Functional Analysis of *AtVAMP714* gene in *Arabidopsis*

Thesis submitted for the degree of Doctor of Philosophy

at the University of Durham

By

Dehiwala Liyanage Champa Kumari M.Sc

Department of Biological & Biomedical Sciences

Durham University

UK

January 2011

Functional Analysis of *AtVAMP714* gene in *Arabidopsis*

Abstract

An activation tagging screen was carried out to identify gain-of-function mutants showing potential auxin defects, with the aim of identifying the new genes regulating plant development. The *conjoined* (*cnj*) mutant isolated from the activation tagged screen exhibits duplication of the seedling axis. Sequencing the insertion locus revealed that the activation tag was positioned between ATP-binding protein and vesicle associated membrane protein genes. Cloned mutant locus and expression studies indicated that the vesicle associated membrane protein gene is upregulated in the activation tagging line. The aim of this work is to investigate the function of the vesicle associated membrane protein gene (*AtVAMP714*), which is a member of an R-SNARE protein family.

To determine the expression pattern of *AtVAMP714*, pro*AtVAMP714*::*GUS* expression in seedlings was examined. GUS activity was observed in the hypocotyl and roots and the strongest expression was observed in the root vascular tissues. The *AtVAMP714* gene is positively auxin regulated. VAMP714::GFP fusion protein localized to Golgi vesicles suggesting it may be involved in the Golgi secretory pathway. Auxin transport levels in roots and shoots found to be greatly reduced in *AtVAMP714* overexpressors compared to the wild type plants. Quantitative real-time RT-PCR showed that transcript levels of *IAA1* and *IAA2* were significantly reduced in *AtVAMP714* overexpressors. Immunolocalization of PIN1 and PIN2 showed strong defects in localization.

To characterize the development role of VAMP714, SALK null mutants of the *AtVAMP714* gene were identified. The mutant phenotype showed an abnormal branching and short root phenotype and *PIN1*, *PIN2* and *PIN4* transcript levels were significantly reduced. Dominant negative transgenics of *AtVAMP714* were also created as a method of knocking out the function of the protein and F2 generation plants were analysed for developmental defects. Consistent with the above results the dominant negative transgenics showed a short root phenotype with dwarfed, branchy shoots. PIN1 and PIN2 proteins were mislocalized in dominant negative transgenics. The results presented provide evidence for a role of AtVAMP714 in auxin transport through a requirement for correct PIN protein secretion and localization.

Declaration

All work recorded in this thesis is original unless otherwise acknowledged in the text or by references, and has not been previously submitted for a degree in this or any other university.

Statement of Copyright

Acknowledgements

I am grateful to my supervisor, Prof. Keith Lindsey for his support and guidance throughout the study. His valuable advice and useful discussions are very much appreciated. I would like to thank Dr. Jennifer Topping for her endless support and patience in the lab, without her help this work would not have been possible.

My special thanks goes to all past and present members of the Lindsey Group, especially Nick for his help in conforcal microscopy, Stuart, Saher, Elie, Mags, Gul, Lucy, Naomi and Jia for their generosity with advice, support through many years and for making my time in the lab enjoyable. I also would like to thank Andrei, Tim, Mike and Lizzy from the Hussey Group for their given support and technical expertise. Many thank to all the people in the Department who helped me in numerous ways to make my work successful.

I am thankful to Durham University Project Sri Lanka Studentship for financial support.

My heartiest thanks to my loving husband Devinda for sharing all good and bad times with me over many years away from home and my family and my friends for their support and encouragement during the period.

Table of Contents

Chapter 2: Materials and Methods

Abbreviations

ACC	1-aminocyclopropane-1-carboxylic acid
BAP	6-Benzylaminopurine
BFA	brefeldin A
bp	base pair (length of a nucleotide)
CaMV	Cauliflower Mosaic Virus
Col-0	*Arabidopsis* ecotype Columbia-0
cDNA	complementary DNA
DAG	days after germination
dNTPs	2'-deoxynucleotide 5' triphosphate
2,4- D	2,4-dichlorophenoxyacetic acids
DNA	deoxyribonucleic acid
DMSO	dimethyl sulphoxide
EDTA	ethylenediaminetetraacetic acid
ER	endoplasmic reticulum
GUS	β- glucoronidase
GFP	Green Fluorescent Protein
GA	gibberellin
HCl	hydrochloric acid
IAA	indole-3- acetic acid
IPTG	isopropylthiogalactoside
Kb	kilobase(s) (length of 1000bp)
KCl	potassium chloride
KOH	potassium hydroxide

MCS	multiple cloning site
$MgCl_2$	magnesium chloride
MW	molecular weight
mRNA	messenger RNA
NaCl	sodium chloride
Na_2HPO_4	disodium hydrogen orthophosphate
NaH_2PO_4	sodium dihydrogen orthophosphate
NaOH	sodium hydroxide
ORF	open reading frame
PCR	polymerase chain reaction
QC	quiescent centre
RNA	ribonucleic acid
RT-PCR	reverse transcriptase polymerase chain reaction
T-DNA	transferred DNA
TIBA	2,3,5-triiodobenzoic acid
Tris	tris(hydroxymethyl) aminomethane
Var	variety
μg	microgram
μl	microlitre
X-Gal	5-bromo-4-chloro-3-indolyl β-D- galactopyranoside
X-Gluc	5-bromo-4-chloro-3-indoyl β-D-glucuronic acid

Chapter 1: Introduction

Chapter 1: Introduction

1.1 Background of the Study

1.1.1 *Arabidopsis thaliana* as a Model for Studying Plant Development

Arabidopsis thaliana is a small dicotyledonous plant in the mustard family (Brassicaceae) that has become the model system of choice for research in plant biology. Significant advances in understanding plant growth and development have been made by focusing on the molecular genetics of this relatively simple angiosperm (Meinke, 1998).

The small size of its genome makes *Arabidopsis thaliana* useful for genetic mapping and sequencing, with about 157 million base pairs and five chromosomes (haploid genome), *Arabidopsis* has one of the smallest genomes among plants. It was the first plant genome to be sequenced, by the *Arabidopsis* Genome Initiative. The most up-to-date version of the *Arabidopsis thaliana* genome is maintained by The *Arabidopsis* Information Resource (TAIR www.arabodpsis.org). Much work has been done to assign functions to its 27,000 genes and the 35,000 proteins they encode (*Arabidopsis* Genome Initiative, 2000). The plant's small size and rapid life cycle are also advantageous for research. It has been used to found several laboratory strains that take about six weeks from germination to mature seed. The small size of the plant is convenient for cultivation in a small space and it produces many seeds (ca. 10,000 per generation). Further, the self-pollinating nature of this plant assists genetic experiments. Also, as an individual plant can produce several thousand seeds, each of the above criteria leads to *Arabidopsis thaliana* being valued as a genetic model organism (Meinke *et al*., 1991, 2010).

Plant transformation in *Arabidopsis* is routine, using *Agrobacterium tumefaciens* to transfer DNA to the plant genome. The floral-dipping method is most commonly used now and involves simply dipping a flower into a solution containing *Agrobacterium* containing the DNA of interest, and a detergent (Clough and Bent 1998). This method avoids the need for tissue culture or plant regeneration.

The *Arabidopsis* gene knockout (insertional mutagenesis) collections are a valuable resource for plant biology made possible by the availability of high-throughput

transformation and funding for genomics resources. The site of T-DNA insertions has been determined for over 300,000 independent transgenic lines, with the information and seeds accessible through online T-DNA databases. Through these collections, insertional mutants are available for most genes in *Arabidopsis* (www.arabidopsis.org).

1.1.2 Insertional Mutagenesis and Activation Tagging

Genetic analysis of mutants of *Arabidopsis* has become a valuable technique for studying and identifying the genes required for development in flowering plants. The genes identified in mutants can be involved in many different aspects of *Arabidopsis* development, from cellular patterning and embryogenesis to maintenance of plant meristems and control of cell differentiation. Mutant studies provide a valuable insight into the function of genes throughout *Arabidopsis* development with wider implications in comparative genetics (Meinke, 1991). An alternative approach is generating gain-of-function mutants through random activation tagging of genes using T-DNA vectors and transcriptional enhancers to drive expression (Weigel *et al*., 2000).

In the *Arabidopsis* post-genomic sequencing era, much effort is being devoted to elucidating the functions of unknown genes (Somerville and Dangl, 2000). The completion of the *Arabidopsis* genome sequence has paved the way for the development of numerous reverse genetics approaches for the determination of gene function. The identification of mutations in the gene of interest is a straightforward, if sometimes laborious process (Krysan *et al*., 1999). However difficulties often arise in the identification of a phenotype that can be associated with the mutation. This is because they may exhibit redundant or highly specialized functions. Homology searching, micro-array based analysis of gene expression and metabolic studies likely will provide some information regarding gene function. In most cases, however a complete understanding of a gene's function will be realized only when this information can be associated with a phenotype at the organismal level. Many of these phenotypes may be manifested as subtle changes in growth or development, underscoring the need for a sensitive and robust methodology for their detection (Douglas *et al*., 2001).

Approaches most commonly used in functional genomics are designed to knock out or alter the function of genes by use of a chemical mutagen, radiation, transposon or T-DNA insertions, which create mainly recessive mutations (Bouche and Bouchez, 2001). However, the limitation of these approaches became obvious when the *Arabidopsis*

and rice genome projects revealed sequence redundancy of more than half of the genes in these genomes (*Arabidopsis* Genome Initiative, 2000; Feng *et al*., 2002; Sasaki *et al*., 2002; Vision *et al*., 2000; Yu *et al*., 2002). It is therefore not difficult to imagine that a gene unique in terms of its sequence may be functionally redundant. In order to circumvent these limitations, activation tagging can be adopted for functional genomic research in plants as an alternative tool to analyse the functions of redundant genes (Jeong *et al*., 2002; Marsch-Martinez *et al*., 2002; Walden *et al*., 1994; Weigel *et al*., 2000; Wilson *et al*., 1996). As activation tagging creates dominant or semi-dominant phenotypes, the effect of wild type loci and functionally redundant genes can be ignored in the mutant lines. Another problem that occurs frequently during the screening of recessive mutants in conventionally tagged resources is that the mutant phenotype often does not segregate with the tag, due to other mutations in the genome (Budziszewski *et al*., 2001).

1.2 *conjoined* Mutant of *Arabidopsis*

In the Lindsey lab at Durham University, an activation tagging screen was carried out to identify gain-of-function mutants showing potential auxin defects with the aim of identifying the new genes regulating plant development (Casson and Lindsey, 2006). A *conjoined (cnj)* mutant was identified following the screening of an activation tagged *Arabidopsis* population (Fig. 1-1). Through sequencing the activation tag it has been positioned in a non-coding region between two genes (Fig. 1-2). One gene is At5g22360, which is predicted to encode a Vesicle-Associated Membrane Protein (AtVAMP 714) and the other gene is At5g22370 which is predicted to encode an ATP-binding protein.

The name *conjoined* was assigned to the mutant, as preliminary characterisation of this mutant exhibited a duplicated seedling axis (Figure 1-1).

Figure 1-1: *conjoined* Mutant of *Arabidopsis*

All four images show the duplicated seedling axis of the *conjoined* mutant. The main characteristic is duplication of seedling axis.

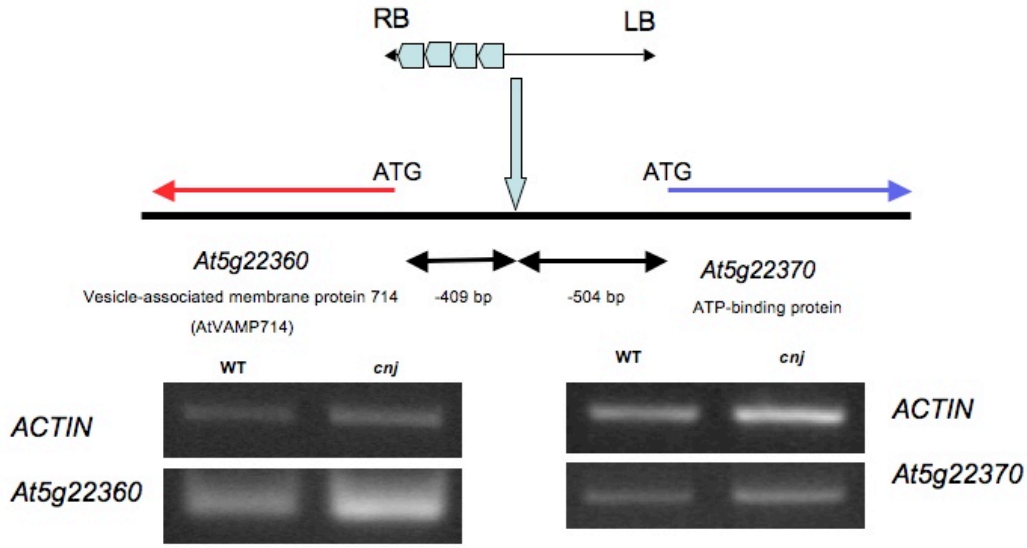

Figure 1-2: *conjoined* Locus

conjoined locus showing the position of the activation tag and the expression analysis of the *At5g22360* and *At5g22370* genes relative to the *ACTIN2* and Col-0 wild type

1.2.1 *CONJOINED* Locus

In activation tagging screens, the overexpressed genes are almost always found immediately adjacent to the inserted T-DNA tag (Weigel *et al*., 2000). Sequencing of the cloned mutant locus and expression studies revealed that At5g22360 gene (*AtVAMP714*) is upregulated in the mutant (Stuart Casson, unpublished data). Bioinformatics analysis of the At5g22360 gene identifies it as a predicted vesicle-associated membrane protein and this gene is a member of an R-SNARE protein family, R-SNARE proteins found in secretary vesicles. They form SNARE complexes that are intrinsic to vesicle fusion and transport (Jahn and Scheller, 2006).

ATP binding protein gene (At5g22370) plays a role in cell division and this function is essential for the correct development of the early embryos (Devic *et al*., 2007). This was published as a mutant affecting embryogenesis after we started this research.

One hypothesis is that At5g22360 is involved in the targeting and/or fusion of transport vesicles to their target membrane (www.uniprot.org). Correct vesicle fusion and transport is essential for cell wall construction and the delivery of key proteins to the cell surface.

1.3 The Vesicle Trafficking Machinery

Many different plants have been used in studies of the plant secretory system; but most labs have focused their attention on the model plant *Arabidopsis thaliana*. The main advantage of *Arabidopsis* is the amount of sequence information and genetic data, both prior to and after the completion of the genome sequencing project (*Arabidopsis* Genome Initiative, 2000).

1.3.1 The Endomembrane System

The endomembrane system is composed of many organelles, each of which must maintain a unique composition of membrane and cargo proteins (Figure1-3; Anton & Natasha, 2003). The endoplasmic reticulum (ER) is a synthesis and transport organelle that branches into the cytoplasm in plant and animal cells (Davidson, 2005). The Golgi apparatus is a series of multiple compartments where molecules are packaged for delivery to other cell components or for secretion from the cell (Graham, 2000).

Vacuoles, which are found in both plant and animal cells (bigger in plant cells), are responsible for maintaining the shape and structure of the cell as well as storing waste products (Lodishet *et al*.,2000). A vesicle is a relatively small, membrane-enclosed sac that stores or transports substances. The plasma membrane, also referred to as the cell membrane, is a protective barrier that regulates what enters and leaves the cell (Figure 1-3; Davidson, 2005).

All of these organelles exchange information through the use of small membrane-enclosed transport vesicles (Bassham *et al*., 2009). These vesicles bud from a donor compartment and then travel to a specific destination where they fuse with the target compartment (Bassham *et al*., 2009). Clearly, some manner of regulation is required to prevent mistargeting of vesicles to the incorrect compartment.

One would expect that each target compartment be uniquely labeled, whereas particular transport vesicles would contain some mechanism for recognizing its target compartment (Bassham *et al*., 2009).

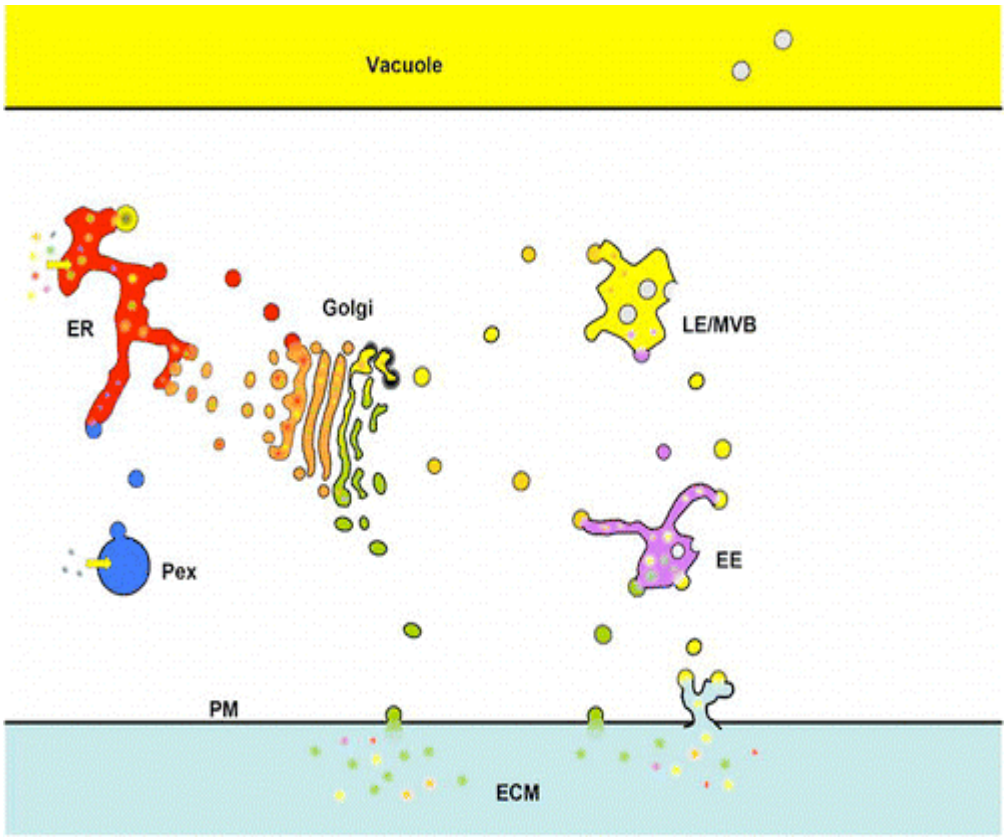

Figure 1-3: The Secretory/Endomembrane System of Arabidopsis

The endomembrane system of all eukaryotes consists of those membrane-bound organelles that exchange lipid and cargo by vesicle trafficking. Despite the constant exchange of vesicles, each organelle/compartment has a relatively constant array of resident membrane and lumenal proteins. In the figure, resident proteins of the endoplasmic reticulum (ER) are red, those of the Golgi are orange, those of the vacuole are yellow, and those of the endosomes (EE) are purple. Secreted proteins (green) end up either in the plasma membrane (PM) or are released into the extracellular matrix (ECM). Peroxisomal (Pex) proteins, some of which are first trafficked through the ER, are indicated in blue (Bassham *et al.,* 2009).

1.3.2 The Vesicle Trafficking Pathway

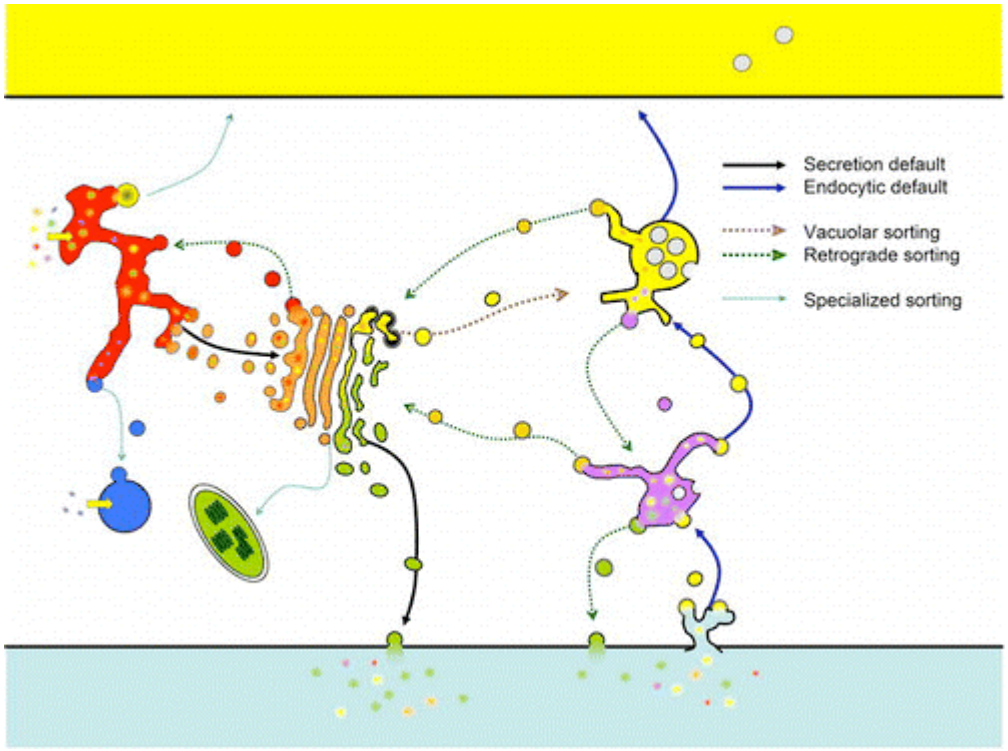

Figure 1-4: The Secretory Pathway, Endocytic Pathway and Retrograde/Recycling Pathways.

The traditional secretory pathway begins by translocation of proteins (yellow arrow) into the endoplasmic reticulum (ER), followed by transport in vesicles to the Golgi by bulk flow (default secretion, solid black line). From the Golgi, secretory proteins are transported to the Plasma Membrane (PM) or extra-cellular matrix (ECM). Also in the Golgi, vacuolar proteins are re-directed to the vacuole (by way of the late endosome) due to specific sorting signals (vacuolar sorting, dashed brown line). Cargo that is endocytosed from the PM/ECM is transported through the endosomes by bulk flow (default endocytosis, solid blue line), first to the early endosomes, then to the late endosomes where endocytic cargo meets vacuolar cargo, and finally the cargo arrives in the vacuole. Many signal-mediated retrograde pathways operate to recycle specific cargo at most compartments (dashed green lines). Finally, several specialized sorting pathways serve to transport peroxisomal proteins from the ER to peroxisomes or to transport some glycosylated proteins from the Golgi to the plastid (dashed cyan lines) (Bassham *et al.*, 2009).

Traffic flows in two main “default” pathways through the secretory system: secretory and endocytic (Figure 1-4). The secretory pathway represents the major biosynthetic route (the “anterograde” direction) that starts with newly synthesized proteins that have been targeted to the endoplasmic reticulum (ER) membrane, then flows first to the Golgi, and subsequently to the plasma membrane (PM)/extracellular matrix (ECM) (Bassham *et al*., 2009). Conversely, the endocytic route represents a counter flow of cargo endocytosed from the PM/ECM, which travels by way of endosomes to the vacuole. Aside from these default pathways; there are several “signal-mediated” pathways that redirect specific proteins from either default pathway. “Retrograde” pathways serve as recycling mechanisms to retrieve material back from later steps in either pathway, or serve to direct newly synthesized cargo destined for the vacuole from the default secretory pathway (Bassham *et al*., 2009). In addition to these bulk-trafficking methods, recent evidence has indicated that peroxisomes may also be a semi-autonomous part of the endomembrane system (Titorenko and Mullen, 2006), and evidence has even suggested that some plastid proteins may travel through the endomembrane system as well (Nanjo *et al*., 2006).

It is widely believed that all of these organelles exchange information through the use of small membrane-enclosed transport vesicles. These vesicles bud from a donor compartment using a complex and ordered system of coat proteins that nucleate on the site of vesicle formation to collect cargo and deform the local membrane until a vesicle is freed by scission. Once free, these vesicles then travel through the cytosol by association with cytoskeletal motors or other docking factors. Finally, through the action of docking and tethering factors as well as members of the SNARE family of proteins, these vesicles must identify their target compartment among all the other possibilities and then fuse their lipid bilayer with the target to deliver their cargo (Natasha & Sanderfoot, 2003).

Research now indicates that such a mechanism exists in the form of proteins from the SNARE super-family (Bassham *et al*., 2009). SNAREs are membrane proteins that each contains a conserved protein motif called the SNARE domain. This domain is made up of a coiled-coil motif (a special type of α–helix) centered on a large hydrophilic residue, and is essential for interactions between SNAREs (Diane and Blatt, 2008).

1.4 Role of SNAREs in Vesicle Trafficking

Energetically, the fusion of a membrane-coated vesicle with a target lipid bilayer is a rather unfavourable process, because of the stability of the membrane structures (Bassham and Blatt, 2008). Eukaryotes have evolved a specialized class of proteins, the soluble *N*-ethylmaleimide sensitive factor adaptor protein receptors (SNAREs) that function as mediators of fusion between vesicular and target membranes. SNARE proteins facilitate vesicle traffic by overcoming the immense dehydration forces associated with bringing two lipid bilayers together in an aqueous environment (Rand and Parsegian, 1989) and by matching vesicles with their destinations to ensure efficient targeting and delivery of specific membrane proteins and soluble cargo. Subsets of SNAREs are found at both vesicles and target membranes, and it is the pairing of the complementary SNARE partners to form a tetrameric bundle of coiled helices that draws the membrane surfaces together for docking and fusion (Diane and Blatt, 2008).

1.4.1 Classification of SNAREs

The various members of the SNARE family of proteins are distributed among the organelles in a specific way. Particular SNAREs label unique target membranes, while others are incorporated into vesicles from only some donor compartments (Bock *et al*., 2001). Since v-SNAREs must travel between compartments, they will be found on more than a single organelle. Due to flexibility in SNARE-SNARE interactions, different combinations of SNAREs can lead to additional levels of organization among the organelles. The members of the SNARE super family have been classified in many ways over the years, based on earlier functional predictions, certain amino acid residues (Fasshauer *et al*., 1998), on characteristics of the SNARE helix alone (Bock *et al*., 2001), and on orthology among the eukaryotic homologues (Sanderfoot *et al*., 2000).

In recent studies, SNAREs are classified either on the basis of their subcellular localization (functional classification) or according to the occurrence of invariant amino acid residues in the centre of the SNARE motif (structural classification). Functional classification divides SNAREs into vesicle-associated and target membrane–associated SNAREs (v- and t-SNAREs, respectively) (Sollner *et al*. 1993), a categorization that can become problematic in the context of homotypic vesicle fusion events and anterograde trafficking routes. Alternatively, under the structural

classification, SNAREs can be grouped as Q- and R-SNAREs owing to the occurrence of either a conserved glutamine or arginine residue in the centre of the SNARE domain (Fasshauer *et al*. 1998). Generally, t-SNAREs correspond to Q-SNAREs, and v-SNAREs correspond to R-SNAREs. The three types of target membrane–localized Q-SNAREs that contribute to the formation of a SNARE complex can be further subdivided into Qa-, Qb-, and Qc-SNAREs (Bock *et al*. 2001). SNAP-25-like proteins constitute a special case because they comprise a Qb- and a Qc-SNARE motif within a single polypeptide chain, possibly as a result of an ancient gene fusion event (Bock *et al*., 2001). For historical reasons, on the basis of their role in synaptic exocytosis, Qa-SNAREs are also frequently referred to as syntaxins (Bennett *et al*. 1992). Likewise, vesicle resident R-SNAREs is often designated as VAMPs (vesicle-associated membrane proteins). R-SNAREs can have a short or long N-terminal regulatory region, further subdividing them into brevins (lat. *brevis*, short) and longins (lat. *longus*, long). Again on the basis of their role in synaptic exocytosis, R-SNAREs with a short N-terminal domain are also frequently referred to as synaptobrevins (Baumert *et al*. 1989). In plants, however, this evolutionarily young class of R-SNAREs is absent; all known plant R-SNAREs belong to the longin category (Uemura *et al*. 2005)

Longins have three main subclasses which are conserved across most eukaryotes including *Arabidopsis* (Table 1-1). The Sec22-like class is involved in ER-to-Golgi traffic (Anton & Natasha, 2003). The Ykt6-like class is involved in many different trafficking events in the cell. The VAMP7-like class is found in most multicellular eukaryotes, and has been extensively duplicated in *Arabidopsis* into two gene families of 4 and 7 members each. The role of these many VAMP7-like SNAREs in *Arabidopsis* remains unclear (Anton & Natasha, 2003).

The greater diversification of SNARE isoforms in plants presumably reflects the necessity for some SNAREs to be devoted to plant-specific biological processes such as the plant-specific type of cytokinesis, gravitropic responses, and the transport of phytohormones (e.g., abscisic acid (ABA) and auxin). Consistent with the role of SNAREs in other eukaryotes, many of these functions appear to be related to the establishment and/or maintenance of polarity at the (sub-) cellular level (Surpin & Raikhel 2004).

1.4.2 Plant R-SNAREs

The R-SNAREs encoded by plant genomes can be grouped into three major subfamilies, the VAMPs, YKT6s, and SEC22s (Table 1-1). Most R-SNAREs are located on trafficking vesicles, anchored by a C-terminal TM domain. A few members, such as AtYKT61 and AtYKT62, are thought to be attached to the vesicular membrane by post-translational addition of lipid anchors, as in the case of their yeast and mammalian counterparts (McNew *et al.* 1997). All plant R-SNAREs are longins, comprising an extended N-terminal stretch (the longin domain; Figure 1-5) that, on the basis of data from human R-SNAREs, may be involved in subcellular localization and SNARE complex formation, by interaction with regulatory polypeptides (Martinez- Arca *et al*. 2003, Uemura *et al*. 2005).

Compared with Q-SNAREs, little is known about the biological roles of plant R-SNAREs. AtVAMP711 suppresses Bax-triggered programmed cell death in yeast, suggesting that intracellular vesicle traffic can regulate the execution of apoptosis (Levine *et al.* 2001). With the exception of a recently discovered salt resistance phenotype (Leshem *et al*. 2006), no further phenotype has been found in any *Arabidopsis* R-SNARE mutant, suggesting that most R-SNAREs act at least partially redundantly, rendering it difficult to infer their function in plants.

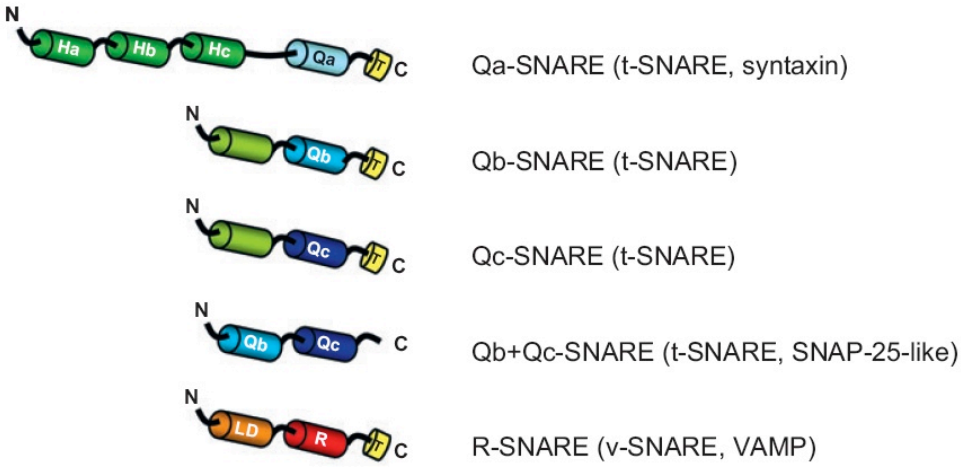

Figure 1-5: Domain structure of Major Plant SNARE sub-families

Scheme of the general domain organization of plant SNARE proteins- shown are Qa-Qb-, and Qc-SNARE motifs, the R-SNARE domain (R), regulatory N-terminal regions of Q-SNAREs, the longin domain (LD) of R-SNAREs, and the C-terminal TM helices (T) present in most SNARE proteins. N and C denote the N- and C-terminal ends of the polypeptides, respectively (Lipka *et al*., 2007).

1.4.3 SNARE Model for Vesicle Trafficking

Current models predict that a vesicle buds from a donor compartment carrying a particular SNARE (a vesicle- or v-SNARE) on its limiting membrane (Bock *et al*., 2001; McNew *et al*., 2000, Diane and Blatt *et al*., 2008). This v-SNARE is capable of interactions with only a particular subset of other SNAREs, and consistent with this, each target membrane has a particular complex of three other SNAREs (target or t-SNAREs). Thus, a single v-SNARE finds its target membrane marked by a t-SNARE complex of three other SNAREs that it can interact with (Figure 1-6). As the vesicle membrane approaches the target membrane, the v-SNARE enters into the 3-helix bundle of the t-SNARE complex, bundling of the 4 SNARE helices drives the two membranes into contact and likely leads to fusion of the vesicle with its target membrane. Experiments have shown that *in vitro*, just the presence of SNAREs embedded in synthetic proteoliposomes are sufficient to drive membrane fusion (Weber *et al*., 1998), and also to maintain some specificity while doing so (McNew *et al*., 2000).

SNARE-domain proteins comprise a superfamily of comparatively small (200–400 amino acids) polypeptides that are characterized by the presence of a particular peptide domain, the SNARE motif (Jahn & Scheller 2006). The SNARE domain is a stretch of 60–70 amino acids consisting of heptad repeat that can form a coiled-coil structure, via hetero-oligomeric interactions; SNAREs mediate fusion events between membranes in the course of intracellular vesicle-associated traffic and therefore occur on vesicles, organelles of the endomembrane system, and the PM. The association of SNAREs with lipid bilayers is usually conferred by C-terminal transmembrane (TM) domains (Figure 1-5). Some SNAREs, however, are attached to membranes via lipid anchors. With the exception of SNAP-25-like SNARE proteins, which harbour two SNARE domains separated by a flexible linker, the vast majority of SNAREs possess one SNARE motif (Figure 1-5). In addition to the SNARE domain and the C-terminal TM domain, many SNAREs contain N-terminal regulatory sequence motifs that control in vivo SNARE protein activity in concert with a range of accessory polypeptides .

SNAREs mediate membrane fusion by intermolecular interactions among complementary vesicle- and target membrane–associated SNAREs. Upon contact, matching types of SNAREs form a highly stable protein association called the SNARE complex. A typical SNARE complex involves three distinct types of SNARE proteins residing on the target membrane and one SNARE polypeptide located on the vesicle that together contribute to a four-helix bundle of intertwined SNARE domains (Brunger 2006, Hong 2005, Jahn & Scheller 2006, Diane and Blatt, 2008). Complex formation is associated with conformational and free energy changes that are commonly believed to drive the membrane fusion process (Figure 1-6).

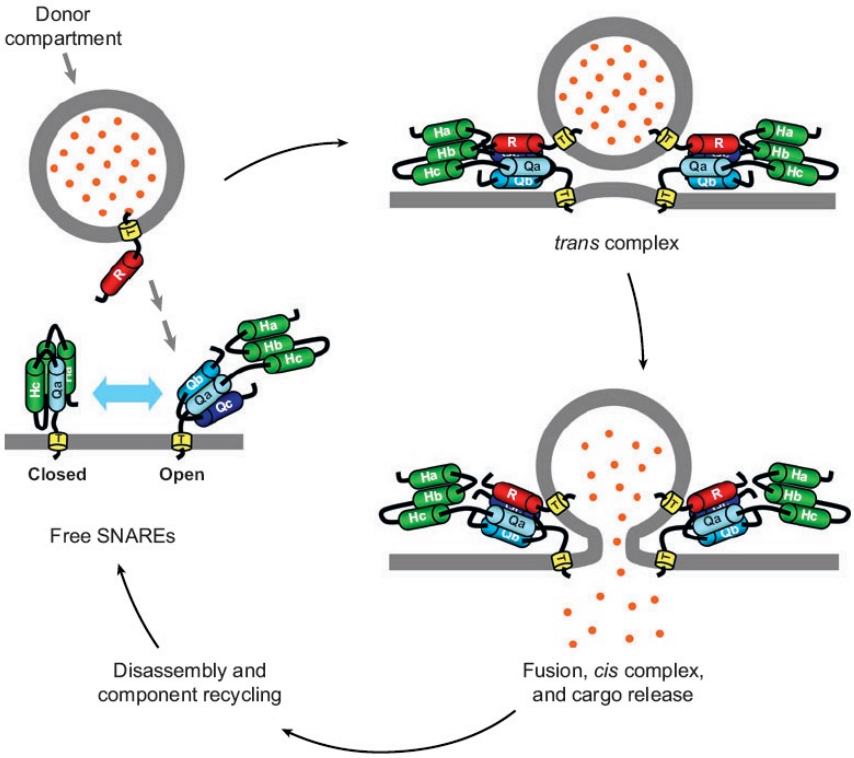

Figure 1-6: Molecular Mechanics of SNARE Complex Formation and Vesicle Fusion

Scheme of the principle of binary and ternary SNARE complex formation. Vesicle fusion is initiated by regulatory protein–mediated opening of the closed conformation of a target membrane–anchored Qa-SNARE. The resulting exposition of the Qa helix allows association with helices provided by a membrane-associated Qb+Qc-SNARE and an R-SNARE. The latter resides in a vesicle, which buds from a donor compartment after cargo loading and is transported to the acceptor compartment. Association in a *trans* complex is accompanied by an increase in core α-helical structure density that drives transition to the *cis* complex, membrane fusion, and the release of vesicle cargo into the acceptor compartment. After energy-dependent disassembly and recycling of the individual complex units, the cycle can restart (Jahn & Scheller 2006). For simplicity, the N-terminal longin domain of the R-SNARE is omitted in this scheme (Lipka *et al*., 2007).

Table 1-1: Types of SNAREs in *Arabidopsis* and Rice (Anton & Natasha, 2003)

SNARE type	SNARE subfamily	*A. thaliana*	*O. sativa*	
Qa		18	14	
	SYP1	9	7	
	SYP2	3	3	
	SYP3	2	1	
	SYP4	3	1	
	SYP8	1	2	
Qb		12	11	
	MEMB	2	1	
	GOS1	2	3	
	VTI1	4	3	
	NPSN1	3	3	
	SEC20	1	1	
Qc		12	16	
	BET1	2	2	
	SFT1	2	2	
	USE1	2	4	
	SYP5	2	3	
	SYP6	1	3	
	SYP7	3	2	
Qb+Qc	SNAP	3	3	
R		15	13	
	VAMP71	4	3	
	VAMP72	7	5	
	YKT6	2	2	
	SEC22	2	3	

1.5 Vesicle Trafficking and Plant Development

1.5.1 Auxin and Plant Development

The plant signalling molecule auxin coordinates many aspects of plant development. Auxin acts as a prominent signal, providing, by its local accumulation in selected cells, a spatial and temporal reference for changes in the developmental programme via the regulation of specific genes (Reinhardt *et al*. 2000, Friml 2003b, Leyser 2006, Esmon *et al*. 2006, Tanaka *et al*. 2006, Dubrovsky *et al*. 2008).

The differential auxin distribution within tissues manifested by local auxin maxima and minima or auxin gradients between cells (Tanaka *et al*., 2006; Sorefan *et al*., 2009). In these cells where auxin accumulates, the different auxin levels trigger a change in the developmental program (Dubrovsky *et al*., 2008; Benkova *et al*., 2009). This developmental reprogramming seems to be pre-programmed and specific for a given cell type. This scenario would also explain the diversity of physiological and developmental auxin effects. Auxin acts as a versatile trigger of change in different contexts and it can be involved in many unrelated, developmental programs (Vanneste and Friml, 2009, Friml, 2010).

Auxin is transported in a regulated, directional fashion in plant tissues (Figure 1-7), which contributes to the generation of differential auxin distribution within plant tissues (Robert and Friml, 2009; Petrasek and Friml, 2009). Auxin distributed through tissues by a directional cell-to-cell transport system is termed polar auxin transport (PAT) that depends on specific auxin carrier proteins (Figure 1-8; Benjamins *et al*. 2005, Blakeslee *et al*. 2005, Kramer & Bennett 2006, Vieten *et al*. 2007). The asymmetric cellular localization of these transporters has been proposed to determine the direction of the flow. Heterologous expression experiments in cultured plant cells, yeast and mammalian cells have demonstrated the auxin-transporting capacity of these carrier proteins (Vieten *et al*., 2007). Expression and localization studies of auxin carrier proteins, as well as specific defects in differential auxin distribution in plants that lack the function of these carriers, established that carrier-dependent PAT is absolutely required for the generation and maintenance of local auxin maxima and gradients (Petrasek and Friml, 2009).

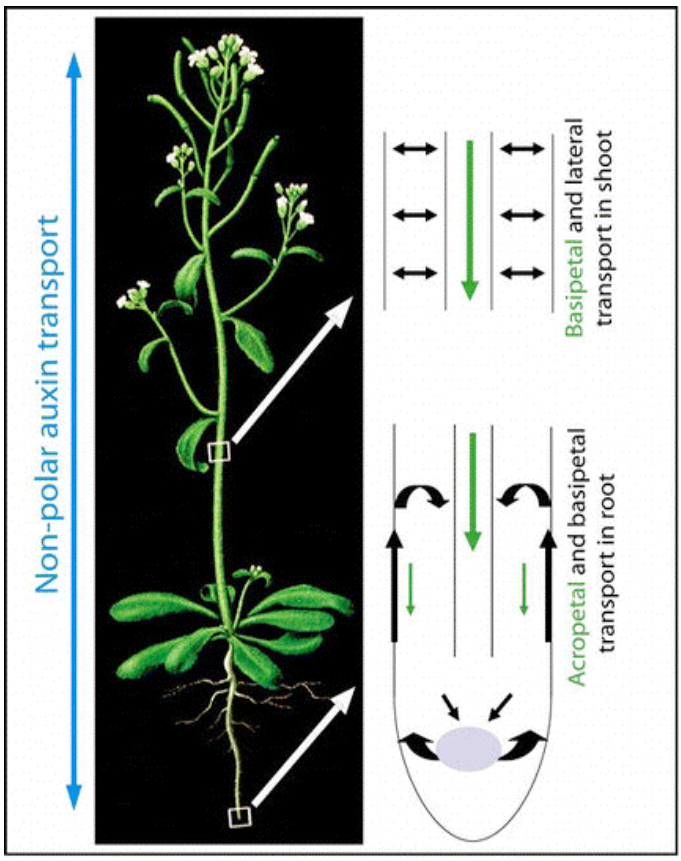

Figure 1-7: A scheme for Non-polar and Polar Auxin Transport in *Arabidopsis thaliana*

Auxin is redistributed throughout all aerial and underground plant body through fast, non-polar transport in phloem (marked by the blue arrows) and slow, cell-to-cell polar auxin transport in other cells (PAT; marked by the green and black arrows). Through PAT, auxin is transported polarly from the aerial apical tissues towards the base through the vasculature (basipetally). This stream continues in the root to the root tip (acropetally) where part of it is redirected upwards (basipetally) through the outer layers. In the shoot, the existence of a short distance lateral transport between the main basipetal stream and outer cell layers is also assumed (Michniewicz and Friml, 2007).

In general, the carrier-mediated transport of auxin can be regulated at three levels: by the regulation of the abundance of a carrier (by regulating its transcription, translation and degradation); subcellular trafficking and targeting of auxin carriers to a specific position on the plasma membrane; and transport activity (through the post-translational modification of carriers, the levels and activity of endogenous inhibitors, the regulation of the plasma membrane pH gradient, the composition of the plasma membrane and the interactions among individual transporters or transport systems) (Petrasek and Friml, 2009).

Auxin efflux carriers of the PIN-FORMED (PIN) family (Galweiler *et al*. 1998, Luschnig *et al*. 1998, Chen *et al*. 1998, Utsono *et al*. 1998, Petrasek *et al.* 2006) show a polar subcellular localization that correlates with and determines the direction of auxin flow through tissues (Friml *et al*. 2004, Wisniewska *et al*. 2006). In plants, polarities of tissue and of individual cells are closely connected by the flow of auxin (Sauer *et al*. 2006), and the cell biological processes depending on vesicle trafficking and polar targeting have an immediate developmental output related to auxin-mediated signalling. At the level of polar auxin transport, many developmental and environmental signals are integrated. By rearranging the subcellular localization of PIN auxin efflux carriers, such signals influence auxin-dependent patterning and contribute substantially to the adaptive and flexible nature of plant development.

1.5.2 AUX1 and Auxin

The existence of specific carriers mediating auxin influx was suggested by the observations that auxin uptake into suspension culture cells (Rubery and Sheldrake, 1974) and tissue segments (Davies and Rubery, 1978) is a saturable process, specific for auxins. A family of amino acid permease-like AUXIN-RESISTANT1/LIKE AUX1 (AUX1/LAX) proteins (Swarup et al., 2001; Swarup et al., 2008) mediates the auxin influx. *AUX1* is a member of a small gene family in *Arabidopsis* consisting of three other *LIKE AUX1* (*LAX*) genes (Swarup *et al.,* 2000).

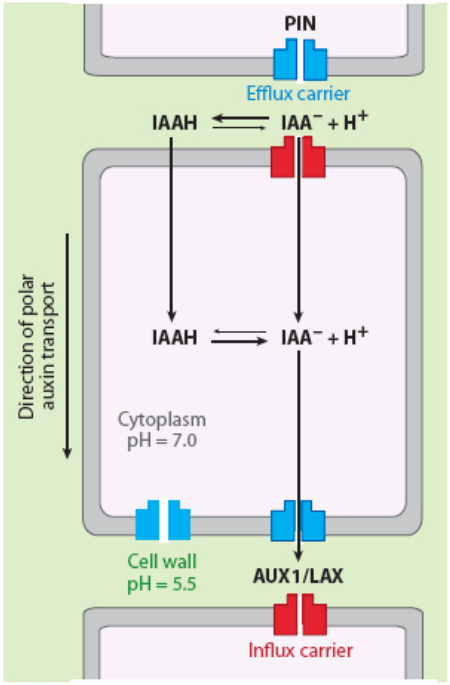

Figure 1-8: Polar Auxin Transport in *Arabidopsis*

PIN-FORMED (PIN) auxin efflux carrier at the plasma membrane determines the auxin exit site from an individual cell. AUX1/LAX1 denotes auxin influx carriers (Vehn and Friml, 2008).

The *aux1* mutant was originally found in a screen for seedlings resistant to 2,4-D (Maher and Martindale, 1980). The auxin resistant and agravitropic root growth phenotype of *aux1* mutants suggested a defect in auxin transport. In *Arabidopsis* root tips, AUX1 is strongly expressed with cell membrane protein localization in protophloem, columella, lateral root cap and epidermal cells. Although in most of these tissues AUX1 appears to be uniformly distributed around all sides of the cells, in the protophloem, AUX1 was found to be enriched at the upper side of cells, that is, opposite to the PIN1 localization in the same cells (Fig. 1-8; Swarup *et a*l., 2001). The plasma membrane localization of AUX1 was also confirmed by biochemical fractionation (Swarup *et al*., 2004). Given the fact that *aux1* root tips contain less auxin than wild type roots suggesting defect in the long-distance auxin distribution down into the root tip AUX1 is involved in unloading auxin from the mature phloem via the protophloem into the PAT system of the root meristem (Swarup *et al*., 2001). In this scenario, an AUX1-dependent system would constitute a connection between phloem-based and PAT routes.

1.5.3. PINs and Auxin

The PIN-FORMED (PIN) protein family is a group of plant transmembrane proteins with a predicted function as secondary transporters. PINs have been shown to play a rate-limiting role in the catalysis of efflux of the plant growth regulator auxin from cells, and their asymmetrical cellular localization determines the direction of cell-to-cell auxin flow, as described above. There is a functional redundancy of PINs and their biochemical activity is regulated at many levels. PINs constitute a flexible network underlying the directional auxin flux (polar auxin transport), which provides cells in any part of the plant body with particular positional and temporal information. Thus, the PIN network, together with downstream auxin signalling system(s), coordinates plant development (Zazimalova *et al*., 2007).

The plasma membrane- localized PIN proteins act as auxin efflux carriers (Petrasek *et al*., 2006) and have been characterized as key regulators involved in multiple developmental processes, including tropic growth (Abas *et al*., 2006; Friml *et al*., 2002a), root meristem patterning (Friml *et al*., 2002b; Blilou *et al*., 2005), lateral organ development (Benkova *et al*., 2003; Reinhardt *et al*., 2003), vascular tissue differentiation and regeneration (Sauer *et al*., 2006a; Scarpella *et al*., 2006; Xu *et al*.,

2006), embryo development (Friml *et al*., 2003; Sauer and Friml, 2004; Weijers *et al*., 2005) and nematode infection (Grunewald *et al*., 2009).

There are eight sequences assigned to PIN proteins in *A. thaliana* (Heisler & Jonsson, 2006) and have different subcellular distributions, including polar, basal, apical, and lateral plasma membrane localizations (Figure 1-9), depending on the PIN protein as well as the cell type (Wisniewska *et al.* 2006). The most typical are basal (root tip–facing) localization of the PIN1 protein in the inner cells of both shoots and roots, apical (shoot apex–facing) localization of PIN2 in the root epidermis and lateral root cap cells, and lateral localization of PIN3 at the inner side of shoot endodermis cells (Galweiler *et al*. 1998; Muller *et al*. 1998; Friml *et al.* 2002b, 2003a). Recently, a subgroup of PIN proteins has been identified that localize not to the plasma membrane but to the endoplasmic reticulum (ER), where they presumably mediate auxin flow to the ER lumen, thus regulating auxin homeostasis (Mravec *et al*., 2009).

From previous reports, there are several indications that PINs have a crucial role in the polar auxin efflux machinery (Morris *et al.*, 2004: Palme & Galweiler, 1999: Morris, 2000: Friml & Palme, 2002); some *pin* mutants were shown to have serious defects in polar auxin transport (Okada *et al*., 1991: Rashotte *et al*., 2000). Polar auxin transport inhibitors can phenocopy loss-of-function *pin* mutations in wild type plants (Friml & Benkova *et al*., 2002: Friml & Wisniewska *et al*., 2002: Galweiler *et al.*, 1998 and Maher & Martindale, 1980).

Plants defective in PIN function show altered auxin distribution and diverse developmental defects, all of which can be phenocopied by chemical inhibition of auxin efflux. These results demonstrate that PINs are essential components of the auxin transport machinery, but the exact mechanism of their action remains unclear (Friml *et al*., 2002, 2003 and Petrásek *et al*., 2006).

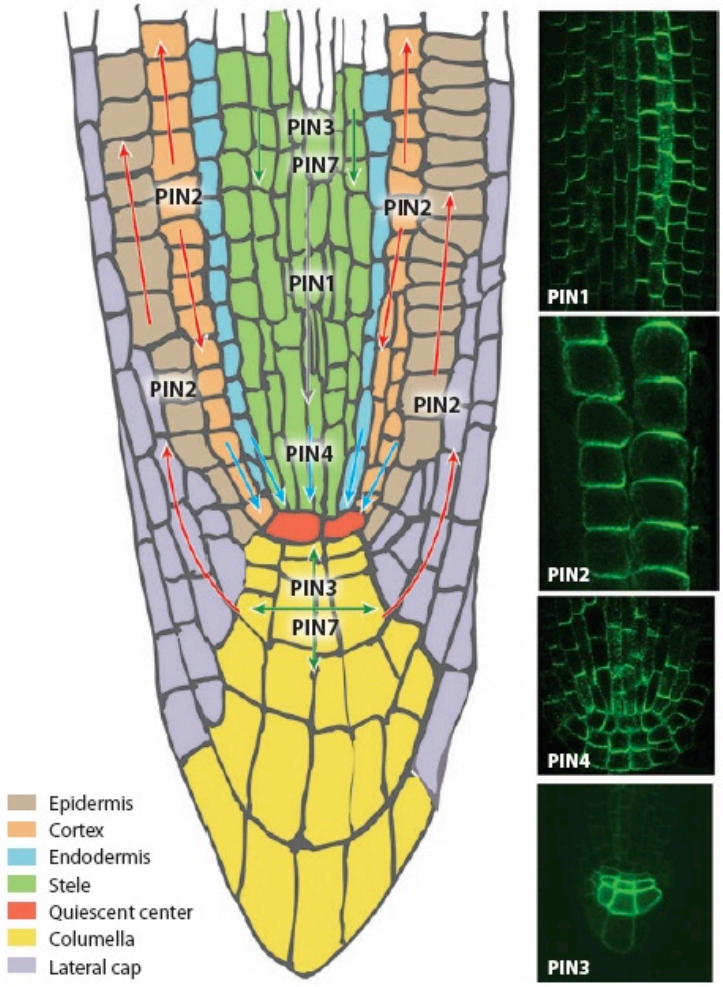

Figure 1-9: Patterns of PIN Protein Localization in the *Arabidopsis* Root tip

Schematic and immunolocalizations of PIN proteins in the *Arabidopsis* root tip. Arrows indicate polar PIN localization at the plasma membrane, illustrating cell type–dependent decisions in the PIN polar localization. PIN1 is localized to basal membrane of stele cells, PIN2 is in epidermis and cortex, note the differential PIN2 targeting in the epidermis (apical) and young cortex (basal) cells, PIN3 is in tiers two and three of root columella cells and PIN4 is in boundaries of the Quiescent centre and surrounding cells (Vehn and Friml, 2008).

1.5.4 Vesicle Trafficking and PIN Targeting

Once the PIN protein is synthesized and post-translational modifications are finished, the protein appears to be loaded into the vesicle trafficking system. In young *Arabidopsis* globular embryos, both basally localized PIN proteins and activity of the *GNOM* gene were shown to be needed for apical-to-basal auxin flow, and PIN1 is mislocalized in *gnom* mutants (Steinmann *et al*., 1999).

An important factor for the delivery of PIN proteins to the plasma membrane is an endosomal regulator of the vesicle trafficking, *GNOM*, which encodes a GDP/GTP exchange factor for adenosyl ribosylation factors (ARF GEF; Shevell *et al*., 1994; Geldner *et al*., 2001, 2003). In *gnom* (also called *emb30*) mutant embryos, the coordinated polar localization of PIN1 is impaired (Steinmann *et al*., 1999). As a consequence, embryonic auxin gradients are not properly established (Friml *et al*., 2003b) and the creation of the apical-basal axis and cotyledon formation is defective (Mayer *et al*., 1991). A range of studies have identified GNOM as a crucial factor in the delivery of PIN proteins as well as other cargos to the plasma membrane. However, whether GNOM plays a specific role in decision on the polarity of PIN targeting remains to be seen (Michniewicz and Friml, 2007).

Knowledge on molecular components controlling cell polarity in plants is scarce (Dhonukshe *et al*.,2005) but it seems that reversible phosphorylation of PIN proteins by the serine/threonine protein kinase PINOID (PID) and proteinphosphatase-2A (PP2A) is important for the decision about apical or basal delivery of PIN proteins (Michniewicz *et al*.,2007). Overexpression of PID or mutants in the PP2A regulatory subunit lead to predominantly apical targeting where as pid loss-of-function leads to basal PIN delivery. The resulting model is that PID phosphorylates PIN proteins, thus supporting their apical targeting, and PP2A antagonizes this action, promoting basal PIN delivery (Friml *et al*., 2004; Michniewicz *et al*., 2007). An important upstream regulator of PID activity is the transcription factor INDEHISCENT (IND) that mediates auxin distribution-dependent fruit development (Sorefan *et al*., 2009).

Genetic and cell biological studies suggested that the correct localization of PIN proteins depends also on the sterol composition of plasma membranes (Souter *et al*. 2002; Willemsen *et al*., 2003; Grebe *et al*., 2003; Pullen *et al*. 2010). The specific sterol composition of the plasma membrane is another factor important for polar PIN delivery

since mutants in the STEROL METHYL TRANFERASE1 (SMT1) enzyme show defective PIN localization (Willemsen *et al*., 2003) in contrast to hydra mutants affected in overall sterol profiles (Souter *et al*., 2002, Souter *et al*., 2004, Lindsey *et al*., 2003). Highlighting the importance of polar PIN delivery for auxin transport-related development, all mutants with defective polar targeting show also pronounced developmental aberrations (Kleine-Vehn and Friml, 2008).

The Arabidopsis mutant *orc* with mutations in the *STEROL METHYLTRANSFERASE1* (*SMT1*) gene, which is involved in sterol biosynthesis, shows cell polarity defects including the impaired polar localization of PINs, accompanied with reduced auxin transport and auxin-related developmental defects (Willemsen *et al*., 2003). Furthermore, sterols and PIN proteins have been shown to have overlapping subcellular trafficking pathways (Grebe *et al*., 2003). Sterol-enriched plasma membrane microdomains, sometimes called lipid rafts, are important for various types of plasma membrane-based signaling processes and have been reported to be also present in higher plants (Martin *et al*., 2005; Bhat and Panstruga, 2005). However, whether PIN proteins and/or related factors are directly associated with these structures, and what eventual functional relevance such associations have, remains unclear.

1.5.5 Endocytic Cycling of PIN Proteins

Genetic evidence for intracellular trafficking of PIN proteins came with the analysis of the *Arabidopsis* mutant *gnom* isolated in a screen for defects in early apical-basal patterning (Mayer *et al*., 1991; Patton *et al*. 1991). *gnom* mutants show a variety of developmental defects. Seedlings always lack a root and also show pronounced defects in the development of apical structures. The most severely affected *gnom* seedlings display a ball-like structure without a recognizable apical-basal axis (Mayer *et al*., 1991; Topping and Lindsey 1997). These developmental defects are reminiscent of auxin- or auxin transport-related defects and the connection between the role of GNOM in vesicle trafficking and auxin biology was established by the observation that in *gnom* mutant embryos, the coordinated polar localization of PIN1 is affected (Steinmann *et al*., 1999). Similarly, in weak *gnom* alleles, PIN1 polar localization is defective in developing lateral root primordia (Geldner *et al*., 2004). These observations suggest that the GNOM protein is a BFA-sensitive regulator of PIN1 subcellular localization. Growing plants on medium supplemented with BFA affects root and hypocotyl gravitropism and elongation as well as lateral root initiation; all processes related to auxin transport

(Geldner *et al*., 2001). Analysis of an engineered BFA-resistant version of GNOM clearly established that GNOM is the endosome-localized regulator of PIN1 exocytic delivery from the endosomes to the PM (Geldner *et al*., 2003). However, it remains unclear whether GNOM is specifically involved in polar exocytosis or in a broader range of exocytic processes. PIN proteins constitutively cycle between endosomes and the PM in a GNOM-dependent manner. These findings complemented earlier physiological studies on the importance of BFA-sensitive vesicle trafficking for the process of auxin transport (Delbare *et al*., 1998; Morris and Robinson, 1998).

1.5.6 Functional Importance of Constitutive Cycling

The constitutive trafficking of PIN proteins would provide a required flexibility for the fast repositioning of PIN carriers to other sides of the cell. This could allow for the rapid redirection of auxin flow in response to environmental or developmental cues (Friml, 2003; Morris, 2000). Rapid PIN relocations were observed during embryonic development (Friml *et al*., 2003b), lateral root formation (Benková *et al*., 2003), phyllotaxis (Heisler *et al*., 2005) and during root gravity response (Friml *et al*., 2002b). In the latter case, PIN relocation occurs within a few minutes after gravity stimulation, thus necessitating a rapid subcellular dynamic. However, the mechanism underlying the rapid PIN polarity changes is unknown and whether it utilizes transcytosis (internalization and subsequent retargeting to the other side of cell) remains to be demonstrated.

It has also been proposed that auxin efflux could be mechanistically analogous to the transport of animal neurotransmitters. In this situation, components of auxin transport could constitutively recycle through the cell in vesicles and facilitate the loading and subsequent release of auxin from cells by polar exocytosis (Friml and Palme, 2002; Baluška *et al*., 2003). It seems that PIN proteins are also functional inside the cell since yeast cells expressing an internalized version of PIN2 accumulate more auxin than control cells (Petrášek *et al*., 2006). Recent results based on immunolocalization of auxin indicated that at least some auxin can be found in BFA-sensitive subcellular compartments (Schlicht *et al*., 2006), however independent confirmation for this important observation is lacking. In transport studies in cultured cells, the amount of PIN protein at the cell surface correlates with auxin efflux, favoring the scenario that PINs function at the plasma membrane (Paciorek *et al*., 2005).

It seems that the constitutive recycling of auxin transport components may be important for the regulation of the directionality and throughput of auxin flow. Whether it is also a

part of a neurotransmitter release-like mechanism and/or receptor-like function remains to be seen (Michniewicz and Friml, 2007).

1.6 Auxin Effect on PIN Internalization

An unexpected mode of auxin action on PAT relates to its effect on subcellular protein trafficking. It has been shown that both exogenously applied and endogenously produced auxin specifically inhibits endocytosis, as evidenced by a reduced uptake of endocytic tracers or the inhibited internalization of several plasma membrane proteins including PINs (Paciorek *et al*., 2005). By inhibiting PIN internalization, auxin increases levels of PINs at the plasma membrane, and thus directly stimulates its own efflux from cells. This provides a mechanism for a positive feedback regulation of auxin transport by auxin itself. The inhibition of endocytosis by auxin requires the activity of a large *Arabidopsis* protein BIG (Gil *et al*., 2001), and it still remains unclear which pathway auxin acts through to exert this effect on endocytosis. It is possible that it will not involve a known TIR1-Aux/IAA-ARF auxin-dependent gene expression pathway (Michniewicz and Friml, 2007). It is intriguing to speculate that auxin may also influence other physiological responses, such as cell elongation, by targeting the subcellular trafficking of other proteins such as the plasma membrane H^+-ATPase, and thereby mediating the acidification and loosening of the cell wall (Michniewicz and Friml, 2007).

1.7 Auxin-dependent Regulation of PIN Polar Targeting

Remarkable rearrangements in PIN polarity have been observed during developmental processes involving the coordinated re-polarization of cells within tissues such as vascular tissue differentiation and regeneration (Scarpella *et al*., 2006; Sauer *et al*., 2006), or lateral roots, leaf and flower initiation (Benkova *et al*., 2003; Reinhardt *et al*., 2003; Heisler *et al*., 2005). Auxin distribution and transport during the formation of vein patterns in developing Arabidopsis leaves revealed interplay between auxin accumulation and the establishment of PIN polarity (Scarpella *et al*., 2006). *PIN1* is first expressed in a broad zone at places of auxin accumulation, but as the leaf matured, this initially wide pattern progressively narrows down. The external application of IAA on the edge of a leaf is also sufficient to induce the strong up-regulation of *PIN1* expression in the vicinity of auxin source, and gradually narrows away from the source and coincides with the establishment of an ectopic vasculature. A progressive formation of *PIN1*-expressing channels, and the polarity of PIN1 protein within the cells, was seen

to be gradually oriented away from the auxin source (Scarpella *et al*., 2006). It seems that auxin functions as the inductive signal, which, through the regulation of PIN1 expression and polarity, defines routes for the formation of new vasculature strands, in part at least via localized activation of the vascular tissue-inducing transcription factor ATHB8 (Pullen *et al*., 2010).

Auxin application onto the *Arabidopsis* root meristem revealed a time- and concentration-dependent repositioning of PIN1 protein from the basal to inner lateral sides of endodermis and pericycle cells. In cortex cells, endogenous PIN2 and ectopically expressed PIN1 relocated to the outer lateral side suggesting that the auxin effect on PIN polarity is modulated by cell type-specific factors (Sauer *et al*., 2006). This system was used to address the molecular mechanism by which auxin influences PIN polarity. Genetic and pharmacological studies revealed that the Aux/IAA-ARF auxin signaling pathway is required for the auxin effects on PIN polarity. For example, in certain dominant stabilized *aux/iaa* mutants (e.g. *axr3/iaa17*), or in specific *arf* mutant combinations e.g. in *arf 7,16,19* or *arf 7,19/ARF17ox* (Sorin *et al*., 2005), the auxin-induced retargeting of PINs was impaired (Sauer *et al*., 2006).

Arabidopsis root meristem regeneration after the ablation of the root quiescent center (QC) did not suggest that auxin redistribution directly affects PIN polarity (Xu *et al*., 2006). The analysis of events happening after the disruption of auxin flow showed that auxin levels were rapidly up-regulated in cells above the ablated QC, which then induced cell-fate changes in this region. Several *PIN* genes, such as *PIN1* and *PIN4*, were strongly down-regulated in the place where the new auxin maximum formed and their expression was shifted to the more proximally positioned cells with unchanged polarity. Only after renewed specification of the QC did *PIN4* become expressed *de novo*, and the protein correctly polarized in these cells. It seems that in the context of root meristem regeneration, auxin primarily influences cell-fate changes and only after proper cell specification, changes in PIN polarity are facilitated (Xu *et al*., 2006).

1.8 Auxin Transport Inhibitors and Vesicle Trafficking

Auxin transport inhibitors (ATIs) are essential tools for manipulating plant development and studying mechanism of auxin transport. They seem to share only limited structural homology and may have several unidentified molecular targets (Katekar and Geissler,

1977). Some of the important representatives of this class of herbicides, such as TIBA or PBA, not only inhibit auxin efflux but also interfere with the subcellular trafficking of PIN and AUX1 proteins and other PAT-unrelated trafficking processes (Geldner *et al*., 2001; Kleine-Vehn *et al*., 2006). PBA and TIBA interfere with organelle motility and the movement of individual vesicles probably by inhibiting actin cytoskeleton dynamics (Dhonukshe *et al.*, 2007b). The cell biological effects of these herbicides are not only restricted to plants but were also detected in yeast and mammalian cells, suggesting a common, evolutionarily conserved target (Dhonukshe *et al*., 2007b). The genetic manipulation of actin dynamics and the chemical stabilization of actin filaments mimic the ATI effect on actin cytoskeleton dynamics and also inhibit auxin efflux, auxin translocation and auxin transport-dependent physiological responses (Dhonukshe *et al*., 2007b). These results, together with the known importance of subcellular dynamics for auxin transport, suggest that the effects of ATIs on actin cytoskeleton dynamics underlie their effect on auxin efflux. The molecular target of ATIs that are relevant for the inhibition of auxin efflux has not been unequivocally identified, and the concentrations needed for the cell biological effects are higher than those required for the physiological effects on auxin transport (Dhonukshe *et al*., 2007b). Therefore, it is possible that effect of ATIs on actin dynamics and auxin efflux reflect two independent molecular targets (Michniewicz and Friml, 2007).

1.9 Aims and Objectives of the Study

Bioinformatics analysis of the *Arabidopsis* gene *AtVAMP714* (At5g22360) identifies it as encoding a vesicle-associated membrane protein of 221 amino acids. This study has been initiated to gain an insight of the function of this gene. This was approached through the characterization of the gene promoter activity in GUS transgenic plants, using GUS histochemical analysis, analyzing the subcellular localization of VAMP714 protein, determining whether VAMP714 has any role in auxin signaling and analysing the loss-of-function and dominant negative mutants.

Chapter 2: Materials and Methods

Chapter 2: Materials and Methods

Described in this chapter are the materials and methods which were used to obtain the results described in the following results chapters.

2.1 Materials

2.1.1 Chemicals

The chemicals used in the following experiments were analytical grade reagents. All the chemicals were obtained from Sigma-Aldrich (Poole, UK), Fisher Scientific Ltd (Loughborough, UK) and BDH (Lutterworth, UK) unless otherwise stated. X-Gluc and IPTG were obtained from Melford Laboratories Ltd (Suffolk,UK), and X-Gal from Bioline (London, UK). Radio-active ^{3}H-IAA was from GE Amersham UK.

2.1.2 Enzymes

Restriction endonucleases, T4 DNA ligase, RQ1 RNase-free DNase, M-MLV reverse transcriptase and RNasin ribonuclease inhibitor were obtained from Promega Ltd. (Southampton, UK). The KOD HOT start PCR system and Proteinase K were from Boehringer Mannheim (Lewes, UK). Shrimp alkaline phosphatase was obtained from Sigma. *Taq* DNA polymerase was from Bioline. Finnzymes Phusion® High-Fidelity DNA polymerase from New England BioLabs.

2.1.3 Kits and Reagents

The Wizard™ Plus SV Minpreps DNA purification system and Access RT-PCR system were from Promega (Southampton, UK). The *High Pure* PCR Product purification kit was from Roche (Mannheim, Germany). The TOPO-TA cloning kit and GATEWAY™ cloning system kits were from Invitrogen (Paisley, UK). The RNeasy Plant RNA extraction kit and the QIAGEN® Plasmid Midi Kit were from Qiagen Ltd (Surrey, UK). The GenElute™ Plasmid Mini prep kit was from Sigma (Poole, UK).

Oligodeoxynucleotide primers used in PCR reactions were obtained from MWG-Biotech (Ebersberg, Germany). The sequences of all oligodeoxynucleotide primers that were used in this work are given in Annex 1.

2.1.4 Bacterial Strains

The *E.coli* strain DH5α was used to prepare competent cells, and as a plasmid host. DH5α cells were used for the propagation of GATEWAY™ Entry and Destination vectors that carry the cyctotoxic *ccd*B gene. The TOP-10 *E.coli* strain used as a host for pCR®2.1 TOPO was supplied as a part of the TOPO-TA cloning kit.

Agrobacterium tumefaciens C58C3 (Dale *et al*., 1989) was used for plant transformations. This strain has been disabled so that it does not cause crown-gall disease but it still has the virulence factors required for T-DNA transfer and insertion into plant genomic DNA. C58C3 carries a chromosomal streptomycin resistance marker, allowing antibiotic selection using 100 µg/ml streptomycin.

2.1.5 Plasmids

The following plasmids were used during this project: pCR®2.1 TOPO (Invitrogen), pΔGUSCIRCE (Topping *et al*., 1991) and pBIN fusion GFP (kindly supplied by Dr. David Dixon, Durham University).

In addition, the following GATEWAY™ compatible vectors were used: pDNOR207, pMDC83, PMDC43 (kindly supplied by the Hussey Group, Durham University), pGHPGWC and pGHGWC (The European Arabidopsis Stock Centre (NASC), Nottingham, UK).

pCR®2.1 TOPO was used for cloning DNA fragments generated by PCR. pΔGUSCIRCE was used in the construction of promoter-GUS construct and contains the β-glucuronidase gene followed by the *NOS* terminator. pBIN fusion GFP was used in the production of VAMP714-GFP fusion and contains the CaMV 35S promoter and terminator. pDNOR207 was used to make GATEWAY™ compatible entry vectors. pMDC 83, pMDC43, pGHGWHC and pGHGWHC were used to make GATEWAY™ expression clones.

All plasmid maps are shown in Annex 2.

2.1.6 Culture Media

All the culture media were sterilized by autoclaving at 121°C for 20 minutes.

2.1.6.1 Bacterial Culture Media

Luria-Bertani (LB) medium: 10 g/ L bacto-tryptone or peptone, 5 g / L bacto-yeast extract, 10 g NaCl and pH adjusted to 7.2 using 0.1M NaOH (Ausubel *et al*., 1997)

LB agar: prepared by adding 15 g bacto-agar to one litre of LB prior to autoclaving.

SOC medium: 20 g/L tryptone, 5 g/l yeast extract, 5.84 g/L NaCl, 10 mM $MgCl_2$, 10 mM $MgSO_4$, 2 g/L glucose and pH adjusted to 6.8 -7.0 using 1 M KOH/HCl. $MgCl_2$, $MgSO_4$ and glucose were added after autoclaving, following filter sterilization using 0.2 µm Minisart® (Sartorius, Germany) filters**.**

Glycerol stock: Aliquots (0.5 ml) from fresh overnight cultures of bacterial strains were combined with an equal volume of sterile 50% v/v glycerol in Eppendorf tubes, and stored either at -20 °C for short-term use, or flash-frozen in liquid nitrogen and kept at -80 °C for long term storage.

2.1.6.2 Plant Culture Media

Seedlings were grown on sterile ½ MS10: 2.2 g/l half strength Murashige and Skoog medium (Sigma M5519), 10g/L sucrose, pH 5.7 adjusted with 1M KOH, 8g/L agar, autoclaved at 121ºC for 20 minutes.

2.1.7 Antibiotics

All the antibiotics and reagents were dissolved in distilled water and filter sterilized using 0.2 µm Minisart® (Sartorius, Germany) filters. Antibiotics were added after cooling the media to 40-50 °C in a water bath. The following antibiotics and reagents were used at different stages of this project:

Table 2.1: Antibiotic and selection reagents

Antibiotic or Reagent	**Stock solution concentration**	**Working concentration**	**Storage temperature**
Ampicillin	25 mg/ml in water	35 - 50 µg/ml	-20 °C
Kanamycin	50 mg/ml in water	50 µg/ml	-20 °C
Chloramphenicol	34 mg/ml in ethanol	10 µg/ml	-20 °C
Carbenicillin	5 mg/ml in water	50-100 µg/ml	-20 °C
Gentamycin	50 mg/ml in water	10 -50 µg/ml	-20 °C
Streptomycin	100 mg/ml in water	100 µg/ml	-20 °C
Rifampicin	20 mg/ml in methanol	100 µg/ml	-20 °C
X- Gal	40 mg/ml in Dimethylformamide	40 µl/100 mm agar plate	-20 °C
IPTG	100 mM in water	10 µl/100 mm agar plate	-20 °C
Nalidixic acid	5 mg/ml in 70% ethanol	25 mg/l	-20 °C

2.1.8 Plant Material

Wild type *Arabidopsis thaliana* var. Columbia (Col-0) and seeds of primary transformants of activation tagged population were kindly supplied by Dr. Stuart Casson.

2.2 Plant Culture Conditions

This section describes the plant culture procedures and growth conditions used during the course of this project.

2.2.1 Seed Sterilisation

Surface-sterilization of seeds is necessary for germination on a nutrient rich medium to prevent contamination by fungi or bacteria. Sterilization was carried out in a laminar flow cabinet, and solutions were transferred using a fresh sterile transfer pipette for each seed sample. Aliquots of seeds were placed in Eppendorf tubes and treated with 70% v/v ethanol for 30-60 seconds to partially de-wax the testa. Seeds were then immersed for 10 minutes in 10% v/v commercial bleach solution with a drop of Tween 20 detergent to enhance wetting and penetration. The seeds were then washed thoroughly in 4-6 changes of sterile distilled water before being plated onto germination medium (½ MS10).

All the washings were collected and filtered through paper towels to remove stray seeds, for autoclaving and disposal.

2.2.2 Plant Growth Conditions

2.2.2.1 Soil based greenhouse culture

Plants in soil were grown in Levington's multipurpose compost mixed 4:1 with silver sand (soil and sand from Klondyke Garden Centre, Chester-le-Street, UK) to ensure adequate drainage in a greenhouse with 16 hour light per day. Seeds were sown in small pots and pre-chilled at 4 °C for three days to break dormancy, before transfer to standard growing conditions (22 °C, 16 hours light: 6 hours dark). Germinated seedlings were transferred at

5-10 days after emergence into 24-well standard tray inserts (LBS Horticulture Ltd., Lancashire UK) containing the standard compost-sand mixture, placed on damp capillary matting. Plants were watered from above using a fine nozzle water dispenser. Separate pools of seeds from individual plants were obtained using the Aracon system (BetaTech, Belgium).

All compost was treated as standard with "Intercept" systemic insecticide (Levinton Horticulture Ltd., UK), at a concentration of 64 mg/24- well trays. The mite *Amblyseius cucumeris* (Syngenta, UK) was introduced every 6 weeks onto the aerial parts of the plant as a biological control against thrips.

2.2.2.2 Culture under Sterile Conditions

Seedlings for analysis were grown in sterile Petri dishes using ½ MS10 media; with plate margins sealed using Micropore^{TM} tape. Prior to germination, seeds were stratified for 3-4 days in the dark at 4°C to promote and synchronize germination. Plates were then transferred to a growth chamber at 22 ± 2 °C set at 'long days' (16 hours light: 6 hours dark).

2.3 Analysis of *VAMP714* Promoter Activity

For analysing the gene promoter activity, plant lines carrying the promoter-GUS fusion and showing segregation with kanamycin selection were germinated in ½ MS 10 plates and incubated in X- Gluc with X- Gluc buffer.

2.3.1 Histochemical GUS Analysis

Adapted from Stomp (1990).

Solutions

X-Gluc stock: 20mM X-Gluc (5-Bromo-4-Chloro-3-Indolyl-β-D-Glucuronide) in N, N-dimethylformamide, stored at -20°C.

X-Gluc buffer: 100mM NaH_2PO_4, 10 mM EDTA, 0.1% (v/v) Triton X-100, 0.5mM potassium ferricyanide ($K_3\{Fe(CN)_6\}$) and 0.5 mM potassium ferrocyanide ($K_4\{Fe(CN)_6\}$),pH 7.0.

X-Gluc staining solution: prepared by mixing 1 volume of X-Gluc stock with 19 volumes of X-Gluc buffer to give a final concentration of 1 mM X-Gluc.

Method

Histochemical localisation of β-glucuronidase (GUS) enzyme activity was carried out by staining plant tissue for up to 16 hours in 1mM X-Gluc staining solution at 37^0C. Stained tissues were then cleared of chlorophyll by soaking in 70% ethanol.

2.3.2 Analysis of GUS Activity during Plant Development

Plant material carrying the pro*AtVAMP714*::GUS construct was incubated for 16 hours under 37º C to generate a comprehensive developmental staining analysis. Seedlings of 3, 5, 8, 11, 14 and 21 days after germination were used for the study.

2.3.3 Hormone Treatments of Seedlings

All phytohormone and inhibitor compounds were made up as 10 mM stock solutions in the relevant solvents, and filter-sterilized using 0.2 µm Minisart® (Sartorius, Germany) filters prior to use. These chemicals were introduced into molten media, cooled to 55°C, before square plates were poured and allowed to cool.

Plant materials carrying the pro*AtVAMP714*::GUS construct were grown in the presence of plant growth regulators and inhibitors, according to the experiment. Seven days after incubation GUS activity was determined by staining plant tissue for up to 16 hours in 1mM X-Gluc staining solution at 37^0C. The following plant growth regulators and inhibitors were used for the study:

- ACC (1- aminocyclopropane-1-carboxylic acid) : ethylene precursor, stock was prepared in distilled water
- BAP (6-benzylaminopurine): cytokinin analogue, stock was prepared by dissolving in a small volume of dilute HCl before making up to volume with distilled water
- IAA (Indole Acetic Acid): naturally active form of auxin, stock was prepared by filter sterilized 70% v/v ethanol
- TIBA (2,3,5-triiodobenzoic acid): auxin transport inhibitor that inhibits the efflux carrier, stock was prepared in 50% v/v DMSO

10 mM stock solutions were made using above plant growth regulators. To make up working solutions using 10 mM stocks, required amounts were added as indicated in Table 2.2 below.

Table 2.2 Amount of 10 mM stock solution to add making working solutions

Desired final concentration	For 1 L	For 400 ml	For 50 ml
1 µM	0.1 ml	40 µl	5 µl
10 µM	1 ml	0.4 ml	50 µl
25 µM	2.5 ml	1.2 ml	125 µl
100 µM	10 ml	4 ml	0.5 ml

2.3.4 Resin Embedding & Tissue Sectioning

Plant material carrying GUS reporter genes were incubated in X-Gluc as described above. Stained material was rinsed three times in 0.1 M phosphate buffer pH 7.

After staining, samples were fixed in a fresh solution of Karnovsky's fixative. A solution of 4% paraformaldehyde and 4% (v/v) glutaraldehyde was made by dissolving paraformaldehyde in de-ionised water at 60^0C, adding 0.1 M KOH drop-wise to bring the pH above 8. The solution was cooled, and brought to pH 7 using 0.1 M HCl. Glutaraldehyde was then added, and combined with 1 volume of 0.2 M phosphate buffer (pH 7) to give a 4% (w/v) paraformaldehyde, 4% (v/v) glutaraldehyde solution in 0.1 M

phosphate buffer. Samples were placed into this fixative for 3 hours in the fridge at 4ºC, then the bathing solution was replaced with fresh fixative for incubation overnight at 4ºC, to ensure penetration into the internal tissues. After this all traces of fixative were removed by rinsing the samples three times in 0.1 M phosphate buffer, for at least 30 minutes each time.

Samples were then embedded using the method recommended for the Historesin™ Embedding Kit (Leica instruments, Heidelberg, Germany), as follows. After fixation, samples were dehydrated through an ethanol series comprising 1 hour in each of 30, 50, 70 and 95% (v/v) ethanol, with a final wash in 95% (v/v) ethanol overnight. Infiltration solution was prepared by mixing LR White with ethanol as follows (Table 2.3). Slides were sealed with clear nail varnish to allow long term storage.

Table 2.3 LR White: Ethanol ratio for infiltration solution

LR White	Ethanol	Duration
1	3	6 hours
1	1	Overnight
3	1	6 hours
1	0	Overnight

Flat bottom embedding (BEEM) capsules (Agar Scientific, Stanstead, UK) were filled with embedding medium. The samples were oriented in this medium using forceps, and left to harden at 60ºC overnight with closed lids.

Capsules were cut away from the hardened resin using razor blades, and the resin trimmed prior to mounting on the cutting block of a Reichert Ultracut Ultramicrotome. 10 µm sections were cut from samples using a glass knife, and floated onto water on Superfrost ™ pre-coated microscope slides (BDH), then left to evaporate on a hotplate. Samples were then mounted in DPX (Fisons Scientific Equipment, Loughborough, UK).

2.4. Root Gravitropic Response Experiments

Tip curvature response (root gravitropic response) experiments were performed to investigate defective auxin signalling in the SALK knockout mutant of *vamp714*. When roots are accidently or experimentally reoriented within the gravity field they undergo a tip-curvature response that ultimately results in a resumption of growth towards gravity (Boonsirichai et al., 2002).

The seeds of the mutant line were plated on ½ MS10 (hard set) and were allowed to germinate. For tip curvature response, 4 day old seedlings were reoriented at 90° angle and the angle of curvature toward gravity was measured after 4, 8, 12 and 24 hours.

2.5 Measurement of Auxin Transport in Roots and Shoots

2.5.1 Acropetal Root Auxin Transport

Arabidopsis plants were germinated on ½ MS_{10} vertical plates with 5 g/L phytogel as gelling agent. 2 days after germination, the plants were transferred to new plates and the plants were tested for auxin transport.

Preparation of the auxin
½ MS_{10} is melted in a microwave and stored in the water bath at 55°C to keep it liquid.

Radioactive auxin media
½ MS_{10} with 1%(w/v) Type M agar (Sigma)
10 µM IAA
500 nM ^{3}H-IAA (GE Amersham UK) – final specific activity is 5.75 µCi/ml ≡ 212.75 MBq/ml
1% DMSO

Normally made in 2 ml batches, once mixed, the agar medium was poured onto a standard glass microscope slide and left to set. Once set the agar was sliced, using a fresh straight edged razor blade, into 2-3 mm-wide strips or blocks.

All plants were lined up with the root tips in a straight line. ^{3}H-IAA was placed onto the top of the roots at the level of just below the root-shoot junction of the seedling with the shortest root. The aim was to make sure that for every root the distance between the application site and the root tip was constant; this distance was measured and the plants were inverted and left for 1 hour per cm.

After this time the distal 5 mm at the root tip was removed and the sample transferred to 4 ml scintillation fluid (EcoScint A, National Diagnostics) and incubated for 48 hours before measuring in the scintillation counter. All data were expressed as counts per minute (CPM).

2. 5.2 Basipetal Shoot Auxin Transport

20 µl of MSMO (minimal media version of MS – Sigma) was pipetted into the bottom of 1.5 ml Eppendorf tubes. 2.5 cm of inflorescence stem segments that did not contain any branches, and which were taken from the very base of the stem, were cut and the apical (upper) end placed in the MSMO media. This was done to prevent entering air bubbles to the transport system.

20 µl of MSMO supplemented with 0.08 µCi/ml ^{3}H-IAA (approx 3.5 µM IAA) was carefully pipetted into the bottom of new tubes. The stem segments were then transferred to these new tubes with the apical end in the MSMO.

Samples were left to incubate for 18 hours before the basal 5 mm of the sample was removed and placed in 4 ml of scintillation fluid. These were then incubated for 48 hours before scintillation.

Non-inverted samples (the basal ends were placed in the medium) were included to control for non-specific transport (abbreviated to NI). Non-radioactive (NR) samples were used to detect baseline activity and contamination.

All the cutting was done with pre-marked glass slides and these were discarded after every treatment type or when liquid could be seen near the cutting section of the segment.

Razor blades were changed every 10 samples. Non-radioactive control traetments were always carried out at the end of each experimental series to detect possible cross contamination.

2.6 Immunolocalization of PIN Proteins in Roots

2.6.1 Solutions

Fixative	for 10 ml
3.7% paraformaldehyde	370 mg
50mM PIPES, pH 6.8	2 ml
5mM EGTA	0.5 ml
2mM $MgSO_4$	0.2 ml
0.4% Triton X-100	40 µl

Enzyme mixture for cell wall digestion for 50 ml

2% w/v Dricelase	
0.4 M Mannitol	3.64 g
5 mM EGTA	2.5 ml
15 mM MES, pH 5.0	97 mg

Stored in 5 ml aliquots at -20°C. Immediately before use the following solutions were added per 1 ml:

10 µl of 100 mM PMSF

1 µl of 10 mg/ ml of leupeptine

1 µl of 1 mg/ ml pepstatine A

PBS Buffer	1 L of 1x
Na_2HPO_4	570 mg
KH_2PO_4	212 mg
NaCl	8 g
Tween 20	0.1 ml
pH 7.0	

2.6.2 Method

Roots were fixed for 60 minutes in the freshly prepared fixative. Then the roots were washed 3 times for 5 minutes each in PBS buffer. Cells were treated with enzyme mixture for 10 minutes at room temperature following two washes with PBS buffer. Then roots were washed with PBS buffer containing 2% bovine serum albumin (BSA) for 30 minutes. Roots were incubated overnight in primary antibody mixture and washed with PBS buffer 3 times for 1 hour each. Roots were incubated again overnight with secondary antibody mixture (PIN antibodies were kindly supplied by Prof. Klaus Palme, University of Freiburg, Germany) and then washed 2 times (30 minutes each) with PBS buffer supplemented with 10 ng/ml DAPI and mounted on a cover-slip for microscopical examination.

2.7 Extraction and Purification of Nucleic Acids

2.7.1 Miniprep of plasmid DNA using the Wizard Plus SV Minpreps DNA purification system

Plasmid DNA from small culture volumes (1-10 ml) was isolated using the SV minipreps DNA purification system from Promega. The resulting plasmid DNA was suitable for DNA sequencing and all cloning purposes.

Method

The bacteria containing the plasmid of interest were grown overnight at 37°C with vigorous shaking in LB medium containing the appropriate antibiotic in a 15 ml test tube. 1.5 ml of overnight culture was transferred to an Eppendorf tube and the bacterial pellet was obtained by centrifugation at 10,000 rpm for 2 minutes. The supernatant was discarded and the pellet was re-suspended in 250 µl of cell re-suspension solution. 250 µl of cell lysis solution was added to each sample and tubes were inverted 4 times to mix the contents. 10 µl of alkaline protease solution was added to the tubes, inverted 4 times, and incubated at room temperature for 5 minutes. 350 µl of Neutralization Solution was added and tubes were inverted 4 times to mix the contents properly. Eppendorf tubes were centrifuged at 13,000 rpm for 10 minutes at room temperature. Minicolumns were assembled by inserting the spin column into the collection tube and clear lysate was decanted into the spin

column. 750 µl of column wash solution was added to the tubes, and centrifuged at 14, 000 x g for 1 minute. Washing was repeated with 250 µl of column wash solution and centrifuged at 14,000 x g for 2 minutes. The spin column was transferred to a 1.5 ml centrifuge tube. 100 µl of nuclease-free water was added and centrifuged at 14, 000 x g for 1 minute at room temperature. The purified DNA was stored at -20 °C until used for further analysis.

2.7.2 Midiprep of plasmid DNA using the QIAGEN® Plasmid Midi Kit

The low copy number plasmids were extracted from a large bacterial culture volume (100-200 ml) using the Qiagen Midi Prep Kit. The resulting DNA was suitable for sequencing, PCR and all other cloning purposes.

A flask of 100 ml of selective LB liquid medium was inoculated with bacteria carrying the plasmid of interest, and grown overnight with vigorous shaking at a temperature to suit the bacterial host. The culture was then transferred to sterile 50 ml Falcon centrifuge tubes, and the cells pelleted by centrifugation at 6,000 x *g* for 15 minutes at 4°C. The supernatant was discarded, and the cells re-suspended in 4 ml of buffer P1, after which 4 ml of lysis buffer P2 was added. The tube was inverted several times to mix the contents thoroughly, and then left to incubate at room temperature for 5 minutes. A further 4 ml of neutralization buffer P3 was added and mixed by inversion, prior to incubation on ice for 15 minutes. The mixture was centrifuged at 20, 000 x *g* for 30 minutes at 4°C to pellet cell debris before the plasmid-containing supernatant was removed to a clean tube, and centrifuged again for a further 15 minutes at 20,000 x *g* at 4°C.

Before the last centrifugation step was completed, a QIAGEN-tip 100 column was prepared to receive the cleared supernatant, by adding 4 ml of buffer QBT to the column and allowing it to drain by gravity flow. The supernatant was removed from the centrifuge tube promptly and applied to the column, where it was also allowed to drain though the membrane under gravity. The QIAGEN-tip 100 was then washed twice, each with 10 ml of buffer QC, before the DNA was eluted into a sterile 15 ml Falcon tube with 5 ml of buffer QF. The plasmid DNA was precipitated by mixing with 3.5 ml of isopropanol at room temperature, the suspension was transferred to Eppendorf tubes and the DNA pelleted by

centrifugation at 15, 000 x *g* at 4 °C for 30 minutes. The pellets were washed with 70 % (v/v) ethanol at room temperature, centrifuged for a further 15 minutes at 15,000 x *g* at 4°C, and the supernatant was removed. The pellets were air-dried until all visible droplets of liquid had disappeared, re-suspended in 100 µl sterile distilled water, and stored at -20 °C.

2.7.3 A Quick genomic DNA Extraction Method for PCR (Edwards *et al.*, 1991)

This method is for extraction of genomic DNA from individual mutants, using leaf tissue.

Extraction buffer: 200 mM Tris.HCl (pH 7.5), 200 mM NaCl, 25 mM EDTA, 0.5 % (w/v) SDS.
TE buffer: 10 mM Tris-Cl (pH 7.5) , 1 mM EDTA. Make from 1M stock of Tris-Cl (pH 7.5) and 500 mM stock of EDTA (pH 8.0).

Method
A small leaf or leaf disc was placed in an Eppendorf tube, frozen on dry ice or in liquid nitrogen and ground to a powder. 400 µl of extraction buffer was added and tissues were ground further for 20 sec whilst tissues were thawing. The mixture was centrifuged at 13,000 rpm for 1 minute. 300 µl of the supernatant was removed and mixed with equal volume of isopropanol. The DNA pellet was precipitated by spinning for 5 minutes at 13,000 rpm and then the pellet was air dried. Dried pellet was redissolved in 50 µl of TE. Genomic DNA obtained from this method was stored at – 20° C until further use. 0.5 – 2 µl of this DNA is sufficient for PCR amplification.

2.7.4 Extraction of DNA using Sigma GenElute™ Plant Genomic DNA Miniprep Kit

GenElute™ Plant Genomic DNA Miniprep Kit (Sigma) was used to extract pure DNA from Columbia wild type plants. Plant tissues were ground into a fine powder in liquid nitrogen using a mortar and pestle and 100 mg of the powder was transferred to a microcentrifuge tube. The sample was kept on ice for immediate use. 350 µl of Lysis solution (Part A) and 50 µl of Lysis solution (Part B) were added to the tube, mixed thoroughly by vortexing and inverting. The mixture was incubated at 65° C for 10 minutes with occasional inversion to

dissolve the precipitate. Then 130 µl of Precipitation solution was added to the mixture and sample was placed on ice for 5 minutes before centrifugation at 13,000 rpm for 5 minutes. Supernatant was carefully pipetted onto a GenElute filtration column (blue insert with 2 ml collection tube) and centrifuged at maximum speed for 1 minute. 700 µl of Binding solution was directly added to the flow through liquid and mixed by inverting. The Binding column was prepared by inserting a GenElute miniprep binding column (with a red o-ring) into a provided microcentrifuge tube. Column preparing solution (500 µl) was added to each miniprep column and centrifuged at 12,000 rpm for 30 seconds to 1 minute, flow-through was discarded. 700 µl of the mixture was carefully pipetted onto the prepared column and centrifuged at 13,000 rpm for 1 minute. Flow-through was discarded and remaining mixture was applied onto the prepared column and repeated the centrifugation as above. Collection tubes and flow-through were discarded. The Binding column was placed into a fresh 2 ml collection tube and 500 µl of diluted wash solution was added to the column. Centrifugation was carried out at 13,000 rpm for 1 minute and flow-through was discarded. Another 500 µl of wash solution was added to the column and centrifuged at maximum speed for 3 minutes to dry the column. The Binding column was transferred to a fresh 2 ml collection tube and 100 µl of pre-warmed (65°C) Elution solution was applied to the column and centrifuged at 13,000 rpm for 1 minute. The elute contains pure DNA and DNA obtained from this method was stored at –20° C until further use.

2.7.5 BAC DNA Preparation Using BAC DNA Miniprep Kit

BAC DNA Miniprep Kit (NORGEN, UK) was used for the rapid preparation of BAC (Bacterial Artificial Chromosomes). Bacterial cultures grown overnight at 37°C in LB medium were used for this procedure. Bacterial culture (1.5 ml) was transferred to a microcentrifuge tube and centrifuged for 20 seconds at 13,000 rpm to pellet the DNA. The supernatant was carefully poured off and the step was repeated with an additional 1.5 ml of bacterial culture. 200 µl of Resuspension buffer was added to the cell pellet and the cells were resuspended by gently vortexing before incubating at room temperature for 5 minutes. Lysis solution (200 µl) was added to the cell suspension and the contents mixed by gently inverting the tube. 200 µl of Neutralization solution was added and immediately mixed by inverting the tube before centrifugation at 13,000 rpm for 10 minutes. The cleared lysate was transferred to a fresh microcentrifuge tube and 2 µl of RNASe T1 was added,

mixed gently before incubating the lysate at 50° C for 30 minutes. After incubation, 60 µl of Binding solution was added to the lysate and mixed well. A spin column with a provided collection tube was assembled and the lysate was transferred into the spin column and centrifuged for 1 minute. The flow-through was discarded and the spin column was reassembled with the collection tube. 600 µl of Wash solution was added to the column and centrifuged at 13,000 rpm for 2 minutes. The flow-through was discarded and the column reassembled with a provided elution tube. 30-50 µl of Elution buffer was added to the column and centrifuged for 2 minutes at 200 rpm. An additional centrifugation was carried out at 14,000 rpm for 1 minute.

2.7.6 RNA Extraction using QIAGEN RNeasy® Plant Kit

The RNeasy kit from Qiagen was used to prepare total RNA from small amounts of tissue (50 - 100 mg). Tissues were frozen in liquid nitrogen prior to RNA extraction.

Method

The sample was ground under liquid nitrogen to fine powder in a mortar and pestle and transferred to an Eppendorf tube containing 450 µl of buffer RLT. 10 µl of β-mercaptoethanol was added per 1 ml of buffer RLT and the sampled was vortexed vigorously. The sample was transferred to the QIAshredder spin column sitting in a 2 ml collection tube and centrifuged for 2 minutes at 14,000 rpm. The supernatant was carefully transferred into a new centrifuge tube. 0.5 volumes (225 µl) of 100 % ethanol was added to the supernatant and mixed immediately by pipetting. The sample was then applied to a pink binding RNeasy mini column and centrifuged for 15 seconds at 10, 000 rpm. Flow-through was discarded. 700 µl of buffer RWI was added to the column and centrifuged at 10, 000 rpm for 15 seconds. The column was then transferred to a new tube, 500 µl of buffer RPE was added onto the column and centrifuged for 15 second at 10,000 rpm. The wash was repeated twice. 30-50 µl of RNase-free water was added for elution and centrifuged for 1 minute at 14,000 rpm. The extracted RNA was stored at -20° C for short term storage and at -80° C for long term storage.

2.7. 7 Quantification of RNA

RNA in solution was quantified using a Thermo Scientific NanoDrop™ 1000 Spectrophotometer (Thermo Fisher Scientific, USA). A 1 µl sample was pipetted onto the end of a fiber optic cable (the receiving fiber). A second fiber optic cable (the source fiber) is then brought into contact with the liquid sample causing the liquid to bridge the gap between the fiber optic ends. The gap is controlled to both 1 mm and 0.2 mm paths. A pulsed xenon flash lamp provides the light source and a spectrometer utilizing a linear CCD array is used to analyze the light after passing through the sample. The instrument is controlled by PC based software, and the data is logged in an archive file on the PC.

2.7.8 DNase treatment of RNA

After Sanyal et al., (1997)
Total RNA was extracted from 7 day old seedlings of all the plant lines required using the QIAGEN, RNeasy Plant Mini Kit. 2 µg of RNA from each sample was DNase treated in 20 µl reactions to give a 100 ng/ µl of each RNA sample. The required volumes of each RNA sample, depending upon their concentrations, were mixed with 2 µl of 10 x DNase buffer, 1 µl of RQ1-DNase (RNase free, Promega Ltd.) and the volume was made up to 20 µl. The reaction was incubated at 37°C for 30 minutes. DNase was inactivated by adding 2 µl of RQ1 DNase stop solution and the reactions were incubated for further 10 minutes at 65 °C.

2.7.9 cDNA synthesis

Reverse transcription reaction was used to synthesise or copy the RNA into its complementary DNA (cDNA) sequence. The cDNA obtained can serve as a template for amplification by PCR. The RETROscript™ RT-PCR kit from Ambion was used to synthesise cDNA from the RNA.

Method
1 µg of total RNA (extracted using Qiagen RNAeasy kit) was mixed with 2 µl of Oligo (dT), the mixture was spun briefly and heated at 70-85° C for 3 minutes. Generally 85°C is more appropriate for targets that are GC-rich or that have a predicted high degree of secondary

structure. The tubes are then removed to ice, spun briefly, and replaced on ice. The remaining reverse transcription components are then added to the mixture: 2 µl of 10 X RT buffers, 4 µl of dNTPs mix, 1 µl of RNase inhibitor, 1 µl reverse transcriptase, and nuclease free water, to make up the volume of the reaction up to 20 µl. All the components are mixed gently, spun briefly, and incubated at 42-44°C for an hour (slowly elevating the temperature to 55°C). The reaction is further incubated at 92°C for 10 minutes to inactivate the Reverse Transcriptase. The cDNA obtained was stored at -20°C until required for PCR.

2.7.10 Purification of DNA from Agarose Gels Using *High Pure* PCR Product Purification Kit

The *High Pure* PCR product purification kit was obtained from Roche Applied Science (Mannheim, Germany) and was used to purify DNA fragments from agarose gels following restriction enzyme digestion or PCR. The following procedure was used for the purification of DNA from a 100 mg agarose gel slice.

The DNA of interest was isolated using agarose gel electrophoresis. The band of interest was cut from the gel using an ethanol-cleaned scalpel or razor blade. The excised gel slice was placed in a sterile 1.5 ml microcentrifuge tube. The weight of the gel slice was determined by first pre-weighing the tube and then reweighing the tube with the excised gel slice. 300 µl of Binding Buffer was added for every 100 mg of agarose gel slice to the microcentrifuge tube. The agarose slice was dissolved by vortexing for 15-30 seconds, incubating the suspension for 10 minutes at 56°C, and further voxtexing the tube for 2-3 minutes. After the agarose gel slice was completely dissolved, 150 µl isopropanol was added for every 100 mg gel slice and the tube was voxtexed thoroughly. *High Pure* filter tubes were inserted into the collection tube. The entire contents of the microcentrifuge tube were pipetted into the filter tube. The tubes were centrifuged at 13,000 rpm for 30-60 seconds. The flowthrough was discarded and 500 µl of wash buffer was added to the filter tube, and centrifuged for 1 minute at 13,000 rpm. The wash was repeated with 200 µl of washing buffer, and centrifuged again at maximum speed for 1 minute. The filter tube was transferred into a new microcentrifuge tube, and 50-100 µl of elution buffer was added to it,

and the tube was centrifuged at 13,000 rpm to pellet the DNA. The eluted DNA was stored at -20° C until further analysed.

2.8 Agarose Gel Electrophoresis

Solutions

1x TAE buffer: 40 mM Tris-acetate, pH 8.0, 1 mM EDTA

10x Loading buffer: 0.25% (w/v) bromophenol blue, 0.25% (w/v) xylene cyanol FF, 0.25% (w/v) acridine orange, 25% (w/v) Ficoll (type 400) in water.

DNA markers: Hyperladder I and Hyperladder II (Bioline) were used according to the manufacturer's instructions.

Method

Gels of 0.7% to 2% (w/v) agarose were prepared in 1x TAE buffer depending on the size of the DNA fragments to be separated. Gels were melted in a microwave, allowed to cool to approximately 50°C before 0.1 µg/ml of ethidium bromide was added and mixed. The molten agarose was immediately poured into a gel tray and allowed to solidify at room temperature for 20-40 minutes. DNA samples were mixed with 1/10 volume of 10x loading buffer and loaded into gel wells by pipetting. DNA markers were mixed with 1/10 volume of 10x loading buffer and loaded into gel wells by pipetting. DNA markers were run alongside sample DNA to enable approximate sizing of fragments. Electrophoresis was performed at 5-10 V/cm in 1x TAE buffer. DNA was visualised on a UV transilluminator (Gel Doc 1000 system with Molecular Analyst version 2.1.1 software, Biorad) and photographed.

2.9 Rubidium Chloride Method for Making Competent *E.coli* Cells

The following method of making chemically competent *E.coli* for transformation is as described by Ausubel *et al.* (1994). Buffer TfbI and TfbII were made up as detailed below, and filter sterilised using 0.2 µm Minisart® filters (Sartorius,Germany) prior to use.

Buffer TfbI

30 mM potassium acetate

100 mM rubidium chloride

10 mM calcium chloride
50 mM manganese chloride
15 % v/v glycerol
pH adjusted to 5.8 (with dilute acetic acid)

Buffer TfbII
10 mM MOPS
75 mM calcium chloride
10 Mm rubidium chloride
15 % v/v glycerol
pH adjusted to 6.5 (NaOH)

To prepare competent cells, a single colony from a fresh LB plate of *E.coli* strain DH5α was used to inoculate 100 ml of sterile LB broth, and grown overnight at 37°C with vigorous shaking to provide aeration. The culture was transferred to 50 ml Falcon centrifuge tubes, and chilled on ice for 15 minutes before centrifuge at 4000 x *g* for 5 minutes at 4°C. The supernatant was discarded, and the cells were resuspended gently in 40 ml of buffer TfbI before resting on ice for 15 minutes. The supernatant was then discarded and the cells re-suspended in 4 ml of buffer TfbII. The cell suspension was rested on ice for 15 minutes before 250 µl aliquots were flash frozen in liquid nitrogen and stored at -80°C until required.

2.10 DNA Cloning into Plasmid Vectors

2.10.1 Digestion of Vector and Insert DNA with Restriction Endonucleases

Restriction enzymes and 10x reaction buffer were obtained from Promega Ltd., and reactions were carried out according to the manufacturer's instructions. Typically, a digestion reaction contained 1-5 µg of DNA, 3 µl of 10x reaction buffer, 1 µl restriction enzymes (10 units/µl) and made up to 30 µl with sterile distilled water. Reactions were left at the required temperature for 1-4 hours (up to an overnight). Following digestion, reaction vector DNA was phosphorylated prior to ligation. Insert DNA was purified by using the *High Pure* PCR clean up kit (Roche labs).

2.10.2 De-phosphorylation of Vector DNA

Following restriction digestion, vector DNA was treated with shrimp alkaline phosphatase (Sigma) to dephosphorylate the 5' ends prior to ligation to prevent re-ligation of vector ends. This was only performed if the vector DNA had been treated with just one restriction enzyme. After digestion, 1 unit of shrimp alkaline phosphatase was added to 1-5 µg of vector DNA with the relevant restriction enzyme in a total volume of 30 µl. The reaction was incubated at 37°C for 30 minutes followed by 10 minutes at 70° C to inactivate the phosphatase.

2.10.3 T- tailing of Vector DNA

After Finney *et al*. (2001). T-tailing of the vector involves the addition of a thymidine nucleotide to the 3' end of DNA stand following vector linearization. This facilitates the cloning of PCR products since *Taq* DNA polymerase adds a 5' adenosine nucleotide. After, cutting the DNA with the restriction enzymes and purifying the DNA fragment from agarose gel. The DNA (10 µl) was mixed with 10 µl of Mg^{++}-free 10x PCR buffer (supplied with *Taq* DNA polymerase from Bioline), 3 µl of 50 mM $MgCl_2$, 20 µl of 5 mM dTTP, 1 µl of *Taq* DNA polymerase (5 units) and made up to 100 µl with sterile distilled water. The reaction was incubated at 75°C for 2 hours and was used in ligation reaction without further purification.

2.10.4 Ligation of DNA Fragments

The enzyme T4 DNA ligase catalyses the formation of a covalent phosphodiester bond between a 5'-phosphoryl group and adjacent 3'- hydroxyl group. In a typical ligation reaction 50-100 ng of vector DNA (cut with suitable restriction enzymes) was mixed with an equal molar amount of insert DNA. To this was added 2 µl of 5x ligation buffer and 1 µl (3 units) of T4 DNA ligase and the volume was made up to 10 µl with sterile distilled water. The contents were mixed and incubated at 4°C overnight before transformation of competent *E.coli* cells.

2.10.5 TOPO Cloning using Invitrogen TOPOTA Cloning® Kit

TOPOTA cloning® was used as a highly efficient, 5 minute, one- step cloning strategy for direct insertion of PCR products into plasmid vector.

2.10.5.1 Ligation of PCR Fragments in pCR®2.1-TOPO

DNA fragments generated by PCR were generally cloned into the pCR® 2.1-TOPO vector from Invitrogen. The vector is supplied linearized with 3' thymidine overhangs for efficient ligation of PCR products. It also utilizes the ligation activity of the topoisomerase enzyme resulting in fast, high efficiency ligation. To 1 µl of the pCR® 2.1-TOPO vector was added 1-2 µl of fresh, unpurified PCR product and the reaction mix made up to 5 µl. The reactants were mixed and left at room temperature for 5 minutes to allow ligation to proceed. The tube was then placed on ice until ready for transformation into TOP10 competent cells (Invitrogen).

2.10.5.2 Transformation of TOP10 One shot ^{TM} Competent Cells

TOP10 One shot™ competent cells were supplied with the TOPOTA Cloning® kit (Invitrogen) along with the ligation ready pCR® 2.1-TOPO vector. Following the ligation of PCR products a tube of TOP10 One shot™ competent cells was defrosted on ice. The TOPO cloning reaction was set up by mixing 2 µl of ligation reaction with 1 µl of salt solution and 3 µl of sterile water in an Eppendorf tube. The reaction mix was incubated on ice for 25-30 minutes before heat shocking by incubation at 42° C for 30 seconds. The tube was then returned to ice for 2 minutes, followed by addition of 250 µl of SOC medium (Section 2.1.6.1). The tube was then incubated for an hour at 37°C with gentle shaking. 50-100 µl of the transformation mix was spread onto LB plates containing 50 µg/ml kanamycin sulphate and 40 µg/ml of X-Gal. Recombinants appear as white colonies following overnight growth at 37°C.

2.10.6 Gateway Cloning using Invitrogen Gateway® Technology

Gateway® Technology is a universal cloning method based on the site-specific recombination properties of bacteriophage lamda (Landy, 1989). It provides a rapid and highly efficient way to move DNA sequences into multiple vector system for function analysis and protein expression (Harley *et al*., 2000). Gateway® Technology provides the following advantages:

- Enables rapid and highly efficient transfer of DNA sequences into multiple vector systems for protein expression and functional analysis while maintaining orientation and reading frame.
- Permits use and expression from multiple types of DNA sequences.
- Easily accommodates the transfer of a large number of DNA sequences into multiple destination vectors.

Lamda recombination is catalyzed by a mixture of enzymes that bind to specific sequences (*att* sites), bring together target sites, cleave them and covalently attach the DNA. Recombination occurs following two pairs of strand exchanges and ligation of the DNAs in a novel form. The recombination proteins involved in the reaction differ depending upon whether lamda utilizes the lytic or lysogenic pathway.

The lysogenic pathway (BP reaction) is catalysed by the bacteriophage λ Integrase (Int) and *E.coli* Integration Host Factor (IHF) proteins (BP Clonase^{TM} enzyme mix) while the lytic pathway (LR reaction) is catalysed by the bacteriophage λ Int and Excisionase (Xis) proteins, and the *E.coli* Integration Host Factor (IHF) protein (LR Clonase^{TM} enzyme mix).

2.10.6.1 Designing *attB* PCR Primers

The *attB* sites were introduced into the PCR product to make it suitable substrate in a BP reaction with a donor vector. The forward primer must contain following structure, to enable efficient Gateway® cloning:

- Four guanine (G) residues at the 5’ end followed by
- The 25 bp *attB* site followed by
- At least 18-25 bp of template or gene-specific sequences

The *attB1* site ends with a thymine (T). In order to fuse the PCR product in frame with an N-terminal tag, the primer must include two additional nucleotides to maintain the proper reading frame with the *attB1* region. These two nucleotides cannot be AA, AG, or GA, because these additions would create translation termination codon.

In order to fuse the PCR product in frame with a C-terminal tag, the primers must include one additional nucleotide to maintain the proper reading frame with the *aatB2* region and any in-frame stop codons between the *attB2* site and the gene of interest must be removed.

2.10.6.2 Producing *attB*-PCR products

The *attB*-PCR products were prepared by amplification of *VAMP714* sequence from TOPO 2.1 vector containing the cloned *VAMP714* sequence using Gateway 360 forward and reverse primers (primer sequences are in Annex 2).

Finnzymes' Phusion ^{TM} High-Fidelity DNA polymerase from New England BioLabs was used to perform a PCR reaction as follows:

Reaction Mixture (50 µl reaction):	
5 x Phusion HF Buffer	10 µl
10 mM dNTPs	1 µl
Forward primer (10 pM/µl)	1.5 µl
Reverse primer (10 pM/µl)	1.5 µl
Phusion DNA Polymerase	0.5 µl
dH_2O	34.5 µl
Template DNA	1 µl

Due to the novel nature of Phusion DNA polymerase, optimal reaction conditions differ from standard enzymes. Phusion DNA polymerase tends to work better at elevated denaturation and annealing temparatures due to a higher salt concentration in its buffer.

Cycling:

Intial denaturation	98°C	30 seconds	1 cycle
Denaturation	98°C	10 seconds	35 cycles
Annealing	60°C	30 seconds	
Extension	72°C	90 seconds	
Final extension	72°C	10 minutes	1 cycle
Hold	4°C	-	

5 µl of PCR product was removed from each tube and was quantified using agarose gel electrophoresis.

The BP recombination facilitates transfer of a gene of interest in an *att*B-PCR product to an *att*P-containing donor vector to create an entry clone. Once the entry clone was created, the gene of interest was shuttled into a large selection of destination vector using the LR recombination reaction.

The entry clone was generated by:

- Performing a BP recombination reaction using the appropriate *att*B- and *att*P-containing substrates
- Transformation of the BP reaction mixture into a suitable *E. coli* host (DH5α) and selection of the entry clone.

Procedure:

- The following components were added to a 1.5 ml microcentrifuge tube and mixed together at room temperature:

attB-PCR product (100 ng)	5 µl
Donor vector (pDONR™207, 150 ng/µl)	1 µl
TE buffer, pH 8.0	2 µl
BP Clonase™II enzyme mix	2 µl

The reaction was incubated at 25°C for an hour. 1 µl of Proteinase K solution was added to each tube to terminate the reaction, vortexed and incubated at 37°C for 10 minutes. The reaction mixture is then transformed into *E. coli* (DH5α) competent cells.

2.10.6.3 Transformation of DH5α Competent Cells

The DH5α™ *E. coli* cells were made competent using the Rubidium Chloride Method (see Section 2.7).

Method

5 µl of the BP reaction was added to 250 µl of DH5α competent cells and mixed gently. The competent cells were then incubated on ice for 30 minutes, followed by heat-shock at 42° C for 30 seconds without shaking. The cells were immediately transferred to ice after heat-shock and incubated for 10 minutes. 1 ml of S.O.C medium was added to the cells at room temperature and tubes were then incubated at 37°C for 1 hour with constant shaking (200 rpm). The cells were spun in a bench top centrifuge for 1 minute at 12,000 rpm and 1 ml of the supernatant was removed. The cell pellet was then resuspended in the remaining supernatant. 50 µl and 100 µl of each transformation mix was then spread on selective media plates and incubated overnight at 37°C.

Sequencing Entry Clones

pDNOR207 Forward and Reverse sequencing primers were used to check the entry clones derived from BP recombination with pDONR 207.

2.10.6.4 The LR Recombination Reaction

After generating the entry clone, the LR reaction was performed to transfer the gene of interest into an *attR*-containing destination vector to create an *attB*-containing expression clone.

An expression clone was generated by performing an LR recombination reaction using the appropriate *attL*- and *attR*-containing substrates, transforming the reaction mixture into a suitable *E.coli* host and selection for expression clone using suitable antibiotic selection.

Procedure:

The following components were added to a 1.5 ml microcentrifuge tube and mixed together at room temperature:

Entry clone (100 ng)	5 µl
Destination vector (150 ng/ µl)	1 µl
TE buffer, pH 8.0	1 µl
LR Clonase™ II enzyme mix	2 µl

LR Clonase™ II enzyme mix was thawed on ice for 2 minutes and vortexed briefly before being added to the reaction mix. The reaction was incubated at 25°C for 1 hour and 1 µl of Proteinase K solution was added to the reaction mixture to terminate the reaction with 10 minutes incubation at 37°C.

5 µl of LR reaction mixture was transformed in 250 µl of DH5α competent cells using the protocol described above, and 100 µl of each transformation mix was then spread on selective media plates and incubated overnight at 37°C.

2.11 DNA Sequencing

The DNA sequencing was performed by the DNA sequencing lab at Durham University, using an ABI 373 DNA sequencer and dye terminator labelling reaction (Perkin Elmer Applied Biosystems). Samples were normally supplied in plasmid form prepared using the Wizard™ SV minipreps DNA purification system from Promega at a concentration of 0.2 µg/µl. Primers for sequencing were supplied at a concentration of 3.2 pmol/ µl.

2.12 Mobilisation of Plasmids into *Agrobacterium* by Triparental Mating

Preparation

Two days before the triparental mating, 5 ml of LB broth was set up for C58C3 culture containing 100 µg/ml streptomycin and 25 µg/ml nalidixic acid as selection agents. The cultures were left to grow for 48 hours at 30°C with constant shaking. The day before the mating, overnight cultures of pRK2013 and of the *E.coli* strain containing the construct to

be transformed into *Arabidopsis* were set up to grow at 37°C in 5 ml LB broth plus 100 mg/ml kanamycin sulphate, with constant shaking.

Method

For triparental mating, 100 µl aliquots from each 5 ml culture were mixed together in a sterile 1.5 ml Eppendorf tube. The remaining liquid cultures were stored at 4°C for future use. The cells were then spun down in a microcentrifuge at 12, 000 rpm for 5 minutes. Supernatants were discarded and the pellets were resuspended in 10 µl of 10 mM $MgSO_4$. The 10 µl droplets were placed onto LB agar plates and incubated overnight at 28-30°C. During this time mobilisation of the plasmids takes place. A patch of the bacterial droplets was streaked on an LB plate containing 50 µg/ml kanamycin sulphate, 25 µg/ml of nalidixic acid and 100 µg/ml of streptomycin for C58C3 selection. The plates were then incubated at 28-30°C overnight. The parental strains were streaked on duplicate plates, as a control.

2.13 *Arabidopsis* Transformation using the Floral Dipping Method

After Clough and Bent (1998).

Solutions and media

5% sucrose (w/v) and 0.05% Silwett L-77 (v/v) (Lehle Seeds, Texas, USA), which acts as a detergent

½ MS10 plates supplemented with antibiotics for selection.

Preparation

Arabidopsis thaliana var. Col was grown in soil in 3.5 inch pots (10-15 plants per pot) with a plastic mesh placed over the soil. Plants were grown for 3-4 weeks until they are 10-15 cm tall and displaying a number of immature, unopened buds. 2-3 days prior to dipping, open flowers and any young siliques were removed.

The *Agrobacterium tumefaciens* strain C58C3 was used for all binary vector constructs. The agrobacteria were grown for 48 hours at 30°C in 200 ml LB supplemented with 25 mg/l nalidixic acid, 100 mg/l streptomycin and 50 mg/l kanamycin sulphate. The culture was pelleted by centrifugation and resuspended in 1 litre of freshly made solution of 5%

sucrose. Once resuspended, Silwett L-77 was added to a final concentration of 0.05% (v/v).

Method

Plants were then fully dipped into the solution and gently agitated for 10-15 seconds before removal. Dipped plants were placed in transparent bags to maintain humidity and placed back in the GM-approved greenhouse in a shaded place overnight. Occasionally a second dipping was carried out 6 days after the first. Following removal from the bags plants were allowed to set seeds and dry out in the greenhouse. Seeds were collected from individual pots of plants and allowed to dry for 2 weeks at 25°C. Seeds were then surface sterilized and germinated on ½ MS10 with antibiotic selection. Antibiotic-resistant plants were transferred to soil and seeds from these plants were tested for segregation of the resistant trait on selective plates.

2.14 Selection of Plants

Transformed plants were selected using ½ MS10 with kanamycin (50 µg/ml for p*VAMP714*::GUS), Basta (15µg/ml for p35S:*VAMP714*:: GFP) and hygromycin (50 µg/ml for pVAMP714::CFP).

2.15 Gene Expression Analysis by Polymerase Chain Reaction (PCR)

2.15.1 Standard PCR

For standard PCR reactions, *Taq* DNA polymerase was obtained from Bioline and was supplied with Mg++-free 10x reaction buffer and 50 mM $MgCl_2$ stock solutions. Oligodeoxynucleotide primers were obtained from MWG-Biotech as lyophilised pellets and resuspended to the desired concentration in sterile distilled water. The template for amplification was genomic DNA, a cDNA or a bacterial colony. A standard PCR reaction contained 10-100 ng of DNA sample, 0.2 µM of each primer, 1.5 µl 50 mM $MgCl_2$ (1.5 mM final concentration), 5 µl Mg++-free 10x reaction buffer, 1 mM dNTP mix and 2.5 units of *Taq* DNA polymerase made up to 50 µl with sterile distilled water in a 0.5 ml Eppendorf tube. Reaction tubes were then placed in a DNA Thermal Cycler (Perkin Elmer, Foster

City, CA, USA). A typical amplification was carried out using the following conditions: denaturation at 94ºC for 1 minute, 1 minute annealing at 55ºC and 1 minute extension at 72ºC. A final extension of 10 minutes at 72ºC was performed after the amplification steps. 10-20 µl of the reaction was run on a 0.7-2% (w/v) agarose gel to check the products.

2.15.2 PCR using Expand ^{TM} KOD HOT Start PCR System

The Expand ^{TM} KOD HOT Start PCR system consists of a mix of both *Taq* and *Pwo* DNA polymerase. Due to the proofreading activity of *Pwo* DNA polymerase, the Expand ^{TM} KOD HOT PCR system results in a 3-fold increase in the fidelity of DNA synthesis (8.5 x 10^{-6} error rate). This system was therefore used when a high degree of sequence fidelity was required. A typical reaction contains: 10-100 ng of DNA sample, 0.2 µM of each primer, 6 µl of 25mM $MgCl_2$ (3.0 mM final concentration), 5 µl of 10x reaction buffer and 10 mM dNTP mix, 2.5 units of enzyme mix, and the volume is made up to 50 µl with sterile distilled water in a 0.5 ml Eppendorf tube. Reactions were then placed in a pre-heated block at 90°C in a Thermal Cycler. A typical amplification was carried out using the following conditions: denaturation at 94°C for 2 minutes; followed by 30 cycles of denaturation at 94°C for 30 seconds, primer annealing at 60°C for 30 seconds, 2 minute of extension at 72°C and final extension step of 10 minutes at 72°C. If the expected product was greater than 3 kb in length then the extension step was carried out at 68°C instead of 72 °C with a general rule of 1 minute extension per kb of target. When the reaction was complete, 5-10 µl of reaction mix was analysed on a 0.7-1% agarose gel.

2.15.3 PCR using Phusion® High-Fidelity DNA Polymerase

The Finnzymes Phusion® High-Fidelity DNA Polymerase (New England BioLabs) was used all PCR amplifications in GATEWAY cloning. The error rate of Phusion DNA Polymerase in Phusion HF buffer is determined to be 4.4 x 10^{-7} which is approximately 50-fold lower than that of *Thermus aquaticus* DNA polymerase. A 50 µl reaction contains: 10-100 ng of DNA sample, 0.5 µM of each primer, 10 µl of 5 x reaction buffer, 1 µl of 10 mM dNTPS, 0.5 µl of Phusion DNA Polymerase and 34.5 µl of water. Due to the high salt concentration in the reaction buffer, Phusion DNA Polymerase tends to work better at elevated denaturation and annealing temperatures.

The following cycling conditions were used to amplify the fragments: initial denaturation at 98°C for 30 seconds, denaturation at 98°C for 10 seconds, annealing at 60°C for 30 seconds, Extension at 72°C for 90 seconds and final extension at 72°C for 10 minutes.

2.15.4 Semi-quantitative Reverse Transcription-mediated Polymerase Chain Reaction (RT-PCR)

Semi-quantitative RT-PCR allows a fairly accurate determination of the relative abundance of specific transcripts within either the same or different cDNA populations. It was important to have a baseline against which the results were normalized. This was done by keeping the amount of RNA in the cDNA synthesis reaction the same (i.e. normalised per mg RNA), using the same level of a specific actin transcript in each cDNA population as a baseline (assuming that this will remain unchanged in the different samples) and by extracting the RNA from same amount of starting material (both in terms of age and weight). The results from the semi-quantitative PCR were confirmed using quantitative Realtime PCR.

Method

The total RNA from each plant was extracted using the QIAGEN RNeasy Kit. The integrity of the RNA was checked by running an agarose gel and was quantified using a NanoDrop spectrophotometer. Equal amounts of RNA from each sample (5 mg) were used to synthesize cDNA. The cDNA synthesis was done using the Ambion Retroscript Kit and the cDNA was diluted to 1:2 to produce a working stock. The efficiency of the primers was checked using a standard PCR reaction. The primers were optimised for $MgCl_2$ concentration and PCR product abundance. Keeping all the parameters the same as the optimisation PCR reaction, the abundance of product produced at defined time points was determined by running the products on a 4% agarose gel. Six time points of 10, 15, 20, 25, 30, 35 and 40 cycles were used. A cocktail was made with all the components of PCR without cDNA in dH_2O. The tubes were labelled with the name of the gene, if more than one gene was used, and the cycle number. The composition of the cocktail for one reaction used was:

cDNA	0.5 µl
10x PCR buffer	2 µl
dNTPs (10 mM)	0.5 µl

$MgCl_2$ (50 mM)	0.5 µl
Taq DNA polymerase	0.1 µl
Forward primer	0.5 µl
Reverse primer	0.5 µl
dH_2O	11.4 µl

The Eppendorf tubes were labelled with gene name and cycle number, and spun briefly in a microcentrifuge. The PCR reaction was performed using the same parameters as optimisation reactions which were: 94°C for 4 minutes, 94°C for 1 minute, 56°C for 1 minute, 72°C for 30 seconds , and 72°C for 10 minutes. The first set of tubes was taken out at the end of 10 cycles, then at the end of 15 cycles and so on until 40 cycles had been completed.

The tubes were removed and put on ice to stop the reaction, stored at 4°C if required and loaded on a 4% agarose electrophoresis gel to quantify the product. Once the optimum number of cycles was decided for an exponential amplification of product, those time points were used to compare the transcript levels of different in a particular line. The same sets of primers were used for doing the semi-quantitative PCR and Real-time PCR. The primers used in all experiments are listed in Annex 2.

2.15.5 Access RT-PCR

The Access RT-PCR System (Promega, UK) is designed for the reverse transcription (RT) and polymerase chain reaction (PCR) amplification of a specific target RNA. This one-tube, two-enzyme system provides sensitive, quick, and reproducible analysis of even rare RNAs. The system uses AMV Reverse Transcriptase (AMV RT) first strand DNA synthesis and the thermostable *Tfl* DNA polymerase from *Thermus flavus* for second strand cDNA synthesis and DNA amplification. The Access RT-PCR System includes an optimized single-buffer system that permits extremely sensitive detection of RNA transcripts without a requirement for buffer additions between the reverse transcription and PCR amplification steps. This simplifies the procedure and reduces the potential for contaminating the samples. In addition, the improved performance of AMV Reverse Transcriptase at elevated temperatures (45°C) in the AMV/*Tfl* 5x Reaction Buffer minimizes problems encountered

with secondary structures in RNA which could prevent full sequence amplification. Reactions were set up as indicated below:

1. The reagents were combined as indicated in below in a 0.5ml reaction tube on ice.

Reagents	Volume	Final Concentration
Nuclease-Free Water (to a final volume of 50 µl)	x µl	
AMV/Tfl 5x Reaction Buffer	10 µl	1x
dNTP Mix (10 mM each dNTP)	1 µl	0.2 mM
Downstream primer	50 pmol	1 µM
Upstream primer	50 pmol	1 µM
25 mM MgSO4	2 µl	1 mM

2. Reagents were mixed by pipetting and the remaining components were added.

AMV Reverse Transcriptase (5u/µl)	1 µl	0.1 u/µl
Tfl DNA Polymerase (5u/µl)	1 µl	0.1 u/µl

3. Reagnets were then gently vortexed and the reactions were initiated by adding:

RNA template	5 µl

First Strand cDNA Synthesis

The following PCR cycling profiles were used:

1 cycle 45°C for 45 minutes reverse transcription

1 cycle 94°C for 2 minutes AMV RT inactivation and RNA/cDNA/primer denaturation

Second Strand Synthesis and PCR Amplification

40 cycles 94°C for 30 seconds denaturation

60°C for 1 minute annealing

68°C for 2 minutes extension

1 cycle (optional) 68°C for 7 minutes final extension

1 cycle 4°C soak

5µl of the reaction products were analyzed by agarose gel electrophoresis.

2.15.6 Real-time PCR

2.15.6.1 Real-time Reaction Mix

A cocktail of following components was made in 20 µl reaction mixes. The cDNA synthesised from the total RNA was diluted in a 1:4 ratio with sterile nuclease-free water and was used as a template for the real-time reaction:

Syber green	10 µl
Forward primer (10 pmol/µl)	0.25 µl
Reverse primer (10 pmol/µl)	0.25 µl
Sterile dH_2O	9 µl
Total	19.5 µl

0.5 µl of template was added and mixed with the rest of the reaction mix in flat topped real-time PCR tubes, and spun briefly. Samples were then run in the RotorGene using the following parameters:

2.15.6.2 Cycling Parameters

A typical profile of Syber Green run used in this experiment was as follows:
Denaturing: 95°C for 4 minutes
Cycling: (40 cycles)
95°C for 20 seconds
55°C for 20 seconds (annealing temperature)
72°C for 20 seconds

Melt:
55°C-99°C, hold 30 seconds on the 1st step, and 5 seconds on subsequent steps. The data from the run were acquired at the annealing temperature using the multi channel, emission at 470 nm and detection at 510 nm.

2.15.6.3 Analysis of Quantitative PCR Data

There are two main ways of analysing the quantitative data, absolute quantification and relative quantification, and either can be used according to the application and the aim of the analysis. In this project, relative quantitation method was used to analyse the data.

2.15.6.3.1 Relative Quantification

The term relative quantitation is used when two or more genes are compared to each other with the result being a ratio. No absolute numbers are detected. An endogenous or a housekeeping gene is normally compared to the gene of interest. Comparative quantification software of the Rotorgene was used to analyse the data in this experiment using *ACTIN2* as a housekeeping gene.

The auxin regulation and tissue-specific gene regulation of four different *VAMP* genes (i.e *VAMP714*, *VAMP713*, *VAMP712* and *VAMP711)* were analysed using the comparative quantification method. Once the primers were optimised using standard PCR and all the parameters of a real-time were optimised, the real-time reaction for each gene was carried out in triplicate. After the completion of the run, the concentration of each reaction sample was calculated by the software, which was then normalised using a 'no template' control. The amplification value for each sample must be above 1 for the amplification to be considered real. These concentrations (in triplicates) for each sample (the mean of the triplicates) were calculated using the Comparative quantification software of the Rotorgene and the values were plotted in a graphical format.

2.16 Transient Expression of VAMP714:GFP

Transient gene expression in onion epidermal cells was carried out by particle (microprojectile) bombardment (Klein *et al*., 1992), to determine the subcellular localization of VAMP714:GFP fusion protein.

2.16.1 Binding DNA to Gold Particles

Onion tissues were used because they lack chlorophyll, allowing clear visualization of GFP. 1 cm sections of gold-coat tubing were covered with DNA bound to the gold particles to function as cartridges for the Helios™Gene gun.

Reagents required:

Fresh 100 % ethanol

PVP (Polyvinylpyrrolidone) 360,000 MW (hydrophilic polymer)

Fresh 0.05 M Spermidine free-base NOT complexed with HCl

1 M $CaCl_2$

Gold particles 1.0 micron (cat no. 1652262)

Plasmid -1 µg/µl concentration, buffered in 10 mM Tris, pH-8.0

Preparation:

A stock solution of 20 mg/ml PVP in 100% ethanol was prepared and stored in a screw-cap tube by sealing the lid with Parafilm. From this stock solution a working stock of 0.05 mg/ml of PVP in 100 % ethanol was prepared.

25 mg of Gold particles were weighed in a 1.5 ml tube.

Method:

500 µl of freshly made spermidine was added to 25 mg gold particles and the gold suspension was vortexed for few seconds. 500 µl of plasmid DNA (1 µg/ µl) was added to the mixture of spermidine and gold particles. In the case of adding multiple plasmids, the plasmids were mixed together before adding to the gold suspension to ensure even coating. The final concentration of the plasmid DNA was maintained at 1 µg/ µl to avoid clumping of particles. The gold suspension together with the plasmid was vortexed for 5 seconds. While vortexing, 500 µl of 1 M $CaCl_2$ was added drop-by-drop to this gold suspension. The mixture was allowed to precipitate at room temperature for 10 minutes and was spun at 5,000 rpm for 15 seconds to remove the supernatant. The pellet was washed twice with 1 ml of 100% ethanol and centrifuged for 5 seconds at 5, 000 rpm between each wash. The pellet was finally resuspended in 3 ml of 0.05 mg/ml PVP and was stored at -20°C until used in a screw-cap tube.

2.16.2 Loading Suspension onto the Plastic Tubing

The tubing prep station (from Bio Rad™) was attached to the nitrogen cylinder using the luer barb fitting on the machine. A 65 cm-long section of the plastic tubing was inserted from the right hand side of the machine into the O-ring at the other end of the cylinder. The ends were trimmed using the Bio Rad™tubing cutter.

The plastic tubing was dried by blowing nitrogen through the tube for 15 minutes. The valve on the top of the nitrogen cylinder was turned anti-clockwise to feed into the regulator. The regulator was turned clockwise until the left-hand gauge registers 2 psi of pressure. The output valve of the tubing prep station was turned anti-clockwise to allow the nitrogen to pass into the tube. 0. -0.4 litres per minute of nitrogen was allowed to flow in to the tubing prep station. After 15 minutes the nitrogen was disengaged by closing both the regulator and the output valve. The plastic tubing was removed from the tubing prep station and one end of the tubing was attached to a syringe.

The gold suspension was vortexed and the free end of the tubing was dipped into the suspension and it was sucked slowly using the syringe, to avoid any bubble formation. The plastic tubing containing the gold suspension is immediately replaced on the tubing prep station and the gold left to settle at the bottom of the tubing for 5 minutes. Once the gold settled at the bottom of the tubing, the ethanol was removed from the tubing at the rate of 1.5-3 cm per second. It takes 30 to 45 seconds to remove all the ethanol from the tubing.

The tubing prep station switch was briefly turned to position II to rotate the tube 180°. The syringe was then detached from the tubing and the switch was tuned to position I. The tube was left to rotate for 30 seconds to allow the gold to smear evenly around the tube. The nitrogen flow was turned on and maintained at 0.35 to 0.4 lites per minute to dry the tube for 5 minutes.

After 5 minutes the rotating tube was stopped and the nitrogen flow was shut down. The tubing was removed from the tubing prep station and the uncoated section of the tubing was chopped using the tubing cutter. 1 cm sections of gold coated tubing were made using the tubing cutter and were used as bullets for the Helios™ Genegun.

2.16.3 Bombarding Gold Particles on Onion Peel Cell using Helios™ Genegun

The onion peel cells were prepared by taking the onion tissues with an intact inner transparent layer. The gold-coated bullets were then inserted into a cartridge holder, leaving the position 1 empty. The cartridge holder was then fitted into the breach of the gun by opening the cylinder lock and push bar. The two O-rings on either side of the breach were quickly checked to ensure that the cartridge holder sits properly and safely. The push bar and the cylinder lack were closed. The cylinder advance lever was squeezed to move to position 1.

The battery was then inserted into the handle of the gun to turn it on. The Swagelok connector from the helium cylinder was attached to the base of the gun and pushed in until it makes a clicking sound. The helium cylinder was opened by turning anti-clockwise. The regulator was adjusted to 250 psi pressure of helium by turning it clockwise. The advance level was squeezed in to allow the helium to kick in the valve and the gun was fired twice to ensure it was pressurised correctly. The Helios™ Gene gun was then placed on to the onion peel on ½ MS10 and the trigger was pulled while holding the safety interlock button to fire. 5-10 bullets were fired onto small section of onion peel.

The ½ MS10 plates containing the bombarded onion peel were covered with aluminium foil and incubated at 22°C in the tissue culture room for 10-15 hours. Both the control and treatment samples must be incubated for equal time to detect any differences in the fluorescence signal.

After incubation, the onion peel was placed on a glass slide with a drop of water under a coverslip and viewed under a Bio Rad confocal microscope to detect fluorescence in the samples.

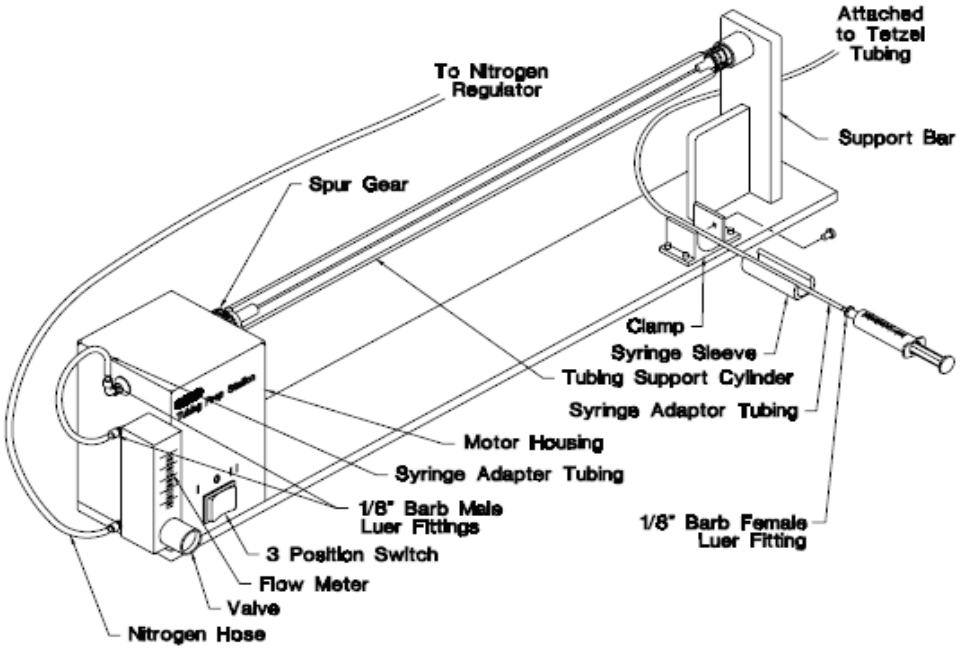

Figure 2.1 Components and control on the tubing prep station, fully assembled

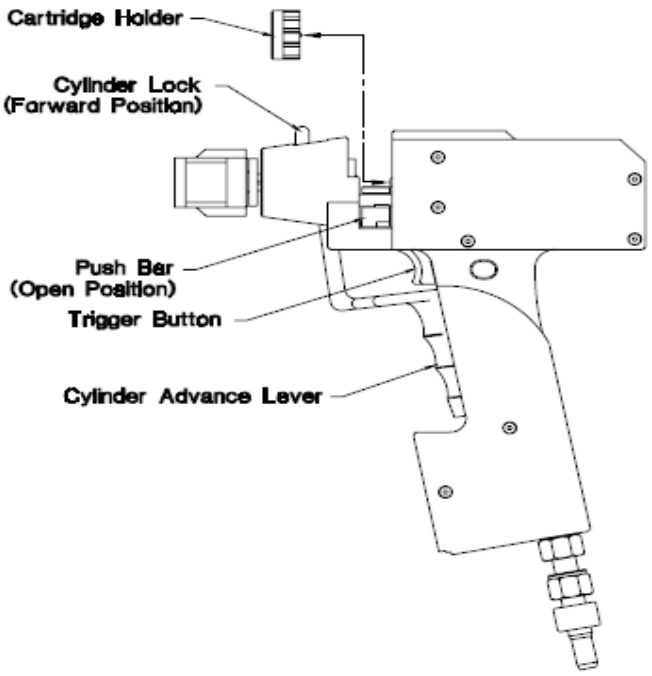

Figure 2.2 inserting a cartridge holder into the Gene gun

2.17 Laser Scanning and Light Microscopy

A Leica SP5 Laser Scanning Microscope (Leica, Germany) was used to analyse the seedling roots of the mutants and overexpressors expressing GFP and CFP. Fresh seedlings carrying GFP and CFP constructs were mounted in dH_2O under a large (32x24 mm) zero-thickness coverslip. The coverslip was placed downwards into the appropriate slot of the motorised stage and examined. This microscope system is based on an inverted DMI 6000 CS microscope base, and the conventional scan head (SP5C) is equipped with three photomultiplier tubes (Hamamatsu R 9624). The system is also equipped with an environment control chamber to maintain optimal conditions for live cell imaging (temperature, carbon dioxide concentration and air humidity). Five lasers, including a 405 nm blue diode laser, provide 9 different laser lines and thus high flexibility for fluorophore excitation. The system includes epifluorescence illumination with DAPI, FITC and Rhodamin filter cubes.

2.17.1 Starting up the Microscope

It was important to switch the machine on in the right sequence in order for it function effectively. All three switches on the TCS control panel (in the order shown on panel with numbers- PC/Microscope, Scanner Power and Laser Power) were switched on and then the key was turned 90° clockwise (for Laser Emission). The computer was turned on and booted up. The objective turret on the microscope stand was set to its lowest position and the condenser was placed in its normal position well clear of the stage. The LAS AF software was started by double clicking the icon on the desktop. The software starts the initialisation of the microscope stand and the scan head, and it cannot be used during this process. After a few minutes, the motorised stage is initialised.

2.17.2 Image Acquisition via the LAS AF Software

The 'Configuration' tab was opened and the 'Laser' icon clicked to open the appropriate window. The required lasers were switched on. When using the Argon laser, 30% power was found to be sufficient for most applications, and prolongs the lifetime of the laser.

2.17.3 Image Resolution and Acquisition of Z-stacks

The image resolution defines how many pixels an image has and the default is 512 x 512, which is sufficient for standard imaging, although a higher resolution of 1024 x 1024 is possible. The higher the resolution resulting file size will be larger. Formats with a ratio other than 1:1, e.g. 1024 x 512, allow imaging at a higher resolution.

For post-acquisition image de-convolution and accurate quantitation, the system always recommended imaging of entire cells or tissue sections in 3 dimensions rather than representative single sections. Programming the acquisition of a Z-stack requires defining the start and end section to be imaged as well as the Z-step (or Z-interval), which defines the stepping of the Z-galvo between the different optical sections. The Z-stack includes display fields of the absolute positions given in micrometers. These fields can also be used to type in the absolute Z-stage positions to define first and last section to be imaged.

2.17.4 Saving Images and Experiments

It is important to know that all the images that have captured, which are displayed in the 'Experiment' menu, are not saved to the hard drive, to avoid accidental deletion. Therefore, it was crucial to constantly save the data to the destination folder on the hard drive in between different scans.

2.17.5 Light Microscopy

For light microscopic analysis a Zeiss Axioscop microscope and an Olympus SZH 10 microscope system were used. The Zeiss Axioscop microscope (Carl Zeiss Ltd, Herts, UK) used DIC/Nomarski optics, and photographs were captured digitally using a Photometrics Coolsnap™ CF camera (Roper Scientific Inc, Trenton, New Jersey, USA) and Openlab 3.1 software. The Olympus SZH 10 is attached to a QIMAGING high performance quantitative digital camera.

2.18 Genotyping of SALK T-DNA Lines

Available T-DNA insertion SALK lines for *AtVAMP714* (SALK_005914 and SALK_005917) were used to characterize loss-of-function mutants. A PCR-based approach was used to identify homozygous insertion mutants among the F1 plants. Seeds obtained from genotyped, homozygous mutant plants were used to characterize the phenotype. The PCR-based genotyping approach involved a genomic PCR using genomic primers, a second PCR using genomic and T-DNA left border primers and third reverse transcriptase PCR (RT-PCR) to confirm the absence of transcripts from the loci. The position of the T-DNA insertions in SALK lines and all the used primers are indicated in Annex 5 and Annex 1 respectively.

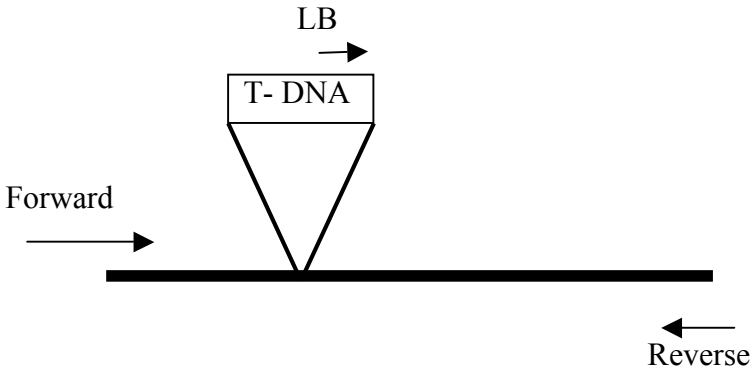

Figure 2.3: Schematic illustration of the SALK insertion and designed primers

Table2.4: Summary of results

SALK Lines	Forward + Reverse primers	LBa1+ Reverse Primer
Homozygous	No Product	Product
Heterozygous	Product	Product
Wild type	Product	No Product

2. 19 Genetic Crosses

Genetic crosses between Arabidopsis plants were made under the Zeiss STEMI SV8 dissecting stereomicroscope (Carl Zeiss Ltd., Welwyn Garden City, Herts, UK). Flowers were selected on the basis of age; examples were chosen for relative maturity of the stigma prior to dehiscence of pollen from the anther, and all other siliques and unsuitable flowers were removed from the stem. Young flowers were emasculated using fine watchmaker forceps (BDH, UK) to gently remove immature anthers, and then mature pollen from the male parent was transferred manually to the stigma, again with forceps.

The stem below the crossed flower was labelled, and the plants were returned to the greenhouse for siliques development. Siliques were harvested upon maturity, but prior to senescence and pod shatter.

Chapter 3: Bioinformatics of the VAMP Family in *Arabidopsis*

Chapter 3: Bioinformatics analysis of the VAMP family in *Arabidopsis*

Arabidopsis VAMP714 is a member of R-SNARE protein family and encodes a Vesicle Associated Membrane Protein (VAMP) of 221 amino acids, with a predicted function in the targeting and/or fusion of transport vesicles to their target membrane. As described in the Introduction, SNAREs locate on the specific organelle membrane to ensure correct vesicular transport by mediating specific membrane fusions. SNAREs are referred to as R- or Q-SNAREs on the basis of the amino acid sequence similarities and specific conserved residues (www.ncbi.nlm.nih.gov).

This chapter describes the Bioinformatics tools used to analyse the *AtVAMP714* gene, for gene expression, protein sequence alignment and *AtVAMP714* promoter analysis. *AtGenExpress* Visualization Tool, Arabidopsis eFP browser and *Arabidopsis* Genevestigator were used to examine the *AtVAMP714* gene expression during plant development.

Prosite (www.expasy.ch/prosite), PFAM (www.pfam.sanger.ac.uk) and SMART (www.smart.embl-heidelberg.de) domain searchers were used to analyse the domain structure and function of the domains of the VAMP714.

R-SNARE protein sequences from *Arabidopsis*, rice, yeast and human downloaded from UniProt/ Swiss-Prot protein database (www.uniport.org/ www.swissport.org) as FASTA format and aligned using ClustalW2 (www.ebi.ac.uk/Tools/clustalw), to examine the VAMP7-1 protein sequence alignments and to construct the phylogenetic tree.

The 2 Kb sequence upstream of *AtVAMP714* promoter region was investigated for transcription initiation sites and *cis* acting elements using the PlantPAN (Plant Promoter Analysis Navigator, http://plantpan.mbc.nctu.edu.tw), and PlantCARE (Plant cis-Acting Regulatory Elements, http://bioinformatics.phs.ugent.be/webtools/plantcare) data bases.

STRING 8.3 (www.string-db.org) known and predicted protein interactions tool was used to analyse the predicted protein interactions with VAMP714 and to find out the conservation of VAMP714 among the other organisms.

3. 1 Domain Structure and Functions of VAMPs

Prosite (www.expasy.ch/prosite), PFAM (www.pfam.sanger.ac.uk) and SMART (www.smart.embl-heldelberg.de) domain searchers were used to analyse the domain structure and function of the domains of the VAMP714.

VAMPs define a group of SNARE proteins that contain three distinct domains, the N-terminal longin domain (LD) of 120-140 amino acids preceding the SNARE motif (SNM) and C-terminal transmembrane domain (TMD). A C-terminal coiled-coil/SNARE domain and single α-helical transmembrane anchor, in combination with variable N-terminal domains, are used to classify VAMPs: those containing long longin N-terminal domains (~150 aa) are referred to as longins, while those with shorter N-termini are referred to as brevins. Longins are the only type of VAMP protein found in all eukaryotes, suggesting that their longin domain is essential.

The longin domain is thought to exert a regulatory function. Longin domains consists of a five-stranded central beta-sheets that is sandwiched by two alpha-helices on one face, and one alpha-helix on the opposite face (Gonzalez *et al*., 2001; Tochio *et al*., 2001).

SNAREs are anchored to membranes by transmembrane segments that not only anchor them, also contribute to SNARE-SNARE interactions and appear to play an active role in the fusion process.

The specificity of membrane fusion is mainly mediated by membrane-associated SNAREs. The SNARE molecules have a highly conserved coiled-coiled domain called SNARE motif. Before the membrane fusion, a trans-SNARE complex consisting of four helical bundles of the SNARE motif from three target-SNAREs (t-SNAREs) and one vesicle-associated SNARE (v-SNARE) (Antonin *et al*., 2001; Diane & Blatt, 2008) is formed. A typical SNARE complex contains one copy of the Qa-, Qb-, Qc- and R-SNARE motif (Fig 1-5). Elements of the SNARE complex differ widely in size and structure, but they share common structural motifs, those contributing to interactions at the core of the SNARE complex (Diane & Blatt, 2008). Complex formation is associated with conformational and free energy changes that are commonly believed to drive the membrane fusion process (Lipka *et al*., 2007).

Figure 3-1: Domain structure of VAMPs

3. 2 Protein Sequence Analysis of VAMP7-1 Sub-family

Arabidopsis possesses eleven genes encoding the VAMP7-like genes, but yeast lacks VAMP7-like genes (Rossi *et al*., 2004). Plants have two major clades of VAMP7-like R-SNAREs. The VAMP7-1 clade (VAMP711 to VAMP714 in *Arabidopsis*) is found in all green plants and is phylogenetically more similar to the VAMP7 SNAREs found in other eukaryotes (Sanderfoot, 2007). The VAMP7-2 group (VAMP721 to 728 in *Arabidopsis*) is only found in green plants (Sanderfoot, 2007), and is involved in secretion (Kwon *et al*., 2008). Table 3-1 listed all *Arabidopsis* R-SNAREs (Sanderfoot, 2007).

Table 3-1: *Arabidopsis* R-SNAREs

SEC22	At1g11890
YKT61	At5g58060
YKT62	At5g58180
VAMP711	At4g32150
VAMP712	At2g25340
VAMP713	At5g11150
VAMP714	At5g22360
VAMP721	At1g04740
VAMP722	At2g33120
VAMP723	At2g33110
VAMP725	At2g32670
VAMP726	At1g04760
VAMP728 (pseudo)	At3g24890
VAMP724	At4g15780
VAMP727	At3g54300
TYN11 (Tomosyn)	At5g05570
TYN12	At4g35560

AtVAMP714 is a member of VAMP7-1 family and has three other family members: *AtVAMP711*, *AtVAMP712* and *AtVAMP713*. To determine the amino acid sequence similarity among the family members, amino acid sequence alignments was carried out using ClustalW2 multiple sequence alignment programme (www.ebi.ac.uk/Tools/clustalw). Multiple alignments of protein sequences are important tools in studying sequences and they provide information to identify the conserved sequence regions. ClustalW2 calculate the best match for the sequences and lines them up according to the identities, similarities and differences (www.ebi.ac.uk/Tools/clustalw). Amino acid sequences were downloaded from UniProt/ Swiss-Prot Protein knowledgebase as FASTA format and align them using ClustalW2.

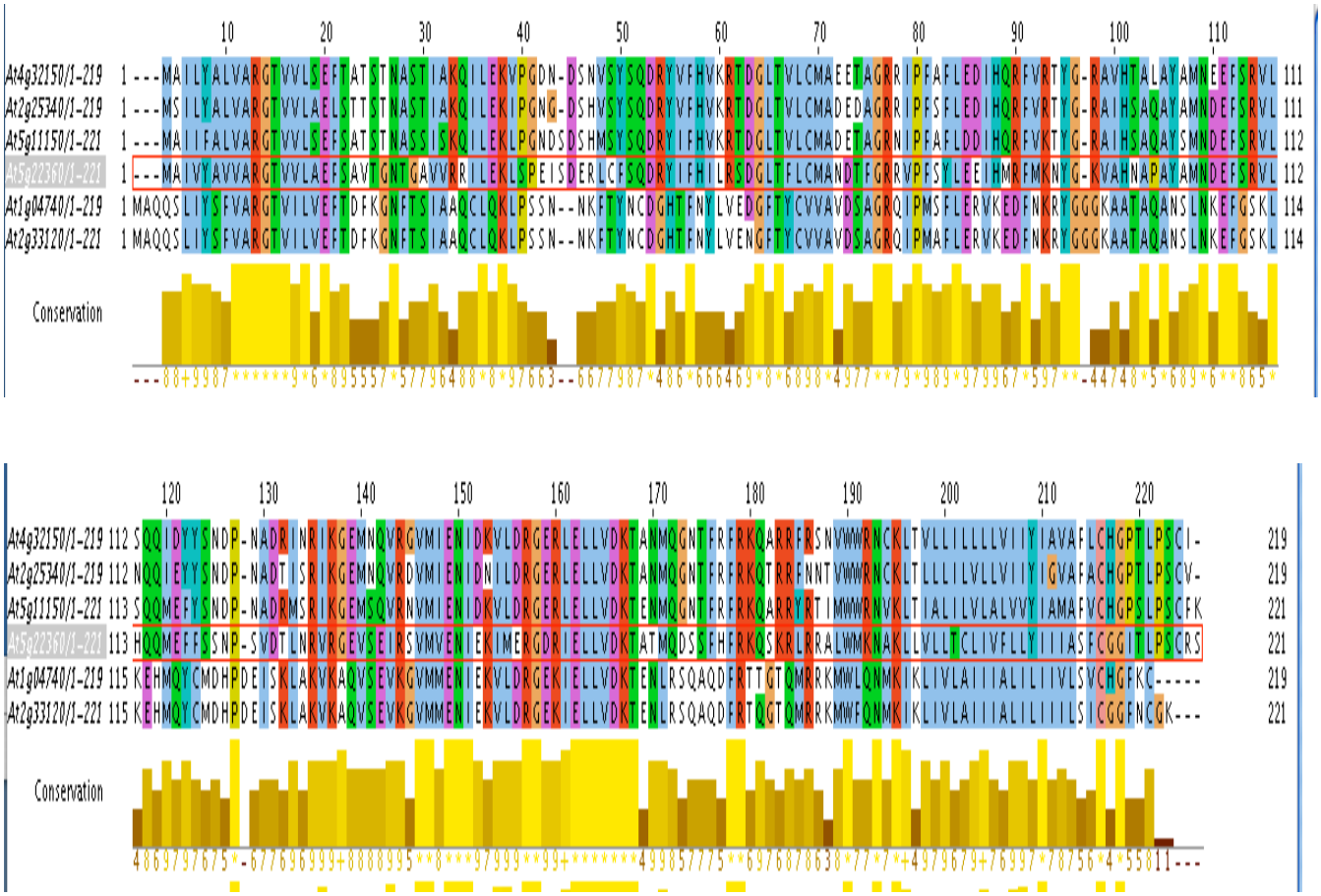

Figure 3-2: Protein sequence alignments and conserved regions of VAMP7-1 family members

The full-length amino acid sequences were used in the analysis. Conserved residues of the *Arabidopsis* VAMP7-1 group are representing in yellow colour bars. Conserved residues of each group of VAMPs are shaded in several colours. At4g32150 (VAMP711), At2g25340 (VAMP712), At5g11150 (VAMP713), At5g22360 (VAMP714), At1g04740, (VAMP721) and At2g33120 (VAMP722)

Aligned sequences and homology searchers showed that vacuolar localized VAMP711, VAMP712 and VAMP713 share over 90% similarities with each other and 80% similarity with Golgi localized VAMP714 (Table 3-2). In spite of the high homology of the VAMP proteins, they showed different subcellular localization. Conserved sequences among the family members were also observed using the same programme (Figure 3-2)

The amino acid sequence analysis of a variety of SNARE proteins from *Arabidopsis*, *Drosophila, C.elegans, S.cerevisiae* and mouse showed that the SNARE domain was highly conserved in each SNARE group. Among the *Arabidopsis* VAMP7 proteins, it was found that, there is an interesting region within the SNARE motif differs depending on the subcellular localization. SNARE proteins localized in plasma membrane/endosome have the 'RSQAQD' sequence in common and SNAREs localized in vacuoles, endosomes and Golgi have 'QGNTER', 'QFQADS' and 'QDSSFH' motifs respectively (Figure 3-3). While these motifs are not conserved in VAMP proteins of other eukaryotes, they might be determinants for the localization of Arabidopsis VAMP proteins (Uemura *et al*., 2004).

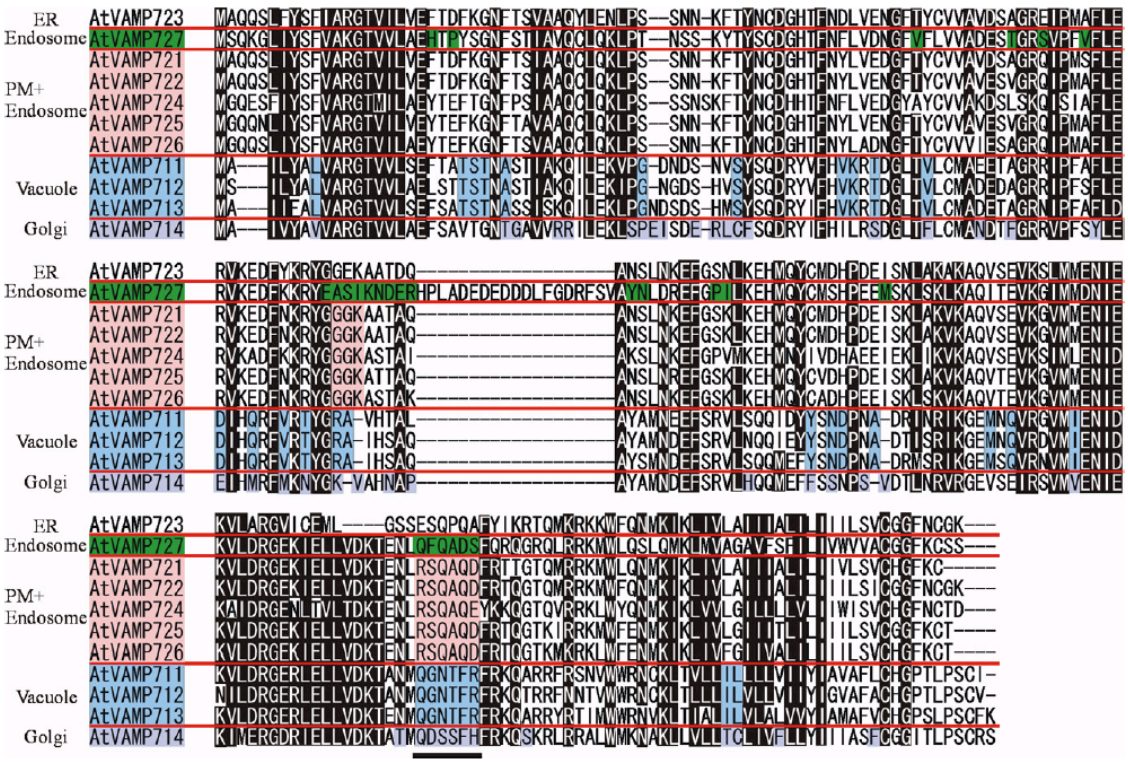

Figure 3-3: Sequence alignment of the *Arabidopsis* VAMP group.

The full-length amino acid sequences were used in the analysis. Conserved residues of the *Arabidopsis* VAMP group are shaded in black. Conserved residues of each group of VAMPs are shaded in several colours. The bar under the alignment represents the regions showing the possible localization signals of Arabidopsis VAMP proteins (Uemura *et al*., 2004).

Table 3-2: Homology of the VAMP7-1 phylogenetic tree group 4

	VAMP714	VAMP713	VAMP712	VAMP711
VAMP714	100			
VAMP713	80	100		
VAMP712	80	90	100	
VAMP711	80	90	90	100

3. 3: Phylogenetic Tree of R-SNARE Proteins

A phylogenetic tree (Figure 3-4) was constructed using R-SNARE protein sequences from *Arabidopsis*, Rice, Yeast and human (all protein sequences downloaded from UniProt/ Swiss-Prot protein database (www.uniport.org) as FASTA format). The programme parameters were adjusted in order to retain the clades with over 70% bootstrap values. To determine the bootstrap values 1000 replicates were performed in the tree. *Arabidopsis* R-SNARE proteins used for this study were listed in Table 3-1.

All the sequences were first aligned into ClustalW2 (www.ebi.ac.uk/Tools/clustalw), exported into NEXUS format and downloaded to PAUP programme. The tree was processed using Adobe Photoshop.

Arabidopsis, rice, yeast and human R-SNAREs make four major groups based on their homology. In-group 1, *Arabidopsis*, yeast and human YKT6 genes grouped together (yellow colour in the tree). *Arabidopsis*, rice and yeast SEC 22 genes grouped into the second group (green colour in the tree). Group 3 is a plant group, all VAMP7-2 genes grouped with rice R-SNAREs (orange colour in the tree). Group 4 (purple colour in the tree) is specific to *Arabidopsis* and all VAMP7-1 genes are grouped together in the group 4 (Figure 3- 4).

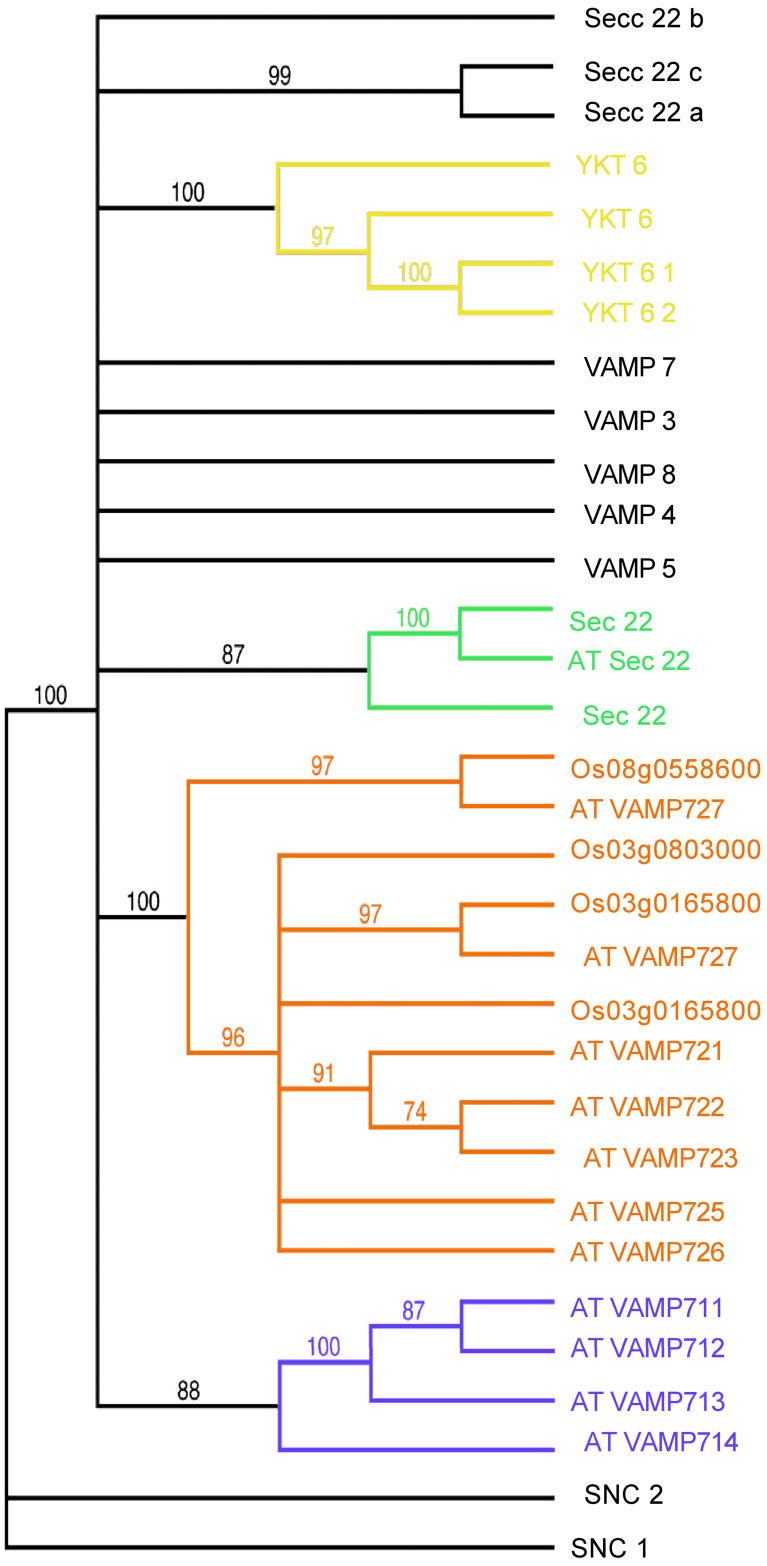

Figure 3-4: Phylogenetic tree of R-SNAREs of *Arabidopsis*, Rice and Yeast

3.4 *AtVAMP714* Gene Expression

AtVAMP714 (At5g22360) gene expression was examined using Arabidopsis eFP browser, *AtGenExpress* Visualization tool and *Arabidopsis* Genevestigator. Arabidopsis eFP browser and *AtGenExpress* visualization and Arabidopsis Genevestigator tools were used to analyse the tissue-specific gene expression and analysing the gene expression in plant development.

3. 4.1 *Arabidopsis* eFP Browser

Arabidopsis eFP browser (Winter *et al*., 2007) was used to analysis of the predicted tissue specificity of *AtVAMP714* expression in Col-0 wild type plants. In Figure 3-5 is illustrated the developmental expression of *VAMP714* in wild type plants.

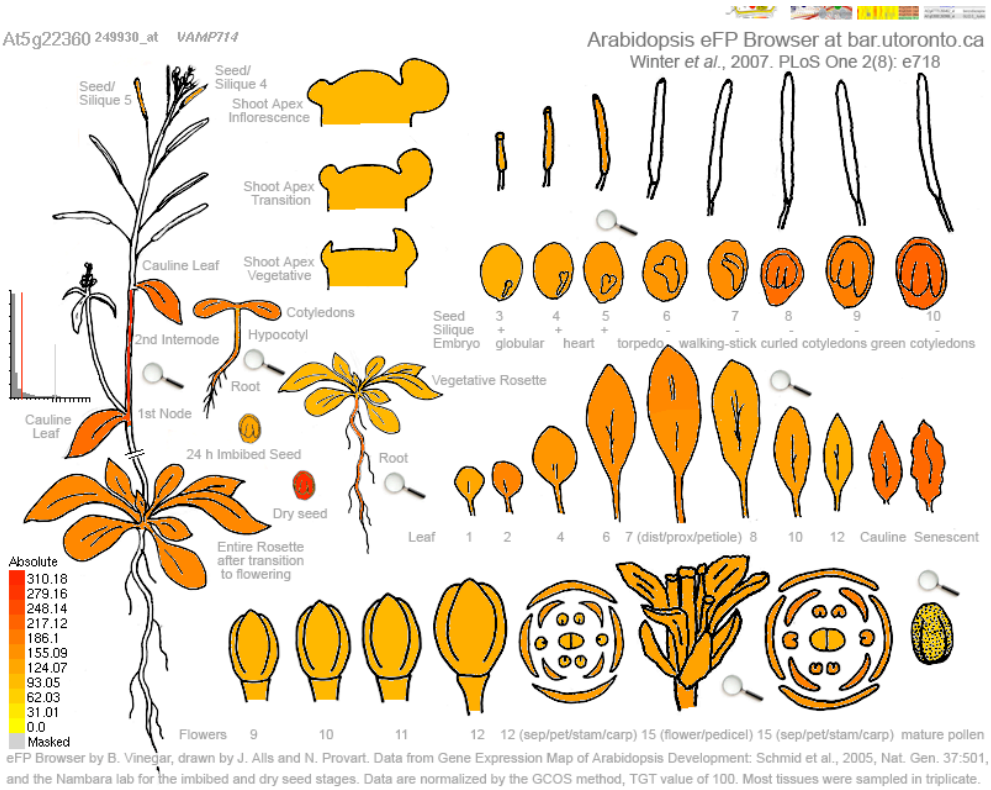

Figure 3-5: Developmental gene expression of *AtVAMP714*

According to this analysis, which is represented graphically in Figure 3-6, the highest gene expression is predicted in stem (second internode), dry seeds, first node, roots, cauline leaves, hypocotyls, floral organs, siliques and rosette leaves. In roots the highest expression is predicted in vascular tissues and no expression is in the root meristem (Figure 3-7).

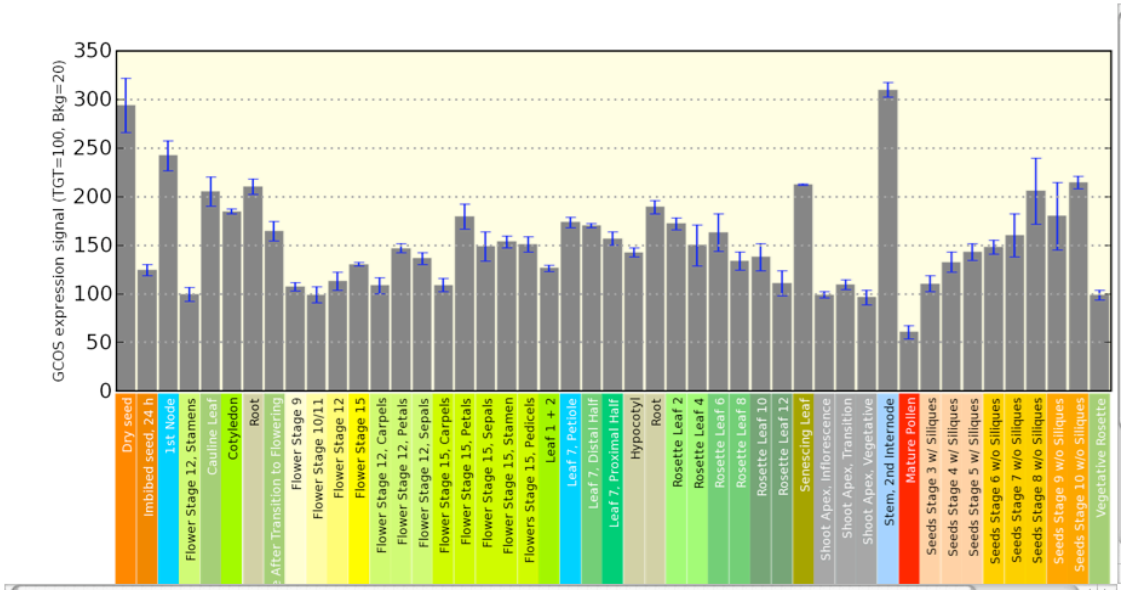

Figure 3-6: Graphical presentation of the tissue specific *AtVAMP714* expression

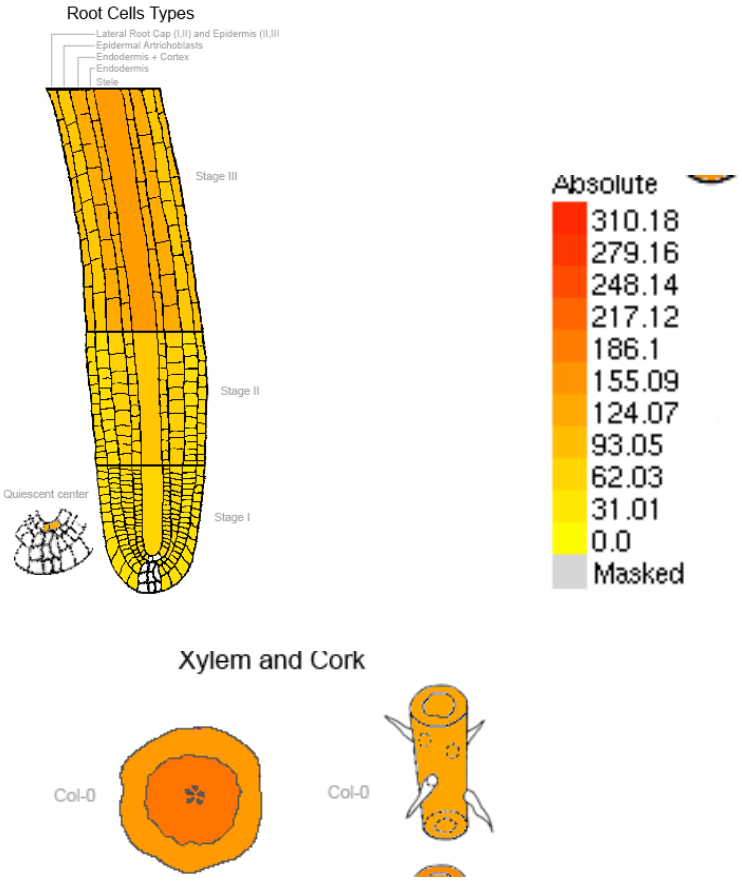

Figure 3-7: *AtVAMP714* gene expression in roots

Tissue specific gene expression in *AtGenExpress* tool indicates that the gene is highly expressed in roots, stems, leaves and floral organs (Figure 3-5, 3-6 and 3-7).

3.4.2 *AtGenExpress* Visualization Tool (AVT)

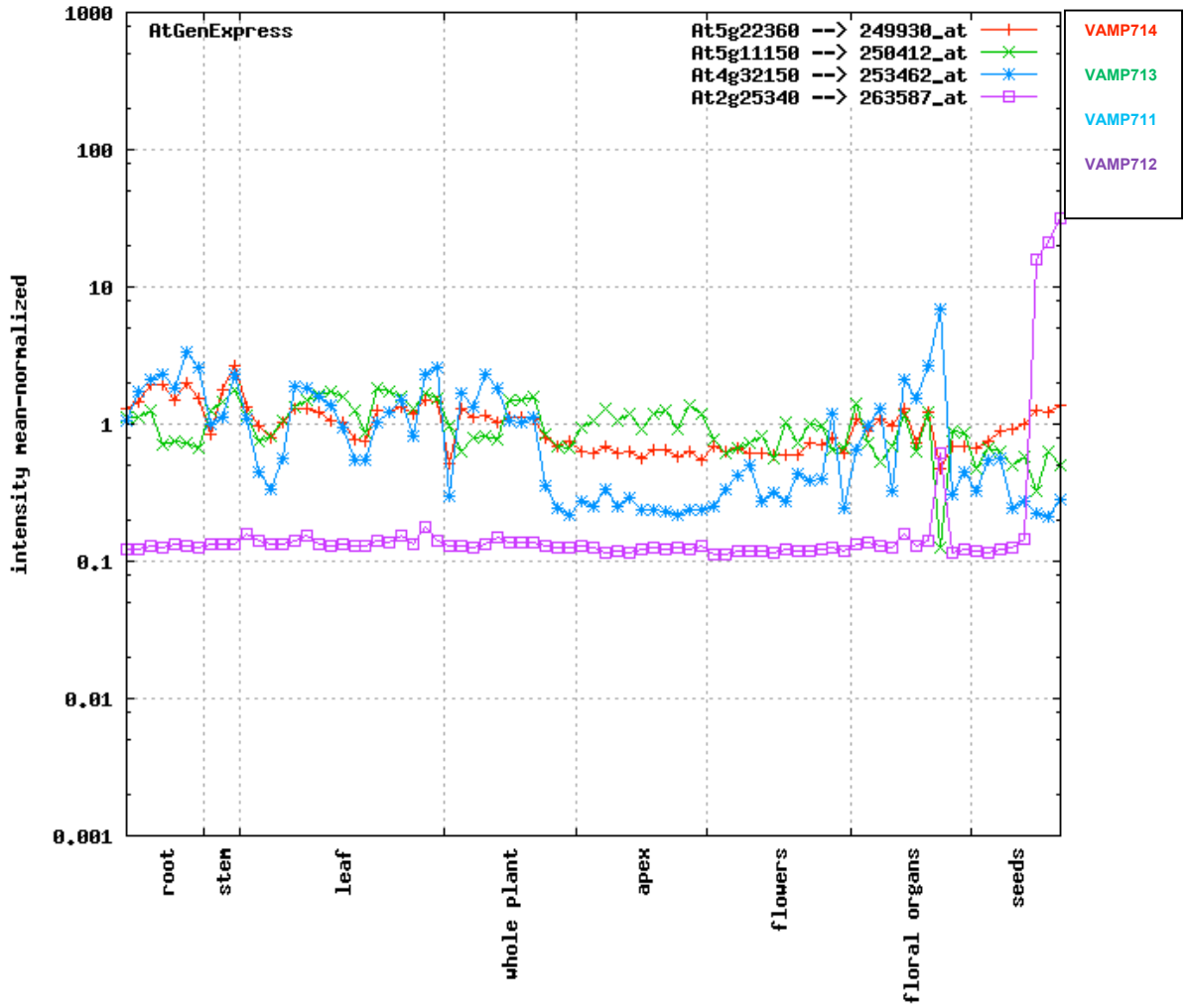

Figure 3-8: *AtGenExpress* Visualization Tool for VAMP7-1 sub-family

According to the *AtGenExpress* visualization tool, *VAMP714* is highly expressed in roots, stem, shoot apex and floral organs.

3.4.3 Genevestigator for Plant Development

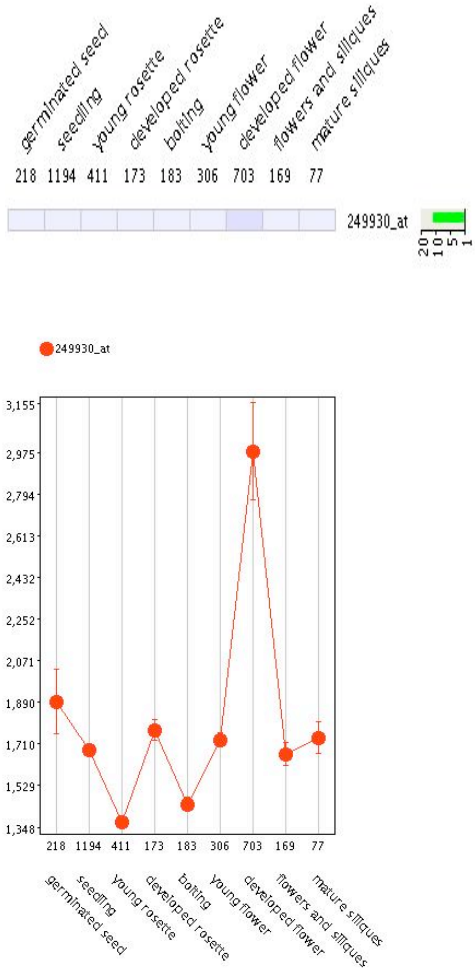

According to the plant development series the gene is highly expressed in developed flowers, and relatively higher expression in germinated seeds, seedlings and rosette layer.

3.5 *AtVAMP714* Promoter Analysis

The 2 Kb sequence upstream (5' to) of *AtVAMP714* was selected as the promoter region and this region was investigated for transcription initiation sites and plant *cis* acting regulatory elements. These were investigated using the PlantPAN, and PlantCARE web sites (http://plntpan.mbc.nctu.edu.tw, http://bioinformatics.phs.ugent.be/webtools/plantcare). These databases are useful for the prediction of transcription initiation sites in the promoter regions of genes of interest. PlantCARE (Plant cis Acting Regulatory Elements) is a database of plant *cis*-acting regulatory elements and a tool for the analysis of promoter sequences. PlantPAN (Plant Promoter Analysis Navigator) recognizes combinatorial *cis*-regulatory elements with a distance constraint in sets of plant genes.

3.5.1 TATA- and CAAT- box

The TATA box is a DNA sequence (cis-regulatory element) found in the promoter region of genes. The *AtVAMP714* promoter contains the TATA-box at around -30 bp from the transcription start site. The CAAT box signal is the binding site for the RNA transcription factor, and is typically accompanied by a conserved consensus sequence. CAAT-box along with the GC box is known for binding general transcription factors. CAAT and GC are primarily located in the region from 100-150bp upstream from the TATA box., which is a common *cis*-acting element (http://bioinformatics.phs.ugent.be/webtools/plantcare) in promoter and enhancer regions.

3.5.2 Light responsive elements

The *AtVAMP714* promoter region contains several *cis*-acting elements involved in light responsiveness. Several light responsive elements found include the GTI motif (GGTTAA), an AAGAA motif, an AE-box (AGAAACAA), a GATA motif, a GAG motif (AGAGAGT) and an ATCC motif described by Park *et al*. (1996); and a G-box described by Arguello-Astoga *et al*. (1996). The G-box has also been proposed as a putative methyl jasmonate (MeJa) responsive element (Rouster *et al*., 1997). The light responsive elements are shown in Annex 7.

3.5.3 Hormone responsive elements

A hormone response element (HRE) is a response element for hormones, a short sequence of DNA within the promoter of a gene that is able to bind a specific hormone response complex and therefore regulate transcription. The *AtVAMP714* promoter region also contains several *cis*-acting elements involved in hormone responsiveness. The promoter contains one TGTCTC or auxin response factor (ARF) binding site in -1346bp upstream of the promoter. ARFs found in early/primary auxin responsive genes (Ulmasov *et al*., 1999)., The Gibberellic Acid responsive element, which binds the GARE factor (Ogawa *et al*., 2005), is also found in the promoter.

In addition, TCA elements involved in salicylic acid responsiveness and a W-box also responsible for salicylic acid inducibility (Chen and Chen, 2003) are found in the *AtVAMP714* promoter.

3. 5.4 Environmental stress responsive elements

The *AtVAMP714* promoter also contains environmental stress responsive motifs such as LTRE (low temperature responsive elements), described by Baker *et al*. (1994). The MBS motif involved in drought-inducibility (Yamaguchi-Shinozaki and Shinozaki, 1994) and the MYB binding site (CAACTG), found in genes that are responsive to water stress (Urao *et al*., 1993) are also present (Annex 7).

3. 5.5 Elicitor responsive elements

The promoter also contains GCC-box and GCN4 motif found in many pathogen-responsive genes. These elements have also been shown to function as ethylene-responsive elements (Brown *et al*., 2003).

3. 6 Proteins Potentially Interacting with VAMP714

STRING (*Search Tool for the Retrieval of Interacting Genes/Proteins*) is a database and web resource of known and predicted protein-protein interactions. The STRING database contains information from numerous sources, including experimental data, computational prediction methods and public text collections. STRING 8.3 Protein Database analyses (www.string.embl.de) were used to investigate predicted interactions between *AtVAMP714* and other proteins. The interactions include direct (physical) and indirect (functional) associations. The associations are derived from four sources Genomic context, High-throughput Experiments, (Conserved) Co-expression and Previous Knowledge. STRING quantitatively integrates interaction data from these sources for a large number of organisms, and transfers information between these organisms where applicable. The database currently covers 2,590,259 proteins from 630 organisms.

According to the STRING 8.3 following proteins show predicted interaction with VAMP714. Different line colours represent the types of evidence for the association (Figure 3-9). Figure 3-7 and 3-8 illustrate the predicted functional partners with VAMP714. Nodes are either coloured (if they are directly link to the input as in the figure 3-8) or white (nodes of a higher iterations/depth). Functional partners often have similar occurrence pattern. Figure 3-10 demonstrates the organisms in which VAMP714 is highly conserved.

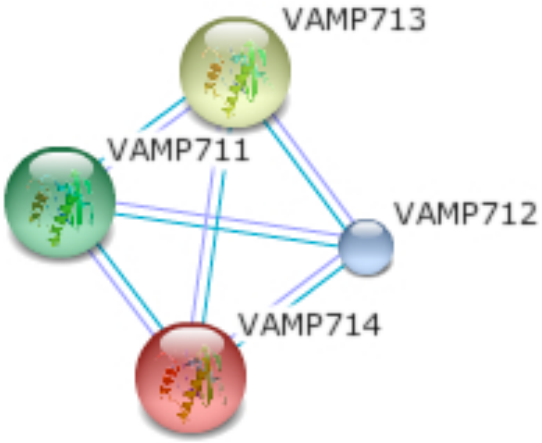

Edges (predicted functional links) consist of up to eight lines: one colour for each type of evidence
Different line colours represent the types of evidence for the association, as shown below

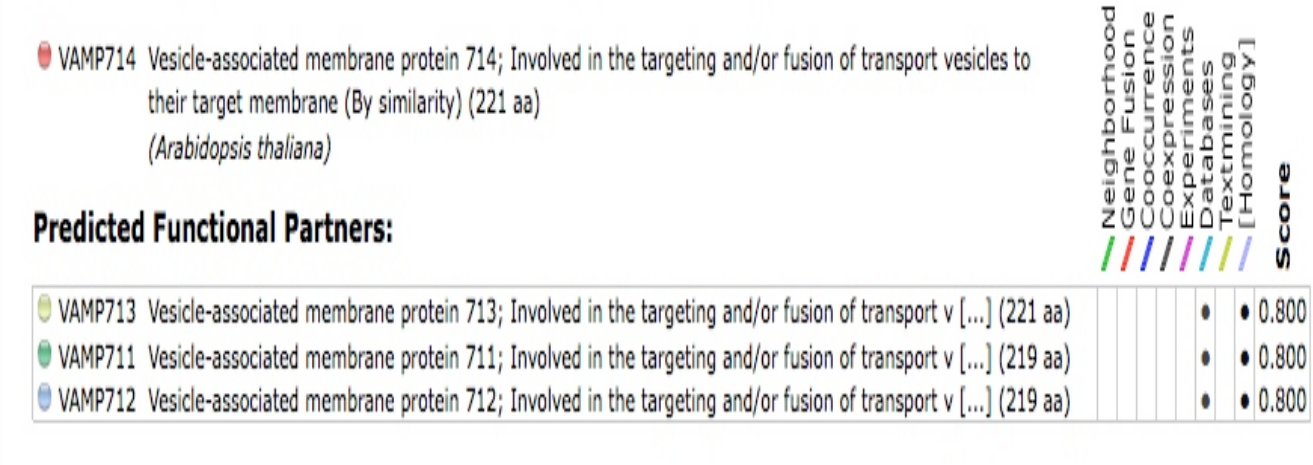

Figure 3-9: Predicted functional partners with VAMP714 (www.string.embl.de)

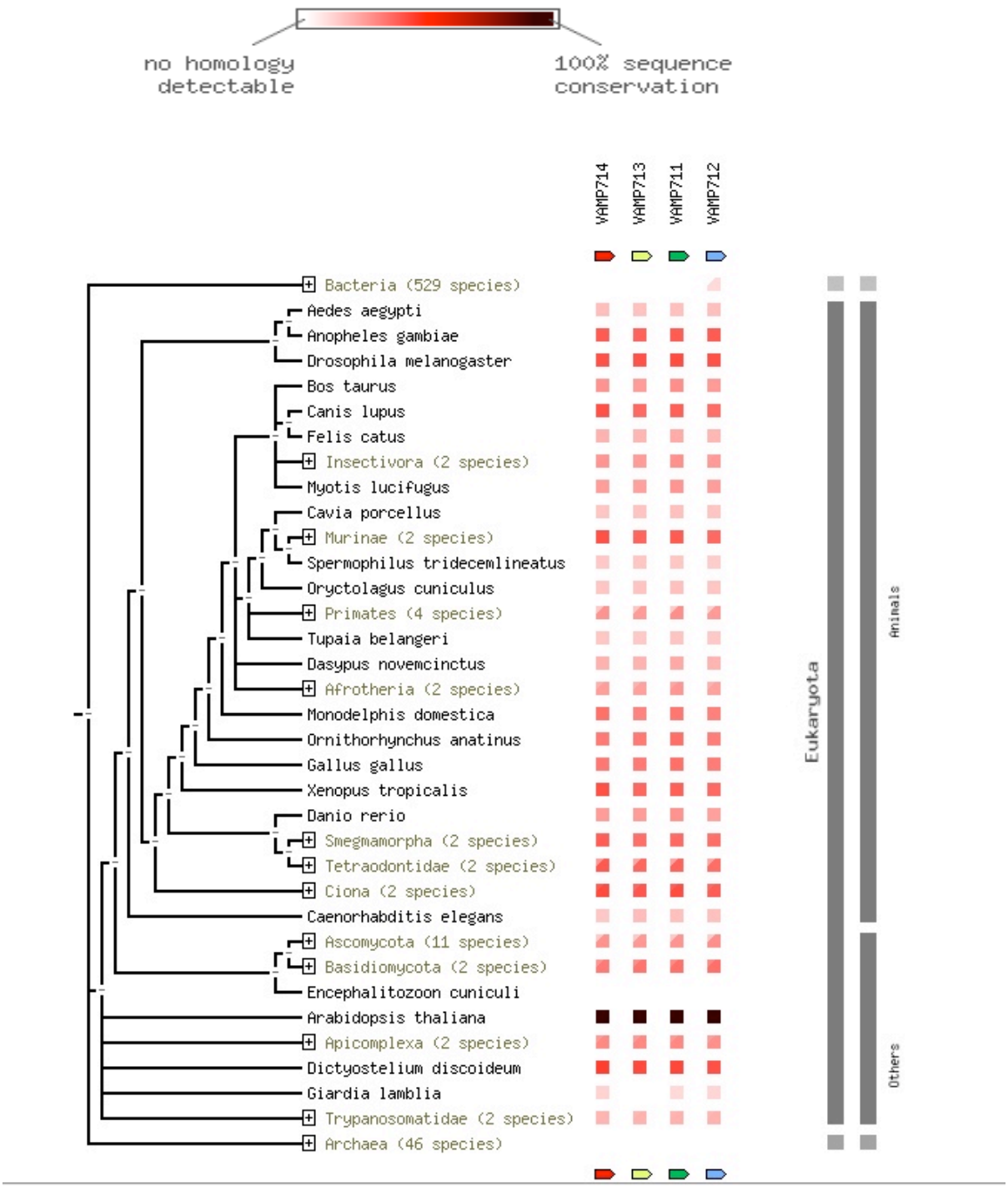

Figure 3-10: Conservation of VAMP714 among the other organisms (STRING 8.3 database)

Phylogenetic Display shows where VAMP714 protein is conserved. Functionally associated proteins often have similar phylogenetic profiles. Input items (proteins) are across the top of the table, and species are down the tree to the left of the table. The presence or absence of an item in an organism is marked a quantitative color scale in Protein-mode (showing the amount of sequence conservation between VAMP714 protein and its best hit in the other species, dark brown being 100% identity as shown in the scale in the top)

Summary

Arabidopsis VAMP7 genes are members of R-SNARE protein family and the completion of the *Arabidopsis* genome sequence has allowed the identification of eleven *VAMP7* genes. These genes are divided into two groups named VAMP7-1 and VAMP7-2. *VAMP711-VAMP714* genes belong to VAMP7-1 sub-group and *VAMP721-VAMP727* genes belong to VAMP7-2 sub-group. VAMP711-VAMP713 shows 90% identity with each other and 80% identity with VAMP714. In spite of the high similarities among the VAMP7 proteins, they show different subcellular localizations. VAMP714 encodes a Vesicle Associated Membrane Protein with 221 amino acids and localized to Golgi (Uemura *et al*., 2005), predicted function as involved in the targeting and/ or fusion of transport vesicles to their target membrane. According to the Gene expression tools *AtVAMP714* is predicted to be expressed in roots, shoot apex, hypocotyls and floral organs.

The VAMP714 has three functional domains named longin, SNARE and transmenbrane. The *AtVAMP714* promoter region, 2kb upstream of the ATG start codon, contains the common promoter motifs TATA-box and CAAT-box. The promoter also contains several *cis*-acting elements involved in light and hormone responsiveness. Motifs associated with response to elicitors and environmental stress are also found.

VAMP714 sequence is highly conserved between *Arabidopsis* and many other organisms.

Chapter 4

Analysis of *AtVAMP714* Gene Expression and AtVAMP714 Protein Localization

Chapter 4: Analysis of *AtVAMP714* Gene Expression and AtVAMP714 Protein Localization

The aim of the work described in this chapter is to investigate experimentally the expression pattern of the *AtVAMP714* gene and the subcellular localization of AtVAMP714 protein in *Arabidopsis* plants. Expression analysis of the *AtVAMP714* gene was carried out using quantitative RT-PCR to determine the abundance of the *AtVAMP714* transcript in different organs, and also by reporter gene fusion analysis to determine the activity of the *AtVAMP714* gene promoter.

Primary transformants of *Arabidopsis* plants containing one of three promoter::reporter gene constructs were used to analyse *AtVAMP714* gene promoter activity and protein localization. The *AtVAMP714* promoter was used for the production of pro*AtVAMP714*::*GUS* and pro*AtVAMP714*::AtVAMP714::CFP expressing plants. The promoter was isolated from *Arabidopsis* Col-0 plants and used to drive the expression of the GUS- (β- glucuronidase-) encoding reporter gene. The promoter was isolated from *Arabidopsis* BAC DNA and used to drive the fusion of CFP (Cerulean Fluorescent Protein) reporter gene. This allowed investigation of the tissue specificity of the promoter activity.

The *AtVAMP714* coding region was used to produce protein fusions with the GFP reporter gene under the control of Cauliflower Mosaic Virus 35S (CaMV 35S) gene promoter. This allowed the analysis of both the phenotypic effects of over-expression of the *AtVAMP714* gene, and determination of the subcellular localization of the AtVAMP714 protein. The constructs are shown in the Figures 4.1 and 4.7 and were introduced into *Arabidopsis* plants by the floral dipping method (Clough and Bent, 1998).

4.1 Development and Hormonal Regulation of the *AtVAMP714* Promoter

To investigate the spatial expression pattern of the *AtVAMP714* promoter in *Arabidopsis* seedlings, pro*AtVAMP714*::*GUS* expression was examined using histochemical localization of GUS activity. Plants expressing pro*AtVAMP714*::*GUS* were isolated and GUS activity was examined during seedling development. These plants were then used to examine the promoter activity in response to various exogenous plant hormones, in order to gain information on the regulation of the promoter.

4.1.1 Cloning of *AtVAMP714* Promoter and Production of pro*AtVAMP714::GUS*

The pro*AtVAMP714*::*GUS* construct was made using the pΔGUSCIRCE vector (Figure 4.1). This construct was introduced into *Arabidopsis* plants by the floral dipping method (for details see Section 2.12). The cloning strategy of pro*AtVAMP714*::*GUS* construct is detailed below.

AtVAMP714 promoter fragment with Sal1 linkers amplified by PCR from *Arabidopsis* Col-0 genomic DNA

↓

Promoter fragment cloned into the pCR®2.1-TOPO vector, sequenced and then excised as a Sal1 fragment

↓

Promoter fragment ligated into the pΔGUSCIRCE vector linearized with Sal1

↓

Recombinant plasmids were isolated and sequenced to verify the construct

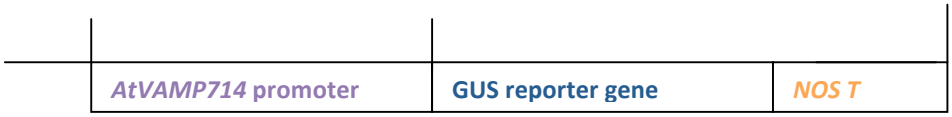

pΔGUSCIRCE

Figure 4.1: Cloning strategy of pro*AtVAMP714*::GUS construct

Approximately two kilobases (kb) of sequence upstream of the ATG of the *AtVAMP714* gene (Annex 3) was selected as the promoter to be used in this work. As most regulatory elements are usually found within 1kb upstream of the ATG of a gene, many of the *cis*-acting elements, which affect transcription of the gene, were expected to have been included in this sequence (see Chapter 3). Two primers were designed to amplify the promoter fragment including Sal1 linkers at the both ends, allowing promoter fragment to be directionally cloned into the pΔGUSCIRCE vector. In addition four internal primers, 360-Prom-1 FOR to 360-Prom-4 FOR and 360-Prom-REV were designed for sequencing of the promoter fragment (Annex 1).

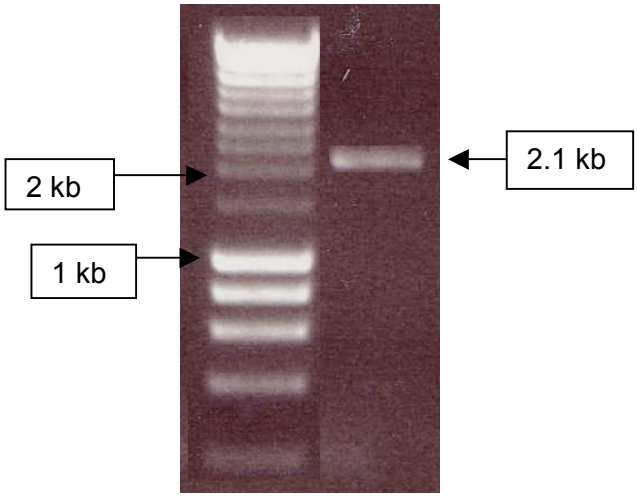

Figure 4-2: PCR amplification of *AtVAMP714* promoter from *Arabidopsis* Col-0 plants

The promoter fragment was amplified from *Arabidopsis* Col-0 genomic DNA prepared using GenElute™ Plant Genomic DNA miniprep kit (Section 2.7.4) and using the Expand™ KOD HOT Start PCR system (Section 2.15.2). The PCR product was analysed by gel electrophoresis (Section 2.8) and a band of 2.1 kb was obtained as expected (Figure 4-2). The PCR product was cloned directly into the pCR®2.1-TOPO vector (Section 2.10.5) and introduced into chemically competent TOP10 One shot™ cells (Section 2.10.5.2). Five positive white colonies were sequenced with universal primers *M13F* and *M13R* and 360 Prom- 2 FOR 360-Prom-3 FOR internal primers. Plasmid DNA was prepared as described in Section 2.7.1. The correctly inserted colony was used for cloning of promoter fragment into the plasmid vector pΔGUSCIRCE.

The promoter fragment was released from the pCR®2.1-TOPO vector with Sal1 linkers. The promoter and pΔGUSCIRCE were both cut overnight with Sal1 (Buffer D at 37^0C as described in Section 2.10.1) and then cleaned with Roche *High Pure* PCR kit (Section 2.7.10). Prior to clean up the pΔGUSCIRCE was treated with Shrimp Alkaline Phosphatase (Section 2.10.2) and incubated at 37^0C for 30 minutes followed by 10 minutes at 70^0C to inactivate the phosphatase. The *AtVAMP714* promoter and pΔGUSCIRCE vector were ligated overnight at 4^0C and then introduced into chemically competent DH5α *E.coli* cells (Section 2.10.6.3). Ten white colonies were used to prepare plasmid DNA (Section 2.7.1) and sequenced with GUS-nested 1 and 360-Prom- FOR 1 and 360-Prom-2 FOR internal primers (Annex 1).

The correctly inserted pro*AtVAMP714*::*GUS* construct in pΔGUSCIRCE was introduced into *Agrobacterium tumefaciens* strain C58C3 by triparental mating (Section 2.12) and positive colonies were identified by PCR, using 5g22360 prom For and GUS-nested 1 primers. A single positive colony was selected and used for introduction of the construct to *Arabidopsis* var Col-0 by the floral dipping method (Section 2.13).

In this construct kanamycin was used as the selectable marker. Kanamycin-resistant T1 seedlings were selected on ½MS10 culture plates containing 50 µg/ml kanamycin sulphate. Kanamycin-resistant seedlings remained green while sensitive seedlings became bleached 7-10 days after germination (DAG) on the selective medium. Kanamycin-resistant primary transformants (T1 plants) were identified and transferred to pots and grown to maturity. Plants were bagged at flowering to prevent cross-pollination and T2 seeds were collected as individual lines for further analysis.

4.1.2 Characterization of pro*AtVAMP714*::*GUS* Expression in *Arabidopsis*

The number of unlinked T-DNA loci in a hemizygous line can be estimated by the ratio of kanamycin-resistant (Kan^R) seedlings to kanamycin-sensitive (Kan^S) sensitive seedlings (Table 4-1).

Table 4-1: Expected segregation ratios and T-DNA loci numbers assuming no linkage between loci

Number of Kan^R	Number of Kan^S	Number of unlinked T-DNA loci
3	1	1
15	1	2
63	1	3
255	1	4

The aim of this work is to identify single locus transgenic lines containing the pro*AtVAMP714*::*GUS* gene fusion. In order to determine the number of T-DNA loci, segregation of kanamycin resistance of T2 seeds was assessed. Nine independent primary (T1) transformants containing pro*AtVAMP714*::*GUS* were obtained using kanamycin selection, and allowed to recover under semi-sterile culture before being grown under greenhouse

conditions. Their progeny were analysed for kanamycin segregation. Seeds from T1 plants (60 seeds from each line) were germinated on ½ MS10 kanamycin (50 µg/ml) medium.

Lines that showed kanamycin resistance with an approximately 3:1 resistance: sensitive segregation ratio was expected to contain T-DNA at a single locus. These lines were used for further analysing of the gene promoter activity.

Table 4-2: Green-white plant selection of pro*AtVAMP714*::*GUS* transgenic seedlings

Line no	Kan^R	Kan^S	Ratio
1	57	3	19:1
2	11	49	1:4
3	52	5	10:1
4	44	6	7:1
5	43	14	**3:1**
6	42	14	**3:1**
7	46	14	**3:1**
8	40	13	**3:1**
9	42	17	**3:1**

Five lines (designated 5-9 in Table 4-2) showed the 3:1 segregation with kanamycin. These lines were used for further analysis.

T2 seeds from each line were surfaced sterilized and germinated on ½ MS10 medium supplemented with Kanamycin (50 µg/ml). Nine days after germination, whole seedlings were stained histochemically for GUS activity (Section 2.3.1). To determine the optimum staining time, seedlings were stained at 37^0C for 3 hours, 6 hours and 16 hours. Microscopic examination of the seedlings indicated that a staining period of 16 hours was required for easy visualization of GUS activity. The staining patterns that were obtained are summarized in Table 4-3.

The T2 seeds from kanamycin-resistant individual plants were subjected to kanamycin segregation analysis described in 4.1.2 to identify the plants homozygous for kanamycin and T-DNA insertion. Line 7, 8 and 9 were shown to be homozygous. Based on this screen, and

GUS analysis, line 7 showed a clear root expression pattern and was selected for further analysis.

Table 4-3: Summary of root expression pattern in five independent T2 pro*AtVAMP714*::GUS transgenic lines

Line	Root staining pattern	Line	Root staining pattern
5	Very weak staining in root/hypocotyl junction and root vasculature	8	No staining
6	Very weak staining in root/hypocotyl junction root vasculature	9	Weak staining in root vasculature
7	Strong staining in root/hypocotyl junction and root vasculature		

Table 4-4: Summary of expression pattern in aerial parts of 5 independent T2 pro*AtVAMP714*::GUS transgenic lines

Line	Staining pattern	
	Mature rosette leaves	**Inflorescence**
5	Centre of the rosette layer, shoot apex	No staining
6	Centre of the rosette, hypocotyls, shoot apex	No staining
7	Strong staining in rosette layer, shoot apex, hypocotyls and stipules	Pollen and stigma
8	No staining	Pollen
9	Strong staining in shoot apex and stipules	Pollen

In order to investigate *AtVAMP714* promoter activity in other organs, T2 GUS line was also grown in soil in greenhouse conditions and mature rosette leaves as well as inflorescences (consisting of stems, floral parts, cauline leaves and siliques) were stained. The staining period used was 16 hours. The expression patterns in these tissues are summarised in Table 4-4.

4.1.3 Developmental Expression of GUS under the *AtVAMP714* Gene Promoter

To investigate the tissue specificity of the *AtVAMP714* gene promoter, the pattern of GUS activity in the pro*AtVAMP714*::*GUS* lines was analysed. Plants expressing the construct were isolated and GUS activity was examined during seedling development. Seedlings were removed at 3, 5, 8, 11, 14 and 21 days after germination and were subjected to histochemical staining for 16 hours at 37^0C followed by de-staining in 70% ethanol before being examined by light microscopy.

Although the expression patterns observed in the seedlings were broadly similar at a given developmnetal stage, there was nevertheless some variability in the level of staining between seedlings. After 16 hours of staining GUS activity could be observed in both primary and lateral roots, though not in root tips, in all stages of development. In all cases where root expression is observed, expression was in the vascular tissues (Figure 4-6A). Table 4-3 & 4-4 summarises the results of GUS staining for five independent transgenic lines. However, representative seedlings and tissues of line 7 are shown in Figures 4-3 and 4-4, and these are now described.

At 3 DAG, GUS expression was seen in the root-hypocotyl junction, shoot apex and in the main root except the root tip. At 5, 8 and 11 DAG, expression was seen in shoot apex, hypocotyl, root-hypocotyl junction and both main and lateral roots except root tips. In all cases GUS activity was strongest at the root-hypocotyl junction and declined towards the root tip. At 14 and 21 DAG, the expression pattern was similar to that at 11 DAG but GUS activity could not be seen in the hypocotyl. At 21 DAG, GUS expression could be seen in mature pollen. GUS activity was also observed in young lateral root primordia, root hairs, trichomes and stipules of the seedlings (Figure 4-4).

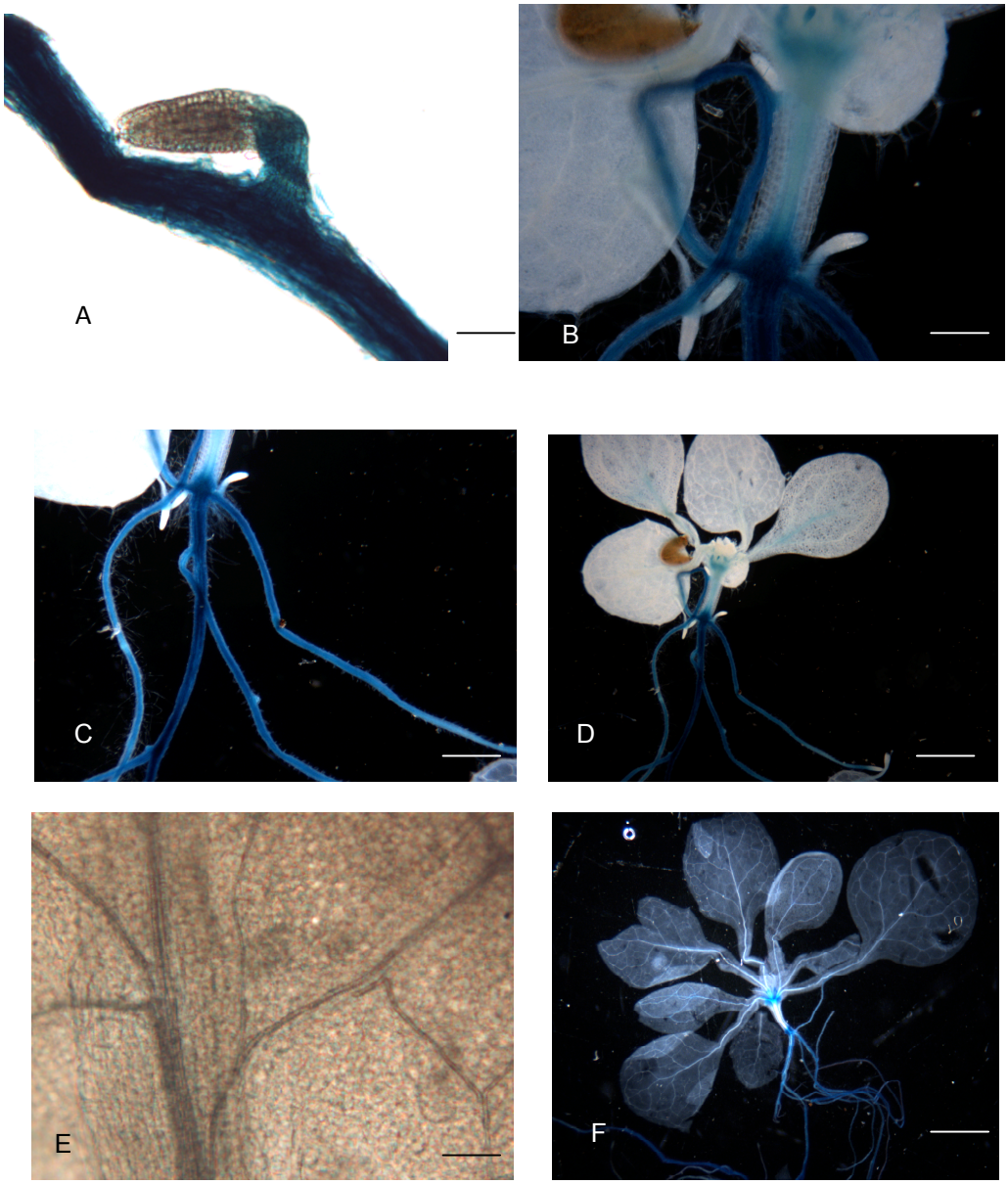

Figure 4-3: Developmental expression of GUS in pro*AtVAMP714::GUS* seedlings

A: No GUS expression in the root meristem of lateral root at day 8 mag. x10,

B: pro*AtVAMP714*::*GUS* expression in hypocotyl at day 8 mag. x6.5,

C: pro*AtVAMP714*::*GUS* expression in primary and lateral roots at day 11 mag. x3,

D: pro*AtVAMP714*::*GUS* expression in a seedling at day 11mag. x1.5,

E: No GUS expression in vascular tissues of leaves at day 11 mag. x10,

F: pro*AtVAMP714*::*GUS* expression of a seedling at day 14 mag. x1.5 (No GUS expression in the hypocotyl), bar=30 µm

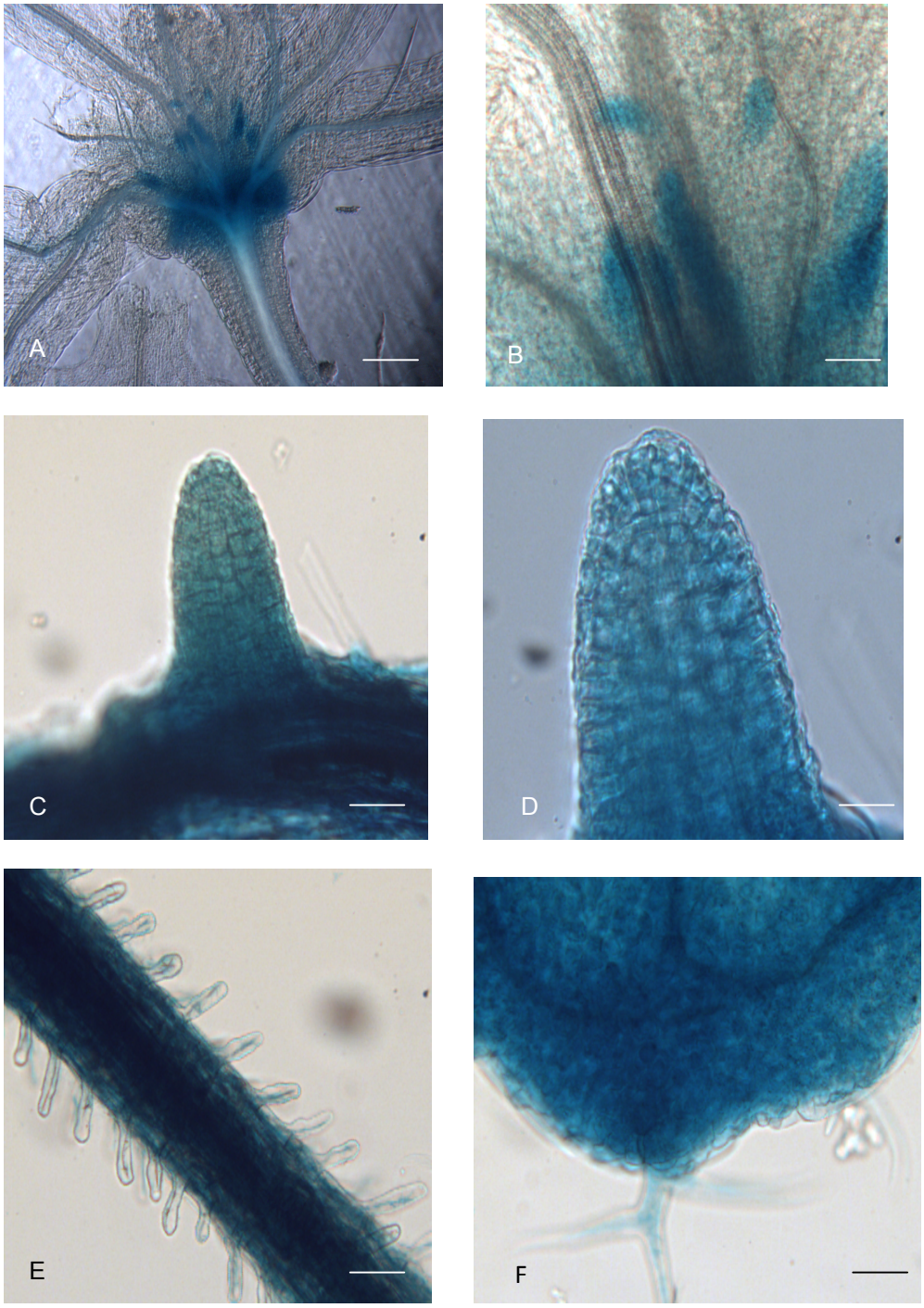

Figure 4-4: Expression pattern of pro*AtVAMP714*::*GUS*

A & **B**: pro*AtVAMP714*::*GUS* expression in stipules at day 14 mag. x7,

C & **D**: pro*AtVAMP714*::*GUS* expression in young lateral roots at day 5 mag. x10,

E: pro*AtVAMP714*::*GUS* expression in main root with root hairs at day 5 mag. x10,

F: pro*AtVAMP714*::*GUS* expression in trichomes at day 14 mag. x 10, bar=30 µm

4.1.4 Response of the *AtVAMP714* Promoter to Plant Growth Regulators

Plants expressing the pro*AtVAMP714*::*GUS* construct were identified and GUS activity was examined during seedling development, as described above. These plants were then used to examine the promoter activity in response to various exogenous plant hormones and inhibitors (IAA, BA, ACC, and TIBA) to determine whether the gene is hormonally regulated.

Seeds from homozygous pro*AtVAMP714*::*GUS* line seven, identified in section 4.1.2 were surface sterilized and germinated on ½ MS10 medium. At 5 days after germination (DAG), seedlings were transferred to ½ MS10 medium supplemented with different plant growth regulators (Table 4-5). Seedlings were removed from this medium at 7 days post transfer and stained histochemically for GUS activity for 16 hours. The seedlings were then cleared using 70% v/v ethanol before being mounted and examined using microscope.

Table 4-5: Working solutions of plant growth regulators

Plant growth regulator	Working concentrations	Action
IAA	10, 25, 100 µM	Enters the cell via influx carrier
BA	10, 25, 100 µM	Cytokinin analogue
ACC	10, 25, 100 µM	Ethylene precursor
TIBA	10, 25, 100 µM	Auxin transport inhibitor

Control seedlings, with no exogenous hormones treatment, showed similar expression pattern to those examined in section 4.1.3 (Figure 4-3 D). Treatment with IAA at all concentrations tested (Table 4-5) led to GUS activity occurring strongly at the tip of the main and lateral roots and cotyledons (Figure 4-5).

Treatment with 25 µM ACC (Figure 4-6 B) and 25 µM BA did not lead to any significant alteration in the pattern or level of GUS activity. Treatments with the auxin efflux carrier inhibitor TIBA led to an upregulation of GUS activity, which was observed in leaves; in contrast, no GUS activity was observed in roots (Figure 4-5).

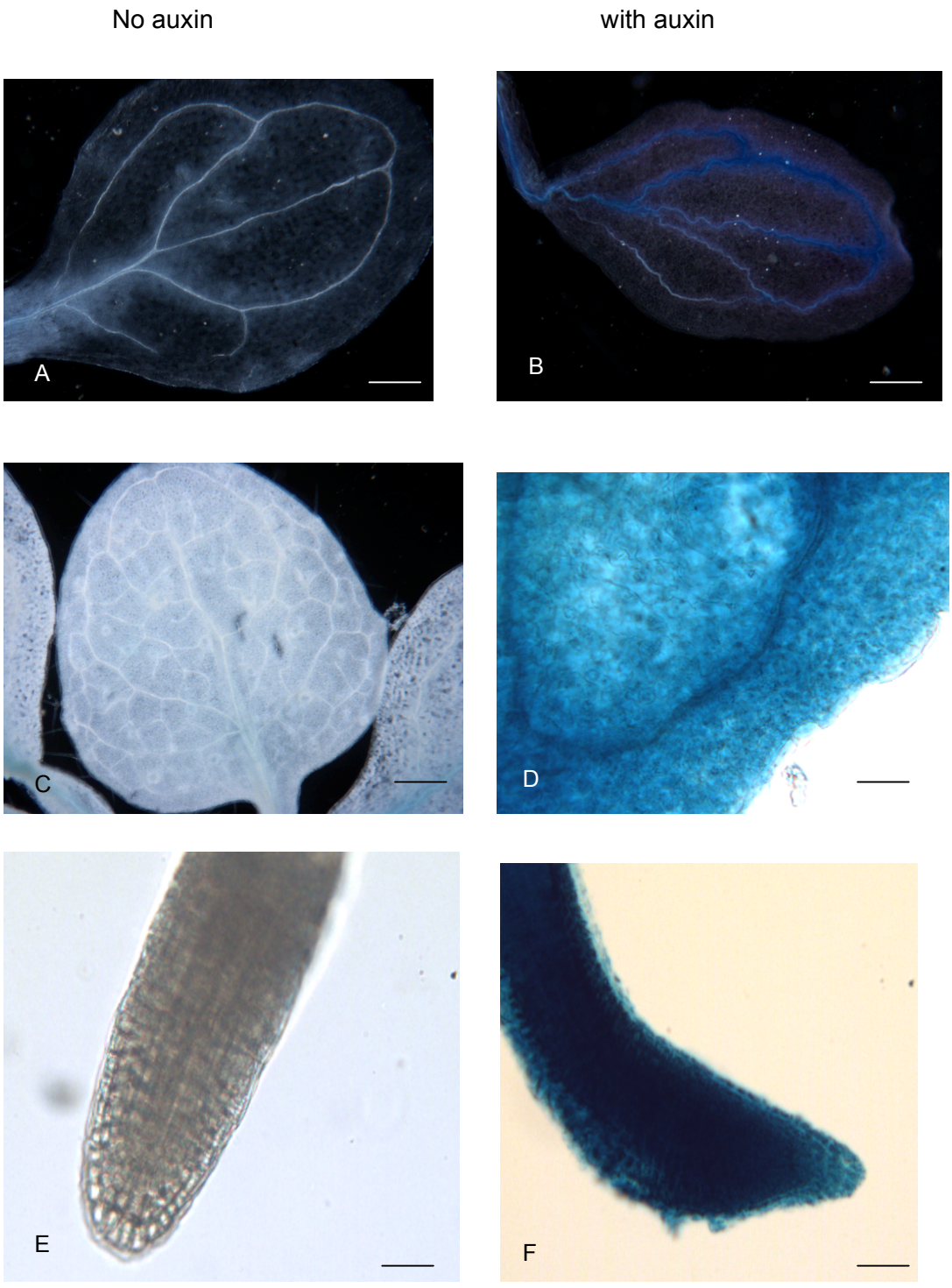

Figure 4-5: Hormonal regulation of pro*AtVAMP714::GUS* expression

A: cotyledon at day 5 with no IAA treatment mag. x5.5

B: cotyledon at day 5 with IAA treatment mag. x5.5

C: leaf at day 14 with no IAA treatment mag. x 10

D: leaf at day 14 with TIBA treatment mag. x 10

E: root tip at day 11 with no IAA treatment mag. x10

F: root tip at day 11 with IAA treatment mag. x10, bar=30 µm

4.1.5 Tissue-specific Expression of pro*AtVAMP714*::*GUS* in *Arabidopsis* Roots

The cell types in which *AtVAMP714* promoter is active, was investigated using transverse sectioning of *Arabidopsis* roots expressing the pro*AtVAMP714*::*GUS* construct.

Seeds were surface sterilized and sown on ½ MS10 medium. Seven days after germination, the seedlings were stained for GUS activity and then embedded in LR White medium (section 2.3.4) before being sectioned. The sections were mounted on slides and examined under the light microscope, as described in section 2.17.5. Sections were taken from the main root just below the root-hypocotyl junction. Examination of transverse root sections showed that GUS activity was present in the vascular tissues both in primary and lateral roots (Figure 4-6 A).

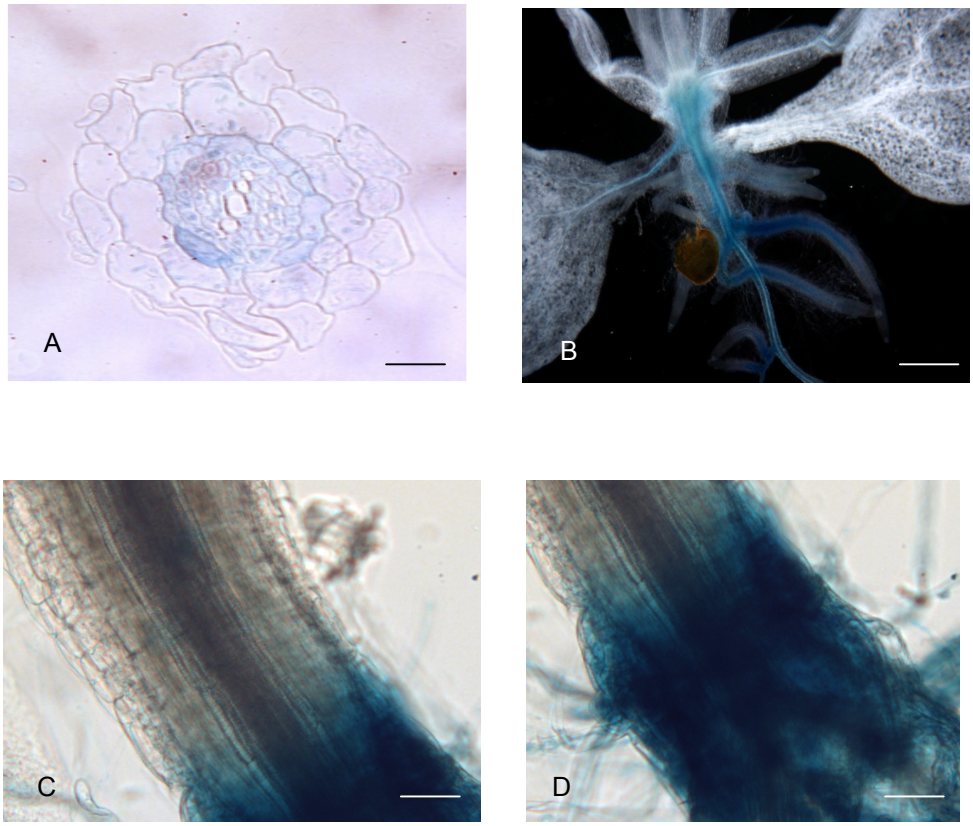

Figure 4-6: pro*AtVAMP714*::*GUS* expression

A: Transverse sections of roots expressing pro*AtVAMP714*::*GUS* mag. x10,

B: pro*AtVAMP714*::*GUS* expressing seedling treated with ACC at day 14 mag. x1.5,

C; pro*AtVAMP714*::*GUS* expressing hypocotyl at day 14 mag. x10,

D: root-shoot junction of a seedling expressing pro*AtVAMP714*::*GUS* at day 14 mag. x10

Bar=30 µm

4.2 Tissue Specific Gene Expression of VAMP Family Members

As described above, *AtVAMP714* is a member of an R-SNARE gene family and belongs to the *VAMP7*-like group. The *VAMP7*-like group has two sub-groups; *VAMP7-1* and *VAMP7-2*. The *VAMP7-1* sub-group has four family members namely *AtVAMP711*, *AtVAMP712*, *AtVAMP713* and *AtVAMP714*. An analysis of the tissue-specific gene expression of all four family members was carried out using gene-specific primers (Annex 1) and qRT-PCR.

4.2.1 RNA Extraction from Different Tissues

Arabidopsis var Col-0 seeds were surfaced sterilized and grown on ½ MS10 medium (Section 2.2.1). Seven days after germination, aerial parts and roots were harvested separately from seedlings and stored at -80^{0}C until required for RNA extraction. *Arabidopsis* Col-0 seeds were sown on soil and grown in greenhouse under controlled conditions. Flowers and siliques were harvested from soil-grown plants and stored as above prior to RNA extraction.

RNA was extracted using the QIAGEN RNAEasy Plant Mini Kit as detailed in section 2.7.6. The extracted RNA was quantified using NanoDrop1000 Spectrophotometry (section 2.7.7). cDNA synthesis was carried out using 1 µg of RNA as detailed in section 2.7. 8.

Real-time PCR was used to examine the tissue specificity of expression. As described in the section 2.15.6, real-time PCR based on the quantitative relationship between the starting target DNA and the amount of amplification product during the exponential phase of a cycling programme. Relative quantification was used to compare the results for each organ. Comparative quantification software of the Rotorgene was used to analyse the data in this experiment using *ACTIN 2* as a housekeeping gene.

The results obtained from this experiment are illustrated in Figure 4-7 and compared with the *AtGenExpress Visualization Tool* and *Arabidopsis eFP* browser (Chapter 3). The *AtVAMP714* gene was highly expressed in shoot, root and floral parts. Similar observations were made for plants transformed with the pro*AtVAMP714*::*GUS* construct, in which GUS activity was observed in shoot apex, hypocotyls, roots and pollen. The tissue-specific gene expression analysis of *AtVAMP713* showed that this gene is highly expressed in floral parts whereas *AtVAMP712* was expressed in the shoots. The expression pattern of *AtVAMP711* was different from other members, whereby relatively high expression was observed in siliques.

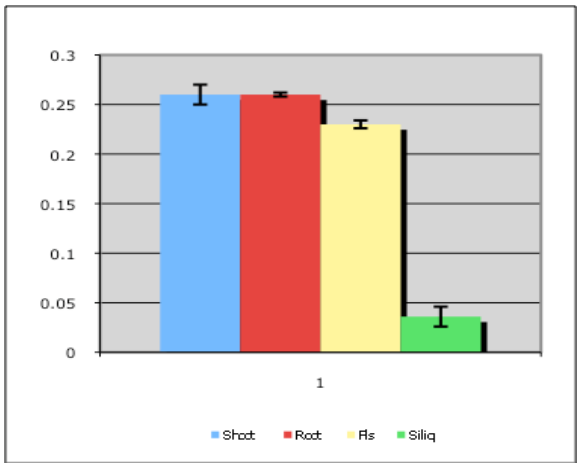

AtVAMP714

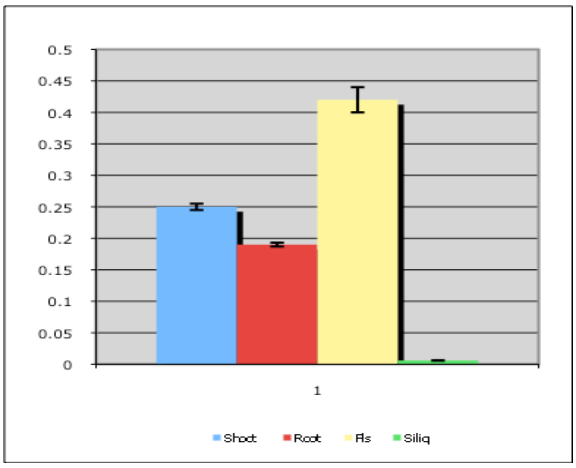

AtVAMP713

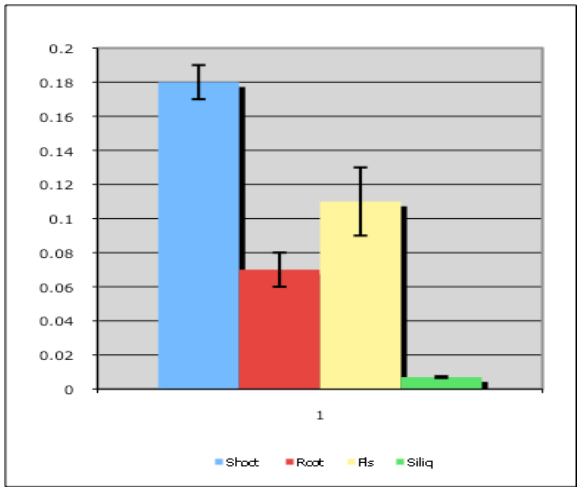

AtVAMP712

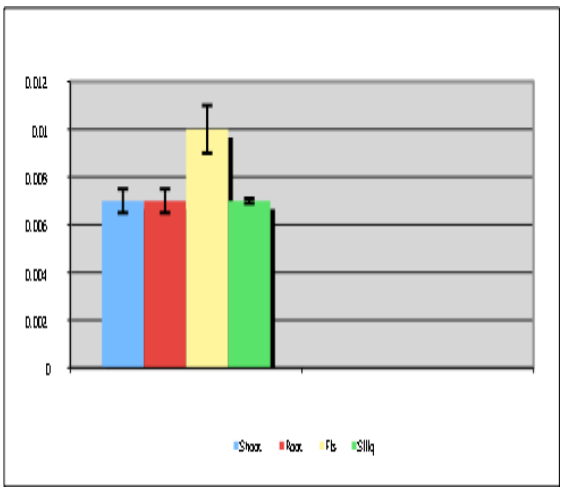

AtVAMP711

Figure 4-7: Tissue specific gene expression of VAMP7-1 family

Quatitative real time RT-PCR analysis of the expression of *AtVAMP711-AtVAMP714* in different tissues in relative to *ACTIN2* in Col-0 wild type plants. These data are representative of two independent experiments using biological replicate samples. The Y-axis represent the relative abundance of the transcripts and error bars represent Standard Error of three technical relicates.

4.3 Localization of the AtVAMP714:GFP Protein Fusion

Green Fluorescent Protein (GFP) is a natural fluorescent protein isolated from the jelly fish *Aequoria victoria*, and is used in many biological systems both in protein fusions to study sub-cellular localization and as a reporter of promoter activity (Hwang *et al*., 1995). A major advantage of GFP is that no substrates other than molecular oxygen are required. GFP may not be easily detectable when driven by weak promoters.

Fusions of GFP with entire proteins of known or unknown function have shown where the proteins are located intracellularly, and whether the proteins move from one compartment to another. GFP and variants with different spectral properties have been deliberately targeted to separate compartments to determine their size, shape, mobility, and dynamic changes during development or environmental response (Stepanenko *et al*., 2008).

In this work AtVAMP714:GFP fusion protein was used as a proxy to study the subcellular localization of AtVAMP714.

4.3.1 Production of Plants Expressing pro35S::AtVAMP714:GFP

A pro35S::AtVAMP714::GFP construct (Figure 4.8) was used to examine the subcellular localization of AtVAMP714. This construct was introduced into *Arabidopsis* plants by floral dipping.

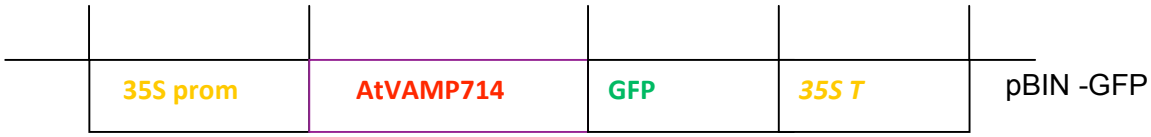

Figure 4.8: pro35S::AtVAMP714::GFP construct

The pBIN-GFP vector (kindly supplied by Dr. David Dixon, Durham University) was used to construct the AtVAMP714::GFP fusion protein. This vector contains the pBIN multiple cloning site (Bevan, 1984), with a GFP cassette and the 35S promoter and terminator. Seven day-old *Arabidopsis* Col-0 seedlings were used to extract RNA to synthesize the cDNA of *AtVAMP714*. Primers 5g22360 Pac 1 For and 5g22360 Bstx 1 Rev were used to amplify the *AtVAMP714* coding region. The Expand™ KOD HOT Start PCR system (section 2.15.2) was used to amplify the fragment from cDNA. The product was analysed by gel electrophoresis (section 2.8) and a band of expected size (220bp) was obtained (Figure 4-9).

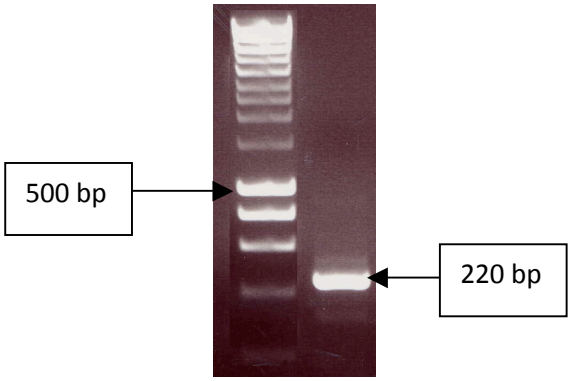

Figure 4-9: PCR amplification of AtVAMP714 from Col-0 gDNA

The PCR product was cloned directly into the pCR®2.1-TOPO vector (section 2.10.5) and introduced into chemically competent TOP10 One shot™ cells (section 2.10.5.2). Five positive white colonies were isolated. The plasmid DNA was prepared as described in section 2.7.1 and was sequenced with universal primers *M13F* and *M13R* and cDNA for-2 and cDNA for-3 internal primers. The correctly constructed sequence from one colony was used for cloning the *AtVAMP714* coding region into the pBIN-GFP vector.

The fragment was sequentially digested from the pCR®2.1-TOPO vector with Pac 1 and then Bstx 1 before being purified with Roche *High Pure* PCR purification kit (section 2.7.10). pBIN-GFP vector was digested with Pac 1 and Bstx 1 and dephosporylated before being ligated with the fragment overnight at 4^0C.

The ligation reaction mixture was introduced into chemically competent *E.coli* DH5α cells. Ten white colonies were used to prepare the plasmid DNA (section 2.7.1) and this was sequenced using pBIN-GFP seq A and 5g22360 Bstx 1 Rev primers. A colony containing the correct insert was identified, and the plasmid was introduced into *A. tumefaciens* strain C58C3 by triparental mating (section 2.12). The pro35S::AtVAMP714::GFP construct was then introduced to *Arabidopsis* var Col-0 by the floral dipping method (section 2.13).

In this construct, Basta was used as the selectable marker. Basta-resistant T1 transgenic seedlings were selected by sowing approximately 0.5 ml of seeds in soil trays. Germination was synchronised by treatment at 4^0C for 3-4 days and seedlings were sprayed first upon emergence and twice afterwards at 3-day intervals with 0.4% Basta (Basta®, 20% glufosinate ammonium). Basta resistant seedlings remained green while sensitive seedlings became bleached 7-10 days after germination (DAG) on the selective medium. Basta-resistant transformed (T1) plants were identified and transferred to pots and grown to maturity. Plants were bagged at flowering to prevent cross-pollination and T2 seeds were collected as individual lines for further analysis.

Table 4-6: Green-white plant selection for pro35S::AtVAMP714::GFP transgenic seedlings

Line no	Bas^R	Bas^S	Ratio
1	57	3	19:1
2	43	15	**3:1**
3	40	17	2:1
4	50	7	7:1
5	52	8	6:1
6	41	9	4:1
7	48	12	**3:1**
8	49	8	8:1
9	58	2	28:1
10	50	8	8:1
11	54	4	13:1
12	32	10	**3:1**
13	45	15	**3:1**
14	47	12	**3;1**
15	54	6	9:1
16	43	14	**3:1**

Lines that showed Basta resistance with an approximately 3:1 segregation ratio were expected to contain T-DNA at a single locus. Six individual lines (line 2, 7,12,13,14 & 16) containing pro35S::AtVAMP714::*GFP* showed the 3:1 segregation with Basta selection (Table 4-6) . This revealed that these plants have single T-DNA insertion. The T3 seeds harvested from above plants were subjected to Basta segregation analysis as above to identify lines that were homozygous for the T-DNA insertion. Lines 2, 7 and 14 shown to be homozygous and the seed were bulked up and T4 seed was used for further experimental analysis.

4.3.2 Transient Expression of *pro35S::AtVAMP714::GFP*

Transient expression of *pro35S*::*AtVAMP714::GFP* construct was observed in onion epidermal peels following microprojectile bombardment using the Helios Gene Gun system. Onion tissues were used because they lack chlorophyll (and no background autofluorescence), allowing clear visualization of GFP. Gold-coated tubing sections (1 cm) were covered with DNA bound to the gold particles to function as cartridges for the Helios Gene Gun (Section 2.16.2) .

The onion tissues were prepared by taking tissues with an intact inner transparent layer. The gold-coated bullets were then inserted into a cartridge holder and then filled into the breach of the gun. After setting up the Helios Gene Gun, the onion section was placed on a petri dish containing wet filter paper. 5-10 bullets were fired onto the onion peel. Plates containing bombarded onion sections were covered with aluminium foil and incubated at 22^0C overnight.

After incubation, the inner layer of the onion tissue was peeled off carefully and mounted on a glass slide with drop of water, covered with a coverslip and viewed under the SP5 Laser Scanning Microscope (section 2.17). The GFP localization pattern was determined (Figure 4-10A).

4.2.3 Co-localization of AtVAMP714:GFP with a Golgi Marker

The expression pattern of *pro35S:: AtVAMP714::GFP* in onion epidermal tissues suggested that the GFP was localized to Golgi. Previous evidence also suggested Golgi localization of AtVAMP714, though vacuolar localization has also been postulated (Umera *et al*., 2005 and Sanderfoot *et al*., 2003, 2007). To confirm this localization pattern, transient experiment was repeated with a Golgi::RFP marker (kindly supplied by Hussey Group, Durham University). The two plasmids (*pro35S:AtVAMP714::GFP* and *Golgi::RFP*) were mixed together and then introduced into onion epidermal cells as described in section 2.16.2. Gold-coated tubing sections (1 cm) were covered with DNA bound to the gold particles to function as cartridges for the Helios Gene Gun were introduced into onion cells and incubated at 22^0C for overnight.

After incubation, the inner layer of the onion tissue was peeled off carefully and mounted on a glass slide with drop of water, covered with a coverslip and viewed under the SP5 Laser Scanning Microscope (section 2.17). Colocalization of the markers was observed, confirming that AtVAMP714 protein is localized to Golgi and Golgi vesicles (Figure 4-10 D & E-G).

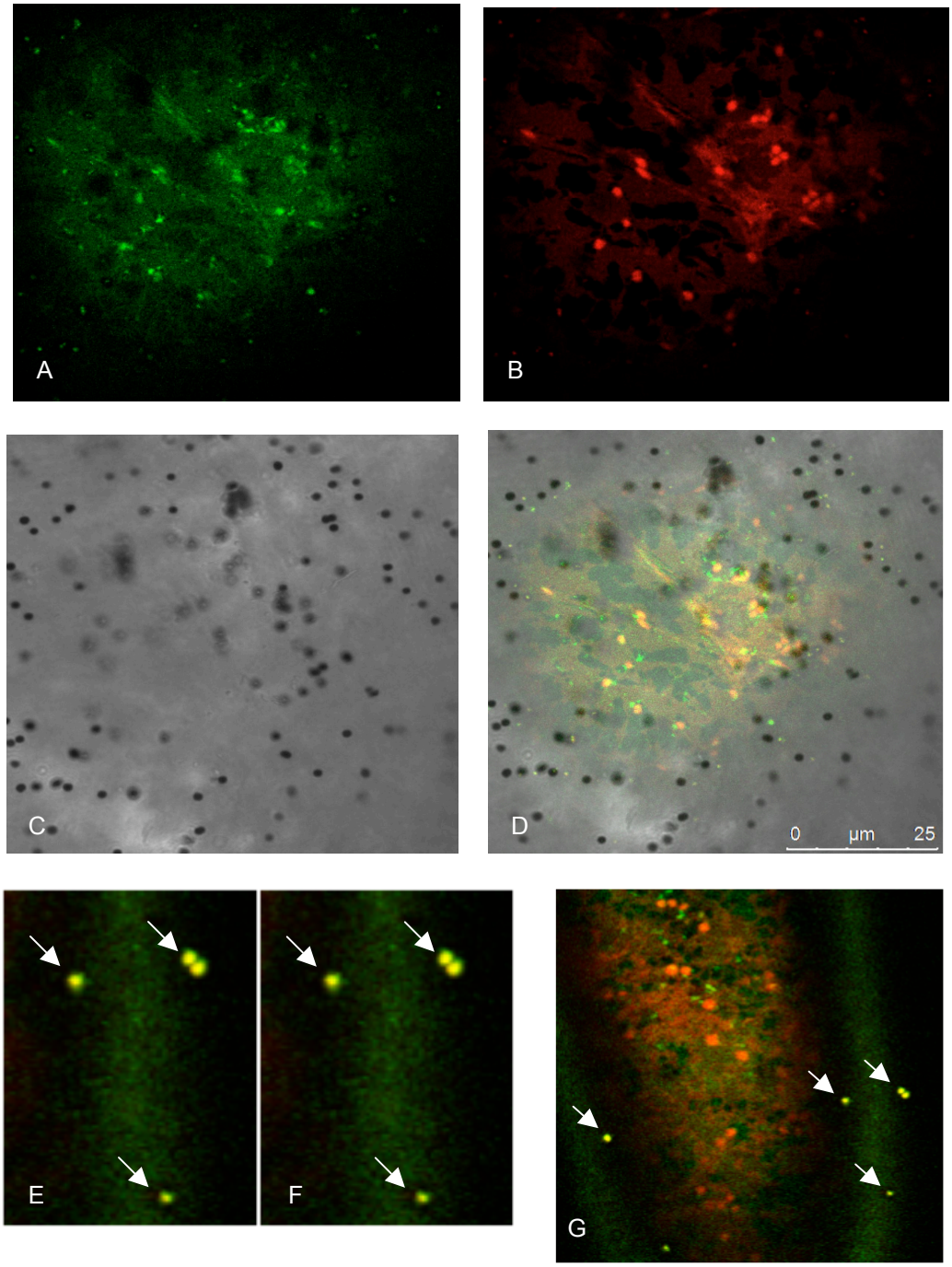

Figure 4-10: Subcellular localization of AtVAMP714

A; Expression pattern of AtVAMP714::GFP on onion epidermal cell

B: Expression pattern Golgi::RFP on onion epidermal cell

C: Insertion of gold particles in onion epidermal cells

D: Merge of AtVAMP714::GFP and Golgi::RFP (A and B)

E, F and **G**: AtVAMP714 localization to Golgi vesicles- Arrows indicate the co-localization with vesicles

4.3.4 pro35S::AtVAMP714*::*GFP Expression in Stable Transformants

Plants expressing pro35S::AtVAMP714::GFP in basta-resistant T4 seedlings which showed 3:1 segregation lines were screened for GFP activity in the roots using a Leica SP5 Laser Scanning Microscope (section 2.17). Roots were analysed because of ease of GFP visualization in the outer cell layers. In all the lines observed, GFP expression is widely observed in vesicles. In some root cells, large round shape structures were observed. It is possible that these structures could represent the aggregation of vesicles, due to protein overexpression. Therefore the pro35S::AtVAMP714::GFP expression pattern in the stable transformants was similar to the observed transient expression (Figure 4-11).

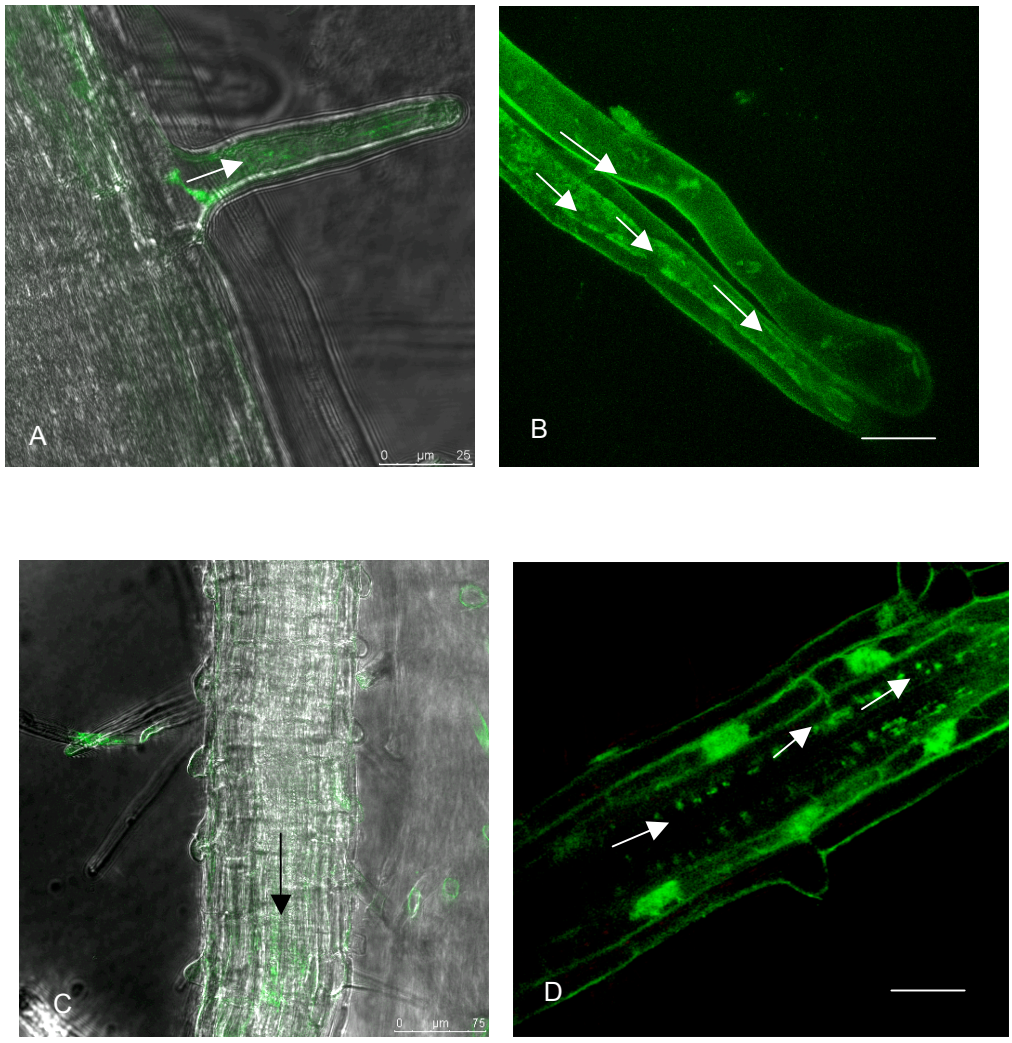

Figure 4-11: GFP expression in stable transformants

A and **B**: GFP expression in root hairs; arrow heads show the GFP expression in vesicles

C: GFP expression in main root;

D: GFP expression in main root showing aggregates of vesicles; arrow heads show the GFP expression in vesicles; scale bar = 30 µm

4.4 Co-localization of AtVAMP714::CFP and PIN1:GFP

The first fluorescent protein emitting in the bluish-green cyan spectral region (CFP; ranging from approximately 470 to 500 nanometers) was discovered simultaneously with BFP during mutagenesis studies that converted the tyrosine residue in the GFP chromophore to tryptophan. This single mutation yielded a chromophore that displays an absorption maximum at 436 nanometers with a very broad fluorescence emission spectral profile centered at 485 nanometers with greater brightness and photostability and as a more useful protein for time-lapse imaging in localization and dynamics studies (Davidson *et al*., 2009).

In Section 4.1 it is described how the *AtVAMP714* promoter is active in root cells, using the *gusA* reporter gene. It was found that the promoter was active in the seedling roots during development and that this expression appeared to be in the vascular tissues of the root. In order to carry out co-localization studies with PIN1::GFP (which is expresed in vascular cells), a construct for the expression of AtVAMP714:CFP fusion protein in vascular cells was made and introduced into *Arabidopsis* by floral dipping.

4.4.1 Construction of the AtVAMP714::CFP

A pro*AtVAMP714*::*AtVAMP714:CFP* construct was made using the Gateway cloning system. A pGHGWC destination vector, which contains CFP (Cerulean Florescence Protein), was used for the insertion of the *AtVAMP714* promoter fragment and coding region. Appoximately 3.5 kilobases (kb) of the sequence (including 2 kb sequence upstream of the ATG of AtVAMP714, were selected as the putative promoter to be used in this work, Annex 3) were amplified using Phusion High Fidelity *Taq* (section 2.15.3). The gene sequence was amplified from the relevant BAC (Bacterial Artificial Chromosome). BAC DNA was prepared using BAC DNA Miniprep Kit (NORGEN, UK) DNA (section2.7.5) and a band of 3.5 kb was obtained as expected (Figure 4.12). The PCR product was cloned directly into the pCR® 2.1 TOPO vector (section 2.10.5) and introduced into TOP10 One shot ^{TM} competent cells (section 2.10.5.2). Putative positive white colonies were checked by preparing plasmid DNA (section 2.7.1) and sequencing using the universal primers *M13* Forward and *M13* Reverse and as well as the internal primers- cDNA for-1, cDNA for-2 and cDNA for 3 (Annex 1) designed for sequencing to verify that no errors had been introduced during the PCR amplification.

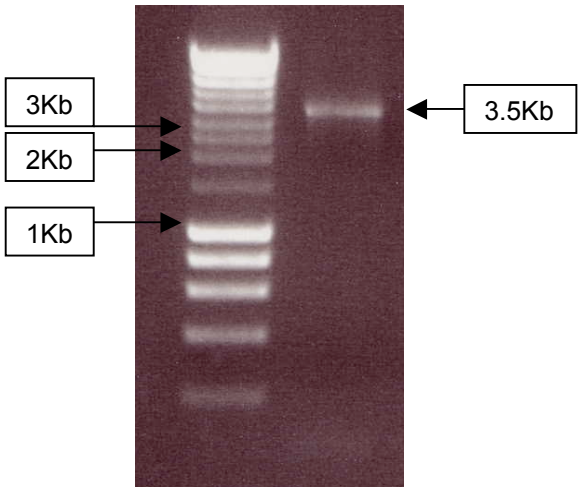

Figure 4-12: PCR amplification of pro*AtVAMP714* and *AtVAMP714* from BAC DNA

The plasmid was then linearized with EcoR V and buffer B for an hour at 72^0C, followed by heat inactivation of the enzyme at 65^0C for 10 minutes. The digest was analysed by gel electrophoresis (section 2.8) and then the plasmid was purified using Roche *High Pure* PCR kit (section 2.7.10). The BP cloning reaction as described in (section 2.9.6.2) was performed into pDNOR207 entry vector and then introduced into chemically competent DH5α *E.coli* cells (section 2.10.6.3). Putative positive colonies were isolated using Gentomycin (35 µg/ml) selection and plasmid DNA was prepared (from five colonies as described in section 2.7.1). DNA from these colonies was sequenced with pDNOR207 Forward and Reverse primers.

The colony 1 was identified as in-frame with gateway *att*R1 and *att*R2 sites and also with the correct insert, and was used to perform LR cloning (section 2.10.6.4). The LR reaction was performed between pDNOR207 containing the *AtVAMP714* promoter sequence and the pGHGWC destination vector. The reaction was introduced into DH5α *E.coli* (section 2.10.6.3) cells and kanamycin resistant colonies were identified. The plasmid DNA from five colonies were prepared (section 2.7.1) and sequenced with 360-cDNA-4 Forward internal primer to check whether the insert was in-frame with gateway sequences. The Gateway cloning strategy for production of pro*AtVAMP714*::*AtVAMP714*::*CFP* was summarized below.

AtVAMP714 promoter fragment amplified by PCR from BAC genomic DNA with *att*B Gateway linkers

↓

Promoter fragment cloned into the PCR® 2.1-TOPO vector, sequenced and TOPO vector linearized with ECOR V

↓

BP reaction performed to transfer *AtVAMP714* promoter to pDNOR207 Donor vector, recombinent plasmids were isolated

↓

LR reaction performed to transfer *AtVAMP714* promoter sequence to pGHGWC Destination vector

↓

Recombinant plasmid isolated and sequenced to verify

The pGHGWC vector containing the *AtVAMP714* promoter and coding sequence CFP fusion was then introduced into *Agrobacterium tumefaciens* strain C58C3 by triparental mating (section 2.12). Then the construct was introduced into *Arabidopsis* var Col-0 and PIN1:GFP plants by the floral dipping method (section 2.13).

4.4.2 pro*AtVAMP714*:: *AtVAMP714::CFP* Expression in PIN1::GFP Plant

T1 seeds from the dipped plants were collected and sown onto ½ MS10 medium supplemented with 20-µg/ml hygromycin and 40 -µg/ml augmentin. Hygromycin-resistant seedlings were selected 7-10 days after germination.

7-10 days after germination the transformed seedlings remained green while untransformed seedlings were brown. Transformed seedlings did not develop any root or shoot system (Figure 4-13). Therefore pro*AtVAMP714*::*AtVAMP714::CFP* expression was observed in F1 transformants.

The expression pattern of PIN1::GFP and AtVAMP714::CFP show localization in the same compartments indicating that the nature proteins are also localized to the same vesicles (Figure 4-14).

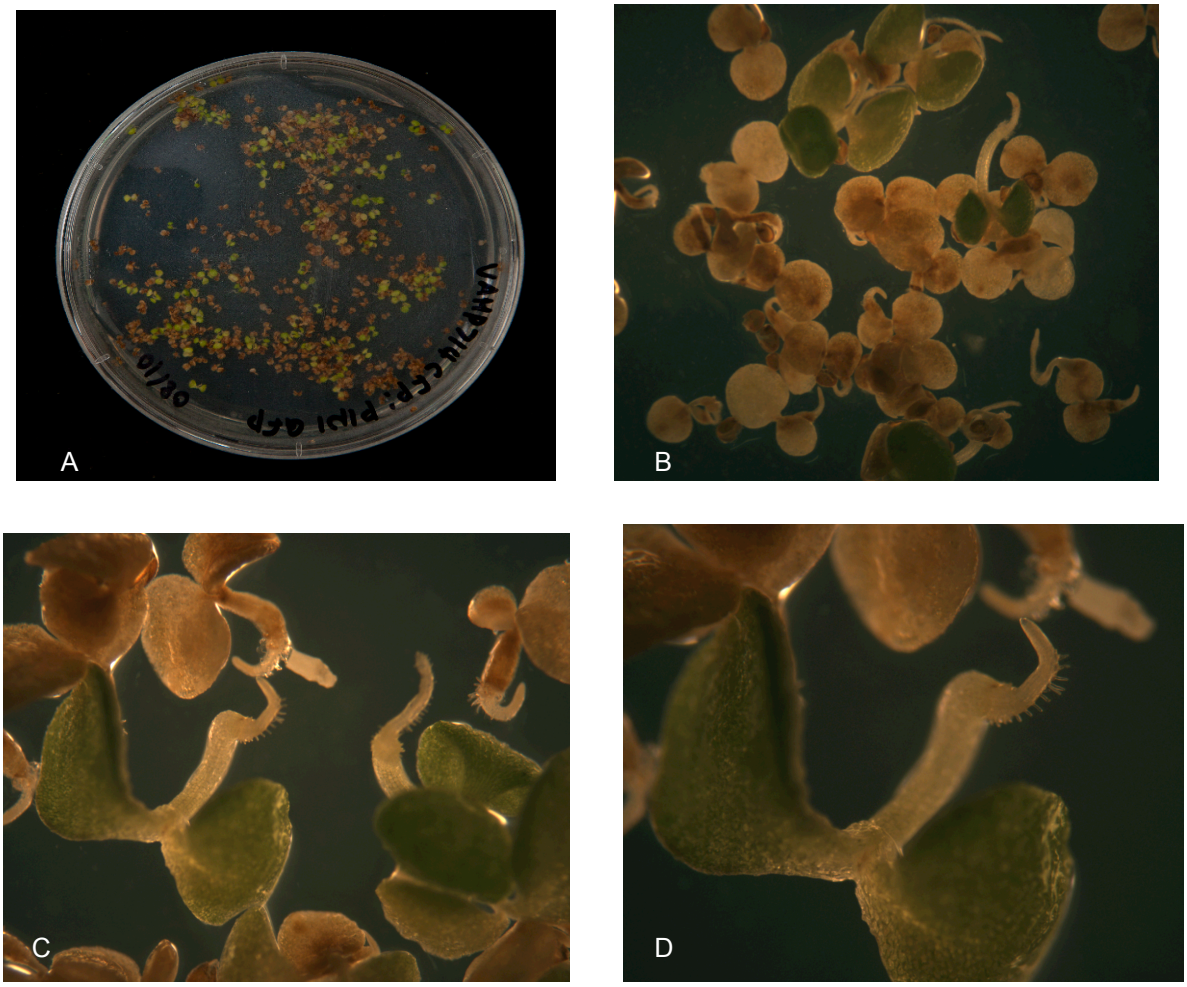

Figure 4-13: PIN1::GFP seedlings expressing pro*AtVAMP714*::AtVAMP714::CFP construct on hygromycin plates

A: Hygromycin selection plate

B: Transformed seedlings with untransformed ones in a selection plate mag x1

C: Transformed seedlings mag x1.5

D: Transformed seedling mag x2

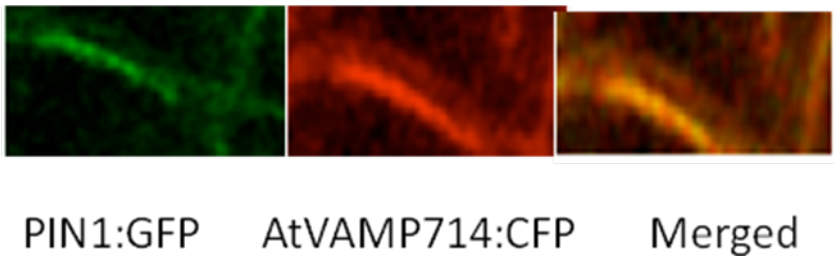

Figure 4-14: AtVAMP714::CFP and PIN1::GFP colocalization

A: PIN1:GFP expression in F1 transformants

B: AtVAMP714: CFP expression in F1 transformants in the same cell

C: Co-localization of: PIN1::GFP and AtVAMP714::CFP

Summary

The results presented in this chapter detailed the analysis of pro*AtVAMP714*::GUS expressing plants. This showed that the *AtVAMP714* promoter was active in the hypocotyl and vascular tissues of the main and lateral roots. The GUS expression was strongest at the root-hypocotyl junction and faded towards the root tip. The activity of the *AtVAMP714* promoter in the vascular tissues was confirmed by the analysis of transverse sections of GUS expressing roots.

Treatments of pro*AtVAMP714*::GUS lines with plant hormones were also carried out to check whether the promoter is hormonally regulated. The naturally occurring auxin IAA appeared to alter the *AtVAMP714* promoter activity and lead to expression of GUS at the root tip and cotyledons. The auxin efflux carrier inhibitor TIBA also alter the expression leading to GUS expression in the leaves of the seedlings due to auxin is trapped in the aerial parts. The ethylene precursor ACC and Cytokinin analog BA did not appear to significantly affect the promoter activity.

Plants carrying p35S:AtVAMP714::GFP localized to Golgi and Golgi vesicles and confirmed by co-localization with RFP Golgi marker.

Finally, plants carrying AtVAMP714::CFP fusion protein under the control of *AtVAMP714* promoter was generated and introduced into PIN1::GFP plants. AtVAMP714::CFP fusion protein and PIN1::GFP show localization in the same compartments.

Chapter 5: Mutation, Overexpression and Dominant Negative Studies

Chapter 5: Mutation, Overexpression and Dominant Negative Studies

The results presented in the previous chapter detailed how *proAtVAMP714::GUS* was active in the hypocotyl and vascular tissues of the main and lateral roots of *Arabidopsis*. The activity of the *AtVAMP714* promoter in the vascular tissues was confirmed by the analysis of transverse sections of GUS-expressing roots. AtVAMP714:GFP fusion protein was found to be localized to Golgi vesicles. *AtVAMP714* gene expression was positively upregulated by auxin. The aim of the work described in this chapter was to analyse the *AtVAMP714* overexpressors for developmental defects, and the production and analysis of *atvamp714* mutants to further investigate the function of the *AtVAMP714* gene.

The *AtVAMP714* overexpressors exhibit reduced apical dominance and short internodal lengths. Young seedlings exhibit abnormal leaf shape (Figure 5-1). This phenotype suggested possible defects in auxin biosynthesis, transport or sensitivity. Auxin is an important regulator of root and shoots growth and development. The distribution of auxin from the site of synthesis, and its relationship to auxin-mediated development has been a major area of study since polar auxin transport was first established (Leyser, 2006). To determine whether the auxin distribution is disrupted in the *AtVAMP714* overexpresses, root and shoot auxin transport levels were measured using a radio-labelled IAA assay. The expression levels of *IAA1* and *IAA2* were determined using qRT-PCR since *IAA* family of genes are well characterized auxin responsive genes (Guilfoyle *et al*., 2002). The establishment of an auxin gradient and maximum in roots is critical for plant development and this is determined by correct PIN localization (Blilou *et al*., 2005). In this project, immunolocalization was used to determine PIN1 and PIN2 localization in *AtVAMP714* overexpressors. *AtVAMP714* is a member of a gene family; the auxin regulated gene expression of the *AtVAMP7-1* family members was determined using qRT-PCR to gain an insight into the auxin regulation of the family.

Arabidopsis SALK knockout lines for *AtVAMP714* were obtained from NASC and screened by PCR for T-DNA insertion in the gene. To characterize the developmental role of the gene, the knockout *atvamp714* mutant phenotype was identified and analysed for developmental defects. To further investigate the function of the gene *AtVAMP714* gene, dominant negative transgenics were generated and studied. This construct was made deleting the transmembrane domain, which plays an essential role in membrane fusion (www.prosite.org). The construct was introduced into *Arabidopsis* plants by floral dipping method, and F2 plants were analysed for developmental defects.

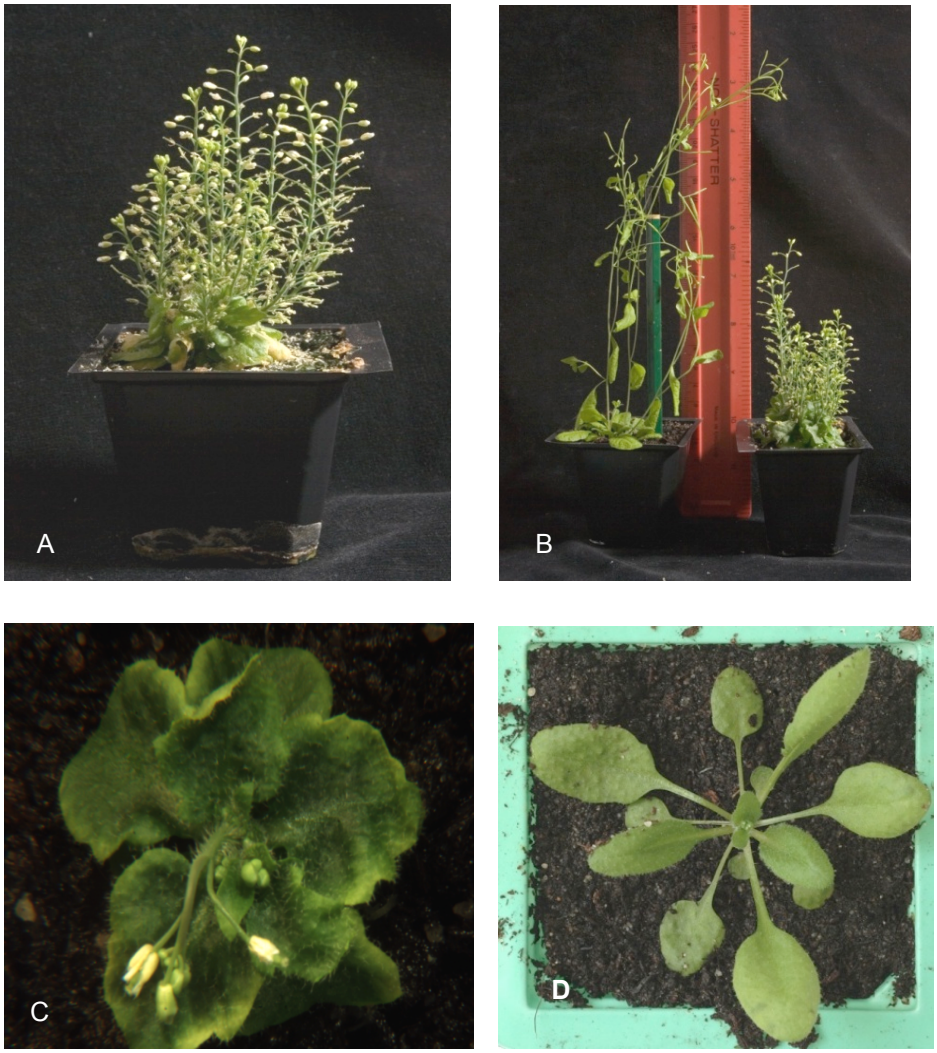

Figure 5-1: *AtVAMP714* overexpressors and Col-0 wild type plants

A: *AtVAMP714* overexpressing phenotype (8 weeks old) showing loss of apical dominance or increase axillary branching with short internodal lengths

B: comparison with a Col-0 Wild type plant and *AtVAMP714* overexpressing phenotype

C: *AtVAMP714* overexpressing seedling (3weeks old) showing abnormal leaf shape

D: Col-0 Wild type seedling showing the leaf shape

5.1 Analysis of *AtVAMP714* Overexpressors

5.1.1 Measurement of Root and Shoot Auxin Transport in *AtVAMP714* Overexpressors

The overexpression of *AtVAMP714* gene lead to a number of developmental defects including loss of apical dominance, short intermodal lengths and abnormal leaf shape similar to developmental defects that resemble those caused by interfering with auxin synthesis, transport or perception (Figure 5-1). To determine whether auxin distribution was disrupted in *AtVAMP714* overexpressors, auxin transport levels in roots and shoots were measured using radioactive IAA transport assay (based on Okada *et al*. 1991).

An acropetal auxin transport level was measured in roots as described in section 2.5.1. ^{3}H-IAA was applied to seedlings just below the root-shoot junction, and transport was allowed to take place for 1 h per cm of root tissue. Root tips were excised and incubated for 48 hours in scintillation fluid (EcoScint A - National Diagnostics) prior to counting, and data were expressed as Counts per Minute (CPM) for each root sample.

Basipetal shoot auxin transport level was measured as described in section 2.5.2. Inflorescence stem segments of 2.5 cm were cut and the apical end placed in the MSMO medium. Non-inverted samples were included to control for non-specific transport (NI) and non-radioactive (NR) samples were used to detect the base line activity and contamination. Samples were incubated in ^{3}H-IAA for 18 h before scintillation counting.

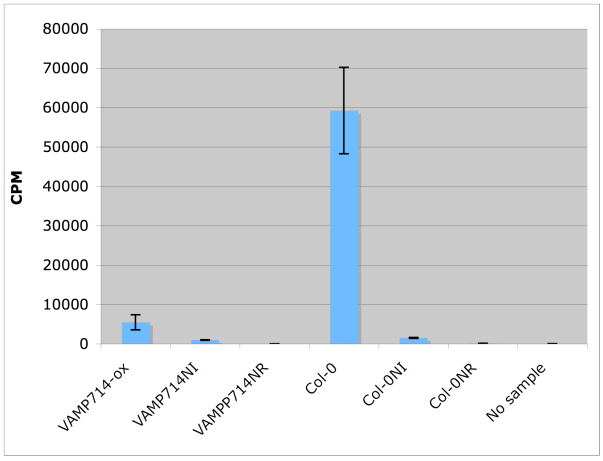

Shoot auxin transport

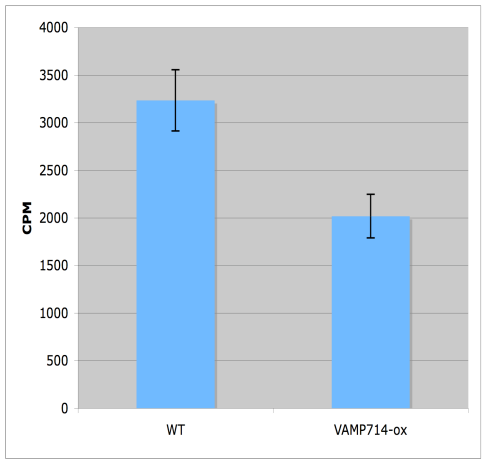

Root auxin transport

Figure 5-2: Root and Shoot auxin transport level of *AtVAMP714* overexpressors and Col-0 wild type plants

Data were taken as Counts per Minutes (CPM) and error bars represent the Standerd Error. In shoot auxin transport; NI=Non-inverted shoot sample, NR= Non-radioactive sample, VAMP714-ox= *AtVAMP714* overexpressors, WT=Col-0 wild type plants

The results, shown in Figure 5-2, show that the levels of root and shoot auxin transport in the *AtVAMP714* overexpressors were significantly reduced compared to *Arabidopsis* Col-0 wild type plants. This results suggests that auxin transport mechanisms are defective in the *AtVAMP714* overexpressors.

5.1.2 Expression Levels of *IAA1* and *IAA2* Genes

The *IAA* family of genes is transcriptionally rapidly up-regulated by auxin (Guilfoyle *et al*., 2002). The expression levels of the *IAA1* and *IAA2* gene were determined using qRT-PCR analysis, in order to determine whether defective auxin transport might also lead to defective auxin responses in the *AtVAMP714* overexpressors. RNA was extracted from *Arabidopsis* Col-0 wild type plants and *AtVAMP714* overexpressors as described in section 2.7.6. cDNA synthesis was carried out as in section 2.7.8 and qRT-PCR was carried out using *IAA1* and *IAA2* primers (Annex 1). Comparative quantification software supplied with the Rotorgene thermal cycler was used to analyse the data. *ACTIN2* was used as a housekeeping gene, for comparative analysis (section 2.15.6.3).

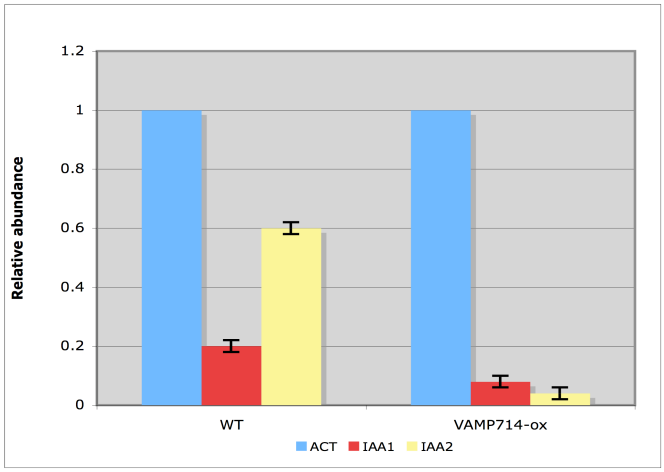

Figure 5-3: *IAA1* and *IAA2* gene expression

Quantitative RT-PCR analysis of the *IAA1* and *IAA2* gene expression in *AtVAMP714* overexpressors (VAMP714-ox) and Col-0 wild type plants (WT) relative to *ACTIN2* at 7 days after germination**.** These data are representative of two independent experiments using biological replicate samples. The error bars represent Standard Error of three technical replicates. Y axis represents the relative abundance of the transcript level

The results show that, in wild-type plants, *IAA1* and *IAA2* expression levels is lower than that of *ACTIN2,* but with *IAA2* being more strongly expressed than *IAA1*. In the *AtVAMP714* overexpressors, however, both *IAA1* and *IAA2* transcripts were lower abundance compared to levels in the the wild-type plants, and *IAA2* was expressed at a particularly low level (Figure 5-3). These results suggest that auxin repsonses, as monitored by the expression levels of these two auxin-responsive genes, are reduced in the *AtVAMP714* overexpressors compared to wild-type.

5.1.3 Auxin-regulated Expression of VAMP7-1 Gene Family

Auxin-regulated expression of the VAMP7-1 gene family members (VAMP714, VAMP713, VAMP712 and VAMP711) was analysed using qRT-PCR with gene specific primers (Annex 1). Auxin-treated *Arabidopsis* Col-0 wild type plants were grown on agar plates for 12, 24 and 36 hours in the presence of 100 µg/ml IAA, and as control, Col-0 wild type plants were grown for the same time on agar plates lacking IAA.

Arabidopsis var Col-0 seeds were surfaced sterilized and germinated on ½ MS10 medium. Approximately 7 days after germination the seedlings were transferred to ½ MS10 medium supplemented with 100 µg/ml IAA. At 12, 24 and 36 hours after auxin treatment, seedlings were harvested and stored at -80ºC. RNA extraction and cDNA synthesis were carried out as

described in 2.7.6 and 2.7.8. qRT-PCR reactions were done using *VAMP714*, *VAMP713*, *VAMP712* and *VAMP711* gene-specific primers (Annex 1). Comparative quantification software provided with the Rotorgene was used to analyse the data using *ACTIN2* as a housekeeping gene.

The results clearly showed that among the VAMP7-1 family members only the *AtVAMP714* gene was upregulated by auxin. For this gene, the relative abundance of the transcript increased up to 24 hours of auxin treatment, and then declined. For all other genes, auxin repressed expression, and *AtVAMP713* was repressed most by the auxin treatment. These results show that *AtVAMP714* is differentially regulated by auxin compared to the other family members (Figure 5-4).

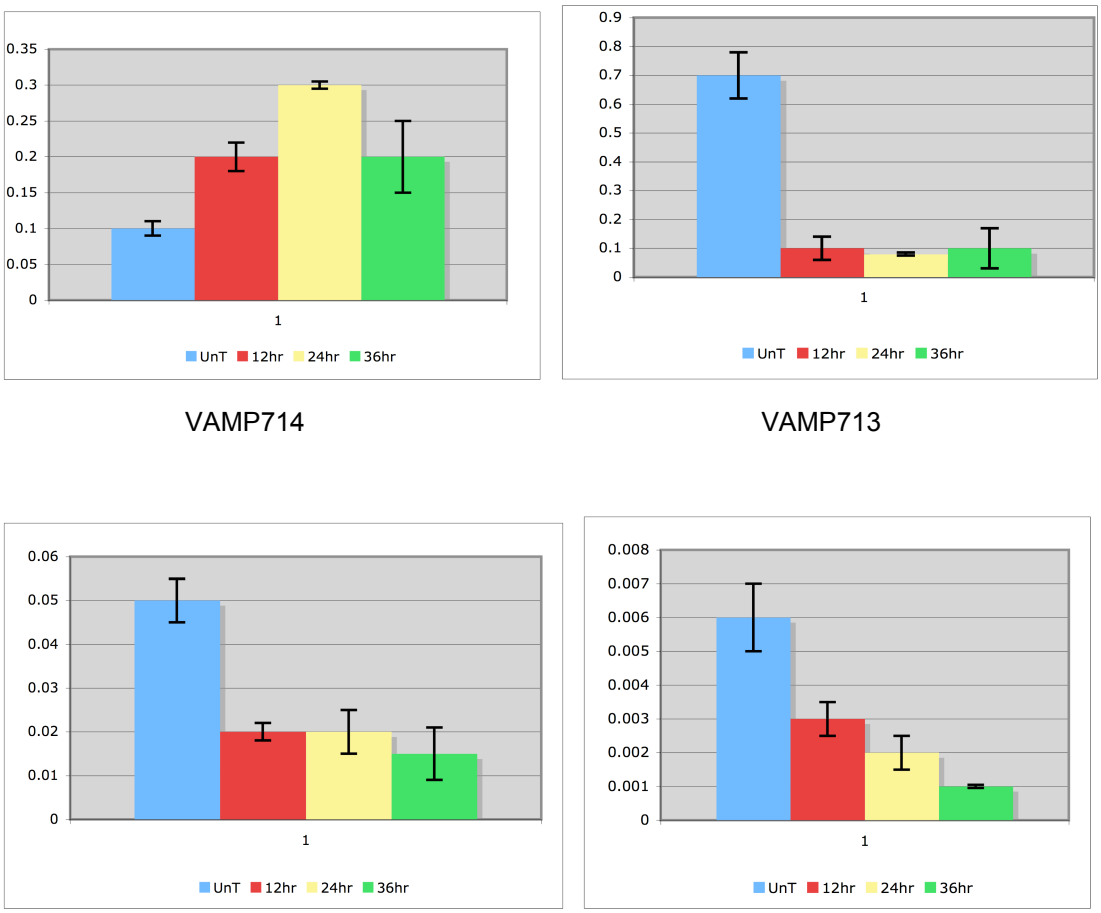

Figure 5-4 Auxin regulated gene expression of VAMP7-1 family

Quantitative RT-PCR analysis of the auxin regulated gene expression of VAMP7-1 family in Col-0 wild type plants relative to *ACTIN2* at 7 days after germination. These data are representative of two independent experiments using biological replicate samples. The error bars represent Standard Error of three technical replicates. Y axis represents the relative abundance of the transcript level.

5.1.4 PIN Localization of *AtVAMP714* Overexpressors

PIN1 and PIN2 localization was analysed in the *AtVAMP714* overexpressors using immunolocalization, and in *Arabidopsis* var Col-0 as a wild-type control. *Arabidopsis* var Col-0 and *AtVAMP714* overexpressing seeds were surfaced sterilized and germinated on ½ MS10 medium. Seven days after germination the seedlings were fixed as described in section 2.6. Then the aerial parts were removed and the roots were incubated with primary anti-PIN1 and anti-PIN2 for 24 hours. Then the roots were incubated with secondary anti-PIN1 and -PIN2 for 24 hours. Roots were examined using the Leica SP5 Laser Scanning Microscope (section 2.17).

In wild-type cells, PIN 1 was localized as expected at the basal membrane of cells in the central cylinder, and PIN2 was localized to the apical membrane of cells in the root cortex and epidermis. In the *AtVAMP714* overexpressors, both PIN1 and PIN2 were severely mis-localized as compared with Col-0 wild type plants. Both proteins were very poorly localized to the membrane, but rather were internalized (Figure 5-5). These results are consistent with the observed defective polar auxin transport seen on the *AtVAMP714* overexpressors, described above (Figure 5-1).

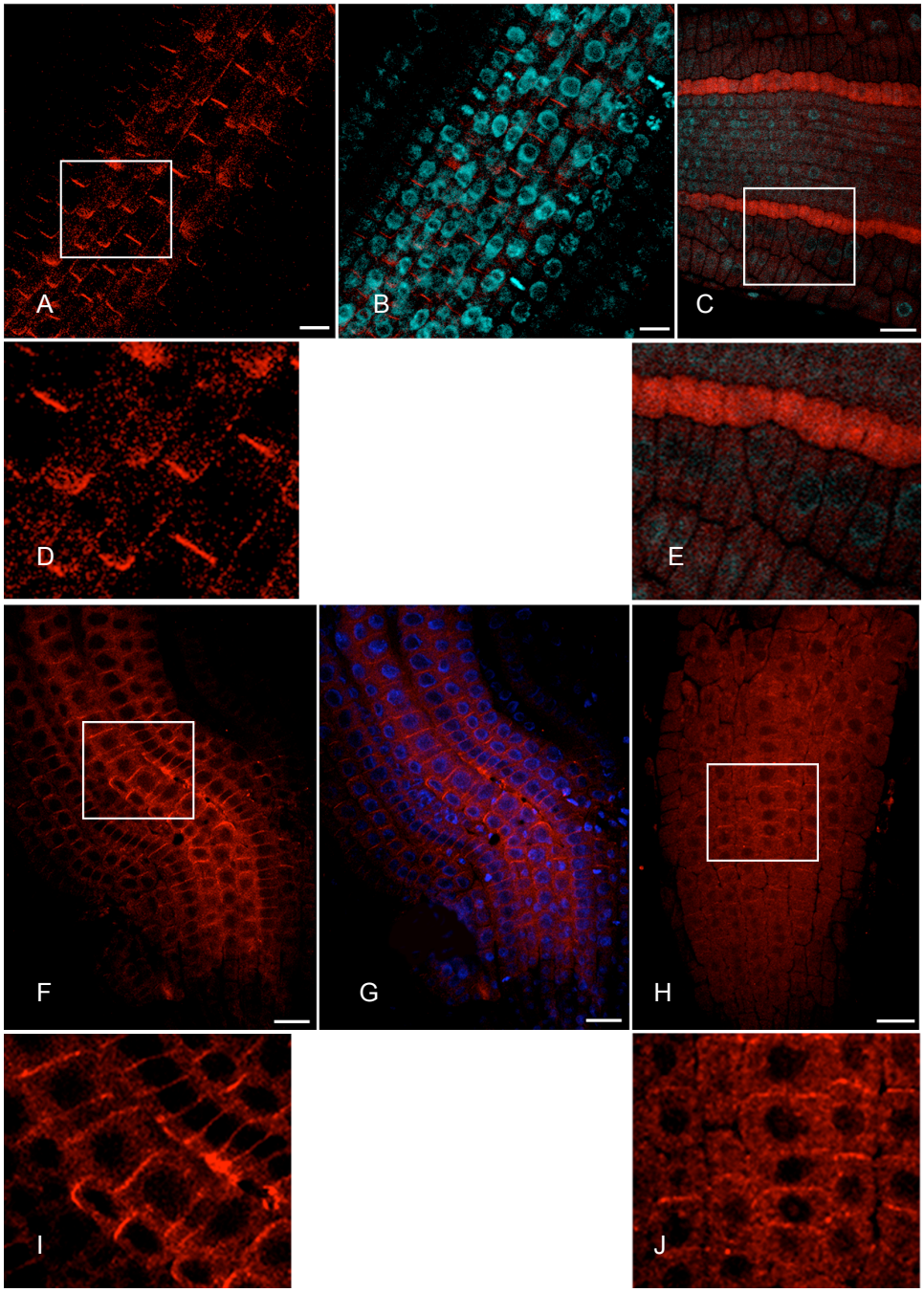

Figure 5-5: Immunolocalization of PIN1 and PIN2 in Col-0 wild type plants and *AtVAMP714* overexpressing plants

A: PIN1 localization in roots of wild type at 5-day post germination (bar =10µm)

B: PIN1 localization in roots of wild type with DAPI staining at 5 day post germination (blue colour represent the nuclei staining, bar=20 µm)

C: PIN1 localization in *AtVAMP714* overexpressing plants **(**bar=20 µm)

D: Close image of PIN1 localization in roots of wild type; PIN 1 localized to basal membrane of cells in the central cylinder (bar=20 µm)

E: Close image of PIN1 localization in *AtVAMP714* overexpressors (bar=20 μm)

F: PIN 2 localization in roots of wild type at 5-day post germination (bar =20μm)

G: PIN 2 localization in roots of wild type with DAPI staining at 5-day post germination (blue colour represent the nuclei staining, bar=20 μm)

H: PIN 2 localization in *AtVAMP714* overexpressing plants **(**bar=20 μm)

I: Close image of PIN2 localization in roots of wild type; PIN 2 localized to apical membrane of cells in the root cortex and epidermis (bar=20 μm)

J: Close image of PIN 2 localization in *AtVAMP714* overexpressors (bar=20 μm)

5.2 Analysis of Loss-of-function Mutants

In addition to the transgenic approach *Arabidopsis* SALK T-DNA insertion mutant lines were screened to identify a *atvamp714* knockout mutant for further analysis of the function of the *AtVAMP714* gene. The SALK insertion lines were screened using a PCR-based approach for a T-DNA insertion in the *AtVAMP714* gene and the both lines screened the T-DNA insertion is in the first intron. As described in the SALK web site the selectable marker is kanamycin resistance. However after several generations of growth, some of the lines show silencing of this gene (www.signal.salk.edu). Therefore, for SALK seedlings segregation analysis with kanamycin was not carried out.

5.2.1 Isolation of SALK knockouts containing an Insertion in the *AtVAMP714* Gene

The SALK T-DNA insertions were originally generated by the vacuum infiltration of Col-0 plants with vector pROK2 (www.signal.salk.edu). A PCR-based genotyping approach was used to identify the T-DNA insertion and homozygous plants among the F1 plants. Seedlings germinated from seed of the genotyped F1 plants were used to characterize the phenotype. The PCR-based genotyping approach involved genomic PCR using genomic primers, a second PCR using genomic and T-DNA left border primers and a third RT-PCR to confirm the absence of the transcript from the At5g22360 locus.

Potential SALK knockout lines for the *AtVAMP714* (At5g22360) gene were identified using the SIGnAL Arabidopsis Gene Mapping Tool (www.signal.salk.edu/cgi-bin/tdnaexpress) and TAIR (www.arabidopsis.org) web site. Two T-DNA insertion mutants were identified (SALK_005914 and SALK_005917) and in both lines the T-DNA insertion was predicted to be in the first intron. The positions of the T-DNA insertions in SALK_005914 and SALK_005917 lines are indicated in Annex 5.

Seeds of both SALK lines were obtained from the Nottingham Arabidopsis Stock Centre (NASC). Seeds were surfaced sterilized and germinated on ½ MS10 medium. After germination seedlings were transferred to soil as described in section 2.2.2.1. When F1 plants were 2-3 weeks old, 20 seedlings from each line were tested for T-DNA insertion by PCR. The results of these analyses are now described in detail.

5.2.2 Analysis of the SALK Insertion Mutants - Verification of Insertion Site in F1 Plants

To confirm the site of T-DNA insertion in the SALK lines, DNA was extracted from SALK seedlings using the DNA extraction method described in section 2.7.3. A genomic PCR amplification was carried out using 360 FOR (+1955) and 360 REV (-2568) primers and 360 REV (-2568) and T-DNA left border primer (LBa1). Using 360 FOR (+1955) as forward primer and 360 REV (-2568) as reverse primer, it was possible to amplify the *AtVAMP714* gene from the wild-type sample but not from the SALK_005914 or SALK_005917, as expected (Figure 5-6, G-PCR). Using 360 REV (-2568) as reverse primer and T-DNA left border sequence as forward primer (specific to amplification of T-DNA flanking sequences), a PCR product was however amplified from SALK line DNA samples, indicating the presence of a T-DNA insertion, but not from the wild type sample (Figure 5-6, LBa1). Results of the genotype analysis are summarised in Table 5-1 (details are in Annex 6, Table 1, 2 and Figure 1).

To determine whether the *AtVAMP714* gene is detectably expressed in the SALK lines, RNA samples were extracted from whole plants, subjected to cDNA synthesis and RT-PCR was performed using 360 FOR (+1955) and 360 REV (-2568) primers. The *AtVAMP714* mRNA was amplified only from the wild-type plant and not from SALK_005917 (Figure 5-6 RT-PCR), consistent with a T-DNA sequence being inserted in the first intron of the gene. The *ACTIN2* gene was used as a positive control for RNA quality and PCR conditions (Figure 5-6 and Annex 6- Figure 1).

Table 5-1: Summary of PCR with SALK T-DNA insertion lines

This summary table shows how we analyse the PCR results. For and Rev indicates forward and reverse primers designed for genomic PCR. LBa1 is the T-DNA left border primer. Forward and reverse primers were possible to give a product with wild type plants not with SALK T-DNA insertions. LBa1 primer and reverse primer were possible to give a product with SALK T-DNA insertions. The analysis of the 20 F1, SALK T-DNA insertion lines for SALK_005914 and SALK_005917 are listed in Annex 6, Table 1 and 2.

For+ Rev	LBa1	Genotype
+	–	Wild type
+	+	Heterozygous
-	+	Homozygous

Among the tested SALK seedlings (SALK_005914 and SALK_005917) two homozygous plants were identified from SALK_005917 (For details; Annex 6 Table 1 and 2; summary table 5-2).

Table 5-2: Genotype of SALK mutants for *AtVAMP714*

This table summarised the genotyping results obtained for SALK_005914 and SALK_005917

SALK line / Genotype	SALK_005914	SALK_005917
WT	14	12
Heterozygous	6	6
Homozygous	0	2

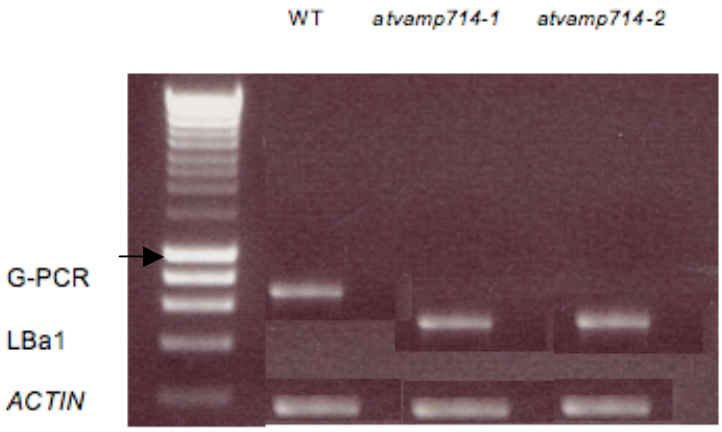

Figure 5-6: PCR for (SALK_005917) homozygous *atvamp714* knockout mutant and Col-0 wild type plant

WT is for Col-0 wild type plant, atvamp714-1 and atvamp714-2 indicate two homozygous lines obtained for SALK_005917 (Annex 5, Table 1). G-PCR indicates the genomic PCR with 360 FOR (+1955) and 360 REV (-2568) primers; product size 642 base pairs (bp). LBa1 indicates PCR using 360 REV (-2568) as reverse primer and T-DNA left border sequence (LBa1) as forward primer; product size 500 bp. Actin is the *ACTIN2* gene used as a positive control for RNA quality and PCR conditions; product size 180 bp. Arrow head= 1000 bp

5.2.3 Characterization of *atvamp714* Knockout Mutant for Developmental Defects

The SALK line 005917, identified as a homozygous knockout (*atvamp714*) mutation of the *AtVAMP714* gene, was used to characterize the developmental role of *AtVAMP714*. Homozygous seedlings were grown on soil and on agar plates for phenotypic analysis. At 14 days after germination, the homozygous mutants displayed similar phenotypes, being dwarfed with abnormal branching. Representative images are shown in Figure 5-8. When germinated on vertical agar plates (½ MS 10), seedlings were found to be smaller than wild-type with a reduced root system (Figure 5-8 A), which is now described.

5.2.3.1 Root Development in the *atvamp714* null Mutant

To further characterize the function of the *AtVAMP714* gene, its role in root development was investigated using *atvamp714* mutants. The seeds of the *atvamp714* mutant and Col-0 wild type were surfaced sterilized and germinated on ½ MS10 vertical plates. Seven days after germination the length of the primary root was measured and the number of lateral roots were counted. The observations were made over 21 days post germination. The primary root of the *atvamp714* mutant is significantly shorter than that of wild type seedlings (1.2±0.2 cm versus 3.5±0.5 cm, n=20, Figure 5-7A). The number of lateral roots was also found to be reduced in *atvamp714* mutants compared to the Col-0 wild type plants (3±1 versus 10±2, n=20, Figure 5-7B). These results show that a functional *AtVAMP714* gene is required for correct primary and lateral root development, since auxin distribution is important in regulating both primary and lateral root development; these observations are consistent with a possible role for *AtVAMP714* in auxin transport-mediated development.

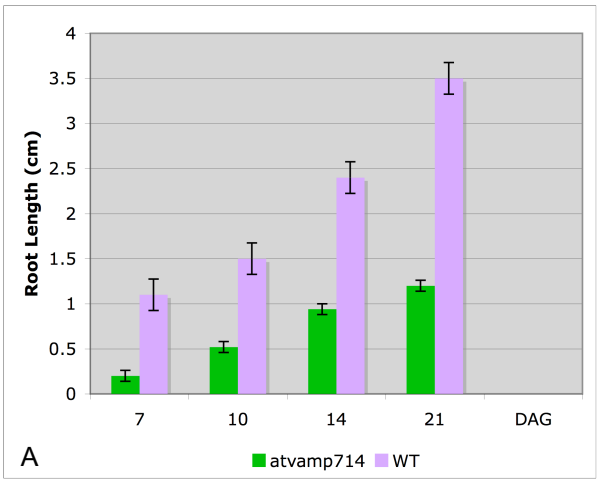

A

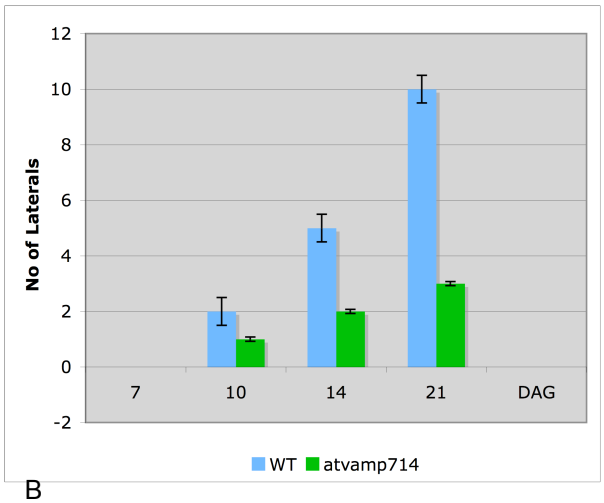

B

Figure 5-7: Length of the primary root (A) and number of laterals (B) in *atvamp714* knockout mutant compared with Col-0 wild type

The length of the primary root was measured and number of laterals was counted over the 21 days of growth (n=20). The error bars represent Standard Error; DAG= Days after Germination

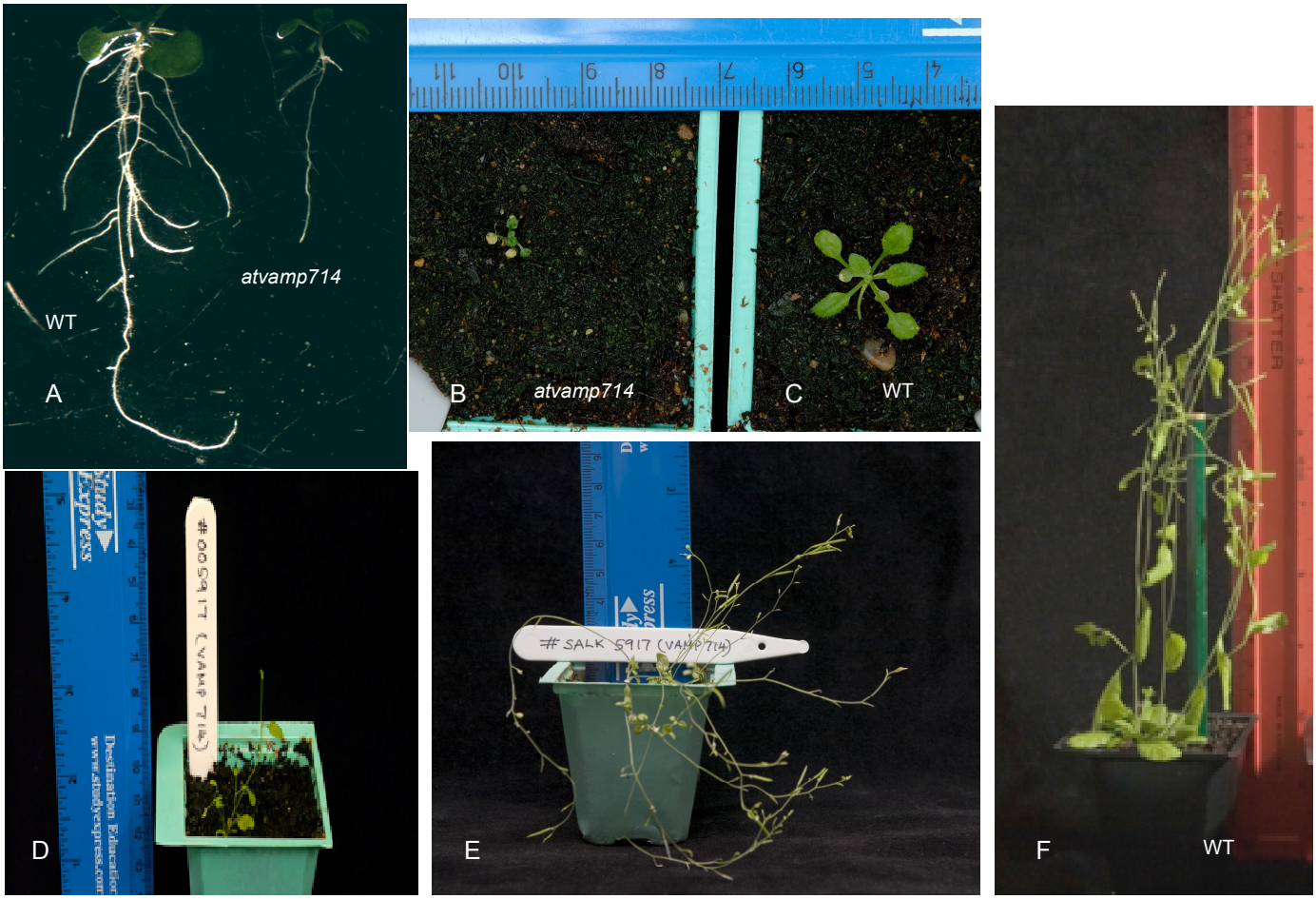

Figure 5-8: *atvamp714* knockout mutant phenotype

A: *atvamp714* knockout mutant (right) and Col-0 wild type (left) at 14 days after germination

B: *atvamp714* knockout mutant at 14 days after germination on soil

C: Col-0 wild type seedling at 14 days after germination on soil

D: *atvamp714* knockout mutant at 28 days after germination

E: *atvamp714* knockout mutant at 42 days after germination

F: Col-0 wild type plant at 42 days after germination

5.2.3.2 Gravitropic Response in the at*vamp714* Mutant

It has been demonstrated that polar auxin transport is important for gravitropic responses. The auxin efflux carrier PIN2, which is distributed asymmetrically within the root epidermal and cortical cells, and the influx carrier AUX1, play an important role in basipetal auxin transport in the gravitropic response of root elongation zone (Muller *et al*., 1999; Marchant *et al*., 1999). To determine whether the *atvamp714* mutants have any defects in auxin transport and it is affected tropic responses, gravitropic curvature was investigated.

atvamp714 mutant and wild type seedlings were grown on ½ MS10 agar plates for 5 days and turned to a 90° angle to measure the angle of bending towards the gravity (Section 2.4). The angle towards the gravity was measured after 8, 12 and 24 hours. The angles were used to compare the degree of bending towards gravity. The *atvamp714* mutant showed less bending towards gravity compared to Col-0 wild type (Figure 5-9 and 5-10). *atvamp714* mutants were found to be less gravitropic than wild type, 10% of *vamp714* mutants roots showed a true gravitropic response compared to 85% wild type (Figure 5-9). Representative seedlings are illustrated in Figure 5-10.

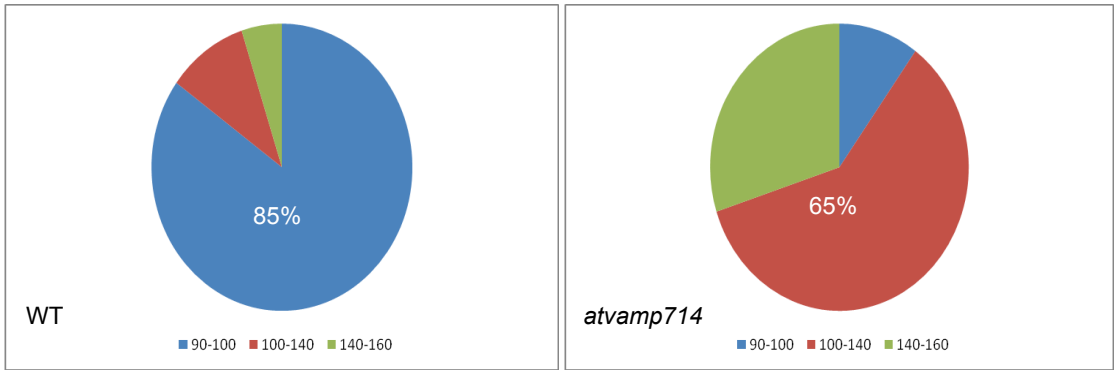

Figure 5-9: Diagrammatic representation of the frequency of Col-0 wild type and *atvamp714* mutants showing different gravitropic responses.

Before turning to 90°

Col-0 WT **vamp714**

8 hours after turning to 90°

12 hours after turning to 90°

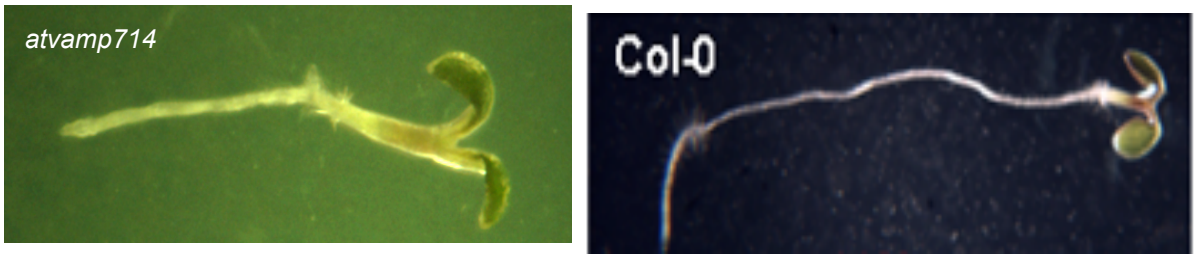

24 hours after turning to 90°

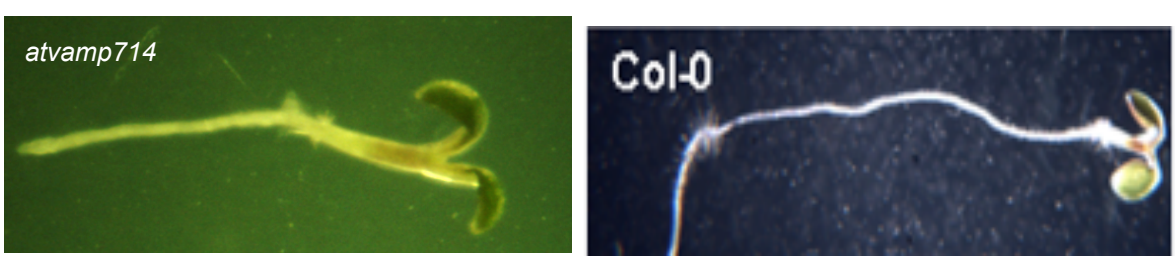

Figure 5-10: Gravitropic responses of Col-0 wild type plant and *atvamp714*

The angle of bending towards gravity at 8 hours, 12 hours and 24 hours after turning the plates at a 90° angle.

5.2.3.3 Characterization of cell identity and auxin distribution in *atvamp714* knockout mutants

QC cells act as a central organizer in the root meristem, the expression of the marker QC25, a marker of QC identity (Sabatini et al., 2003), was examined in the *atvamp714* null mutant to determine whether the observed root growth defects were associated with an inability to correctly specify QC cells. QC25 and *atvamp714* seeds were surfaced sterilized and germinated on ½ MS10 medium. Seven days after germination the seedlings were transferred to soil as described in section 2.2.2.1 and maintained in the greenhouse. When the plants started flowering the QC25 marker lines were crossed into *atvamp714* mutants as described in section 2.19. F1 plants were grown up to collect F2 seeds. Due to time constraints F2 seed was not analysed further.

The expression of the DR5::GUS reporter, a marker of auxin distribution or response (Sabatini et al. 1999) was examined in *atvamp714* mutants to determine whether the auxin distribution was disrupted or altered compared to wild-type. Both DR5::GUS and *atvamp714* seeds were surfaced sterilized and germinated on ½ MS10 plates and transferred to soil as described above. At the flowering stage the DR5::GUS marker line was crossed with the *atvamp714* mutant as described in section 2.19. F1 plants were grown up to collect F2 seeds. Due to time constraints F2 seed was not analysed further.

5.2.3.4 *PIN* gene Expression and Protein Localization in *atvamp714* null Mutants

The establishment of an auxin gradient and maximum in the root is critical for correct meristem organization, and this is determined by correct PIN protein expression and localization (Blilou et al., 2005; Grieneisen et al., 2007). To determine the *PIN* gene expression in *atvamp714* mutants, transcription analysis and PIN::GFP localization was carried out.

Transcript levels of *PIN1*, *PIN2* and *PIN4* in wild-type and *atvamp714* mutant seedlings were measured using qRT-PCR. Seeds were surfaced sterilized and germinated on ½ MS10 medium. Two weeks after germination seedlings were harvested; RNA extraction and cDNA synthesis were carried out as described in 2.7.6 and 2.7.8. qRT-PCR reactions were carried out using *PIN1*, *PIN2* and *PIN4* gene-specific primers (Annex 1). Comparative quantification software provided with the Rotorgene was used to analyse the data using *ACTIN2* as a housekeeping gene.

The results of the quantitative RT-PCR analysis are shown in Figure 5-11. In the wild-type, *PIN1* and *PIN2* genes are expressed at relatively high levels, with *PIN4* being expressed at a lower relative level, consistent with the more limited spatial expression gain for PIN4 (Friml *et al*., 2002, Wisniewaka *et al*., 2006). In the *atvamp714* mutant, the levels of transcript abundance of all three *PIN* genes is reduced compared with wild-type, with the levels of *PIN2* and *PIN4* being particularly low. This is interesting given a role for *AtVAMP714* in vesicle trafficking and auxin trasport, and is consistent with the view that a feedback regulation exists between auxin concentration and PIN expression/levels (Blilou *et al*., 2005; Grieneisen *et al*., 2007).

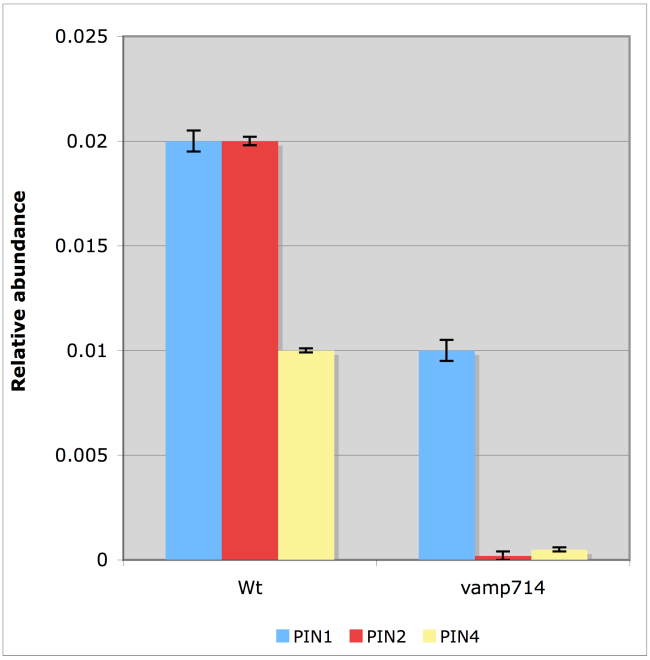

Figure 5-11: Transcript levels of *PIN* genes in the *atvamp714* mutant

Quantitative RT-PCR analysis of the PIN gene expression of *atvamp714* and Col-0 wild type plants relative to *ACTIN2* at 7 days after germination**.** These data are representative of two independent experiments using biological replicate samples. The error bars represent Standard Error of three technical replicates. Y axis represents the relative abundance of the transcript level.

To determine whether the reduced *PIN* gene transcript levels seen in the *atvamp714* mutant are reflected in PIN protein levels or localization, immunolocalization studies were carried out. *Arabidopsis* var Col-0 and *atvamp714* mutant seeds were surfaced sterilized and germinated on ½ MS10 medium. Seven days after germination the seedlings were fixed as described in section 2.6. Then the aerial parts were removed and the roots were incubated with primary anti-PIN1 and -PIN2 antibodies for 24 hours. Then the roots were incubated with secondary

anti-PIN1 and -PIN2 antibodies for 24 hours. Regions of interest of the roots were selected for imaging using the Leica SP5 Laser Scanning Microscope (section 2.17).

In wild-type cells, PIN 1 was localized as expected at the basal membrane of cells in the central cylinder, and PIN2 was localized to the apical membrane of cells in the root cortex and epidermis. In the *atvamp714* mutants, both PIN1 and PIN2 were localized in similar pattern as with Col-0 wild type plants. But both proteins were very poorly localized to the membrane, rather were internalized. Therefore PIN1 and PIN2 accumulation in membrane and cytoplasm were measured using *Image J* software and the membrane to cytoplasm ratios were calculated (Figure 5-12).

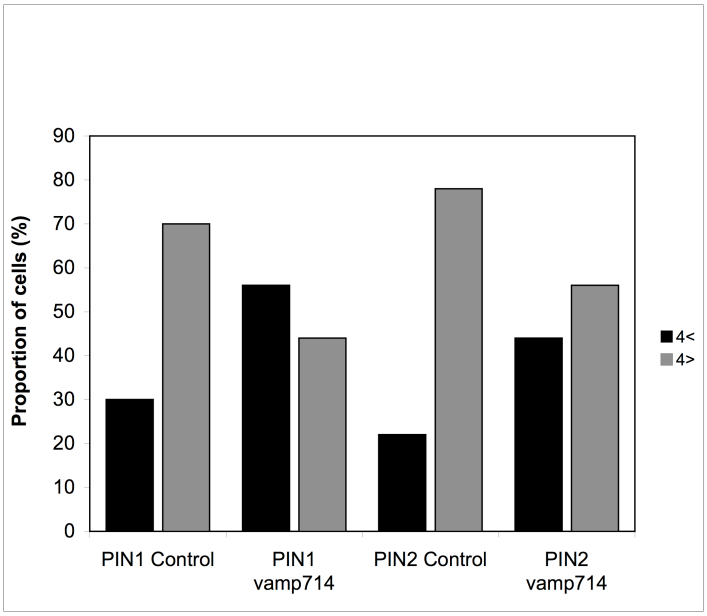

Figure 5-12: PIN1 and PIN2 accumulation

PIN1 and PIN2 accumulation (fluoresence signal) in both membrane and cytoplasm were measured in populations of cells using *Image J* software, and membrane to cytoplasm ratios were calculated (n=100 cells). Black bars represent the proportion of cells in which the ratio of fluorescence signal between membrane and cytoplasm is less than 4. Grey bars represent population of cells in which the ratio of fluorescence signal between membrane and cytoplasm is greater than 4.

The results show that, in the controls, most cells (>70%) exhibited PIN1 and PIN2 localization predominantly at the plasma membrane, as expected. In the *atvamp714* mutant, both PIN1 and PIN2 accumulated to lower relative levels at the plasma membrane, with a relatively high intracellular accumulation. These results are consistent with the *atvamp714* mutant being defective in its ability to localize correctly PIN1 and PIN2 (Figure 5-13 and 5-14).

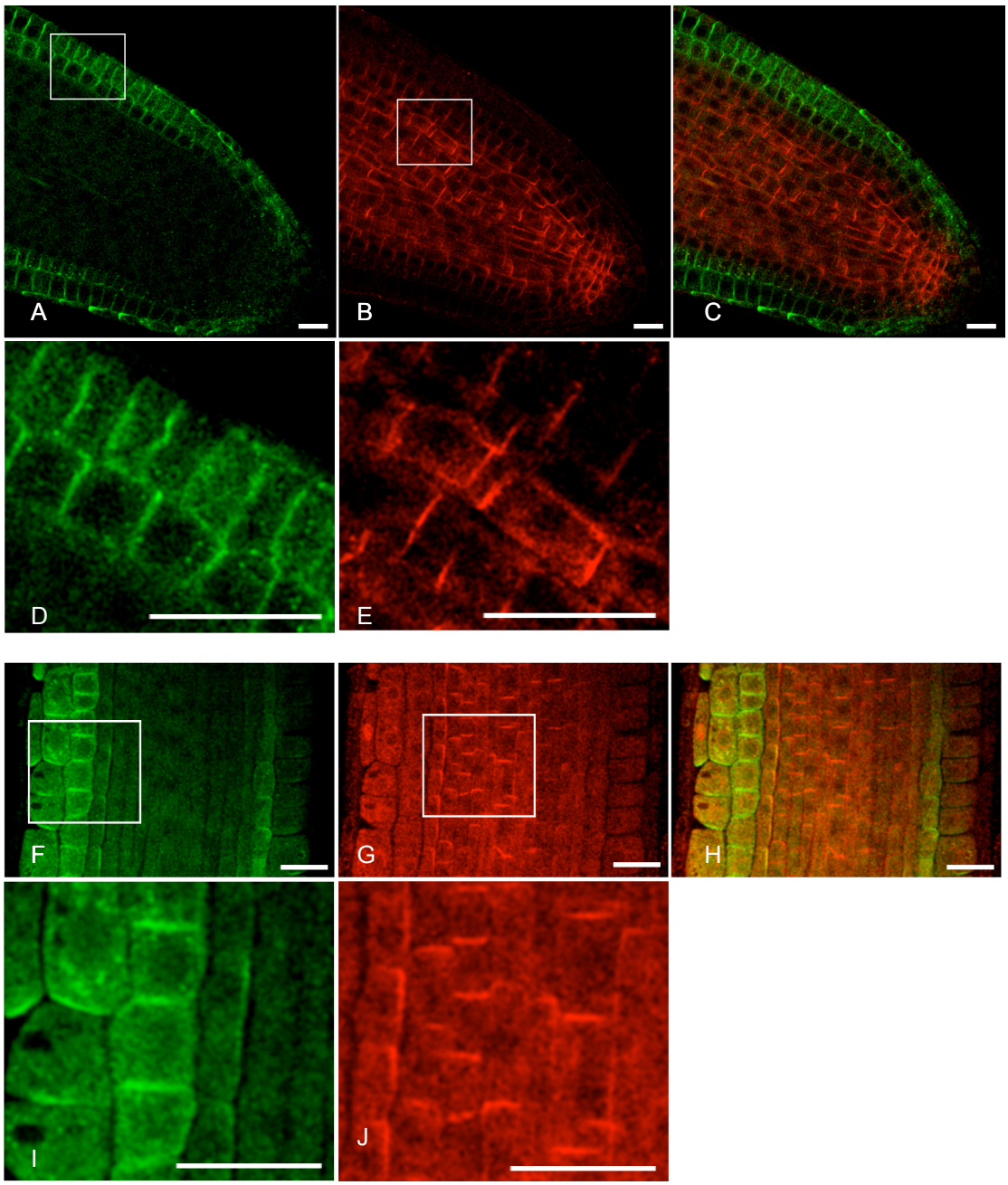

Figure 5-13: Immunolocalization of PIN1 and PIN2 in Col-0 wild type and *atvamp714* mutants

A: PIN 2 localization in roots of wild type at 5-day post germination; PIN 2 localized to apical membrane of cells in the root cortex and epidermis

B: PIN 1 localization in roots of wild type at 5-day post germination; PIN 1 localized to basal membrane of cells in the central cylinder,

C: Overlay of PIN 1 and PIN 2 localization in roots of wild type at 5-day post germination

D: Close image of PIN 2 localization in roots of wild type

E: Close image of PIN 2 localization in roots of wild type

F: PIN 2 localization in roots of *atvamp714* at 5-day post germination

G: PIN 1 localization in roots of *atvamp714* at 5-day post germination

H: Overlay of PIN 1 and PIN 2 localization in roots of *atvamp714* at 5-day post germination

I: Close image of PIN 2 localization in roots of *atvamp714* mutants

J: Close image of PIN 1 localization in *atvamp714* mutants

Bar represent 20 µm

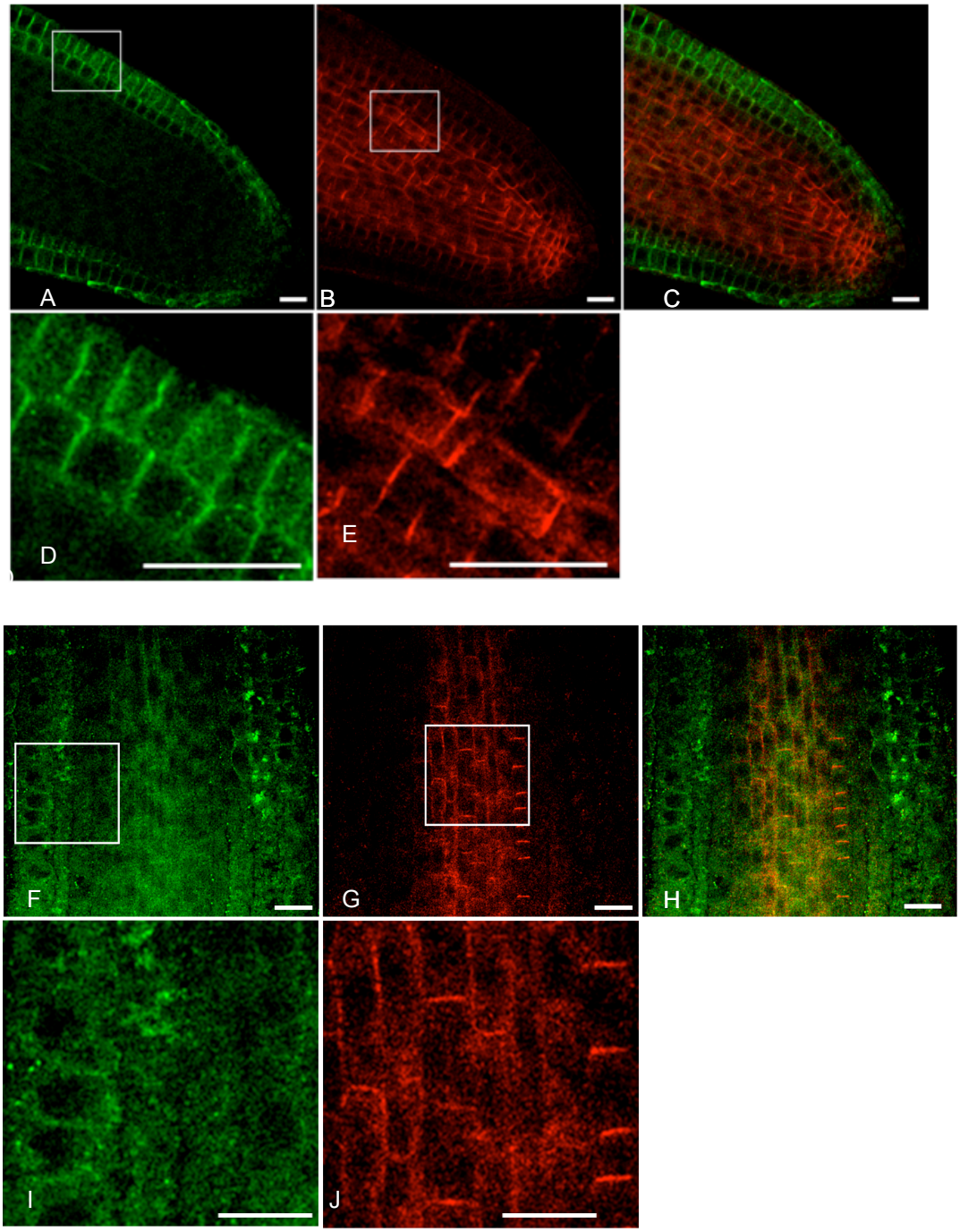

Figure 5-14: Immunolocalization of PIN1 and PIN2 in Col-0 wild type and *atvamp714* mutants

A: PIN 2 localization in roots of wild type at 5-day post germination; PIN 2 localized to apical membrane of cells in the root cortex and epidermis

B: PIN 1 localization in roots of wild type at 5-day post germination; PIN 1 localized to basal membrane of cells in the central cylinder,

C: Overlay of PIN 1 and PIN 2 localization in roots of wild type at 5-day post germination

D: Close image of PIN 2 localization in roots of wild type

E; Close image of PIN 2 localization in roots of wild type

F: PIN 2 localization in roots of *atvamp714* at 5-day post germination

G: PIN 1 localization in roots of *atvamp714* at 5-day post germination

H: Overlay of PIN 1 and PIN 2 localization in roots of *atvamp714* at 5-day post germination

I: Close image of PIN 2 localization in roots of *atvamp714* mutants

J: Close image of PIN 1 localization in *atvamp714* mutants

Bar represent 20 μm

5.3 Dominant Negative Transgenics for Gene Knockouts

The studies on mutants of the *AtVAMP714* gene support an essential role for this gene in auxin transport and plant development. An additional way to investigate the function of the VAMP714 protein is to create and characterize dominant negative mutant transgenics. The aim of this approach is to express a non-functional fragment of the AtVAMP714 protein which would bind to the Qa, Qb and Qc complex of SNARE and inhibit the binding of the native protein. This strategy has previously been used successfully to characterize the functions of other SNAREs (Tyrrell and Blatt, 2007).

5.3.1 Production of Dominant Negative Mutant Transgenics

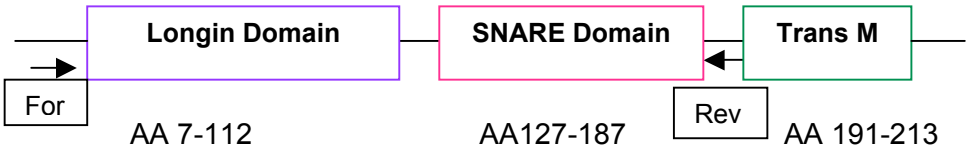

Figure 5-15: Domain structure of AtVAMP714

This figure illustrate the three main domains of AtVAMP714 (Longin domain, SNARE domain and Transmembrane domain (Trans M) with the length of the amino acids. For and Rev indicates the position of forward and reverse primers designed for amplifying the Longin and SNARE domains.

The transmembrane domain (Trans M, Figure 5-15) of SNAREs plays a key role in membrane fusion, and so the objective was to create a mutant AtVAMP714 protein lacking this domain, for introduction into wild-type *Arabidopsis* plants. Primers were designed to amplify only the Longin and SNARE domains (Figure 5-15), using the Oligos primer designing tool. This construct was made using Gateway cloning system and pMDC43 as destination vector. The cloning strategy is explained below.

Longin and SNARE domains were amplified from Col-0 wild type cDNA (Annex 4) using Dom-Neg For and Dom-Neg Rev primers (Annex 1). The Phusion Taq High Fidelity PCR system (section 2.15.3) was used to amplify the fragment (170 bp; figure 5-16). This PCR product was cloned directly into the pCR®2.1-TOPO vector (section 2.10.5) and introduced into chemically competent TOP10 One shot™ cells (section 2.10.5.2). Plasmid DNA was prepared as described in section 2.7.1 and five positive white colonies were sequenced with universal primers *M13F* and *M13R* and 360-cDNA For-2, 360-cDNA Rev internal primers, designed for sequencing to verify that no errors had been introduced during the PCR amplification. The

correct sequence was used for cloning of the gene fragment into pDNOR 207 entry vector (Annex 2).

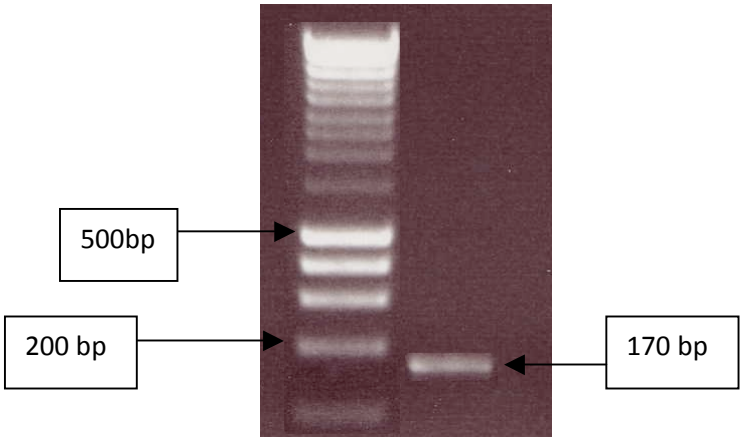

Figure 5-16: Amplification of Longin and SNARE domains from Col-0 wild type plants

The plasmid was then linearized with EcoR V and buffer B for an hour at 72^0C and followed by heat inactivation of the enzyme at 65^0C for 10 minutes. The digest was analyzed by gel electrophoresis (section 2.8) and then the plasmid was purified using Roche *High Pure* PCR kit (section 2.7.10). The BP cloning reaction (section 2.10.6.2) was performed into the pDNOR207 entry vector and then introduced into chemically competent DH5α *E.coli* cells (section 2.10.6.3). Putative positive colonies were selected on Gentomycin (35 µg/ml) and plasmid DNA was prepared from five colonies (section 2.7.1). DNA from these colonies was sequenced with pDNOR207 Forward and Reverse primers (Annex 1).

One colony (number 3) was in-frame with gateway *att*R1 and *att*R2 sites and also with the right insert, and was used to perform LR cloning (section 2.10.6.4). The LR reaction was performed between pDNOR207 containing the Longin and SNARE sequence and pMDC43 destination vector (Annex 2). The plasmid was introduced into DH5α *E.coli* (section 2.10.6.3) cells and kanamycin resistant colonies were identified. The plasmid DNA from five colonies was prepared (section 2.7.1) and sequenced with 360-cDNA-2 Forward and 360-cDNA-4 Forward internal primer to check whether the insert was in-frame with gateway sequences. The Gateway cloning strategy for production of dominant negative transgenics is summarized below.

Longin and SNARE domains amplified by PCR from Col-0 cDNA with *att*B Gateway linkers

↓

Domain fragment cloned into the PCR® 2.1-TOPO vector, sequenced and TOPO vector linearized with ECOR V

↓

BP reaction performed to transfer Domain fragment to pDNOR207 Donor vector, recombinent plasmids were isolated

↓

LR reaction performed to transfer Domain fragment sequence to pMDC43 Destination vector

↓

Recombinant plasmid isolated and sequenced to verify

The pMDC43 vector containing the domain sequence was then introduced into *Agrobacterium tumefaciens* strain C58C3 by triparental mating (section 2.12). Then the construct was introduced into Arabidopsis var Col-0 by the floral dipping method (section 2.13).

T1 seeds from the dipped plants were collected and sown onto ½ MS10 medium supplemented with 20 mg/L hygromycin and 40 mg/L augmentin to kill the *Agrobacterium*. Hygromycin resistant seedlings remained green while sensitive seedlings became bleached 7-10 days after germination on the selective medium. Hygromycin resistant transformed (T1) plants were identified and transferred to soil 7-10 days after germination. T2 seed was harvested as individual lines.

The number of unlinked T-DNA loci in a hemizygous line can be estimated by the ratio of hygromycin-resistant ($Hygro^R$) seedlings to hygromycin-sensitive ($Hygro^S$) seedlings (Table 4-1). Ten independent hygromycin-resistant T2 lines were isolated and germinated on ½ MS10 medium supplemented with 20 mg/L hygromycin. Approximately 7-10 days after germination the plates were scored for the ratio of $Hygro^R$ seedlings to $Hygro^S$ seedlings (Annex 8, Table 1). This revealed that plant numbers 2, 4, 5 and 8 have single T-DNA insertion.

The T3 seeds harvested from above four plants were subjected to hygromycin segregation analysis as above to identify lines that were homozygous for the T-DNA insertion. Lines 2, 4 and 5 shown to be homozygous and the seed were bulked up and T4 seed was used to

analysis of the dominant negative phenotype. T4 seed was surfaced sterilized and germinated on ½ MS10 medium supplemented with 20 mg/L hygromycin. 7-10 days after germination, expression analysis of the *AtVAMP714* gene was carried out using quantitative RT-PCR to determine the abundance of the *AtVAMP714* transcript and seedlings were also observed for developmental defects.

5.3.2 Analysis of the Dominant Negative Transgenics

5.3.2.1 RNA Extraction from Dominant Negative Transgenics

Arabidopsis var Col-0 seeds and dominant negative T4 seeds were surfaced sterilized and grown on ½ MS10 medium (Section 2.2.1). Seven days after germination, seedlings were harvested separately and stored at -80^{0}C until required for RNA extraction.

RNA was extracted using the QIAGEN RNAEasy Plant Mini Kit as detailed in section 2.7.6. The extracted RNA was quantified using NanoDrop1000 Spectrophotometry (section 2.7.7). cDNA synthesis was carried out using 1 µg of RNA as detailed in section 2.7. 8.

Real-time PCR was used to examine the abundance of the dominant negative *AtVAMP714* transcript in Col-0 wild type and dominant negative transgenics. PCR primers were designed to detect the truncated form of the dominant negative transcript (Longin and SNARE domains). As described in the section 2.15.6, real-time PCR based on the quantitative relationship between the starting target DNA and the amount of amplification product during the exponential phase of a cycling programme. Relative quantification was used to compare the results. Comparative quantification software of the Rotorgene was used to analyse the data in this experiment using *ACTIN 2* as a housekeeping gene.

The results showed that the relative abundance of the transcript of *AtVAMP714* was higher in dominant negative transgenics than that of Col-0 wild type plants (Figure 5-17).

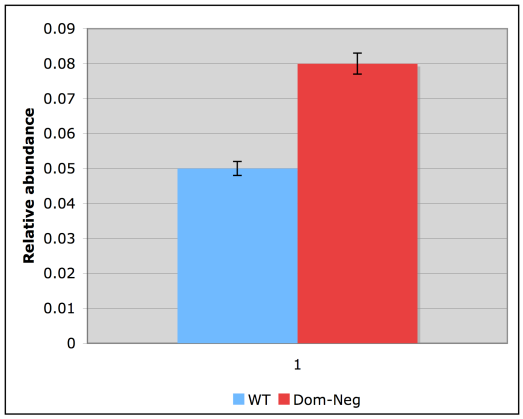

Figure 5-16: *AtVAMP714* gene expression in the dominant negative transgenics

Quantitative RT-PCR analysis of the *AtVAMP714* gene expression of dominant negative transgenics and Col-0 wild type plants relative to *ACTIN2* at 7 days after germination**.** These data are representative of two independent experiments using biological replicate samples. The error bars represent Standard Error of three technical replicates. Y axis represents the relative abundance of the *AtVAMP714* transcript level.

5.3.2.2 Analysis of Dominant Negative Transgenics for Developmental Defects

Dominant negative transgenics (T4) were evaluated for developmental defects. T4 seed was surface sterilized and germinated on ½ MS 10 medium supplemented with 20 mg/L hygromycin. Seven days after germination seedlings were observed for developmental defects. The developmental defects observed over the growth of the seedlings are illustrated in figure 5-17. The observed phenotype exhibits short roots with dwarf and branchy shoots. In older plants exhibit reduced apical dominance (Figure 5-17 E and F). This phenotype suggested defects in auxin transport or sensitivity in dominant negative transgenics.

5.3.2.3 PIN localization in Dominant Negative Transgenics

To determine the PIN protein localization in dominant negative transgenics, immunolocalization studies were carried out. *Arabidopsis* var Col-0 and dominant negative transgenic seeds were surfaced sterilized and germinated on ½ MS10 medium. Seven days after germination the seedlings were fixed as described in section 2.6. Then the aerial parts were removed and the roots were incubated with primary anti-PIN1 and -PIN2 antibodies for 24 hours.

The roots were incubated with secondary anti-PIN1 and -PIN2 antibodies for 24 hours. Regions of interest of the roots were selected for imaging using the Leica SP5 Laser Scanning Microscope (section 2.17).

The results showed strong defects in PIN1 and PIN2 localization in dominant negative transgenics suggesting defects in auxin transport. (Figure 5-18).

In wild-type cells, PIN 1 was localized as expected at the basal membrane of cells in the central cylinder, and PIN2 was localized to the apical membrane of cells in the root cortex and epidermis. In the dominant negative transgenics, both PIN1 and PIN2 were severely mis-localized as compared with Col-0 wild type plants. Both proteins were very poorly localized to the membrane, but rather were internalized (Figure 5-18).

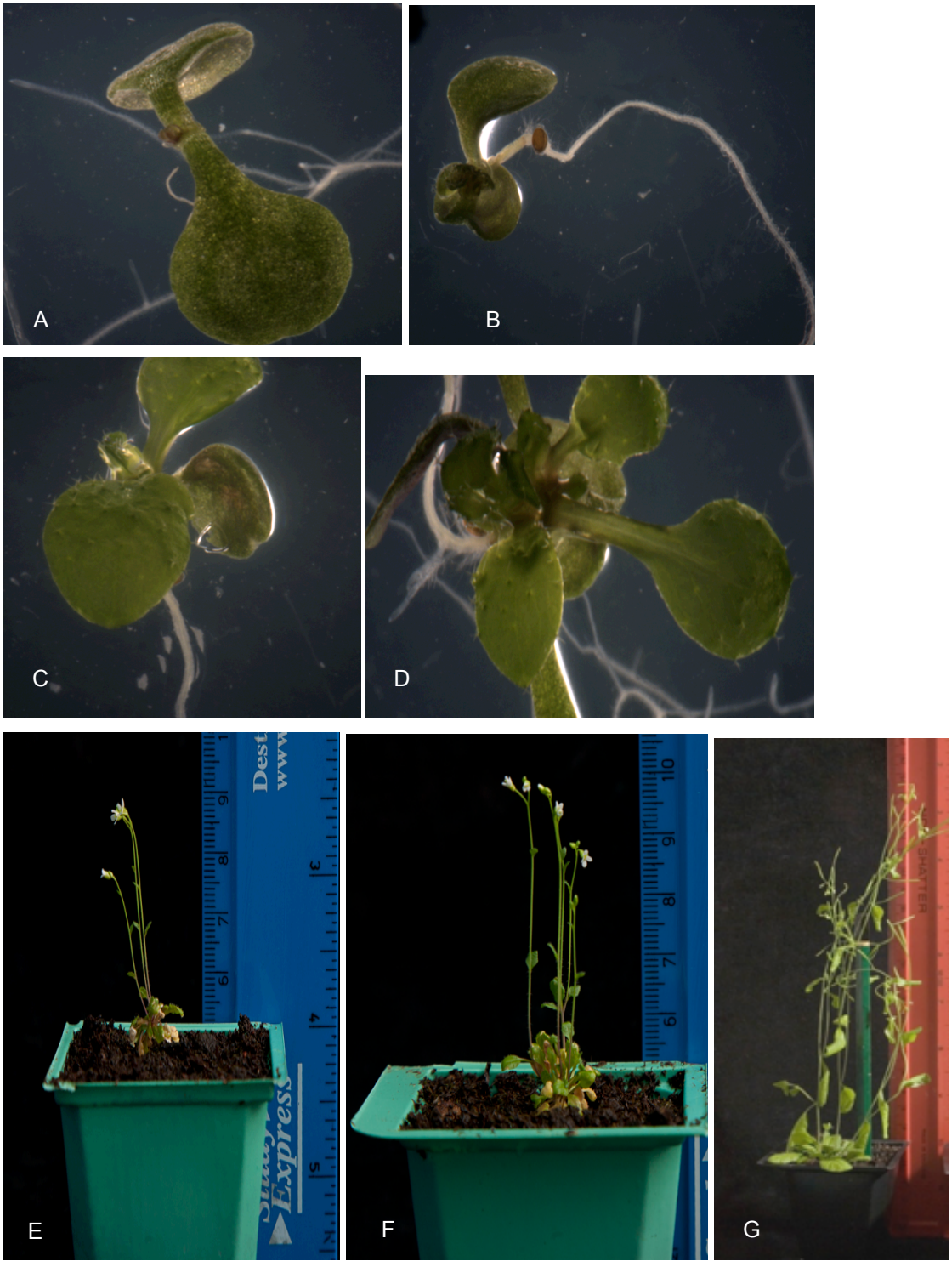

Figure 5-17: Developmental stages of Dominant Negative transgenics

Dominant negative transgenics on selection plate and soil media showing developmental defects

A: Dominant negative transgenic seedling on selection plate; two cotyledon stage at 5 day

B: Dominant negative transgenic seedling on selection plate at 10 day

C: Dominant negative transgenic seedling on selection plate at 10 day; D: Dominant negative transgenic seedling on selection plate at 15 day

E: Dominant negative transgenic plant at 21 day

F: Dominant negative transgenic plant at 40 day and **G**: Col-0 wildtype plant at 40 days

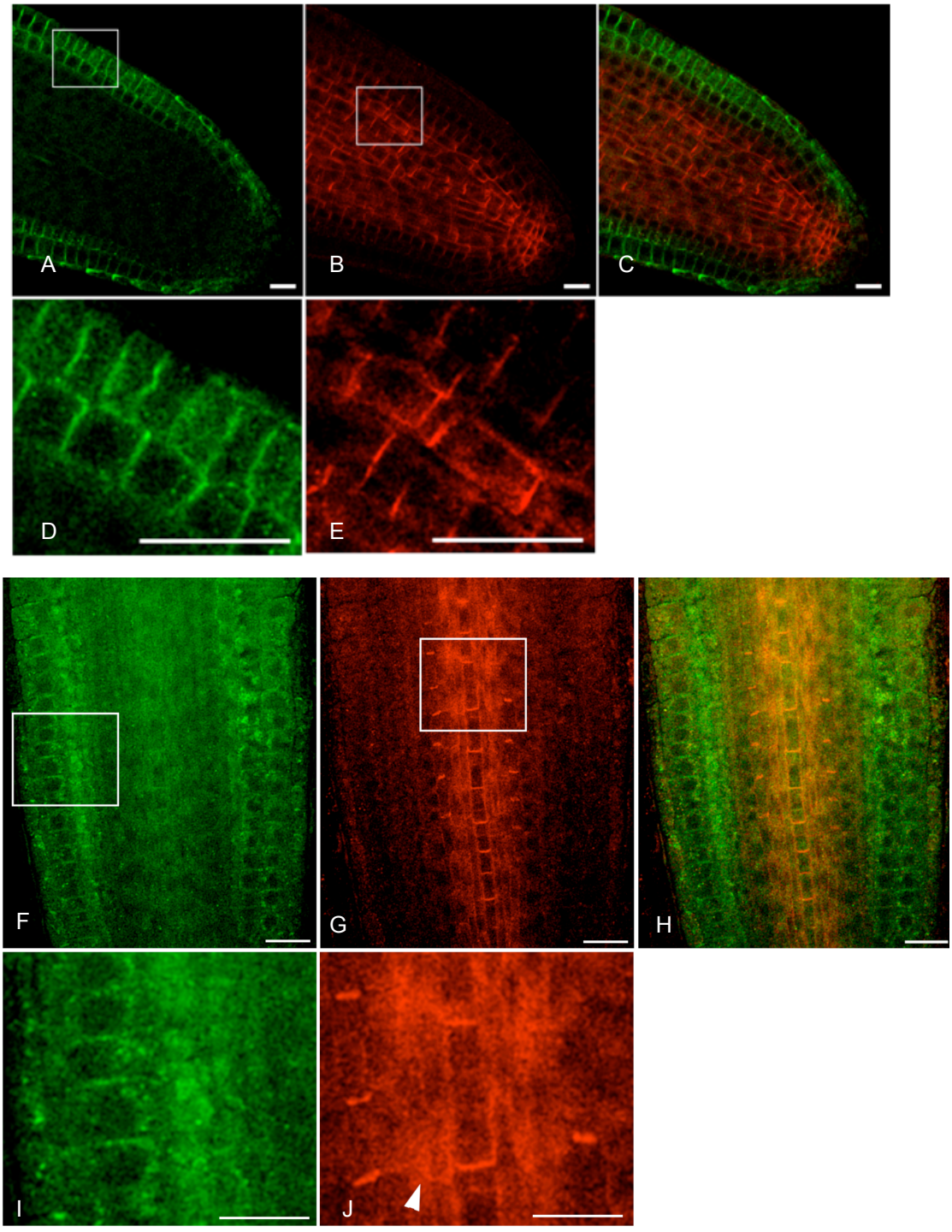

Figure 5-18: Immunolocalization of PIN1 and PIN2 in Col-0 wild type and Dominant negative transgenics

A; PIN 2 localization in roots of wild type at 5-day post germination; PIN 2 localized to apical membrane of cells in the root cortex and epidermis

B: PIN 1 localization in roots of wild type at 5-day post germination; PIN 1 localized to basal membrane of cells in the central cylinder

C: Overlay of PIN 1 and PIN 2 localization in roots of wild type at 5-day post germination

D: Close image of PIN 2 localization in roots of wild type

E; Close image of PIN 1 localization in roots of wild type

F: PIN 2 localization in roots of Dominant negative transgenics at 5-day post germination

G: PIN 1 localization in roots of Dominant negative transgenics at 5-day post germination

H: Overlay of PIN 1 and PIN 2 localization in roots of Dominant negative transgenics at 5-day post germination

I: Close image of PIN 2 localization in roots of Dominant negative transgenics mutants

J: Close image of PIN 1 localization in Dominant negative transgenics mutants; arrow head shows the internalization of the PIN1

Bar represent 20 µm

Summary

The results presented in this chapter detail the analysis of the *AtVAMP714* overexpressors, *atvamp714* knockout mutants and dominant negative mutant transgenics. *AtVAMP714* overexpressors exhibited developmental defects that resemble those caused by interfering with auxin synthesis, transport or perception. Measurement of shoot and root auxin transport levels were found to be reduced in *AtVAMP714* overexpressors, and PIN1 and PIN2 proteins showed strongly defective localization. qRT-PCR confirmed that transcript levels of the auxin-responsive *IAA1* and *IAA2* genes were significantly reduced in *AtVAMP714* overexpressors.

SALK null mutants of the *AtVAMP714* gene were identified and showed an abnormal branching and short root phenotype, also consistent with altered auxin responses. qRT-PCR showed that *PIN1*, *PIN2* and *PIN4* transcript levels were significantly reduced in *atvamp714* null mutants. Immunolocalization of PIN1 and PIN2 did not show any defects in *atvamp714*, but accumulations of PIN1 and PIN2 in membranes were lower than that of Col-0 wild type plants.

Dominant negative mutant transgenics of *AtVAMP714* were created as a method of knocking out the protein and F2 generation was analysed for developmental defects. Consistent with the above results the dominant negative transgenics also showed short root phenotype with dwarfed, branchy shoots. PIN proteins were also mislocalized in dominant negative transgenics.

Chapter 6: Discussion

Chapter 6: Discussion

The plant signalling molecule auxin regulates many aspects of plant growth and development. Auxin is distributed through tissues by the polar auxin transport (PAT) system (Lomax *et al*. 1995). Both auxin influx (AUX1/LAX protein family) and efflux (PIN protein family) carriers show polar subcellular localization and determine the direction of the auxin flow through tissues (Swarup *et al*. 2001, Galweiler *et al*. 1998, Friml *et al*., 2004, Friml, 2010). The PIN proteins (with the exception of PIN5, whose function appears to be in auxin homeostasis; Mravec *et al*. 2009) have been shown to drive auxin efflux from cells, providing directionality in the root tip and in the shoot apex. This directionality in the root tip produces a gradient of auxin that maintains the patterning and function of the root meristem, in a regulatory loop that involves the PLETHORA (PLT) transcription factors (Blilou *et al*., 2005; Galinha *et al*., 2007; Grienelsen *et al*., 2007). PLT proteins in turn promote PIN gene expression and auxin distribution. The MERISTEM-DEFECTIVE protein, a likely transcriptional regulator, is also required to maintain *PIN* and *PLT* gene expression, auxin distribution and root meristem function (Casson *et al*. 2009). With the aim of identifying new genes regulating plant development, an activation tagging screen was carried out for gain of function mutants. The *AtVAMP714* gene was found to be upregulated in one activation tagging line (Casson and Lindsey, unpublished data) and bioinformatics analysis identified it as a member of the *VAMP7* gene family encoding a predicted protein of 221 amino acids.

This study has aimed to investigate the function of the *AtVAMP714* gene in *Arabidopsis thaliana*. AtVAMP714 is a member of R-SNARE protein family. R-SNAREs are divided into two sub classes, longins and brevins (Uemura *et al*. 2005). Longins are classified into three groups and VAMP7 is one of them. In *Arabidopsis* there are eleven genes encoding VAMP7-like and VAMP7-like group further sub divided into two sub groups, VAMP7-1 and VAMP7-2. *AtVAMP714* is a member of a VAMP7-1 sub group and this work describes the functional characterization of this gene.

6.1 Expression analysis of *AtVAMP714* gene

The work described in this thesis supports a role for AtVAMP714 in auxin transport, via its proposed molecular function in vesicular transport of PIN proteins to the plasma membrane. This hypothesis is based on a number of key observations, relating to the spatial expression of the gene, the regulation of the gene by auxin, the gain- and loss-of-function phenotypes of mutant and transgenic seedlings, the subcellular localization of the protein and its co-localization with PIN proteins.

Determination of the expression pattern of *AtVAMP714* was carried out using transgenic lines expressing a promoter-GUS fusion and by qRT-PCR. The promoter sequence was analysed for conserved motifs using bioinformatics tools. The promoter activity during plant development and in response to exogenously applied plant hormones was investigated using promoter-GUS fusion analysis. pro*VAMP714*::*GUS* transgenic seedlings were histologically stained and roots were sectioned to determine the specific cell type in which the *AtVAMP714* promoter is active. In addition, VAMP714 protein localization was carried out using a GFP reporter gene fusion. To further analyse the function of the gene, loss-of-function mutants and dominant negative transgenics were analysed. A *proVAMP714:VAMP714::CFP* gene was used to show that VAMP714 and PIN1 proteins are localized to the same vesicles.

6.1.1 Identification of conserved motifs in, and hormonal regulation of, the *AtVAMP714* promoter

Sequence analysis of 2 kb of the 5' flanking region upstream of the *AtVAMP714* gene start codon was carried out using the PlantPAN (Plant Promoter Analysis Navigator) and PlantCARE (Plant cis-Acting Regulatory Elements) databases. This revealed that there are motifs for several promoter activities in the region (section 3.5).

Analysis of the 2 kb promoter sequence revealed the presence of the auxin response element (AuxRE) motif (TGTCTC). This sequence was originally identified in the soybean GH3 promoter, and was subsequently used to make the DR5 synthetic promoter that directs high auxin inducibility in several species including *Arabidopsis* (Ulmasov *et al*., 1995, Ulmasov *et al*., 1997). This element was also found to be enriched in the 5' flanking region of genes upregulated by IAA (Goda *et al*., 2004). The AuxRE was identified at the position of -1346 in the *AtVAMP714* promoter.

The AuxRE binding site is found in promoters of primary or early auxin response genes of *Arabidopsis*. Genetic and molecular experimental approaches have demonstrated that AuxREs function as transcription factor binding sites on primary auxin response genes (Hagen and Guilfoyle, 2002). Therefore, genes that contain TGTCTC AuxREs would be expected to be transcriptionally activated in response to auxin.

The use of exogenous plant hormone and inhibitor application is a simple approach for the initial investigation of the response of promoter-reporter fusions, as a means to investigate the regulation of expression of a gene of interest. The response of the *AtVAMP714* gene promoter

to exogenous plant hormones can be summarised as follows. IAA altered the spatial *AtVAMP714* promoter activity and led to an activation of GUS activity in the root tip and cotyledon vascular tissues. The cytokinin analogue BA and ethylene precursor ACC did not appear to affect significantly promoter activity.

Exogenously applied auxin transport inhibitors interfere with auxin distribution and thus perturb plant development. TIBA (2, 3, 5-triiodobenzoic acid) inhibits auxin efflux and thus blocks polar auxin movement between cells. Treatment of *proAtVAMP714::GUS* seedlings with the auxin transport inhibitor TIBA led to a increased level of GUS expression in leaves, consistent with an accumulation of auxin in these organs, which synthesize auxin. This result is consistent with an upregulation of *AtVAMP714* expression by auxin, potentially as a mechanism to remove auxin from tissues accumulating high levels.

Numerous sequences that have a functional role in the up-regulation or down-regulation of genes by auxin have been described (Abel and Theologis, 1996; Guilfoyle, 1999). Early achievements in molecular studies of the auxin response were the identification of auxin-response-factor (ARF) proteins and their binding to a *cis*-regulatory element, the auxin-response element (AuxRE; TGTCTC), in primary auxin-response gene promoters (Ulmasov *et al*., 1997). Some ARFs act as transcriptional activators and some as repressors. ARF functions are inhibited by direct binding of members of the AUX/IAA protein family, identified as products of primary auxin-response genes (Hagen *et al*., 2002). Auxin influences gene expression by promoting rapid degradation of AUX/IAA proteins via the TIR1 protein complex, thereby allowing ARFs to regulate transcription (Kepinski and Leyser, 2005, Dharmasiri *et al*. 2005). Mutants impaired in the degradation of AUX/IAA proteins are altered in auxin responses (Berleth and Jurgens, 1993, Hamann *et al*., 1999, 2002).

The *AtVAMP714* gene promoter contains the AuxRE TGTCTC at a position -1346 from the ATG codon. This is consistent with regulation of the gene by auxin. This was demonstrated by qRT-PCR, which showed that the transcript levels of *AtVAMP714* were increased with treatment of wild-type seedlings with exogenous IAA (Figure 5-3).

The gibberellic acid responsive element, which binds the GARE factor (Ogawa *et al*., 2003), is also found in the *AtVAMP714* promoter. Gibberellin enhances cell division and elongation (Thomas and Sun, 2004). In addition, TCA elements involved in salicylic acid responsiveness and a W-box, also responsible for salicylic acid inducibility (Chen and Chen, 2003), are found in the *AtVAMP714* promoter. Salicylic acid (SA) promotes disease resistance responses and ethylene synthesis (Klessig *et al*., 2009). A growing body of evidence indicates that many plant

pathogens can either produce auxin themselves or manipulate host auxin biosynthesis to interfere with the host's normal developmental processes (Manulis *et al*., 1998 and Vandeputte *et al*., 2005). In response, plants probably evolved mechanisms to repress auxin signalling during infection as a defence strategy (Dong *et al*., 2007). Plants over-accumulating SA frequently display morphological phenotypes that are reminiscent of auxin-deficient or auxin-insensitive mutants (Dong *et al*., 2007), indicating that SA might interfere with auxin responses.

AtVAMP714 promoter region also contains several motifs potentially involved in light responsiveness and environmental stress responsive motifs, such as LTRE (low temperature responsive elements), described by Baker et al. (1994) and also the MBS motif involved in drought-inducibility (Yamaguchi-Shinozaki and Shinozaki, 1994). The *AtVAMP714* promoter contains a GCC-box and GCN4 motif found in many pathogen-responsive genes. These elements have also been shown to function as ethylene-responsive elements.

Although several motifs were identified in the *AtVAMP714* promoter, this does not in itself prove that *AtVAMP714* gene expression is influenced by these sequences, and further work would be required to investigate their possible functions. Nevertheless, given the auxin inducibility of the *AtVAMP714* gene, and the interactions between auxin and other hormones such as ethylene, salicyclic acid and gibberellins (Aaron and Estelle, 2009), it is possible that the expression of this gene is influenced by multiple hormonal signals, or may act to regulate interactions between these various signalling systems. Experimental observations on the regulation of *AtVAMP714* are now discussed in more detail.

6.1.2 The *AtVAMP714* promoter is active in vascular tissues

The expression analysis of *proVAMP714::GUS* was examined in transgenic seedlings by GUS histochemistry over a development time course, to investigate the spatial expression pattern of the *AtVAMP714* gene (section 4.1). The response of promoter-GUS transgenic lines to exogenously applied plant hormones was also investigated (section 4.1.3 and 4.1.4).

The data presented in Figures 4-3 and 4-4 demonstrated that the *AtVAMP714* promoter is active at the hypocotyl-root junction, especially at relatively young stages of seedling development (2-10 days post germination) and in both primary and lateral roots. The roots of seedlings which expressed the *proVAMP714::GUS* gene were sectioned to determine whether GUS expression occurs in specific cell layers. Sections were taken from the main root adjacent to the hypocotyl in all cases. Examination of *proVAMP714::GUS* lines by sectioning indicated that the *AtVAMP714* promoter is active in endodermis, pericycle and vasculature of mature roots in *Arabidopsis*. *proVAMP714::GUS* expression was also observed in developing lateral

roots and root hairs. The *Arabidopsis* eFP browser is also predicted the *AtVAMP714* gene expression in vascular tissues of the roots (bar.utoronto.ca/efp).

In plants, auxin is transported by two distinct pathways. Throughout the plant, auxin is transported away from the source tissues (young leaves and flowers) by an unregulated bulk flow in the mature phloem. In addition a slower, regulated, carrier-mediated cell-to-cell directional transport moves auxin in the vascular cambium and the protophloem from the shoot towards the root apex (Goldsmith, 1977, Swarup *et al* 2001) and also mediates short-range auxin movement in different tissues. Once auxin reaches the root apex, part of it is redirected back upwards (basipetally) mainly through the root epidermis into the root elongation zone (Rashotte *et al*., 2000) where it can be recycled back into the vascular stream (Blilou *et al*., 2005). These two pathways appear to be connected at the level of phloem loading in leaves (Marchant *et al*., 2002) and phloem unloading in roots (Swarup *et al*., 2001).

proVAMP714::GUS expression was observed in developing lateral roots. Lateral root formation is initiated close to the root tip, first seen as divisions in pericycle cells and giving rise to lateral root primordia (Dolan *et al*., 1993; Dubrovsky *et al*., 2000). The subsequent development of the primordia follows a series of highly ordered cell divisions that ultimately lead to the emergence of lateral roots (Malamy and Benfey, 1997a). As auxin represents a key regulator of lateral root development, studies have shown that IAA, the major endogenous auxin in plants, is necessary for both the initiation and the later development of lateral roots (Celenza *et al*., 1995; Reed *et al*., 1998). *AtVAMP714* gene expression was observed in developing lateral roots in *Arabidopsis*, consistent with the evidence that developing lateral roots need a supply of auxin for their initiation and subsequent elongation. Developing lateral root primordia are proposed to obtain IAA via polar auxin transport (Reed *et al*., 1998). Recently, [Malcolm Bennett's paper in Nature Cell Biology and others on the LAX genes] has shown that the auxin influx carriers are required for auxin transport into the young lateral root primordium, and the auxin efflux carrier PIN2 is also required for lateral root initiation. Several other auxin-related mutants (eg the *alf* mutants) have been described in *Arabidopsis* that arrest lateral root formation at various stages of development (Celenza *et al*., 1995). The observation that the *atvamp714* mutant described in section 5.2 has reduced lateral root development supports a role for the AtVAMP714 protein in lateral root initiation or maintenance, presumably through a role in auxin transport.

Interestingly, the *AtVAMP714* promoter-GUS fusion is not active in root meristems, although these cells represent a relatively high concentration of auxin (Blilou *et al*., 2007). This suggests that the promoter is not simply activated by relatively high auxin, but is also presumably regulated by tissue-specific factors in addition to auxin, to determine tissue-specific expression

patterns, and so the cells in which the AtVAMP714 protein is functional. This would suggest that AtVAMP714 would only have a role in the vesicle trafficking of PIN (and perhaps other) proteins in specific cell types, and would not normally be required for the correct localization of PIN proteins found in the root tip, such as PIN3 and PIN4 (Blilou *et al*., 2005). However, *AtVAMP714* expression is activated in the root tip of seedlings grown in the presence of exogenous auxin, and we can speculate that this activation may be a response of the plant to remove excess auxin from the root tip.

proVAMP714::GUS expression was also prominent in root hairs. The plant hormone auxin controls root epidermal cell development in a concentration-dependent manner (Sabatini *et al*., 1999; Blilou *et al* 2005; Grieneisen *et al*., 2007) Root hairs are produced on a subset of epidermal cells as they increase in distance from the root tip. Auxin is required for their initiation (Knox *et al*., 2003: Grebe *et al*., 2002; Fischer *et al*., 2006: Masucci *et al*., 1994) and continued growth (Pitts *et al*., 1998: Rahman *et al*., 2002: Lee *et al*., 2006: Cho *et al*., 2007). AUX1-dependent auxin transport through non-hair cells maintains an auxin supply to developing hair cells as they increase in distance from the root tip, and sustains root-hair outgrowth (Angharad *et al*., 2008). The expression of *AtVAMP714* in these cells may suggest either a role for the protein in these cells, or simply an induction of expression by auxin

In developing leaves of *Arabidopsis* expression of the auxin responsive DR5:GUS reporter is observed in stipules, indicating relatively high levels of free auxin in this site (Aloni *et al*., 2003). *AtVAMP714* promoter-GUS expression was also observed in stipules, which given the observed auxin-inducibility of the promoter (section 4.1) is consistent with these tissues being high in auxin concentration.

6.1.3 Analysis of *AtVAMP714* transcript levels in different plant organs

As described in section 4.2, the wild-type transcript levels of *AtVAMP714* were determined by qRT-PCR. *AtVAMP714* was expressed at similar levels in roots and aerial parts of developing seedlings. *proVAMP714::*GUS expression was observed in hypocotyls, stipules, roots and pollen. Consistent with the results obtained by qRT-PCR, similar results were found using the *AtGenExpress Visualization Tool* and *Arabidopsis eFP* browsers (chapter 3). Transcript levels of the other members of the family were also analysed using qRT-PCR. The tissue-specific pattern of expression of *AtVAMP714* was found to be distinct from that of the other family members (Section 4.2).

Although the *AtVAMP714* transcript was detected in roots and aerial parts, the promoter-GUS activity was only seen strongly in roots throughout the plant development. In aerial parts, promoter-GUS expression was only observed in hypocotyls and stipules. There are several reasons why the activity of the promoter as determined by the GUS reporter gene may not correlate exactly with levels of the *AtVAMP714* transcript itself.

One possibility is that the expression levels of promoter-GUS in aerial parts are too low for detection using the GUS assay. Increasing the staining time during the GUS histochemical assay is a simple way to investigate this possibility. It is also possible that there is not be a direct correlation between the amount of GUS protein that is present and the amount of *AtVAMP714* transcript. It has been shown that the *GUS* transcript and the GUS protein levels do not correlate well in tissues (Topping *et al*., 1991). Therefore it is possible that, there is also poor correlation *AtVAMP714* transcript and GUS protein levels. It is also possible that the cloned *AtVAMP714* promoter does not contain all of the required regulatory elements, or the genomic context in which the transgene is located affects its expression, a phenomenon that is known as 'position effect' (Topping et al. 1991). Arguing against this latter possibility is the observation that independent transgenic lines showed similar promoter-GUS expression patterns (Section 4.1). The *AtGenExpress* visualization tool and Arabidopsis eFP browser also revealed that *AtVAMP714* gene is highly expressed in root vascular tissues and hypocotyls.

On the basis of these observations, it can be hypothesised that the *AtVAMP714* gene is activated by auxin to promote auxin transport out of the stem into the root. Auxin is transported mainly through the vascular tissues, and consistent with this, *AtVAMP714* promoter-GUS expression was observed in vascular tissues of the roots.

6.2 Subcellular Localization of AtVAMP714

Proteins must be localized to their appropriate subcellular compartment to perform their correct function. Determining subcellular localization is important for understanding protein function and is a critical step in genome annotation. AtVAMP714 localization was carried out using the onion epidermal cells transient expression system. This system has been used previously to show, for example, the subcellular localization of other VAMP family members (Uemura *et al*. 2004).By comparing localization with a Golgi:RFP marker (Nebenfuhr *et al*., 1999), it was revealed that the AtVAMP714:GFP fusion protein is localized to Golgi and, by implication, is involved in the Golgi trafficking pathway. The Golgi apparatus consists of a large number of small independent stacks.

The individual Golgi stacks can appear as perfectly round discs, as short lines or in the shape of small rings, depending on orientation and status (Nebenfuhr *et al*., 1999). The Golgi marker may also show weak ER labeling, resulting from the continuous recycling of Golgi resident proteins through the ER (Brandizzi *et al*., 2002). The only known marker proteins for post-Golgi organelles are directly involved in trafficking to or from these organelles (e.g. Rab proteins, Molendijk *et al*., 2004; SNAREs, Uemura *et al*., 2004; or sorting receptors, Tse *et al*., 2004), and may interfere with the normal functioning of the organelle.

The Golgi apparatus in plants is organized as a multitude of individual stacks that are motile in the cytoplasm and in close association with the endoplasmic reticulum (Boevink *et al*., 1998). The Golgi apparatus is required for operating as a sorting centre for cargo molecules, providing modification and redirection to other organelles as appropriate. In the post-Golgi direction, these include vacuole and plasma membrane, and specialized transport routes to each are required to prevent mislocalization. Golgi-derived secretory vesicles carry proteins to the plasma membrane (Pauly *et al*., 1999; Fry, 2004) Secretory and endocytic traffic through the post-Golgi endomembrane system regulates the abundance of plasma-membrane proteins such as receptors, transporters and ion channels, modulating the ability of a cell to communicate with its neighbours (Jurgens *et al*., 2009). The localization of AtVAMP714 to the Golgi suggests a role for this protein in Golgi transport system.

Interestingly other members of the VAMP7-1 family (*AtVAMP711*, *AtVAMP712* and *AtVAMP713*) are localized to vacuolar membrane (Uemura *et al*., 2005) and involved in the transport to the vacuole from the PVC (Uemura *et al*., 2004). The tissue specific pattern of expression and auxin regulation of *AtVAMP714* is distinct from other family members and these are proposed to be differently localized.

6.2.1 AtVAMP714 and PIN1 proteins co-localize with each other

The PIN proteins are critical for directional auxin transport and are localized to specific faces of the cell at the plasma membrane. Correct PIN localization is a function of the PIN protein sequence and its phosphorylation status. The actin cytoskeleton is required for correct PIN localization, presumably in part by Golgi vesicle-mediated transport to the plasma membrane and by endocytotic recycling at the plasma membrane (Geldner *et al*., 2003 and 2004). However, molecular components of any Golgi vesicle transport pathway of PIN proteins are still not known.

Therefore, although PIN proteins have been intensively studied (Benková *et al*., 2003; Friml *et al*., 2003b; Geldner *et al*., 2001; Geldner *et al.,* 2003a), the cellular mechanism of their polarized positioning within the cells (Geldner *et al*., 2003a; Steinmann *et al*., 1999; Willemsen *et al*., 2003) and the cellular basis of early PIN localization remains poorly understood. It has been shown that the protein kinase PINOID (PID) plays an important role in this process (Benjamins, 2004; Friml *et al*., 2004). PIN polarity is controlled by differential PIN phosphorylation, which appears to be the result of the antagonistic activities of the serine-threonine kinase PINOID (PID) and a phosphatase containing the subunit PP2A (Friml *et al*., 2003; Michniewicz *et al*., 2007). *PID* overexpression leads to a shift in the polarity of at least PIN1, PIN2 and PIN4 from the basal (lower) to the apical (upper) membrane in root cortex and lateral root cap cells (Friml *et al*., 2003b). These PID dependent polarity changes can be reverted by increasing the expression of *PP2A*, which suggests that PIN polarity and auxin efflux are at least in part controlled by PID-dependent phosphorylation (Michniewicz *et al*., 2007).

Immunocytochemistry and PIN:GFP fusions have been used to explore the cellular processes involved in PIN localization. Targeting of PIN1 protein to the basal plasma membrane requires PIN1 recycling from the plasma membrane to endosomes and is mediated by GNOM, an endosomal GDP/GTP exchange factor for ARF GTPases (Geldner *et al*., 2003). PIN2 is transported through endosomes expressing SORTING NEXIN 1 (SNX1) and distinct from GNOM-positive endosomes (Jaillais *et al*., 2006). PIN proteins are continuously trafficked through endosomal compartments, which are central to their correct localization and function (Geldner *et al*., 2003). However, the mechanism of apical versus basal targeting of PIN proteins is poorly understood as are the specific sorting signals of PINs and the endosomal compartments that are part of their trafficking routes.

It has therefore been suggested that the establishment and maintenance of polarity in plant cells is a post-mitotic event, involving endocytic and exocytic processes. Evidence has also been obtained suggesting that the Golgi apparatus functions as a junction between the exocytic and endocytic pathways for PIN trafficking (Boutte *et al*., 2007). Actin might be involved in this, either by modulating the movement of both Golgi stacks and PIN-labelled compartments or by mediating the transport of Golgi-derived products to the cell surface, but not by directing endocytic recruitment. In addition, it was found that microtubules play an indirect role in PIN localisation, as their prolonged disruption leads to a reorganization of growth axis and cell polarity in plant cells. These data suggest that the Golgi network is actively involved in trafficking of the PIN proteins (Boutte *et al*., 2007).

To investigate whether AtVAMP714 is involving PIN1 protein trafficking we carried out experiment to evaluate colocalization of PIN1:GFP with AtVAMP714:CFP. An *AtVAMP714:*CFP gene construct was introduced into PIN1:GFP plants, and results demonstrated co-localization of the two fusion proteins (Section 4.4). This indicates that PIN1 and AtVAMP714 are found in the same vesicles, supporting the hypothesis that AtVAMP714 is functionally related to PIN protein localization via its role in vesicle trafficking. This possibility was investigated further by analysing PIN localization and auxin transport in plants disrupted in AtVAMP714 function.

The protein serine/threonine kinase PINOID (Christensen *et al*., 2000; Benjamins *et al*., 2001) is the only as yet identified molecular component directly involved in the regulation of polar delivery of PIN proteins. The PINOID (PID) catalyzes PIN phosphorylation and crucially contributes to the regulation of apical-basal PIN polarity. Loss of PINOID (PID) function causes an apical- to-basal shift in PIN polarity, correlating with defects in embryo and shoot organogenesis. PID gain-of-function results in an opposite basal-to-apical PIN polarity shift, which leads to auxin depletion from the root meristem, ultimately leading to its collapse (Friml *et al*., 2004). These results indicate that PID-dependent phosphorylation leads to preferentially apical PIN localization, whereas low phosphorylation levels result in basal PIN targeting. *MERISTEM-DEFECTIVE* (*MDF*) gene of *Arabidopsis* plays an essential role in regulating *PIN* and meristem transcription factor gene expression, and in establishing the correct auxin distribution, meristem pattern and function (Casson *et al*., 2009). The *PLETHORA* (*PLT*) genes also regulate *PIN* gene transcript distribution, which further acts to stabilize the auxin maximum (Blilou *et al*., 2005). As a result of functional redundancy, mutations in individual *PLT* or *PIN* genes often display only very minor defects in root meristem organization and activity (Aida *et al*., 2004). Other molecular components directly involved in the regulation of polar delivery of PIN proteins still remains unclear.

6.3 Functional analysis of *AtVAMP714*

Functional analysis of the *AtVAMP714* gene was performed by overexpressing the *AtVAMP714* coding sequence under the control of the 35S promoter, and by the generation and analysis of loss-of-function mutants using dominant negative transgenics and SALK knockout mutants.

6.3.1 Requirement for *AtVAMP714* in auxin transport

As described in Chapter 5, overexpression of the *AtVAMP714* gene was carried out in transgenics under the control of 35S promoter. The expression level of *AtVAMP714* was determined in the overexpressors using RT-PCR. It was confirmed that *AtVAMP714* gene is expressed to a higher level in the overexpressors than the wild type plants.

Overexpression of the *AtVAMP714* gene led to a phenotype exhibiting reduced apical dominance with short internodal lengths. Younger plants exhibited abnormal leaf shapes. This phenotype resembles developmental defects caused by interfering with auxin synthesis, transport or perception. Measurement of rates of polar auxin transport in these transgenic plants revealed a reduced rate of auxin transport. This is consistent with a role for AtVAMP714 in auxin transport.

In aerial parts of the adult plant, IAA is transported basipetally from its site of synthesis at the shoot apex toward the roots in a process referred to as polar auxin transport (Lomax *et al*. 1995). In roots, auxin moves in the opposite direction in different cell types, acropetally through the root stele and basipetally through epidermal cells (Tsurumi and Ohwaki 1978; Meuwly and Pilet 1991). Disruption of auxin transport affects critical processes such as embryo development in the seed, vascular differentiation, stem elongation, flower and root development, apical dominance, leaf shape and tropic responses (Lomax *et al*. 1995).

Physiological studies have indicated that the polar auxin transport system requires the activity of AUX1 and PIN carriers located on the plasma membrane of transporting cells. These carriers act to move auxin through files of cells by successively transporting auxin into and out of adjacent cells in the file. Net auxin movement is polar because the efflux carriers are asymmetrically localized in transporting cells (Lomax *et al*. 1995).

Consistent with the observed defective auxin transport in overexpressing transgenics, immunolocalization of PIN1 and PIN2 in these plants showed strong defects in their subcellular distribution, with very poor localization to the plasma membrane in root tissues (Section 5.1). Associated with reduced auxin transport in these plants is a reduction in auxin responses and the level of gene expression. The genes *IAA1* and *IAA2* (Abel and Theologis, 1996) respond rapidly in their transcription levels in response to auxin (Abel and Theologis, 1996); *IAA1* has been shown to be reduced in transcript abundance in the *polaris* mutant, which is defective in auxin transport and responses (Casson *et al*. 2002). qRT-PCR analysis showed that transcript levels of *IAA1* and *IAA2* were significantly reduced in *AtVAMP714* overexpressors. These

results further support the idea that AtVAMP714 is required to regulate auxin transport and downstream responses, consistent with the observed developmental defects in the overexpressing plants.

6.3.2 Loss-of-function mutants of *AtVAMP714*

Further supporting evidence for a role for AtVAMP714 in auxin transport came from analysis of SALK T-DNA insertion mutants and dominant negative transgenics.

Among the two SALK lines screened (salk_005914 and salk_005917), salk_005917 (*vamp714*) is a null mutant for *AtVAMP714* and exhibited an abnormal phenotype. Homozygous mutant *vamp714* seedlings had a reduced primary root length, a reduced number of lateral roots and an altered root gravitropic response, compared to wild type plants (Section 5.2). This suggested that AtVAMP714 has a function in root growth and gravitropic response, consistent with a requirement for correct PIN protein localization and polar auxin transport. All the plants homozygous for the mutation also showed a dwarf phenotype with high branching, again consistent with a defective auxin transport system. For example, the *axr1* and *axr3* mutants, defective in auxin responses, have enhanced branching (Estelle *et al*., 1995); and the *max* mutants of *Arabidopsis*, and related mutants in pea and rice, that are defective in auxin-strigolactone signaling, similarly show reduced apical dominance (Bennett and Leyser 2006; Gomez-Roldan *et al*. 2008; Umehara *et al*. 2008).

6.3.3 Dominant-negative mutant analyses clarify AtVAMP714 functions in plant development

Further support for a role for AtVAMP714 in PIN protein localization came from the construction and analysis of dominant negative mutant transgenic plants. Dominant negative mutations involve the functional inactivation of a wild-type gene product by co-expression of a mutant allele of that gene. Analyses of dominant-negative mutations are therefore useful to elucidate functions of genes. Such a mutant protein will disturb its own functions and also inhibit the function of any iso-variants expressed in the same cells. Examples of the use of this approach to investigate protein function includes,making use of dominant negative inhibitors complementary to selected SNAREs. This was first employed by Leyman *et al*. (1999) to explore the role for the tobacco SNARE NtSYP121 in K^+ and Cl^- channel control and was subsequently used to examine the functioning of the same SNARE and in membrane vesicle traffic and development (Geelen *et al*., 2002). The disruption of NtSYP121 function by

expressing a dominant-negative, cytosolic fragment *in vivo* had severe effects on growth, tissue development and traffic to the plasma membrane (Geelen *et al.*, 2002; Tyrrell *et al*., 2007).

SNAREs are anchored to membranes by transmembrane segments that not only anchor them, also contribute to SNARE-SNARE interactions and appear to play an active role in the fusion process. Transgenic *Arabidopsis* plants were established expressing a form of the AtVAMP714 protein that lacks the transmembrane domain. The aim was to test the dominant negative mutant strategy for analyzing the role of AtVAMP714. The rationale of this method lies in the ability of the protein fragment genetically engineered from the full-length sequence to bind the native protein partners, thereby preventing completion of the normal SNARE function. The specificity of dominant negative SNARE fragments *in vivo* suggests that this approach will find much wider application in studies of trafficking in plants (Scales *et al*., 2000; Tyrrell *et al*., 2007).

It was found that the dominant-negative phenotype of *AtVAMP714* showed a short root and a branchy dwarfed aerial phenotype. Consistent with the auxin transport defects observed in the overexpressors and loss-of-function mutants, PIN1 and PIN2 localization was severely abnormal in the dominant negative seedlings. It is interesting that the dominant negative mutant, and SALK loss-of-function mutants, exhibited a similar phenotype to the overexpressors. This suggests that overexpression of the ATVAMP714 protein leads to a loss-of-function phenotype, possibly due to an altered stoichiometry between AtVAMP714 and putative interacting protein partners, which adversely affect vesicle trafficking (and PIN protein targeting) function. While there are some differences in phenotypes observed between the dominant negative and the loss-of-function mutants, both types of mutant exhibit common features that strongly suggest an essential role for AtVAMP714 in correct PIN localization and polar auxin transport.

6.4 Conclusions

In this study we discovered that the activation-tagged *conjoined* mutant of *Arabidopsis* overexpresses *AtVAMP714*, which may act to generate a dominant negative phenotype. AtVAMP714 is a vesicle-associated protein that co-localizes with a Golgi marker and is potentially involved in Golgi trafficking pathway. AtVAMP714 is expressed in vascular tissues, and is required for correct PIN localization and polar auxin transport. *AtVAMP714* may be activated by auxin to promote auxin transport out of cells, such as from the stem into the root. Plants defective in AtVAMP714 function showed reduced expression of auxin-inducible genes, and defective root and shoot development and root gravitropism, consistent with auxin signalling problems. As such, this work represents the first direct evidence for a role for VAMP R-SNARE proteins in PIN protein localization. A model for the role of AtVAMP714 is summarized in Figure 6-1.

6.5 Future Work

This study has raised a number of avenues for future investigation. Since *atvamp714* mutants show an agravitropic response, one of the most important points is to investigate the localization of PIN3 and PIN4 proteins in *atvamp714* mutants. Gravitropic curvature of *Arabidopsis* roots requires changes in IAA transport at the root tip (Muday and Rahman, 2008). The *pin3* mutant exhibits slightly reduced rates of gravitropic curvature (Harrison and Masson, 2007), and PIN3 is localized in the columella cells, which are the site of gravity perception (Blancaflor *et al*., 1998; Friml *et al*., 2002). The PIN3 protein relocates to membranes on the lower side of columella cells after gravitropic reorientation, consistent with a role in facilitating asymmetric IAA transport at the root tip (Friml *et al*., 2002; Harrison and Masson, 2007).

It would also be interesting to determine the free IAA level in *atvamp714* mutants. It can be predicted that, since the polar auxin transport system appears to be defective in the mutants, the concentration of accumulated auxin in the root tip will be reduced, but this requires confirmation. During this project, the auxin responsive DR5::GFP fusion gene has been introduced into *atvamp714* mutant background, but in the time available it was not possible to analyse. This is expected to provide information on the distribution of auxin in the root tip of the mutants (Sabatini *et al*., 1999).

Another important area that requires future experimentation is the identification of proteins with which AtVAMP714 interacts. There are a number of possible approaches that can be used,

including the yeast 2 hybrid system (Pierre-Olivier *et al*., 2004), bimolecular fluorescence complementation ('split YFP' analysis) Kerppola, 2006) and co-precipitation experiments combined with proteomics (Elaine, 2007). For the first two approaches, candidate interacting proteins must be identified for cloning (ie into yeast expression vectors or as YFP fusions, respectively), perhaps based on the bioinformatics predictions described in Chapter 3. For the third approach (pull-down studies), it is necessary either to raise antibodies against ATVAMP714, or generate a tagged version of the protein (eg HIS-tagged; Bill, 2008), so that it can be purified from protein extracts in association with interacting proteins; mass spectrometry can be used to identify associated proteins. Further studies, such as colocalization analysis, eg of fluorescent protein fusions, can be carried out to further confirm interactions with ATVAMP714. Mutant analysis or dominant negative studies could then allow us to investigate whether these proteins are, like ATVAMP714, essential for PIN localization or auxin transport. This work would allow us to build up a network of interacting proteins essential for auxin signalling in the root tip.

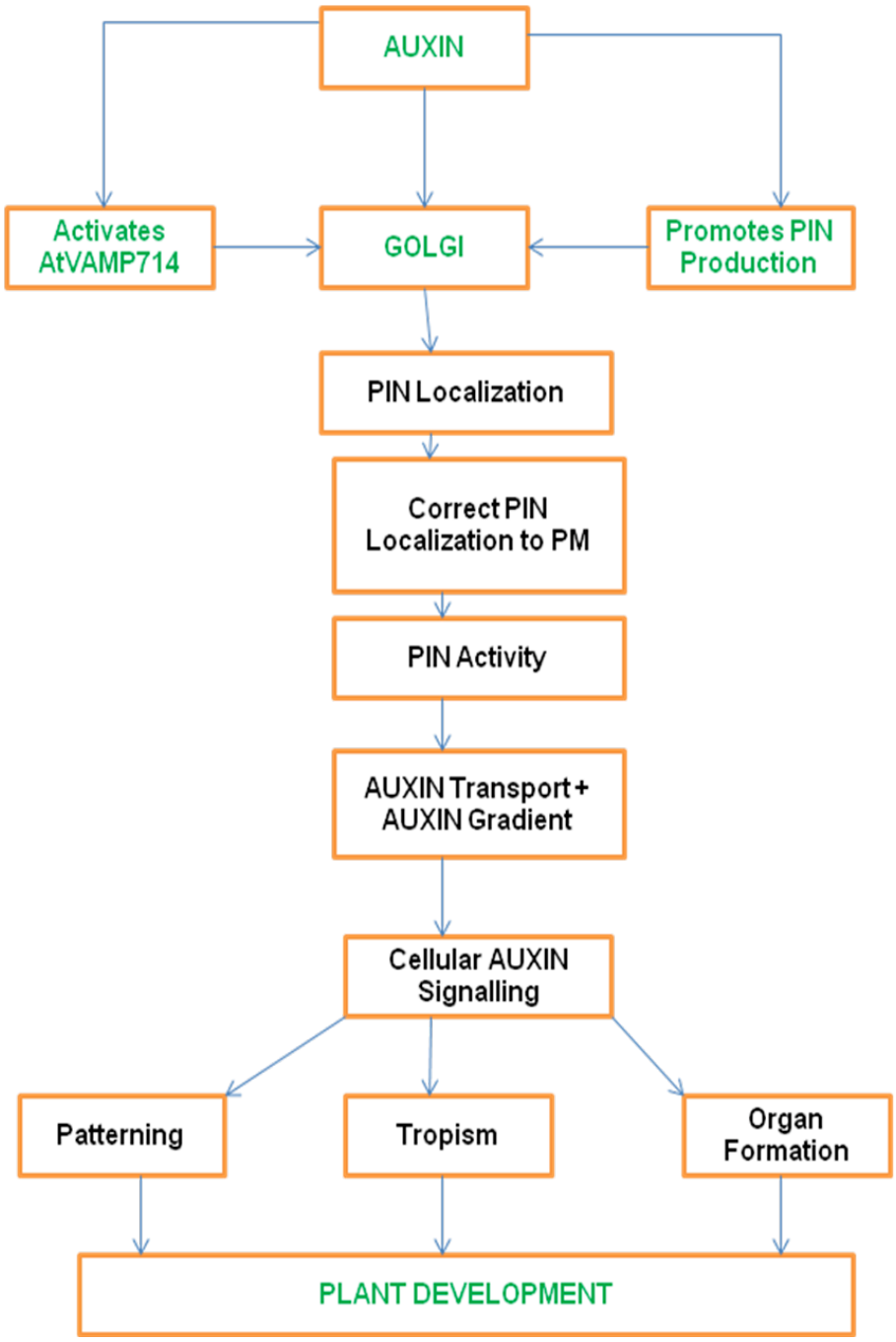

Figure 6-1: Diagram showing Auxin Transport pathway with links to Golgi trafficking and AtVAMP714

REFERENCES

REFERENCES

Aaron Santner and Mark Estelle (2009). Recent advances and emerging trends in plant hormone signalling. *Nature,* 459 -25

Abas L, Benjamins R, Malenica N, Paciorek T, Wisniewska J, *et al*. (2006). Intracellular trafficking and proteolysis of the *Arabidopsis* auxin-efflux facilitator PIN2 are involved in root gravitropism. *Nat. Cell Biol.* 8:249–56

Abe H, Urao T, Ito T, Seki M, Shinozaki K, Yamaguchi-Shinozaki K. (1993) Arabidopsis AtMYC2 (bHLH) and AtMYB2 (MYB) function as transcriptional activators in abscisic acid signaling. *Plant Cell* 15: 63-78 (2003)

Abel S, Theologis A. (1996) Early genes and auxin action. *Plant Physiol*.11:9–17

Aida, M., Beis, D.,Heidstra, R., Williamsen, V., Blilou, I., Galinha, C., Nussaume, L., Noh, Y.S., Amasino, R. and Scheres, B. (2004) The *PLETHORA* genes mediate patterning of the Arabidopsis root stem cell niche. *Cell*, 119, 109-120

Aloni R., Schwalm K., Langhans M., Ullrich C.I. *(2003)* Gradual shifts in sites of free-auxin production during leaf-primordium development and their role in vascular differentiation and leaf morphogenesis in *Arabidopsis. Planta 216:841–853*

Angharad R. Jones, Eric M. Kramer, Kirsten Knox, Ranjan Swarup, Malcolm J. Bennett, Colin M. Lazarus, H. M. Ottoline Leyser, Claire S. Grierson. (2008). Auxin transport through non-hair cells sustains root-hair development. *Nature Cell Biology* 11, 78 - 84

Anton A Sanderfoot and Natasha V Ralkhel (2003) The Secretory System of Arabidopsis; The Arabidopsis Book, *American Society of Plant Biologists*

Arabidopsis Genome initiative (2000) Analysis of the genome sequence of the flowering plant *Arabidopsis thaliana*. *Nature*, 408, 796-815

Argüello-Astorga GR, Herrera-Estrella LR (1996). Ancestral multipartite units in light-responsive plant promoters have structural features correlating with specific phototransduction pathways*. Plant Physiology ,* 112*:*1151-1166

Ausubel FM, Brent R, Kingston RE, Moore DD, Seidman JG, Smith JA, Struhl K. (1994) Current protocols in molecular biology. New York: John Wiley & Sons

Baker SS, Wilhelm KS, Thomashow MF (1994) The 5'-region of Arabidopsis thaliana cor15a has cis-acting elements that confer cold-, drought- and ABA-regulated gene expression. *Plant Mol Biol* 24:701-713

Baluška, F., J. Samaj, and D. Menzel. (2003). Polar transport of auxin: carrier-mediated flux across the plasma membrane or neurotransmitter-like secretion? *Trends Cell Biol* 13:282–285

Bassham DC, Brandizzi F, Otegui MS, Sanderfoot AA (2009) The Secretory System of Arabidopsis: The Arabidopsis Book. Rockville, MD: American Society of Plant Biologists. http://www.aspb.org/publications/arabidopsis/

Baumert M, Maycox PR, Navone F, Decamilli P, Jahn R. (1989). Synaptobrevin: an integral membrane-protein of 18000 daltons present in small synaptic vesicles of rat-brain. *EMBO J.* 8:379–84

Bednarek, S.Y., and Raikhel, N.V. (1992) Intracellular trafficking of secretory proteins. *Plant Mol. Biol.* 20, 133-150

Benjamins R, Quint A, Weijers D, Hooykaas P, Offringa R. (2001). The PINOID protein kinase regulates organ development in *Arabidopsis* by enhancing polar auxin transport. *Development* 128:4057–67

Benjamins, R., N. Malenica, and C. Luschnig. (2005). Regulating the regulator: the control of auxin transport. *Bioessays* 27:1246–1255

Benková, E., M. Michniewicz, M. Sauer, T. Teichmann, D. Seifertová, G. Jürgens, and J. Friml. (2003). Local, efflux-dependent auxin gradients as a common module for plant organ formation. *Cell* 115:591–602

Benkova Eva, Maria G. Ivanchenko, Jiril Friml, Svetlana Shishkova and Joseph G. Dubrovsky (2009). A morphogenetic trigger: is there an emerging concept in plant developmental biology? Trends in Plant Science Vol.14 No.4

Bennett MK, Calakos N, Scheller RH. 1992. Syntaxin: a synaptic protein implicated in docking of synaptic vesicles at presynaptic active zones. *Science* 257:255–59

Bennett, M. J., A. Marchant, H. G. Green, S. T. May, S. P. Ward, P. A. Millner, A. R. Walker, B. Schulz, and K. A. Feldmann. (1996). Arabidopsis AUX1 gene: a permease-like regulator of root gravitropism. *Science* 273:948–950

Bennett, M.J., Marchant, A., May, S.T., and Swarup, R**.** (1998). Going the distance with auxin: Unravelling the molecular basis of auxin transport. Philos. Trans. R. Soc. Lond. B 353**,** 1511–1515

Berleth T and Jurgens G (1993) The role of the monopteros gene in organising the basal body region of the *Arabidopsis* embryo. *Development*, 118, 575–587

Bhat, R. A. and R. Panstruga. (2005). Lipid rafts in plants. *Planta* 223:5–19

Bill Brizzard (2008). Epitope tagging. *BioTechniques*, Vol. 44, (5), 693–695

Blakeslee, J. J., W. A. Peer, and A. S. Murphy. (2005). Auxin transport. *Curr. Opin. Plant Biol* 8:494–500

Blatt M.R, Campanoni P, (2007) Membrane trafficking and polar growth in root hairs and pollen tubes. *J Exp Bot* 58: 65–74

Blilou, I., J. Xu, M. Wildwater, V. Willemsen, I. Paponov, J. Friml, R. Heidstra, M. Aida, K. Palme, and B. Scheres. (2005). The PIN auxin efflux facilitator network controls growth and patterning in Arabidopsis roots. *Nature* 433:39–44

Bock JB,Matern HT, Peden AA, Scheller RH (2001) A genomic perspective on membrane compartment organization. *Nature* 409: 839–841

Bock, J.B., Klumperman, J., Davanger, S., and Scheller, R.H. (1997) Syntaxin 6 functions in *trans*- Golgi network vesicle trafficking. *Mol.Biol. Cell* 8, 1261-1271

Boevink P, Oparka K, Santa Cruz S, Martin B, Betteridge A, Hawes C (1998) Stacks on tracks: the plant Golgi apparatus traffics on an actin/ER network. *Plant J* 15:441–447

Bonifacino J.S, Lippincott-Schwartz J. (2003). Coat proteins: shaping membrane transport. *Nat. Rev. Mol. Cell Biol.* 4(5):409–14

Boonsirichai K, Guan C, Chen R, Masson PH. (2002) Root gravitropism: an experimental tool to investigate basic cellular and molecular processes underlying mechanosensing and signal transmission in plants. *Annual review of plant biology*. 53:421-47.

Bouche, N and Bouchez, D. (2001) Arabidopsis gene knockout; phenotypes wanted. *Curr.Opin. plant Biol*. 4, 111-117

Boutte Y, Ikeda Y, Grebe M. (2007). Mechanisms of auxin-dependent cell and tissue polarity. *Curr. Opin. Plant Biol.* 10(6):616–23

Boutté, Y., M. T. Crosnier, N. Carraro, J. Traas, and B. Satiat-Jeunemaitre. (2006). The plasma membrane recycling pathway and cell polarity in plants: studies on PIN proteins. *J. Cell Sci* 119:1255–1265

Budziszewski, G.J, Lewis, S.P, Glovel, L.W et al., (2001) Arabidopsis genes essential for seedling variability: isolation of insertional mutants and molecular cloning. *Genetics*, 159 1765-1778

Busch, M., U. Mayer, and G. Jurgens. (1996). Molecular analysis of the Arabidopsis pattern formation of gene GNOM: gene structure and intragenic complementation. *Mol. Gen. Genet* 250:681–91

Brandizzi, F., Snapp, E., Roberts, A., Lippincott-Schwartz, J. and Hawes, C. (2002) Membrane protein transport between the ER and Golgi in tobacco leaves is energy dependent but cytoskeleton independent: evidence from selective photobleaching. *Plant Cell*, 14, 1293–1309

Brunger AT. 2006. Structure and function of SNARE and SNARE–interacting proteins. *Q. Rev. Biophys.* 38:1–47

Carter C, Pan SQ, Jan ZH, Avila EL, Girke T, Raikhel NV. (2004). The vegetative vacuole proteorne of *Arabidopsis thaliana* reveals predicted and unexpected proteins. *Plant Cell* 16:3285–303

Carter CJ, Bednarek SY, Raikhel NV. (2004). Membrane trafficking in plants: new discoveries and approaches. *Curr. Opin. Plant Biol.* 7(6):701–7

Carter, C., S. Pan, J. Zouhar, E. L. Avila, T. Girke, and N. V. Raikhel. (2004). The vegetative vacuole proteome of Arabidopsis thaliana reveals predicted and unexpected proteins. *Plant Cell* 16:3285–3303

Casson, S.A. & Lindsey, K**.** (2006). The turnip mutant of Arabidopsis reveals that LEC1 expression mediates the effects of auxin and sugars to promote embryonic cell identity. *Plant Physiology* 142: 526-541

Casson SA, Chilley PM, Topping JF, Evans IM, Souter MA, Lindsey K. (2002) The POLARIS gene of Arabidopsis encodes a predicted peptide required for correct root growth and leaf vascular patterning. *Plant Cell* 14:1705-21

Celenza, J.L., Grisafi, P.L., and Fink, G.R**.** (1995). A pathway for lateral root formation in *Arabidopsis thaliana*. Genes Dev. **9,** 2131– 2142

Chang, W.C., T.Y. Lee, H.D. Huang*, H.Y. Huang and R.L. Pan (2008) PlantPAN: Plant Promoter Analysis Navigator, for identifying combinatorial cis-regulatory elements with distance constraint in plant gene group, *BMC Genomics*, 9:561

Chatre, L., F. Brandizzi, A. Hocquellet, C. Hawes, and P. Moreau. (2005). Sec22 and Memb11 are v-SNAREs of the anterograde endoplasmic reticulum-Golgi pathway in tobacco leaf epidermal cells. *Plant Physiol* 139:1244–1254

Chen Y, Shin YK, Bassham D.C. (2005). YKT6 is a core constituent of membrane fusion machineries at the *Arabidopsis* trans-Golgi network. *J. Mol. Biol.* 350:92–101

Chen, R., P. Hilson, J. Sedbrook, E. Rosen, T. Caspar, and P. H. Masson. (1998). The Arabidopsis thaliana AGRAV-ITROPIC 1 gene encodes a component of the polar-auxin-transport efflux carrier. *Proc. Natl. Acad. Sci.* 95:15112–15117

Chen, Y., Y. K. Shin, and D. C. Bassham. (2005). YKT6 is a core constituent of membrane fusion machineries at the Arabidopsis trans-Golgi network. *J. Mol. Biol* 350:92–101

Chen, Y.A. and R.H. Scheller, SNARE-mediated membrane fusion, *Nat. Rev. Mol. Cell Biol.* 2 (2001), pp. 98–106

Cho, M., Lee, S. H. & Cho, H.-T. (2007) P-Glycoprotein4 displays auxin efflux transporter-like action in *Arabidopsis* root hair cells and tobacco cells. *Plant Cell* 19, 3930–3943

Chow CM, Neto H, Foucart C, Moore I. (2008). Rab-A2 and Rab-A3 GTPases define a trans-Golgi endosomal membrane domain in *Arabidopsis* that contributes substantially to the cell plate. *Plant Cell* 20(1):101–23

Christensen, S.K., Dagenais, N., Chory, J., and Weigel, D. (2000). Regulation of auxin response by the protein kinase PINOID. *Cell* 100, 469–478

Clough, S.J and Bent, A.E (1998) Floral dip: a simplified method for *Agrobacterium*-mediated transformation of *Arabidopsis thaliana*, *Plant J*, 16, 735-743

Cooper, Geoffrey (2000). The Mechanism of Vesicular Transport *The Cell: A Molecular Approach*. *Sinauer Associates*, Inc. *http://www.ncbi.nlm.nih.gov/books/*

Corina Vlot, Maris Amick Dempsey,and Daniel F. Klessig (2009) Salicylic Acid, a Multifaceted Hormone to Combat Disease; *Annu. Rev. Phytopathol*. 47:177–206

David W. Meinke(1991). Perspectives on Genetic Analysis of Plant Embryogenesis. *Plant Cell* 3, 857-866

Davidson, Michael (2005). The Endoplasmic Reticulum *Molecular Expressions*. Florida State University. http://micro.magnet.fsu.edu/cells/endoplasmicreticulum/

Davies, P. J. (2004). Plant Hormones: biosynthesis, signal transduction, action!. Kluwer Academic Publishers. Dordrecht, Netherlands

Davies, P. J. and P. H. Rubery. (1978). Components of auxin transport in stem segments of Pisum sativum. *Planta* 142:211–219

Delbarre, A., P. Muller, and J. Guern. (1998). Short-lived and phosphorylated proteins contribute to carrier-mediated efflux, but not to influx, of auxin in suspension-cultured tobacco cells. *Plant Physiol* 116:833–844

Devic M, Lahmy S, Guilleminot J, Schmit AC, Pelletier G, Chaboute ME, (2007). QQT proteins colocalize with microtubules and are essential for early embryo development in Arabidopsis. *Plant J*. 50(4):615-26

Dhonukshe P, Grigoriev I, Fischer R, Tominaga M, Robinson D, et al. 2008a. Auxin transport inhibitors block vesicle motility and actin cytoskeleton dynamics in diverse eukaryotes. *Proc. Natl. Acad. Sci.* 105(11):4489–94

Dhonukshe, P., F. Aniento, I. Hwang, D. Robinson, J. Mravec, Y-D. Stierhof, and J. Friml. (2007a). Clathrin-mediated constitutive endocytosis of PIN auxin efflux carriers in Arabidopsis. *Curr. Biol* in press

Dhonukshe, P., Kleine-Vehn, J., Friml, J., (2005). Cell polarity, auxin transport and cytoskeleton mediated division planes: who comes first? *Protoplasma* 226, 67–73

Dhonukshe P,Samaj J, Baluska F, Friml J. (2007b). A unifying new model of cytokinesis for the dividing plant and animal cells. *Bioessays* 29:371–81

Diane C. Basshan and Michael R. Blatt (2008). SNAREs: Cogs and Coordinators in Signaling and Development. *Plant Physiology*, 147, 1504-1515

Dolan, L., Janmaat, K., Willemsen, V., Linstead, P., Poethig, S., Roberts, K. and Scheres, B. (1993) Cellular organisation of the *Arabidopsis thaliana* root. *Development*, 119, 71–84

Dong Wang, Karolina Pajerowska-Mukhtar,Angela Hendrickson Culler, and Xinnian Dong (2007). Salicylic Acid Inhibits Pathogen Growth in Plants through Repression of the Auxin Signaling Pathway. *Current Biology* 17, 1784–1790

Douglas C. Boyes, Adel M. Zayed, Robert Ascenzi, Amy J. McCaskill, Neil E. Hoffman, Keith R. Davis and Jorn Gorlach (2001). Growth Stage-Based Phenotypic analysis of Arabidopsis. *Plant Cell* 13, 1499-1510

Dubrovsky J, Sauer M, Napsucialy-Mendivil S, Ivanchenko M, Friml J, et al. (2008). Auxin acts as a local morphogenetic trigger to specify lateral root founder cells. *Proc. Natl. Acad. Sci. USA.* Invited for revision

Dubrovsky, J.G.*,* Doerner, P.W.*,* Colón-Carmona, A. *and* Rost, T.L. *(*2000*)* Pericycle cell proliferation and lateral root initiation in Arabidopsis*. Plant Physiol.* 124*,* 1648–1657

Edwards K, Johnstone C, Thompson C. (1991). A simple and rapid method for the preparation of plant genomic DNA for PCR analysis. *Nucleic Acids Res*. 19:1349

Elaine A. Elion (2007). Detection of Protein-Protein Interactions by Coprecipitation, *Current Protocols in Immunology*, 10.1002/0471142727 (Online publication)

Elliot M. Meyerowitz (2001). Prehistory and History of Arabidopsis Research, *Plant Physiol*, Vol. 125, pp. 15

Esmon, C. A., A. G. Tinsley, K. Ljung, G. Sandberg, L. B. Hearne, and E. Liscum. (2006). A gradient of auxin and auxin-dependent transcription precedes tropic growth responses. *Proc. Natl. Acad. Sci* 103:236–241

Estelle M*,* Timpte C, Lincoln C, Pickett FB, Turner J,. (1995). The AXR1 and AUX1 genes of Arabidopsis function in separate auxin-response pathways. Plant J. 8 (4), 561-9

Fasshauer D, Sutton RB, Brunger AT, Jahn R. (1998). Conserved structural features of the synaptic fusion complex: SNARE proteins reclassified as Q- and R-SNAREs. *Proc. Natl. Acad. Sci. USA* 95:15781–86

Feng, Q., Zhang, Y., Hao, P. et al., (2002) Sequence and analysis of rice chromosome 4. *Nature*, 420, 316-320

Finney Michael, Paul E. Nisson, Ayoub Rashtchian (2001) Molecular Cloning of PCR Products**,** *John Wiley and Sons*, Inc. Lab Protocoals

Fischer, U. *et al*. (2006) Vectorial information for *Arabidopsis* planar polarity is mediated by combined AUX1, EIN2, and GNOM activity. *Curr. Biol.* 16, 2143–2149

Friml J, Vieten A, Sauer M, Weijers D, Schwarz H,. , T. Hamann, R. Offringa, and G. Jürgens. (2003b). Efflux-dependent auxin gradients establish the apical-basal axis of *Arabidopsis*. *Nature* 426:147–53

Friml J, Yang X, Michniewicz M, Weijers D, Quint A, *et al*. (2004). A PINOID-dependent binary switch in apical basal PIN polar targeting directs auxin efflux. *Science* 306:862–65
Friml, J. (2003). Auxin transport - shaping the plant. *Curr. Opin. Plant Biol* 6:7–12

Friml, J. and K. Palme. (2002). Polar auxin transport - old questions and new concepts? *Plant Mol. Biol* 49:273–284

Friml, J., E. Benková, I. Blilou, J. Wisniewska, T. Hamann, K. Ljung, S. Woody, G. Sandberg, B. Scheres, G. Jürgens, and K. Palme. (2002a). AtPIN4 mediates sink-driven auxin gradients and root patterning in Arabidopsis. *Cell* 108:661–673

Friml, J., E. Benková, U. Mayer, K. Palme, and G. Muster. (2003a). Automated whole-mount localization techniques for plants. *Plant J* 34:115–24

Friml, J., J. Wisniewska, E. Benková, K. Mendgen, and K. Palme. (2002b). Lateral relocation of auxin efflux regulator PIN3 mediates tropism in Arabidopsis. *Nature* 415:806–809

Friml, J., X. Yang, M. Michniewicz, D. Weijers, A. Quint, O. Tietz, R. Benjamins, P. B. Ouwerkerk, K. Ljung, G. Sandberg, P. J. Hooykaas, K. Palme, and R. Offringa. (2004). A PINOID-dependent binary switch in apical basal PIN polar targeting directs auxin efflux. *Science* 306:862–865

Fry, S.C. (2004) Primary cell wall metabolism: tracking the careers of wall polymers in living plant cells, *New Phytol*. 161 641–675

Galinha C, Hofhuis H, Luijten M, Willemsen V, Blilou I, Heidstra R, Scheres B. (2007). PLETHORA proteins as dose-dependent master regulators of Arabidopsis root development. *Nature*. 25;449 (7165):1053-7

Gälweiler, L., C. Guan, A. Müller, E. Wisman, K. Mendgen, A. Yephremov, and K. Palme. 1998. Regulation of polar auxin transport by AtPIN1 in Arabidopsis vascular tissue. *Science* 282:2226–2230

Geelen D, Leyman B, Batoko H, Di Sansebastiano G, Moore I, Blatt M, Di Sansabastiano G (2002) The abscisic acid-related SNARE homolog NtSyr1 contributes to secretion and growth: evidence from competition with its cytosolic domain. *Plant Cell* 14**:** 387–406

Geldner, N., J. Friml, Y. D. Stierhof, G. Jürgens, and K. Palme. (2001). Auxin transport inhibitors block PIN1 cycling and vesicle trafficking. *Nature* 413:425–428

Geldner, N., N. Anders, H. Wolters, J. Keicher, W. Kornberger, P. Muller, A. Delbarre, T. Ueda, A. Nakano, and G. Jürgens. (2003). The Arabidopsis GNOM ARF-GEF mediates endosomal recycling, auxin transport, and auxin-dependent plant growth. *Cell* 112:219–230

Geldner, N., S. Richter, A. Vieten, S. Marquardt, R. A. Torres-Ruiz, U. Mayer, and G. Jurgens. (2004). Partial loss-of-function alleles reveal a role for GNOM in auxin transport-related, post-embryonic development of Arabidopsis. *Development* 131:389–400

Gerst J,E. (2003). SNARE regulators: matchmakers and match-breakers. *Biochim. Biophys. Acta* 1641:99–110

Gil, P., E. Dewey, J. Friml, Y. Yhao, K. C. Snowden, J. Putterill, K. Palme, M. Estelle, and J. Chory. (2001). BIG: a calossin-like protein required for polar auxin transport in Arabidopsis. *Genes Dev* 15:1985–1997

Giuliano G, Pichersky E, Malik VS, Timko MP, Scolnik PA, Cashmore AR (1988) An evolutionarily conserved protein binding sequence upstream of a plant light-regulated gene. *Proc Natl Acad Sci* 85:7089-7093

Goda H, Sawa S, Asami T, Fujioka S, Shimada Y, Yoshida S **(**2004) Comprehensive comparison of auxin-regulated and brassinosteroid-regulated genes in *Arabidopsis***.** *Plant Physiol* , 134**:**1555-1573

Goldsmith, M. H. M**.** (1977). Polar transport of auxin. *Annu. Rev. Plant Physiol. Plant Mol. Biol.* 28, 439-478

Gomez-Roldan V., Fermas S., Brewer P.B., Puech-Pages V., Dun E.A., Pillot J.P., *et al* (2008) *Strigolactone inhibition of shoots branching. Nature 455:189-194*

Gonzalez L.C., Jr., W.I. Weis and R.H. Scheller, A novel SNARE N-terminal domain revealed by the crystal structure of Sec 22b (2001), *J. Biol. Chem.* 276,. 24203–24211
Graham, Todd R. (2000). Eurekah Bioscience Collection Cell Biology University of New South Wales and Landes Bioscience. http://www.ncbi.nlm.nih.gov/books/

Grebe, M., J. Xu, W. Mobius, T. Ueda, A. Nakano, H. J. Geuze, M. B. Rook, and B. Scheres. (2003). Arabidopsis sterol endocytosis involves actin-mediated trafficking via ARA6-positive early endosomes. *Curr. Biol* 13:1378–1387

Grebe, M. *et al*. (2002) Cell polarity signaling in Arabidopsis involves a BFA-sensitive auxin influx pathway. *Curr. Biol.* 12, 329–334

Grieneisen, V.A., Xu.J., Maree, A.F.M., Hogeweg, P. and Scheres, B, (2007). Auxin transport is sufficient to generate a maximum and gradient guiding root growth. *Nature*, 449, 1008-1013

Grunewald, W., Cannoot, B., Friml, J., Gheysen, G., (2009). Parasitic nematodes modulate PIN-mediated auxin transport to facilitate infection. *PLoS Pathog*. 5

Guilfoyle, T**.** (1999). Auxin-regulated genes and promoters. In Biochemistry and Molecular Biology of Plant Hormones, P. Hooykaas, M. Hall, and K. Libbenga, eds (New York: Elsevier Science), pp. 423–459

Guilfoyle, TJ; Ulmasov, T; Hagen, G. The ARF family of transcription factors and their role in plant hormone-responsive transcription. Cell. Mol. Life Sci. 1998. 54(7):619-27

Hadfi, K., Speth, V. and Neuhaus, G. (1998) Auxin- induced developmental patterns in Brassica juncea embryos. *Development* 125, 879-887

Hagen G, Guilfoyle TJ. (2002). Auxin-responsive gene expression: genes, promoters and regulatory factors. *Plant Mol Biol*.; 49:373–385

Hamann T, Benkova E, Baurle I, Kientz M and Jurgens G (2002) The *Arabidopsis BODENLOS* gene encodes an auxin response protein inhibiting MONOPTEROS-mediated embryo patterning. *Genes Dev*, 16, 1610–1615

Hamann Thorsten, Ulrike Mayer and Gerd Jurgens (1999). The auxin-insensitive bodenlos mutation affects primary root formation and apical-basal patterning in the Arabidopsis embryo, *Development* 126, 1387-1395

Hartley, J. L., Temple, G. F., and Brasch, M. A. (2000). DNA Cloning Using *in vitro* Site-Specific Recombination. *Genome Research 10*, 1788-1795

Hay, J.C., and Scheller, R.H. (1997) SNAREs and NSF in targeted membrane fusion. *Curr.Opin.Cell Biol*. 9, 505-512

Heisler, M.G. and Jonsson, H. (2006) Modeling auxin transport and plant development. *J Plant Growth Regul*. 25, 302-312

Heisler MG, Ohno C, Das P, Sieber P, Reddy GV, et al. (2005). Patterns of auxin transport and gene expression during primordium development revealed by live imaging of the *Arabidopsis* inflorescence meristem. *Curr. Biol.* 15:1899–911

Hong, W. (2005). SNAREs and traffic. *Biochim. Biophys. Acta* 1744:493–517

Jahn R, Scheller R.H. (2006). SNAREs: engines for membrane fusion. *Nat. Rev. Mol. Cell Biol.* 7:631–43

Jahn, R.,T. Lang and T.C. Sudhof, Membrane fusion, *Cell* 112 (2003), pp. 519–533.
Jaillais Y, Fobis-Loisy I, Miege C, Rollin C, Gaude T. 2006. AtSNX1 defines an endosome for auxin-carrier trafficking in *Arabidopsis*. *Nature* 443(7107):106–9

Jaillais Yvon, Isabelle Fobis-Loisy, Christine Miège, Claire Rollin and Thierry Gaude (2006). AtSNX1 defines an endosome for auxin-carrier trafficking in *Arabidopsis. Nature* 443, 106-109

Jan Petrasek, Jozef Mravec, Rodolphe Bouchard, Joshua J. Blakeslee, Melinda Abas, Daniela Seifertova , Justyna Wisniewska, Zerihun Tadele, Martin Kubes, Milada Covanova, Pankaj Dhonukshe,3 Petr Skupa,1,2 Eva Benkova, Lucie Perry, Pavel Krecek, Ok Ran Lee, Gerald R. Fink, Markus Geisler, Angus S. Murphy, Christian Luschnig, Eva Zazımalova´ ,Jırıl Friml (2006) PIN Proteins Perform a Rate-Limiting Function in Cellular Auxin Efflux; *Science* 312, 914

Jefferson, R.A., Kavanagh, T.A. and Bewan, M.W.(1987) GUS fusions- beta-glucuronidase as a sensitive and versatile gene fusion marker in higher-plants. *EMBO journal*. 6, 3901-3907

Jeong, D.H., An, S., Kang, H.G., Moon, S., Han, J.J., Park, S., Lee, H.S., An, K. and An, G. (2002) T-DNA insertional mutagenesis for activation tagging in rice. *Plant Physiol*. 130, 1636-1644

Jiri Friml, (2010) Subcellulat trafficking of PIN auxin efflux carriers in auxin transport. *European Journal of Cell Biology* 89: 231-135

Jurgens, G. Membrane trafficking in plants, (2004) *Annu. Rev. Cell Dev. Biol.* 20, 481–504

Jürgen Kleine-Vehn, Fang Huang, Satoshi Naramoto, Jing Zhang, Marta Michniewicz Remko Offringa and Jiríl Friml (2009). PIN Auxin Efflux Carrier Polarity Is Regulated by PINOID Kinase-Mediated Recruitment into GNOM-Independent Trafficking in *Arabidopsis, The Plant Cell* 21:3839-3849

Kaplan B, Davydov O, Knight H, Galon Y, Knight MR, Fluhr R, Fromm H (2006) Rapid Transcriptome Changes induced y Cytosolic Ca^{2+} Transients Reveal ABRE related sequences as Ca^{2+} Responsive cis elements in Arabidopsis. *Plant Cell*, 18:2733-2748

Kepinski, S. and Leyser, O. (2002) Ubiquitination and auxin signaling: a degrading story. *Plant Cell* 14, S81–S95

Kepinski, S., and Leyser, O. (2005). The Arabidopsis F-box protein TIR1 is an auxin receptor. *Nature*, 435, 446–451

Katekar, G. F. and A. E. Geissler. (1977). Auxin Transport Inhibitors: III. Chemical requirements of a class of auxin transport inhibitors. *Plant Physiol* 60:826–829

Kim DW, Lee SH, Choi SB, Won SK, Heo YK, Cho M, Park YI, Cho HT. (2006) Functional Conservation of a Root Hair Cell-Specific cis-Element in Angiosperms with Different Root Hair Distribution Patterns. *Plant Cell*. 18:2958-2970

Klein Theodore, Rene Arentzen, Paul A. Lewis and Sandra Fitzpatrick-McElligott (1992) Transformation of Microbes, Plants and Animals by Particle Bombardment. *Nature Biotechnology* 10, 286 - 291

Kleine-Vehn J, Dhonukshe P, Sauer M, Brewer P, Wisniewska J, *et al*. (2008a). ARF GEF-dependent transcytosis and polar delivery of PIN auxin carriers in *Arabidopsis*. *Curr. Biol.* 18:526–31

Kleine-Vehn, J., P. Dhonukshe, R. Swarup, M. Bennett, and J. Friml. (2006). A novel pathway for subcellular trafficking of AUX1 auxin influx carrier. *Plant Cell* 18:3171–3181

Klessig DF, Park SW, Kaimoyo E, Kumar D, Mosher S,.(2007) Methyl salicylate is a critical mobile signal for plant systemic acquired resistance *Science*. 318(5847):113-6

Klessig DF, Park SW, Liu PP, Forouhar F, Vlot AC, Tong L, Tietjen K,.(2009). Use of a synthetic salicylic acid analog to investigate the roles of methyl salicylate and its esterases in plant disease resistance, *J Biol Chem*. 13;284(11):7307-17

Knox, K., Grierson, C. S. & Leyser, O. (2003). AXR3 and SHY2 interact to regulate root hair development. *Development* 130, 5769–5777

Kramer, E. M. and M. J. Bennett. (2006). Auxin transport: a field in flux. *Trends Plant Sci* 11:382–386

Krysan, P.J., Young, J.C., and Sussman, M.R.(1999). T-DNA as an insertional mutagen. *Plant Cell* 11**,** 2283-2290

Kwon, C., C. Neu, S. Pajonk, H. S. Yun, U. Lipka, M. Humphry, S. Bau, M. Straus, M. Kwaaitaal, H. Rampelt, F. El Kasmi, G. Jürgens, J. Parker, R. Panstruga, V. Lipka, and P. Schulze-Lefert. (2008). Co-option of a default secretory pathway for plant immune responses. *Nature* 451:835–840

Lam E, Chua NH (2003) ASF-2: A factor that binds to the cauliflower mosaic virus 35S promoter and a conserved GATA motif in cab promoters. *Plant Cell* 1:1147-1156

Landy, A. (1989). Dynamic, Structural, and Regulatory Aspects of Lambda Site-specific Recombination. *Ann. Rev. Biochem*. *58*, 913-949

Laskowski, M.J., Williams, M.E., Nusbaum, C., and Sussex, I.M**.** (1995). Formation of lateral root meristems is a two-stage process. *Development* 121**,** 3303–3310

Lee, S. H. & Cho, H. T. PINOID positively regulates auxin efflux in *Arabidopsis* root hair cells and tobacco cells. *Plant Cell* 18, 1604–1616 (2006)

Leshem Y, Melamed-Book N, Cagnac O, Ronen G, Nishri Y, *et al.* (2006). Suppression of *Arabidopsis* vesicle-SNARE expression inhibited fusion of H2O2 containing vesicles with tonoplast and increased salt tolerance. *Proc. Natl. Acad. Sci.* 103:18008–13

Levine A, Belenghi B, Damari-Weisler H, Granot D. (2001). Vesicle-associated membrane protein of *Arabidopsis* suppresses Bax-induced apoptosis in yeast downstream of oxidative burst. *J. Biol. Chem.* 276:46284–89

Leyman B, Geelen D, Quintero FJ, Blatt MR (1999) A tobacco syntaxin with a role in hormonal control of guard cell ion channels. *Science* 283**:** 537–540

Leyser O. (2006). Dynamic integration of auxin transport and signaling. *Curr. Biol.* 16(11): 424–433

Leyser HM, Lincoln CA, Timpte C, Lammer D, Turner J, Estelle M. (1993) Arabidopsis auxin-resistance gene AXR1 encodes a protein related to ubiquitin-activating enzyme E1. *Nature*. 364:161–164

Lindsey K, Pullen ML, Topping JF (2003) Importance of plant sterols in pattern formation and hormone signalling. *Trends Plant Sci* 8: 521–525

Lodishet, Harvey (2000). Organelles of the Eukaryotic Cell, *Molecular Cell Biology*. W. H. Freeman and Company. http://www.ncbi.nlm.nih.gov/books/

Lomax TL, Muday GK, Rubery PH. Auxin transport. In: Davies PJ, editor (1995). Plant hormones: Physiology, biochemistry and molecular biology. Dordrech, Netherlands: Kluwer Academic Publishers;.509–530

Luschnig, C., R. A. Gaxiola, P. Grisafi, and G. R. Fink. (1998). EIR1, a root-specific protein involved in auxin transport, is required for gravitropism in Arabidopsis thaliana. *Genes Dev* 12:2175–2187

Maarten Koornneef and David Meinke (2010). The development of Arabidopsis as a model plant*, Plant Journal* 61, 909–921

Maher, E. P. and S. J. B. Martindale. (1980). Mutants of Arabidopsis thaliana with altered responses to auxins and gravity. *Biochem. Genet* 18:1041–1053

Malamy, J.E. and Benfey, P.N. (1997a) Organisation and cell differentiation in lateral roots of *Arabidopsis thaliana*. *Development*, 124, 33–44

Manulis, S., Haviv-Chesner, A., Brandl, M.T., Lindow, S.E., and Barash, I. (1998). Differential involvement of indole-3-acetic acid biosynthetic pathways in pathogenicity and epiphytic fitness of Erwinia herbicola pv. gypsophilae. *Mol. Plant Microbe Interact*. 11, 634–642

Marchant, A., J. Kargul, S. T. May, P. Muller, A. Delbarre, C. Perrot-Rechenmann, and M. J. Bennett. (1999). AUX1 regulates root gravitropism in Arabidopsis by facilitating auxin uptake within root apical tissues. *EMBO J* 18:2066–2073

Marsch-Martinez, Greco, R, Van Arkel, G< Herrera Estrella, L and Pereira, A (2002) Activation tagging using the En-1 maize transposon system in Arabidopsis, *Plant Physiol*, 129, 1544-1556

Marta Michniewicz, Marcelo K. Zago, Lindy Abas, Dolf Weijers, Alois Schweighofer, Irute Meskiene, Marcus G. Heisler, Carolyn Ohno, Jing Zhang, Fang Huang, Rebecca chwab, Detlef Weigel, Elliot M. Meyerowitz, Christian Luschnig, Remko Offringa, and Jirı Friml (2007). Antagonistic Regulation of PIN Phosphorylation by PP2A and PINOID Directs Auxin Flux, *Cell* 130, 1044–1056

Martin, S. W., B. J. Glover, and J. M. Davies. (2005). Lipid microdomains-plant membranes get organized. *Trends Plant Sci* 10:263–265

Martinez-Arca S, Rudge R, Vacca M, Raposo G, Camonis J, *et al*. (2003). A dual mechanism controlling the localization and function of exocytic v-SNAREs. *Proc. Natl. Acad. Sci. USA* 100:9011–16

Maruyama-Nakashita A, Nakamura Y, Watanabe-Takahashi A, Inoue E, Yamaya T, Takahashi H. (2005) Identification of a novel cis-acting element conferring sulfur deficiency response in Arabidopsis roots. *Plant J*. 42: 305-314

Masucci, J. D. & Schiefelbein, J. W. The *rhd6* mutation of *Arabidopsis thaliana* alters root-hair initiation through an auxin- and ethylene-associated process. *Plant Physiol.* 106, 1335–1346 (1994)

Mayer, U., R. A. T. Ruiz, T. Berleth, S. Misera, and G. Jurgens. (1991). Mutations affecting body organization in the Arabidopsis embryo. *Nature* 353:402–407

McNew, J.A., Parlati, F., Fukuda, R., Johnston, R.J., Paz, K., Paumet, F., Sollner, T.H., and Rothman, J.E. (2000) Compartmental specificity of cellular membrane fusion encored in SNARE proteins. *Nature* 407, 153-9

Meinke DW, Cherry JM, Dean C, Rounsley SD, Koornneef M (1998) *Arabidopsis thaliana*: A model plant for genome analysis. *Science* 282: 662-682

Meuwly P, Pilet PE. (1991) Local treatment with indole-3-acetic acid influences differential growth responses in Zea mays L. roots. *Planta*.185:58–64

Michniewicz M, Brewer PB, Friml J (2007) Polar Auxin Transport and Asymmetric Auxin Distribution: (2007). The Arabidopsis Book. Rockville, MD: American Society of Plant Biologists. voi: 10.1199/tab.0108, http://www.aspb.org/publications/arabidopsis/

Michniewicz, M., Zago, M.K., Abas, L., Weijers, D., Schweighofer, A., Meskiene, I., Heisler, M.G., Ohno, C., Zhang, J., Huang, F., Schwab, R., Weigel, D., Meyerowitz, E.M., Luschnig, C., Offringa, R., Friml, J., (2007). Antagonistic regulation of PIN phosphorylation by PP2A and PINOID directs auxin flux. *Cell* 130, 1044–1056

Molendijk, A.J., Ruperti, B. and Palme, K. (2004) Small GTPases in vesicel trafficking. *Curr. Opin*. *Plant Biol*. 7, 694–700

Morris, D. A. and J. S. Robinson. (1998). Targeting of auxin carriers to the plasma membrane: differential effects of brefeldin A on the traffic of auxin uptake and efflux carriers. *Planta* 205:606–612

Morris, D. A., J. Friml, and E. Zažímalová. (2004). The transport of auxins. In Plant Hormones: biosynthesis, signal transduction, action! pp 437–470. Davies, P. J., editor. (ed.). Kluwer Academic Publishers

Morris, D.A. (2000) Transmembrane auxin carrier systems-dynamic regulators of polar auxin transport. *Plant Growth Regul*. 32, 161-172

Mravec, J.,Skupa, P.,Bailly,A.,Krecek, P.,Hoyerova , K.,Bielach,A.,Petrasek, J., Zhang, J.,Gaykova,V.,Stierhof,Y.-D.,Schwarzerova, K.,Rolcık, J.,Dobrev,P., Seifertova , D.,Luschnig,C.,Benkova , E.,Zazımalova ,E.,Geisler,M., Friml,J., (2009). Subcellular homeostasis of phytohormone auxin is mediated by the ER-localized PIN5 transporter. *Nature* 459, 1136–1140

Mravec,J.,Kubes,M.,Bielach,A.,Gaykova,V.,Petrasek,J.,Skupa,P.,Chand,S.,Benkova, E.,Zazımalova , E.,Friml,J.,(2008) .Interaction of PIN and PGP transport mechanisms in auxin distribution-dependent development. *Development,* 135, 3345–3354

Muday, G. K. and A. DeLong. (2001). Polar auxin transport: controlling where and how much. *Trends Plant Sci* 6:535–542

Müller, A., C. Guan, L. Gälweiler, P. Tänzler, P. Huijser, A. Marchant, G. Parry, M. Bennett, E. Wisman, and K. Palme. (1998). AtPIN2 defines a locus of Arabidopsis for root gravitropism control. *EMBO J* 17:6903–6911

Nanjo, Y., H. Oka, N. Ikarashi, K. Kaneko, A. Kitajima, T. Mitsui, F. J. Muñoz, M. Rodríguez-López, E. Baroja-Fernández, and J. Pozueta-Romero. (2006). Rice plastidial N-glycosylated nucleotide pyrophosphatase/phosphodiesterase is transported from the ER-golgi to the chloroplast through the secretory pathway. *Plant Cell* 18:2582–2592

Nathan S. Claxton, Scott G. Olenych and Michael W. Davidson (2009) National High Magnetic Field Laboratory, 1800 East Paul Dirac., The Florida State University, Tallahassee, Florida

Nebenfuhr, A., Gallagher, L., Dunahay, T.G., Frohlick, J.A., Masurkiewicz, A.M., Meehl, J.B. and Staehelin, L.A. (1999) Stopand- go movements of plant Golgi stacks are mediated by the acto-myosin system. *Plant Physiol*. 121, 1127–1141

Nichols, B.J., Ungermann, C., Pelham, H.R.B., Wickner, W.T., and Haas, A. (1997) Homotypic vacuolar fusion mediated by t-and v-SNAREs. *Nature* 387, 199-202

Nihal Dharmasiri, Sunethra Dharmasiri and Mark Estelle (2005). The F-box protein TIR1 is an auxin receptor, *Nature*; Vol 435, 441-445

Niko Geldner, Jirí Friml, York-Dieter Stierhof, Gerd Jürgens, Klaus Palme (2001) Auxin transport inhibitors block PIN1 cycling and vesicle trafficking. *Nature* 413, 425-428

Ogawa M, Hanada A, Yamauchi Y, Kuwahara A, Kamiya Y, Yamaguchi S **(**2003) Gibberellin biosynthesis and response during *Arabidopsis* seed germination. *Plant Cell* 15**:**1591-1604

Okada, K., Ueda, J., Komaki, M. K., Bell, C, J and Shimura, Y.(1991) Requirement of the auxin polar transport system in the early stages of *Arabidopsis* floral bud formation. *Plant Cell* 3, 677-684

Paciorek, T., E. Zažímalová, N. Ruthardt, J. Petrášek, Y. D. Stierhof, J. Kleine-Vehn, D. A. Morris, N. Emans, G. Jürgens, N. Geldner, and J. Friml. (2005). Auxin inhibits endocytosis and promotes its own efflux from cells. *Nature* 435:1251–1256

Palme, K. and Galweiler, L. (1999) PIN- pointing the molecular basis of auxin transport. *Curr. Opin. Plant Biol*. 2, 375-381

Paponov, I.A., Teale, W.D., Trebar, M., Bliiou, I. and Palme, K. (2005) The PIN auxin efflux facilitators: evolutionary and functional perspectives. *Trends Plant Sci*. 10, 170-177

Park , S. C., H. B. Kwon and M. C. Shih (1996) Cis-Acting Elements Essential for Light Regulation of the Nuclear Gene Encoding the A Subunit of Chloroplast Glyceraldehyde 3-Phosphate Dehydrogenase in Arabidopsis thaliana. *PLANT PHYSIOLOGY* , 112: 4 1563-1571

Patton, D. A., L. H. Franzmann, and D. W. Meinke. (1991). Mapping genes essential for embryo development in Arabidopsis thaliana. *Mol. Gen. Genet* 227:337–47

Pauly, M., Albersheim, P., Darvill, A., York, W.S. (1999) Molecular domains of the ellulose/xyloglucan network in the cell walls of higher plants, *Plant J*. 20 629–639

Petrásek J, Friml J (2009) Auxin transport routes in plant development. *Development* 136:2675–2688

Petrášek, J., J. Mravec, R. Bouchard, J. J. Blakeslee, M. Abas, D. Seifertová, J. Wisniewska, Z. Tadele, M. Kubeš, M. Covanová, P. Dhonukshe, P. Skupa, E. Benková, L. Perry, P. Krecek, O. R. Lee, G. R. Fink, M. Geisler, A. S. Murphy, C. Luschnig, E. Zažímalová, and J. Friml. (2006). PIN proteins perform a rate-limiting function in cellular auxin efflux. *Science* 312:914–918

Pfeffer, S.R. (1999) Transport- vesicle targeting: tethers before SNAREs. *Nat. Cell Biol*. **1**, E17-22

Pierre-Olivier Vidalain, Mike Boxem, Hui Ge, Siming Li, and Marc Vidal (2004). Increasing specificity in high-throughput yeast two-hybrid experiments, *Methods* 32, 363–370

Pitts, R. J., Cernac, A. & Estelle, M. Auxin and ethylene promote root hair elongation in *Arabidopsis*. *Plant J.* 16, 553–560 (1998)

Pullen, M., Clark, N., Zarinkamar, F., Topping, J. & Lindsey, K**.** 2010. Analysis of vascular development in the hydra sterol biosynthetic mutants of Arabidopsis. *PLoS ONE* 5(8): e12227

Rahman, A. *et al*. Auxin and ethylene response interactions during *Arabidopsis* root hair development dissected by auxin influx modulators. *Plant Physiol.* **130**, 1908–1917 (2002)

Rand RP, Parsegian VA (1989) Hydration forces between phospholipid bilayers. Biochim *Biophys Acta* 988: 351–376

Rashotte, A. M., S. R. Brady, R. C. Reed, S. J. Ante, and G. K. Muday. (2000). Basipetal auxin transport is required for gravitropism in roots of Arabidopsis. *Plant Physiol* 122:481–490

Reed RC, Brady SR, Muday GK. (1998) Inhibition of auxin movement from the shoot into the root inhibits lateral root development in Arabidopsis. *Plant Physiol*.118, 1369–1378

Reichardt L, Stierhof YD, Mayer U, Richter S, Schwarz H, Schumacher K, Jurgens G (2007) Plant cytokinesis requires de novo secretory trafficking but not endocytosis. Curr Biol 17: 2047–2053

Reinhardt, D., E. R. Pesce, P. Stieger, T. Mandel, K. Baltensperger, M. Bennett, J. Traas, J. Friml, and C. Kuhlemeier. (2003). Regulation of phyllotaxis by polar auxin transport. *Nature* 426:255–260

Reinhardt, D., T. Mandel, and C. Kuhlemeier. 2000. Auxin regulates the initiation and radial position of plant lateral organs. *Plant Cell* 12:507–518

Richter S, Voss U, Jürgens G. (2009) Post-Golgi traffic in plants, *Traffic*. 10(7):819-28

Robinson, D.G., Hinz, G., and Holstein, S.E. (1998) The molecular characterization of transport vesicles. *Plant Mol. Biol*. 38, 49-76

Rossi, V. R. Picco, M. Vacca, M. DEsposito, M. DUrso, T. Galli and F. Filippini, (2004) VAMP subfamilies identified by specific R-SNARE motifs, *Biol. Cell* 96, 251–256

Rossi, V.D.K. Banfield, M. Vacca, L.E. Dietrich, C. Ungermann, M. D'Esposito, T. Galli and F. Filippini, (2004) Longins and their longin domains: regulated SNAREs and multifunctional SNARE regulators, *Trends Biochem. Sci.* 29,. 682–688

Rouster J, Leah R, Mundy J, Cameron-Mills V **(**1997) Identification of a methyl jasmonate-responsive region in the promoter of a lipoxygenase 1 gene expressed in barley grains. Plant J 11**:** 513–523

Rubery, P. H. and A. R. Sheldrake. (1974). Carrier-mediated auxin transport. *Planta* 188:101–121

Sabatini, S. *et al* (1999). An auxin-dependent distal organizer of pattern and polarity in the *Arabidopsis* root. *Cell* 99, 463-472

Sabatini, S., Heidstra, R., Wildwater, M., and Scheres, B. (2003). SCARECROW is involved in positioning the stem cell niche in the Arabidopsis root meristem. *Genes Dev.* 17**:** 354–358

Sachs, T. (1981). The control of patterned differentiation of vascular tissues. *Adv. Bot. Res* 9:151–262

Sanderfoot AA, Kovaleva V, Bassham DC, Raikhel NV. (2001a). Interactions between syntaxins identify at least five SNARE complexes within the Golgi/prevacuolar system of the *Arabidopsis* cell. *Mol. Biol. Cell* 12:3733–43

Sanderfoot AA, Pilgrim M, Adam L, Raikhel NV. (2001b). Disruption of individual members of *Arabidopsis* syntaxin gene families indicates each has essential functions. *Plant Cell* 13:659–66

Sanderfoot AA, Raikhel N. (2003). The secretory system of *Arabidopsis*. In *The Arabidopsis Book*, ed. CR Somerville, EM Meyerowitz. Rockville, MD: *Am. Soc. Plant Biol*. available at http://www.aspb.org/publications/arabidopsis*/*

Sanderfoot, A. A. (2007). The expansion of SNARE gene families parallels the rise of multicellularity among the green plants. *Plant Physiol* 144:6–17

Sanderfoot, A. A., V. Kovaleva, D. C. Bassham, and N. V. Raikhel. (2001b). Interactions between syntaxins identify at least five SNARE complexes within the Golgi/prevacuolar system of the Arabidopsis cell. *Mol. Biol. Cell* 12:3733–3743

Sanderfoot, A.A., and Raikhel, N.V. (1999) The specificity of vesicle trafficking: coat proteins and SNAREs. *Plant Cell* 11, 629-42

Sanyal**,** A., O'Driscoll, S.W., Bolander, M.A., and Sarkar, G**. (**1997). An effective method of completely removing contaminating genomic DNA from an RNA sample to be used for PCR. *Mol. Biotechnol*. 8**,** 135–137

Sasaki, T., Matsumoto, T., Yamamoto, K.*et al*. (2002) The genome sequence and structure of rice chromosome 1. *Nature*, 420, 312-316

Sauer, M., J. Balla, C. Luschnig, J. Wisniewska, V. Reinohl, J. Friml, and E. Benková. (2006). Canalization of auxin flow by Aux/IAA-ARF-dependent feedback regulation of PIN polarity. *Genes Dev* 20:2902–11

Scarpella, E., D. Marcos, J. Friml, and T. Berleth. (2006). Control of leaf vascular patterning by polar auxin transport. *Genes Dev* 20:1015–1027

Scales SJ, Chen YA, Yoo BY, Patel SM, Doung YC, Scheller RH (2000) SNAREs contribute to the specificity of membrane fusion. Neuron 26**:** 457–464

Schlicht, M., M. Strnad, M. J. Scanlon, S. Mancuso, F. Hochholdinger, K. Palme, D. Volkmann, D. Menzel, and F. Baluška. (2006). Auxin Immunolocalization Implicates Vesicular Neurotransmitter-Like Mode of Polar Auxin Transport in Root Apices. *Plant Signaling and Behaviour* 1:122–133.

Sheen,J., Hwang, S.B. et al.(1995) Green –Fluorescent Protein as a new vital marker in plant cells. *Plant Journal* 8, 777-784

Shevell, D. E., W. M. Leu, C. S. Gillmor, G. Xia, K. A. Feldmann, and N. H. Chua. (1994). EMB30 is essential for normal cell division, cell expansion, and cell adhesion in Arabidopsis and encodes a protein that has similarity to Sec7. *Cell* 77:1051–1062

Shiv B. Tiwari, Gretchen Hagen, and Tom Guilfoyle (2003). The Roles of Auxin Response Factor Domains in Auxin-Responsive Transcription. *Plant Cell*; 15(2): 533–543

Simpson SD, Nakashima K, Narusaka Y, Seki M, Shinozaki K, Yamaguchi-Shinozaki K. (2003) Two different novel cis-acting elements of erd1, a clpA homologous Arabidopsis gene function in induction by dehydration stress and dark-induced senescence. *Plant J*. 33: 259-270

Sorefan,K.,Girin,T.,Liljegren,S.J.,Ljung,K.,Robles,P,Galvan-Ampudia,C.S.,Offringa, R.,Friml,J.,Yanofsky,M.F.,Østergaard,L.,(2009.) A regulated auxin minimum is required for seed dispersal in Arabidopsis. *Nature* 459, 583–586

Sorin, C., J. D. Bussell, I. Camus, K. Ljung, M. Kowalczyk, G. Geiss, H. McKhann, C. Garcion, H. Vaucheret, G. Sandberg, and C. Bellini. (2005). Auxin and light control of adventitious rooting in Arabidopsis require ARGONAUTE1. *Plant Cell* 17:1343–1359

Souter M, Topping J, Pullen M, Friml J, Palme K, *et al*. (2002) *hydra* mutants of *Arabidopsis* are defective in sterol profiles and auxin and ethylene signalling. *Plant Cell* 14: 1017–1031

Souter MA, Pullen ML, Topping JF, Zhang X, Lindsey K (2004) Rescue of defective auxin-mediated gene expression and root meristem function by inhibition of ethylene signalling in sterol biosynthesis mutants of *Arabidopsis*. *Planta* 219: 773–783

Steinmann, T., N. Geldner, M. Grebe, S. Mangold, C. L. Jackson, S. Paris, L. Gälweiler, K. Palme, and G. Jürgens. (1999). Coordinated polar localization of auxin efflux carrier PIN1 by GNOM ARF GEF. *Science* 286:316–318

Stepanenko OV, Verkhusha VV, Kuznetsova IM, Uversky VN, Turoverov KK (2008). Fluorescent proteins as biomarkers and biosensors: throwing color lights on molecular and cellular processes *Curr. Protein Pept. Sci.* 9 (4): 338–69

Stefan Kepinski and Ottoline Leyser (2005). The Arabidopsis F-box protein TIR1 is an auxin receptor, *Nature*: Vol 435, 447-451 *The Plant Journal*: 51, 1126–1136

Stomp, A.M. (1992). Histochemical localization of β-glucuronidase. In: *GUS Protocols: Using the GUS Gene as a Reporter of Gene Expression (*Gallagher, S.R., ed.). San Diego: Academic Press, 103 113

Stuart A. Casson, Jennifer F. Topping, Keith Lindsey (2009). MERISTEM-DEFECTIVE, an RS domain protein, is required for the correct meristem patterning and function in Arabidopsis, The *Plant Journal*, Vol 57 (5), 857-869

Somerville, C. and Dangl, J. (2000) Genomics. Plant biology in 2010. Science, 290, 2077-2078

Surpin, M. and N. Raikhel. (2004). Traffic jams affect plant development and signal transduction. *Nature Rev. Mol. Cell Biol* 5:100–109

Surpin, M., H. Zheng, M. T. Morita, C. Saito, E. Avila, J. J. Blakeslee, A. Bandyopadhyay, V. Kovaleva, D. Carter, A. Murphy, M. Tasaka, and N. Raikhel. (2003). The VTI family of SNARE proteins is necessary for plant viability and mediates different protein transport pathways. *Plant Cell* 15:2885–2899

Sutter JU, Campanoni P, Blatt MR, Paneque M. (2006a). Setting SNAREs in a different wood. *Traffic* 7:627–38

Sutter JU, Campanoni P, Tyrrell M, Blatt MR. (2006b). Selective mobility and sensitivity to SNAREs is exhibited by the *Arabidopsis* KAT1 K+ channel at the plasma membrane. *Plant Cell* 18:935–54

Sutter, J., P. Campanoni, M. R. Blatt, and M. Paneque. (2006). Setting SNAREs in a different wood. *Traffic* 7:627–638

Sutton, R.B.,D. Fasshauer, R. Jahn and A.T. Brunger, Crystal structure of a SNARE complex involved in synaptic exocytosis at 2.4 Å resolution (1998), *Nature* 395, 347–353

Swarup, R., A. Marchant, and M. J. Bennett. (2000). Auxin transport: providing a sense of direction during plant development. *Biochem. Soc. Trans* 28:481–485

Swarup, R., E. M. Kramer, P. Perry, K. Knox, H. M. Leyser, J. Haseloff, G. T. Beemster, R. Bhalerao, and M. J. Bennett. (2005). Root gravitropism requires lateral root cap and epidermal cells for transport and response to a mobile auxin signal. *Nat. Cell Biol* 7:1057–1065

Swarup, R., J. Friml, A. Marchant, K. Ljung, G. Sandberg, K. Palme, and M. Bennett. (2001). Localization of the auxin permease AUX1 suggests two functionally distinct hormone transport pathways operate in the Arabidopsis root apex. *Genes Dev* 15:2648–2653

Swarup, R., J. Kargul, A. Marchant, D. Zadik, A. Rahman, R. Mills, A. Yemm, S. May, L. Williams, P. Millner, S. Tsurumi, I. Moore, R. Napier, I. D. Kerr, and M. J. Bennett. (2004). Structure-function analysis of the presumptive Arabidopsis auxin permease AUX1. *Plant Cell* 16:3069–3083

Swarup K, Benkova E, Swarup R, Casimiro I, Peret B, et al. (2008). The auxin influx carrier LAX3 promotes lateral root emergence. *Nat. Cell Biol.* 10:946–54

Tanaka, H., P. Dhonukshe, P. B. Brewer, and J. Friml. (2006). Spatiotemporal asymmetric auxin distribution: a means to coordinate plant development. *Cell Mol. Life Sci* 63:2738–54.

Terzaghi WB, Cashmore AR (1995) Light-regulated transcription. *Annu Rev Plant Physiol* 46:445-474

Thomas, S.G. and Sun, T.P. (2004). Update on Gibberellin signaling: A tale of the tall and short. *Plant Physiology*, 135, 668-676

Thorsten Hamann, Eva Benkova, Isabel Bäurle, Marika Kientz, and Gerd Jurgens (2002). The *Arabidopsis BODENLOS* gene encodes an auxin response protein inhibiting MONOPTEROS-mediated embryo patterning, *GENES & DEVELOPMENT* 16:1610–1615

Thorsten Hamann, Ulrike Mayer and Gerd Jurgens (1999). The auxin-insensitive bodenlos mutation affects primary root formation and apical-basal patterning in the Arabidopsis embryo, *Development* 126, 1387-1395

Titorenko, V. I. and R. T. Mullen. 2006. Peroxisome biogenesis: the peroxisomal endomembrane system and the role of the ER. *J. Cell Biol* 174:11–17

Tochio, H., M.M. Tsui, D.K. Banfield and M. Zhang, An autoinhibitory mechanism for nonsyntaxin SNARE proteins revealed by the structure of Ykt6p, *Science* 293 (2001), 698–702

Tom K. Kerppola (2006). Design and Implementation of Bimolecular Fluorescence Complementation (BiFC) Assays for the Visualization of Protein Interactions in Living Cells. *Nat Protoc*. 1(3): 1278–1286

Tom Bennett, Tobias Sieberer Barbara, Willett Jon Booker, Christian Luschnig and Ottoline Leyser (2006). The *Arabidopsis MAX* Pathway Controls Shoot Branching by Regulating Auxin Transport, *Current Biology* 16, 6, 553-563

Topping, J.F., Wei, W.B. and Lindsey, K. (1991). Functional Tagging of Regulatary Elements in the Plant Genome, *Development*, 112, 1009-1019

Tse, Y.C., Mo, B., Hillmer, S., Zhao, M., Lo, S.W., Robinson, D.G. and Jiang, L. (2004) Identification of multivesicular bodies as prevacuolar compartments in Nicotiana tabacum BY-2 cells. *Plant Cell*, 16, 672–693

Tsurumi S, Ohwaki Y. (1978) Transport of 14C-labeled indoleacetic acid in Vicia root segments. *Plant Cell Physiol*. 9:1195–1206

Tyrrell, M., Campanoni, P., Sutter, J. U., Pratelli, R., Paneque, M., Sokolovski, S., and Blatt, M. R. 2007 Selective targeting of plasma membrane and tonoplast traffic by inhibitory (dominant-negative) SNARE fragments *The Plant Journal* 51, 6, 1099-1115

Ueda, T., T. Uemura, M. H. Sato, and A. Nakano. 2004. Functional differentiation of endosomes in Arabidopsis cells. *Plant J* 40:783–789

Uemura T, Sato MH, Takeyasu K. (2005). The longin domain regulates subcellular targeting of VAMP7 in *Arabidopsis thaliana*. *FEBS Lett.* 579:2842–46

Uemura, T., T. Ueda, R. L. Ohniwa, A. Nakano, K. Takeyasu, and M. H. Sato. (2004). Systematic analysis of SNARE molecules in Arabidopsis: dissection of the post-Golgi network in plant cells. *Cell Struct. Funct* 29:49–65

Ulmasov T, Hagen G, Guilfoyle TJ(1999) Dimerization and DNA binding of auxin response factors. *Plant J* 19:309-319

Ulmasov, T., J. Murfett, G. Hagen, and T. Guilfoyle. 1997. Aux/IAA proteins repress expression of reporter genes containing natural and highly active synthetic auxin response elements. *Plant Cell* 9:1963–1971

Ulmasov, T, Liu, Z B., Hagen, G and T J Guilfoyle. (1995). Composite structure of auxin response elements. *Plant Cell*, 7(10): 1611–1623

Umehara M., Hanada A., Yoshida S., Akiyama K., Arite T., Takeda-Kamiya N., *et al* (2008) Inhibition of shoot branching by new terpenoid plant hormones. *Nature;455:195-200*

Urao T, Yamaguchi-Shinozaki K, Urao S, Shinozaki K An Arabidopsis myb homolog is induced by dehydration stress and its gene product binds to the conserved MYB recognition sequence. *Plant Cell* 5:1529-1539

Utsuno, K., T. Shikanai, Y. Yamada, and T. Hashimoto. (1998). Agr, an Agravitropic locus of Arabidopsis thaliana, encodes a novel membrane-protein family member. *Plant Cell Physiol* 39:1111–1118

Vandeputte, O., Oden, S., Mol, A., Vereecke, D., Goethals, K., El Jaziri, M., and Prinsen, E. (2005). Biosynthesis of auxin by the gram-positive phytopathogen Rhodococcus fascians is controlled by compounds specific to infected plant tissues. *Appl. Environ. Microbiol*. 71, 1169–1177

Vanneste S, Friml J (2009) Auxin: A trigger for change in plant development. *Cell* 136: 1005–1016

Vieten A, Sauer M, Brewer PB, Friml J (2007) Molecular and cellular aspects of auxin-transport-mediated development. *Trends Plant Sci* 12:160–168

Vieten, A., S. Vanneste, J. Wisniewska, E. Benková, R. Benjamins, T. Beeckman, C. Luschnig, and J. Friml. (2005). Functional redundancy of PIN proteins is accompanied by auxin-dependent cross-regulation of PIN expression. *Development* 132:4521–4531

Vision, T.J., Brown, D.G. and Tanksley, S.D. (2000). The origins of genomic duplications in Arabidopsis. *Science*, 290, 2114-2117

Volker Lipka, Chian Kwon and Ralph Panstruga (2007), SNARE-Ware: The Role of SNARE-Domain Proteins in Plant Biology. *Annu. Rev. Cell Dev. Biol*. 2007. 23:147–74

Walden, R., Fritze, K., Hayashi, H., Miklashevichs, E., Harling, H. and Schell, J (1994) Activation tagging: a means of isolating genes implicated as playing a role in plant growth and development. *Plant Mol. Biol*. 26, 1521-1528

Waters, M.G., and Hughson, F.M. (2000) Membrane tethering and fusion in the secretory and endocytic pathways. *Traffic*.1, 588-97

Weber T, Zemelman BV, McNew JA, Westermann B, Gmachl M, Parlati F, Sollner TH, Rothman JE (1998) SNAREpins: minimal machinery for membrane fusion. *Cell* 92: 759–772

Weigel,D., Ahn, JH., Blazquez, MA.et al., (2000) Activation tagging in Arabidopsis. *Plant Physiol,* 122, 1003-1013

Weijers, D.,Friml,J.,(2009). Snap Shot: auxin signalling and transport. *Cell* 136, 1172

Weijers,D.,Sauer,M.,Meurette,O.,Friml,J.,Ljung,K.,Sandberg,G.,Hooykaas,P.Offringa, R.,(2005). Maintenance of embryonic auxin distribution for apical- basal patterning by PIN-FORMED-dependent auxin transport in Arabidopsis. *Plant Cell17*,2517–2526

Willemsen, V., J. Friml, M. Grebe, A. Van den Toorn, K. Palme, and B. Scheres. (2003). Cell polarity and PIN protein positioning in Arabidopsis require STEROL METHYL-TRANSFERASE1 function. *Plant Cell* 15:612–625

Wilson, K., Long, D., Swineburne, J. And Coupland, G.(1996) A dissociation insertion causes a semi-dominant mutation that increases expression of TINY, an Arabidopsis gene related to APETALA2. Plant cell 8, 659-671

Winter D, Vinegar B, Nahal H, Ammar R, Wilson GV, et al. (2007) An “Electronic Fluorescent Pictograph” Browser for Exploring and Analyzing Large-Scale Biological Data Sets. *PLoS ONE* 2(8): e718

Wiśniewska, J., J. Xu, D. Seifertova, P. B. Brewer, K. Ruzicka, I. Blilou, D. Rouquie, E. Benková, B. Scheres, and J. Friml. (2006). Polar PIN localization directs auxin flow in plants. *Science* 312:883

Xu, J. and B. Scheres. (2005). Dissection of Arabidopsis ADP-RI-BOSYLATION FACTOR 1 function in epidermal cell polarity. *Plant Cell* 17:525–536

Xu, J., H. Hofhuis, R. Heidstra, M. Sauer, J. Friml, and B. Scheres. (2006). A molecular framework for plant regeneration. *Science* 311:385–388

Yamaguchi-Shinozaki, K. and Shinozaki,K. (1994). A novel cis-Acting Element in an Arabidopsis Gene is Involved in Responsiveness to Drought, Low Temperature or High Salt Stress. *Plant Cell*, 6,251-264

Yang T, Poovaiah BW (2002). A calmodulin-binding/CGCG box DNA-binding protein family involved in multiple signaling pathways in plants. *J Biol Chem*. 277:45049-45058

Yohann Boutté, Marie-Thérèse Crosnier, Nicola Carraro, Jan Traas and Béatrice Satiat-Jeunemaitre**.** (2006**).** The plasma membrane recycling pathway and cell polarity in plants: studies on PIN proteins, *Journal of Cell Science* 119, 1255-1265

Yu D, Chen C, Chen Z (2001) Evidence for an important role of WRKY DNA binding proteins in the regulation of NPR1 gene expression *Plant Cell* 13: 1527-1540

Yu, J., Hu, S., Wang, J. et al. (2002) A draft sequence of the rice genome (*Oryza sativa* L. ssp. indica). *Science*, 296, 79-92

Zazımalova E, Krecek P, Skupa P, Hoyerova K, Petrasek J. (2007). Polar transport of the plant hormone auxin—the role of PIN-FORMED (PIN) proteins. *Cell Mol. Life Sci.* 64(13):1621–37

Annex 1

Primers Used

Primers for GUS and GFP Cloning

5g22360 Prom For GTCGAGCAGAGATCCTAGTTAGTGAGTCC

5g22360 Prom Rev GTCGAGGTGATTCGATGACAGAGAGTGGAG

5g22360 Pac1 For TTAATTAACGCGATTGTCTATGCTGTTGTAGCG

5g22360 Bstx1 Rev CAGATTTTAAGATCTGCATGATGG

Gateway Primers

GW-360-FOR

GGGGACAAGTTTGTACAAAAAAGCAGGCTCAGAGATCCTAGTTAG
TGAGTCC

GW-360-REV

GGGGACCACTTTGTACAAGAAAGCTGGGTCAGATCTGCATGATGGTAAAGTG

Dom-Neg For

GGGGACAAGTTTGTACAAAAAAGCAGGCTTCGTTGTAGCGAGAGGTACCGTG

Dom-Neg Rev

GGGGACCACTTTGTACAAGAAAGCTGGGTCCTATTAGCATTTTTCATCCAAAG

Nested Primers

Nest-360- For AGCAGAGCGAGGATCTTGAC

Nest-360-Rev CATAAGCAAGGAGGACCATGAC

Domneg- Nest- For GTTGTAGCGAGAGGTACCGTG

Domneg-Nest-Rev TTAGCATTTTTCATCCAAAG

Actin Primers

Act2 For GGATCGGTGGTTCCATTCTTGC

Act2 Rev AGAGTTTGTCACACACAAGTGCA

qPCR Primers

VAMP714-FOR	GAGATTCGATCGGTCATGGT
VAMP714-REV	GGTAAAGTGATTCCTCCG
VAMP713-FOR	TTGTGAAAACATATGGCCGA
VAMP713-REV	CTAGCAACTCCAAACGCTCC
VAMP712-FOR	AACGTACTGATGGCCTCACC
VAMP712-REV	ATGTTCGCGGTTTTATCGAC
VAMP711-FOR	GGTGGAGAAACTGCAAGCTC
VAMP711-REV	ACACACTTCGCAAAGCAATG
IAA1-B FOR	GGAAGTCACCAATGGGCTTA
IAA1-B REV	GAGATATGGAGCTCCGTCCA
IAA2-B FOR	CACCAGTGAGATCTTCCCGT
IAA2-B REV	AGTCTAGAGCAGGAGCGTCG

Internal Primers for sequencing

360-cDNA For-1	GCGATTGTCTATGCTGTTGTAGC
360-cDNA For-2	TCCATTTTCGTATTTGGAAGAGAT
360-cDNA For-3	GGATTGAGCTTCTTGTTGATAAA
360-cDNA Rev	TACAGGAGCTTAGCATTTTTCATCC
360-Prom-1 For	TTCCAGCCAGTCAATGTTTTTCTCC
360-Prom-2 For	CGAGGGACAGCGAAACAATCAATA
360-Prom-3 For	GCTCGTAGCACAATAGAAATCGGAAAT
360-Prom-4 For	GTATCCGAACCCAAACCGAAAAGT
360-Prom Rev	GATTCGATGACAGAGAGTGGAGAT

GUS Primers

GUS nested 1 CGTAAGTCAGACCTAGCG

GUS nested 2 GGGAATACAATGCAGGAC

Primers for SALK genotyping

AtVAMP714

360 FOR (+1955)	GTATCCGAACCCAAACCGAAAAGT
360 REV (-2568)	CCTGAAAATCCAATCACCAACACATC
SALK_LBa1	TGGTTCACGTAGTGGGCCATCG

pDNOR primers

pDNOR207 For	TCGCGTTAACGCTAGCATGGATCTC
pDONR207 Rev	GTAACATCAGAGATTTTGAGACAC

Annex 2

Vector Maps

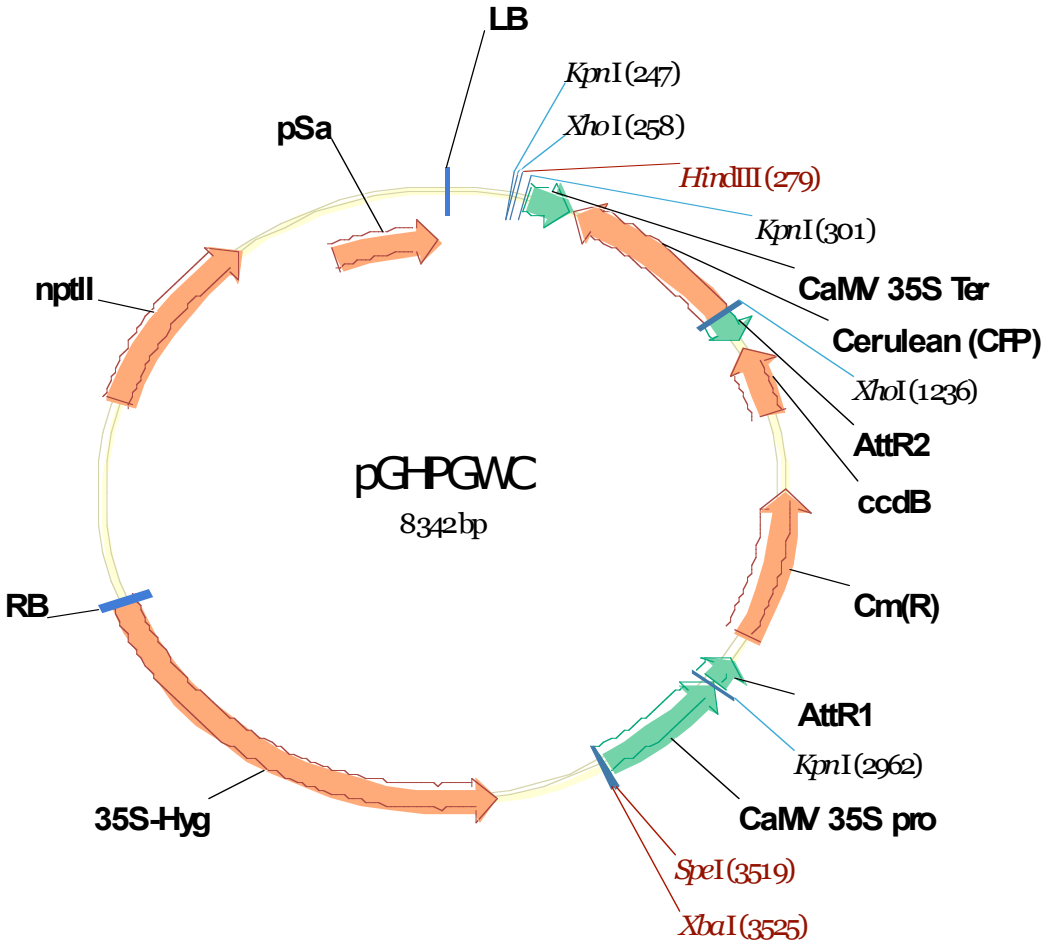

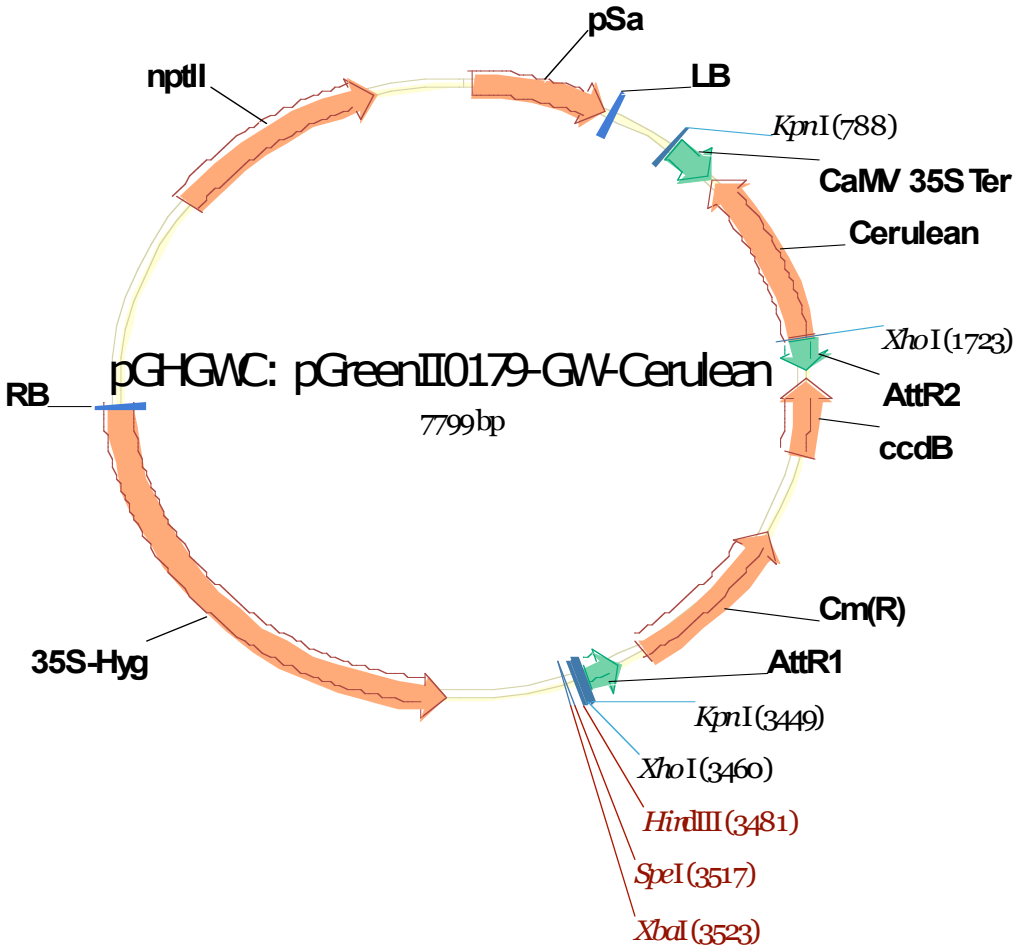
pSa
LB
KpnI (788)
CaMV 35S Ter
Cerulean
XhoI (1723)
AttR2
ccdB
Cm(R)
AttR1
KpnI (3449)
XhoI (3460)
HindIII (3481)
SpeI (3517)
XbaI (3523)
35S-Hyg
RB
nptII
pGHGWC: pGreenII0179-GW-Cerulean
7799 bp

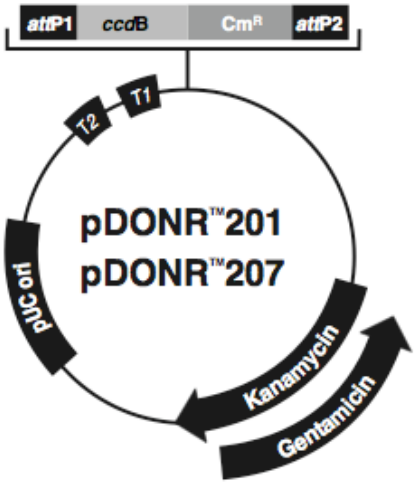

Comments for:	pDONR™201 4470 nucleotides	pDONR™207 5585 nucleotides
*rrn*B T2 transcription termination sequence (c):	73-100	73-100
rrnB T1 transcription termination sequence (c):	232-275	232-275
Recommended forward priming site:	300-324	300-324
*attP*1:	332-563	332-563
*ccd*B gene (c):	959-1264	959-1264
Chloramphenicol resistance gene (c):	1606-2265	1606-2265
*attP*2 (c):	2513-2744	2513-2744
Recommended reverse priming site:	2769-2792	2769-2792
Kanamycin resistance gene:	2868-3677	---
Gentamicin resistance gene (c):	---	3528-4061
pUC origin:	3794-4467	4909-5582

(c) = complementary strand

Invitrogen™
life technologies

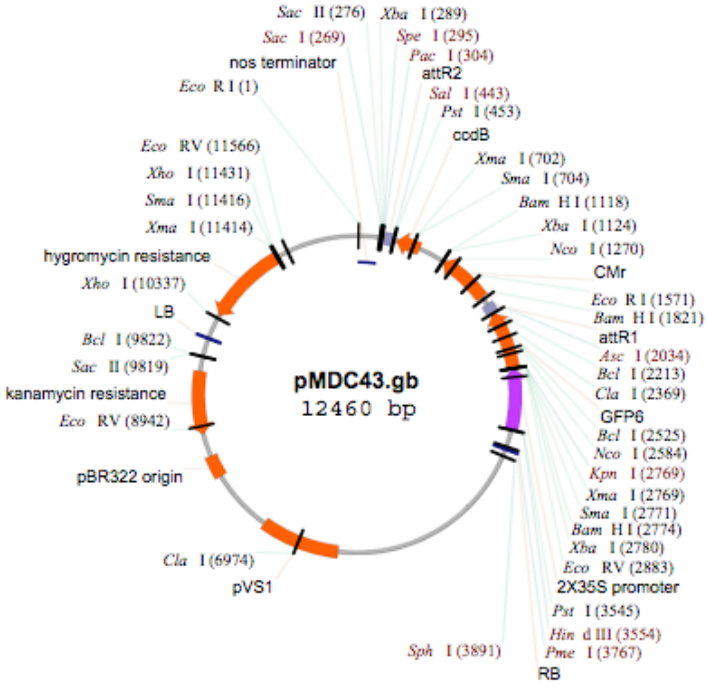
pMDC43.gb
12460 bp
Sac II (276)
Xba I (289)
Sac I (269)
Spe I (295)
Pac I (304)
nos terminator
attR2
Eco R I (1)
Sal I (443)
Pst I (453)
codB
Eco RV (11566)
Xma I (702)
Xho I (11431)
Sma I (704)
Sma I (11416)
Bam H I (1118)
Xma I (11414)
Xba I (1124)
Nco I (1270)
hygromycin resistance
CMr
Xho I (10337)
Eco R I (1571)
LB
Bam H I (1821)
attR1
Bcl I (9822)
Asc I (2034)
Sac II (9819)
Bcl I (2213)
kanamycin resistance
Cla I (2369)
Eco RV (8942)
GFP6
Bcl I (2525)
Nco I (2584)
pBR322 origin
Kpn I (2769)
Xma I (2769)
Sma I (2771)
Bam H I (2774)
Xba I (2780)
Cla I (6974)
Eco RV (2883)
pVS1
2X35S promoter
Pst I (3545)
Hin d III (3554)
Sph I (3891)
Pme I (3767)
RB

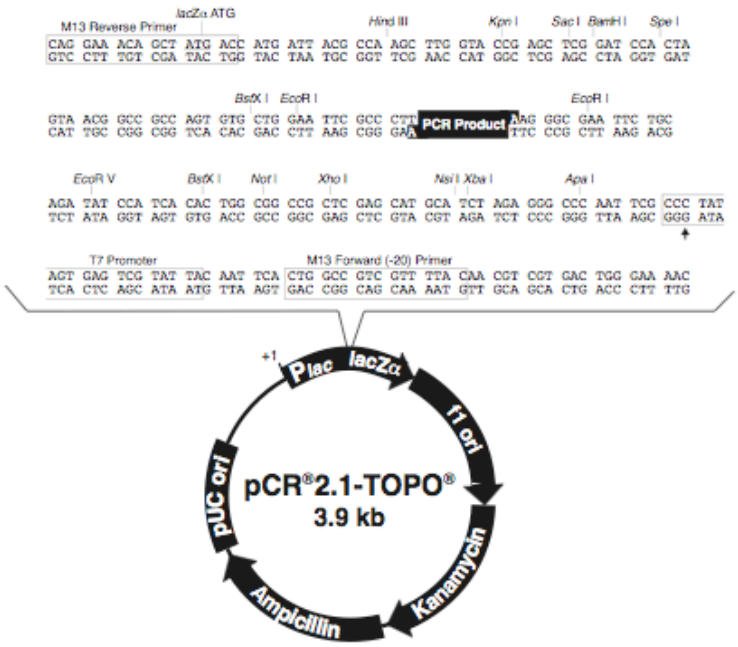

Comments for pCR®2.1-TOPO®
3931 nucleotides

LacZα fragment: bases 1-547
M13 reverse priming site: bases 205-221
Multiple cloning site: bases 234-357
T7 promoter/priming site: bases 364-383
M13 Forward (-20) priming site: bases 391-406
f1 origin: bases 548-985
Kanamycin resistance ORF: bases 1319-2113
Ampicillin resistance ORF: bases 2131-2991
pUC origin: bases 3136-3809

Invitrogen™
life technologies

pΔGUS-CIRCE

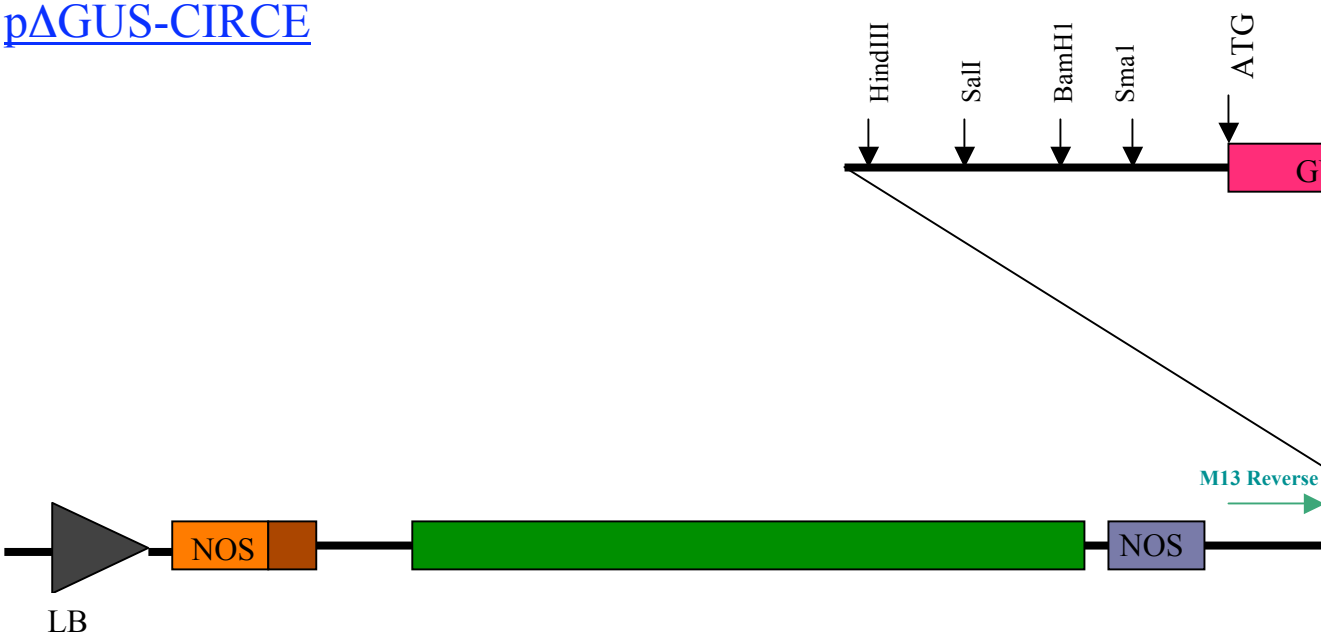

Promoter from the *NOS* gene

Leader sequence from TMV

Terminator and polyadenylation sequences from the *NOS* gene

Annex 3

AtVAMP714 **Promoter and Gene sequence**
Designed Primers are in different colours

pink=nester for primer
red = GW 5g22360Prom For
blue = GW 5g22360Prom REV
green = ATG
Org=cDNA For-1
Purple= cDNA For-2
Red= cDNA For-3
Pur= cDNA Rev
GW-360-Rev-new
TAA = stop codon
green = nested Rev-new

```
   1  TAAAGTTTCA AGCACTGTTC TCAGTCTTGT ATTTCCTCAT CTTCCATGTA
  51  CTTCTCCTGT ACAGCTGCGA CTGTGAAGAC TATCGTCAAA GAAACAATTC
 101  TTTTGTAGTA GACGTAAAAC TAAACTCAAG AGTTATTGAG AGAAGTAATG
 151  GTTAAGAAAT CCAAAATGCT AAAAAAGGAT ATCTGTTATA ATCCCAATCA
 201  GTTTGACCAA TTGCAATCTT GCTGTATTCA ACCACACTTG CATCAATGCC
 251  GGCAAATATG TATCCATTGC TCTTGTCGAT GAGCTTTACT AGATCCCCAA
 301  CACTTTCTTT ATCCTGAAAA CAAAAAAGAA AATTGCGAAA AGATGCTTGT
 351  ACAGAGAGAA AGAGAGAGAG AGGTAAAGGA AATCGCAAAC CTGAATATCC
 401  AAGGTTGTAA AATTAACAAG ACTGTAATCT TCAATGACAC TACATAGCTC
 451  TTTTGTTAGT TTTCTGCAAT GAGAAACATC AAGCTCATGA GATATTGAGC
 501  ATGCTTCTAA ATGGATAATT ATTAACCGTT CAATGTGTAT TCAGATGATG
 551  TTTACATCGA ACCTGTACTT AGCAGAGCGA GGATCTTGAC TAAGATGGTG
 601  CTCCAAGTAT GACAAGTCTT GAACATCGGT ATAGAAATCT AAATTGAAAG
 651  CTACATGCAC AGAGATCCTA GTTAGTGAGT CCACAGTATA CATTTGAAAA
 701  TTCGATGTTA TGAGAACAAA ACCATAGATA GATTATTAAT ACCTAGCTTC
 751  CCGTAGCTTC CAATCAGATC GATTTTAGAC AATACATTGA CATGTGGGAG
 801  TTCCATGTGA AGCATTGTGG ATAAGGAGAG AAGTAGCGAA CTTACGTAGT
 851  TCCCGGGATC ACAACATAGA TGGGAATCAA TTAGTTGCAC AGCAGTTAAC
 901  TGCAGAACAA AGAAATTCAT CAGATATGTA GACTCCTAAG TAAGGTTCAT
 951  TTAGCAAGTT AGTAATAAGT GAAGTAAAGC ACATACTCTA AGGTTCAATG
1001  ATTTAATCAG CTTCGTGAGA ACATTCTTGG TACTGTCATG AATGAAGAAC
1051  AATTCCACTT GGCCAGGAAA ATCAAAGAGA ATGTAATGAT CTGCAAACAA
1101  TTCAAAACGT TTTACTTTAA GAAAGAGATA TTATGACCAC GAAAAGAAGA
1151  AGAAGAAGAA GGGACATATC GTTGCTAACC CTTCAGAAGA GGCTTTAGTT
1201  TAGATTCCAG CCAGTCAATG TTTTTCTCCA AGTACTCCAT ACAATATACA
1251  AGACCTGTCA CATTAGAAAG TTTCTTTGTT AATTTGACCA AAGATTAAAA
1301  TCAAAAGTAA GAAGAAAAGG GAAAATCAAG ATGGCAAAAT TCACCTCCAT
1351  TAGGACCAAG CGAGTGTTCC GACATAACAT CTTCTAACTT GATCAATTCT
1401  TCTATATTCA CACCACACTC ATAACTAAAA TCAATGTCAA GAAACAACAT
1451  ACACCTGCAA TTTTTAACAA TTTTGTTGTA TTTGGCTTGA AAAGGATACG
1501  GTAATGCATC ATTTGCAGGA TCCAGATTAA CAATAGCAAC CTTCCTGCAA
1551  CAACAACAAA ATAGTAACTC AACGTTAAGA GAATTTACTT ACAGAGAAGT
1601  TCTCACGAAT CTGCAAATCT CTCTACCAAA AACAAAGACA AGGCAACAAC
1651  ATTTCACAAT GACTCTGCTC AAAAGTCAGA CAATTCAAAT TTCTGGAATT
1701  CAACACTATT ATTTACTAAA GTTTGCAACT TGTAAACTTT ACAATGCGAG
1751  GGACAGCGAA ACAATCAATA CAAACAGAAT TACAGATACA AAAGCCAAGT
1801  AAGCTTCATT CTTTGATCCA AAAAGAGAAG AGAAGAGAAA GAACATGAAA
1851  CCTGCCCATT AGAGAGAGGA ACTGAGACAT TCCATTGCAA TAAGTGGTCT
1901  TTCCCGATCC TGGAGGACCT ATTACTACTT GTCCAAACAC CATGCTTCTG
1951  AAGACGAAGA AGAAGATTGA TACCAATCGG AGTCAAACAC GTTGTATAAT
2001  ATCAGAGCCA GTCAGACAAA AAAACACAGT AATTGCAAAG CAAAATCATC
2051  TAATCATCAA ACTAACATAA CATGAATATT CAATAGAGAA CATCAAAACC
2101  CTTCTAAACA CTGAGCTCGT AGCACAATAG AAATCGGAAA TGTCATTTGT
2151  TCGTCGGACA CAGAATACAA ACACAATCCT CCAATATTAT TAACCCAATT
2201  CCTAAACCTC GTTTATAATA CAACAAACAA TTCACTGGAG AAAGAGAAGC
2251  AGAGAAACAA TTTGCTTCAA GAGCATATTC ATTATATCAG AAGCAACTGG
2301  AGACACAGAA GAAAATAAAT AGAGAAGCTC GCCTGTGTAG TTAGCCGGAG
2351  AGAGAAGCAA TGACAGGTCT GTTTGCCGGA GCAAGAGAAA CTCGCAGCCG
2401  GAGACTCGTC GAAGACTCGA TTCAAGGCGA AGTAAGCTCG CCGAAGACTC
2451  GATCGGTATA TTTAAATTAG GGCTTTAATT TTAATTCGGT TTATTCGTGC
2501  TATACTCGAA CCGAACCGGA TAATCGAAAT TAAAAAGAAG GAAACGATCA
2551  AGTTATTATT GGAGTATCCG AACCCAAACC GAAAAGTGAA TTTCGGGTCG
2601  GTTTGTTTTC GGATAAGTTA CCAAGGCCTA ATAAATTGGT AAACCGTAAA
2651  CCGATGCATC AGGGTTTAAA ATGTAACAAA ATAATATTTT AGGTGACAAT
2701  TAAAAACGTA ACAATAAAAC AAGGGGTTAT ATTCGAAACG TTTGCACCTA
2751  ACCTTATAAC TTCGCATTTT TATACTCTGT TCTGATCGCA GCAAAGCCGA
2801  CGTTGAACTT TCTCGCCGCC GGAGCGCGTG ATCTCCACTC TCTGTCATCG
2851  AATCACTCTA ATTGAAGATT CTCCGATGGC GATTGTCTAT GCTGTTGTAG
2901  CGAGAGGTAC CGTGGTATTA GCTGAATTCA GCGCCGTTAC GGGAAACACA
2951  GGCGCCGTGG TGCGACGGAT CCTCGAGAAG CTTTCACCGG AAATCTCCGA
```

```
3001  TGAAAGACTT TGTTTCTCTC AAGATCGTTA TATCTTCCAT ATTCTTAGAT
3051  CTGATGGTCT TACCTTTCTC TGTATGGCCA ATGATACCTT TGGAAGTAAG
3101  TATTTTTCAC TTTCTCCGAA TCGTAATCTC TCTTAAGAAG ATTTAGTCTT
3151  TGTAATTGAT TCTGAGTTTT ATGTTTTGAT GTGTTGGTGA TTGGATTTTC
3201  AGGGAGGGTT CCATTTTCGT ATTTGGAAGA GATTCATATG AGATTCATGA
3251  AAAACTATGG CAAAGTGGCT CATAATGCTC CAGCTTATGC AATGAATGAT
3301  GAATTCTCAA GGGTTTTGCA TCAGCAGATG GAGTTCTTCT CTAGTAATCC
3351  TAGTGTTGAT ACTCTCAATC GTGTTAGAGG AGAAGTCAGT GAGGTATAAT
3401  TGTTTCTTCG TATGATCTCT AGATATTACT CAGCTATATC CATTGAAAAG
3451  GTTGAATTTT TATGAGTTAT TACGCCTTCT TGGCTCACAC AGGCTTCTTT
3501  AAATCTGTCT TGGGTGAAAG ATGAAGTTTG TTATCTCATT GTTGTGTTAT
3551  CGTGTTTACA GATTCGATCG GTCATGGTAG AGAACATTGA GAAGATAATG
3601  GAAAGAGGTG ATAGGATTGA GCTTCTTGTT GATAAAACAG CAACAATGCA
3651  AGATAGCTCG TTTCACTTCA GGAAGCAATC TAAGCGCCTT CGCCGAGCTC
3701  TTTGGATGAA AAATGCTAAG CTCCTGTAAG GATCTCTCTC ACTTCTAGAT
3751  TCTCTTCATT CCTTTTCTTT GCTAACTAAG AGATACGCTC TTCTACATTC
3801  TAGGTGTTTC AACTCGCCTT TGCAGCATAG TTTATTGATA TGTTTCTTAA
3851  ACTAGAGATA CAGTAGTTCT AAGATTCAAC ATTATTTTCG ATTTTGGGAA
3901  ATTCTCCTCG ACAAAATATC TAATTTTTGG CTGATAGGAA CTACACTGCC
3951  TTGATTCCAC CTCTGCTTAA AGAAATTTCA TTATTGTTTT GTTTTGATGC
4001  TTGAGTTCCA GATCACTTTT ATTAATCAAC AAAACTGCTT TTCTTGTTTG
4051  TGTTCGGCAG GGTCTTGTTG ACATGCTTGA TAGTTTTCTT GCTGTACATA
4101  ATAATCGCAT CTTTCTGCGG AGGAATCACT TTACCATCAT GCAGATCTTA
4151  AAATCTGGCG GCCTTATCTA AGGTATACTG AAACGGACCA CTGTTTTTGT
4201  AAATCAACTC AGTCGCATCA TTTCGATTTG AAGCCTTGGT TTTGTCATGA
4251  AAATGACTGT GAGTTTGAAG TTACATGTCA TGGTCCTCCT TGCTTATGTA
4301  ACTCTTGTAA ATGTCAAAAT CAAAATGATA CAGAGGTTCA TTGAACTCTT
4351  GCCTTGTCTT TTAGATTTAG TCACGTGAGT GAGTTTGTTC TCTGTATTTC
4401  CAAAACTTTA TCCGCTGTGT CTTTATAATT TTTGCATTTG CAATGTACAT
4451  CACATATTCG TTATTTTTGT TGTTAAAATT ACTTCAGTTT TCATCTTTGT
4501  TTAATAACAT TTCTGATTCA CAAATA
```

Annex 4

AtVAMP714 Domain Structure

For primer (Pink) and Reverse primer (Blue) used to amplify the Longin and SNARE domains to create Dominant Negative transgenic plants

At5g22360/ VAMP714
Longin Domain
SNARE Domain
Trans-membrane Domain
For primer
Reverse primer

```
   1  CATTTTTATA CTCTGTTCTG ATCGCAGCAA AGCCGACGTT GAACTTTCTC
  51  GCCGCCGGAG CGCGTGATCT CCACTCTCTG TCATCGAATC ACTCTAATTG
 101  AAGATTCTCC GATGGCGATT GTCTATGCTG TTGTAGCGAG AGGTACCGTG
 151  GTATTAGCTG AATTCAGCGC CGTTACGGGA AACACAGGCG CCGTGGTGCG
 201  ACGGATCCTC GAGAAGCTTT CACCGGAAAT CTCCGATGAA AGACTTTGTT
 251  TCTCTCAAGA TCGTTATATC TTCCATATTC TTAGATCTGA TGGTCTTACC
 301  TTTCTCTGTA TGGCCAATGA TACCTTTGGA AGGAGGGTTC CATTTTCGTA
 351  TTTGGAAGAG ATTCATATGA GATTCATGAA AAACTATGGC AAAGTGGCTC
 401  ATAATGCTCC AGCTTATGCA ATGAATGATG AATTCTCAAG GGTTTTGCAT
 451  CAGCAGATGG AGTTCTTCTC TAGTAATCCT AGTGTTGATA CTCTCAATCG
 501  TGTTAGAGGA GAAGTCAGTG AGATTCGATC GGTCATGGTA GAGAACATTG
 551  AGAAGATAAT GGAAAGAGGT GATAGGATTG AGCTTCTTGT TGATAAAACA
 601  GCAACAATGC AAGATAGCTC GTTTCACTTC AGGAAGCAAT CTAAGCGCCT
 651  TCGCCGAGCT CTTTGGATGA AAAATGCTAA GCTCCTGGTC TTGTTGACAT
 701  GCTTGATAGT TTTCTTGCTG TACATAATAA TCGCATCTTT CTGCGGAGGA
 751  ATCACTTTAC CATCATGCAG ATCTTAAAAT CTGGCGGCCT TATCTAAGGT
 801  ATACTGAAAC GGACCACTGT TTTTGTAAAT CAACTCAGTC GCATCATTTC
 851  GATTTGAAGC CTTGGTTTTG TCATGAAAAT GACTGTGAGT TTGAAGTTAC
 901  ATGTCATGGT CCTCCTTGCT TATGTAACTC TTGTAAATGT CAAAATCAAA
 951  ATGATACAGA GGTTCATTGA ACTCTTGCCT TGTCTTTTAG ATTTAGTCAC
1001  GTGAGTGAGT TTGTTCTCTG TATTTCCAAA ACTTTATCCG CTGTGTCTTT
1051  ATAATTTTTG CATTTGCAAT GTACATCACA TATTCGTTAT TTTTGTTGTT
1101  AAAATTACTT CAGTTTTCAT CTTTGTTTAA TAACATTTCT GATTCACAAA
1151  TA
```

AtVAMP714 Interleaved Sequences

Domains are in different colours (Longin, SNARE and Transmembrane)

```
    Met Ala Ile Val Tyr Ala Val Val Ala Arg Gly Thr Val Val Leu Ala Glu     17
112 ATG GCG ATT GTC TAT GCT GTT GTA GCG AGA GGT ACC GTG GTA TTA GCT GAA

    Phe Ser Ala Val Thr Gly Asn Thr Gly Ala Val Val Arg Arg Ile Leu Glu     34
163 TTC AGC GCC GTT ACG GGA AAC ACA GGC GCC GTG GTG CGA CGG ATC CTC GAG

    Lys Leu Ser Pro Glu Ile Ser Asp Glu Arg Leu Cys Phe Ser Gln Asp Arg     51
214 AAG CTT TCA CCG GAA ATC TCC GAT GAA AGA CTT TGT TTC TCT CAA GAT CGT

    Tyr Ile Phe His Ile Leu Arg Ser Asp Gly Leu Thr Phe Leu Cys Met Ala     68
265 TAT ATC TTC CAT ATT CTT AGA TCT GAT GGT CTT ACC TTT CTC TGT ATG GCC

    Asn Asp Thr Phe Gly Arg Arg Val Pro Phe Ser Tyr Leu Glu Glu Ile His     85
316 AAT GAT ACC TTT GGA AGG AGG GTT CCA TTT TCG TAT TTG GAA GAG ATT CAT

    Met Arg Phe Met Lys Asn Tyr Gly Lys Val Ala His Asn Ala Pro Ala Tyr    102
367 ATG AGA TTC ATG AAA AAC TAT GGC AAA GTG GCT CAT AAT GCT CCA GCT TAT

    Ala Met Asn Asp Glu Phe Ser Arg Val Leu His Gln Gln Met Glu Phe Phe    119
418 GCA ATG AAT GAT GAA TTC TCA AGG GTT TTG CAT CAG CAG ATG GAG TTC TTC

    Ser Ser Asn Pro Ser Val Asp Thr Leu Asn Arg Val Arg Gly Glu Val Ser    136
469 TCT AGT AAT CCT AGT GTT GAT ACT CTC AAT CGT GTT AGA GGA GAA GTC AGT

    Glu Ile Arg Ser Val Met Val Glu Asn Ile Glu Lys Ile Met Glu Arg Gly    153
520 GAG ATT CGA TCG GTC ATG GTA GAG AAC ATT GAG AAG ATA ATG GAA AGA GGT

    Asp Arg Ile Glu Leu Leu Val Asp Lys Thr Ala Thr Met Gln Asp Ser Ser    170
571 GAT AGG ATT GAG CTT CTT GTT GAT AAA ACA GCA ACA ATG CAA GAT AGC TCG

    Phe His Phe Arg Lys Gln Ser Lys Arg Leu Arg Arg Ala Leu Trp Met Lys    187
622 TTT CAC TTC AGG AAG CAA TCT AAG CGC CTT CGC CGA GCT CTT TGG ATG AAA

    Asn Ala Lys Leu Leu Val Leu Leu Thr Cys Leu Ile Val Phe Leu Leu Tyr    204
673 AAT GCT AAG CTC CTG GTC TTG TTG ACA TGC TTG ATA GTT TTC TTG CTG TAC

    Ile Ile Ile Ala Ser Phe Cys Gly Gly Ile Thr Leu Pro Ser Cys Arg Ser    221
724 ATA ATA ATC GCA TCT TTC TGC GGA GGA ATC ACT TTA CCA TCA TGC AGA TCT
    Stop                                                                   221
```

Annex 6

Table 1: PCR results for SALK_005917 seedlings

PLANT NO	PCR RESULTS			GENOTYPE
	FOR+REV	FOR+LBa1	RT-PCR	
1	†	—		Wild type
2	†	—		Wild type
3	†	—		Heterozygous
4	†	—		Wild type
5	—	†		Heterozygous
6	†	—	—	**Homozygous**
7	—	†		Wild type
8	†	†		Heterozygous
9	†	—		Wild type
10	†	†	—	**Homozygous**
11	†	—		Wild type
12	†	—		Wild type
13	†	†		Heterozygous
14	†	—		Wild type
15	†	†		Wild type
16	†	†		Wild type
17	†	—		Wild type
18	†	—		Wild type
19	†	†		Wild type
20	†	—		Wild type

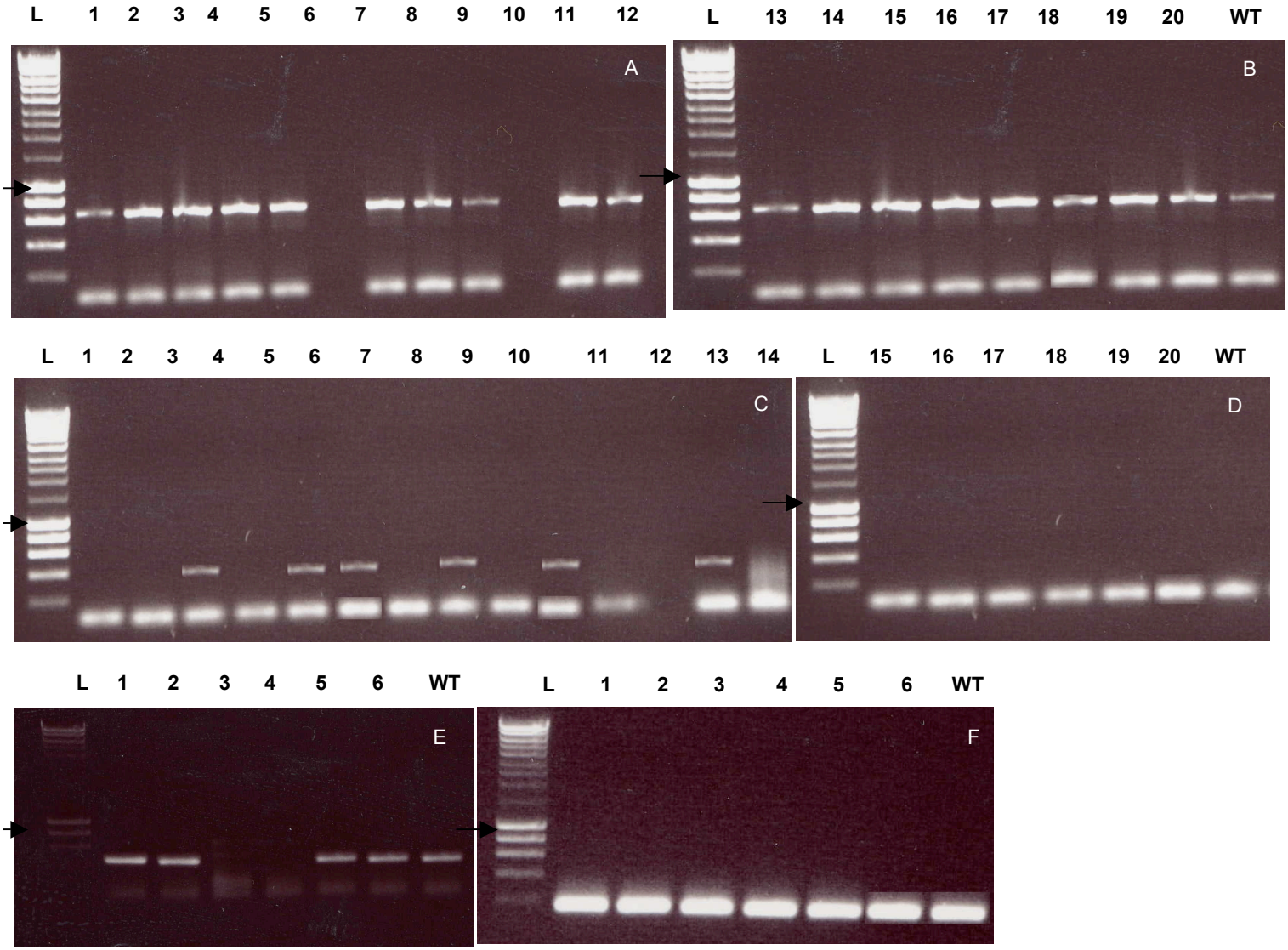

Figure1: PCR Results of SALK_005917 (Arrow head= 1000bp)

A and **B**: PCR results of 20 seedlings with 360 (+1955) Forward and 360 (-2568) Reverse primers (product size= 642bp), Plant numbers 6 and 10 not giving bands

C and **D**: PCR results of 20 seedlings with 360 (-2566) Reverse and LBa1 primers (product size= 500bp), Plant numbers 3, 5,6, 8, 10 and 13 giving bands

E: Plant numbers 3, 5,6, 8, 10 and 13 -RT-PCR with 360 (+1955) Forward and 360 (-2568) Reverse primers

Lane 1- Plant number 3

Lane 2-Plant number 5

Lane 3-Plant number 6

Lane 4-Plant number 10

Lane 5-Plant number 5

Lane 6-Plant number 13

F: Plant numbers 3, 5,6, 8, 10 and 13 PCR with *ACTIN2* primers (product size=180bp)

Table 2: PCR results for SALK_005914 seedlings

PLANT NO	PCR RESULTS			GENOTYPE
	FOR+REV	FOR+LBa1	RT-PCR	
1	†	—		Wild type
2	†	—		Wild type
3	†	—		Wild type
4	†	—		Wild type
5	**—**	**†**		Wild type
6	†	—		Wild type
7	**—**	**†**		Wild type
8	†	†		Heterozygous
9	†	—		Wild type
10	†	†		Heterozygous
11	†	—		Wild type
12	†	—		Wild type
13	†	†		Heterozygous
14	†	—		Wild type
15	†	†		Heterozygous
16	†	†		Wild type
17	†	—		Wild type
18	†	—		Wild type
19	†	†		Heterozygous
20	†	—		Wild type

Annex 7

***AtVAMP714* Promoter analysis**

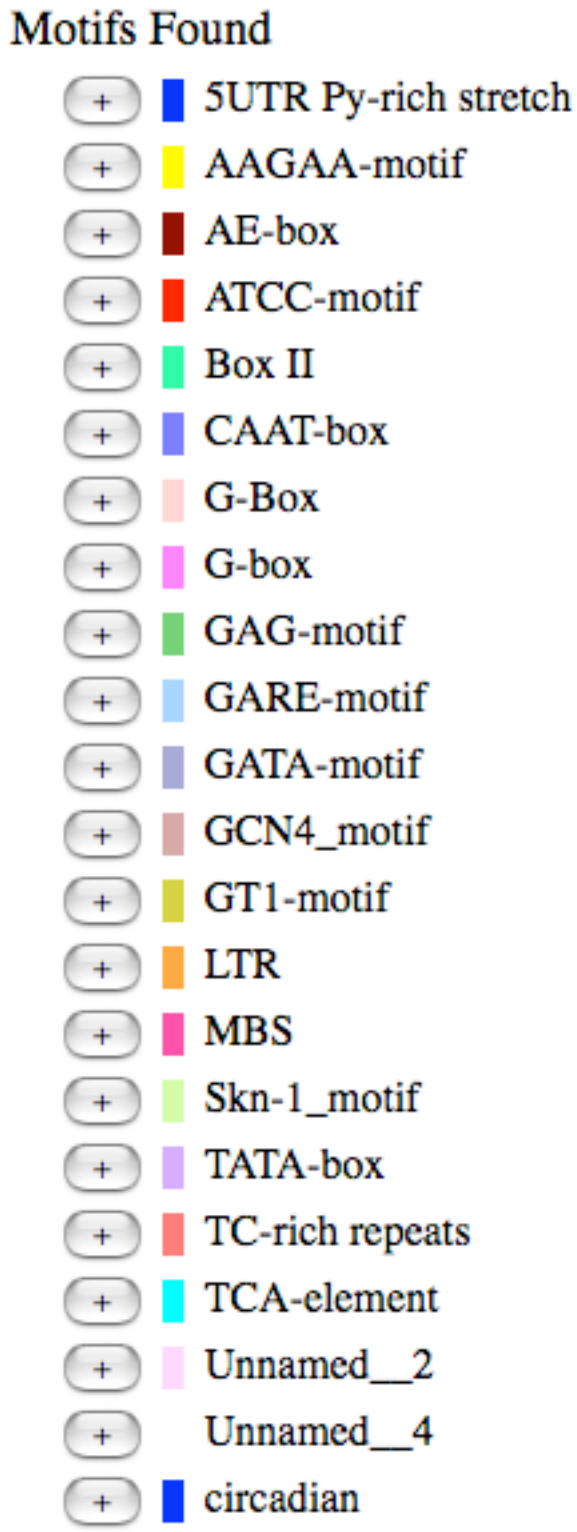

AtVAMP714 Promoter Analysis

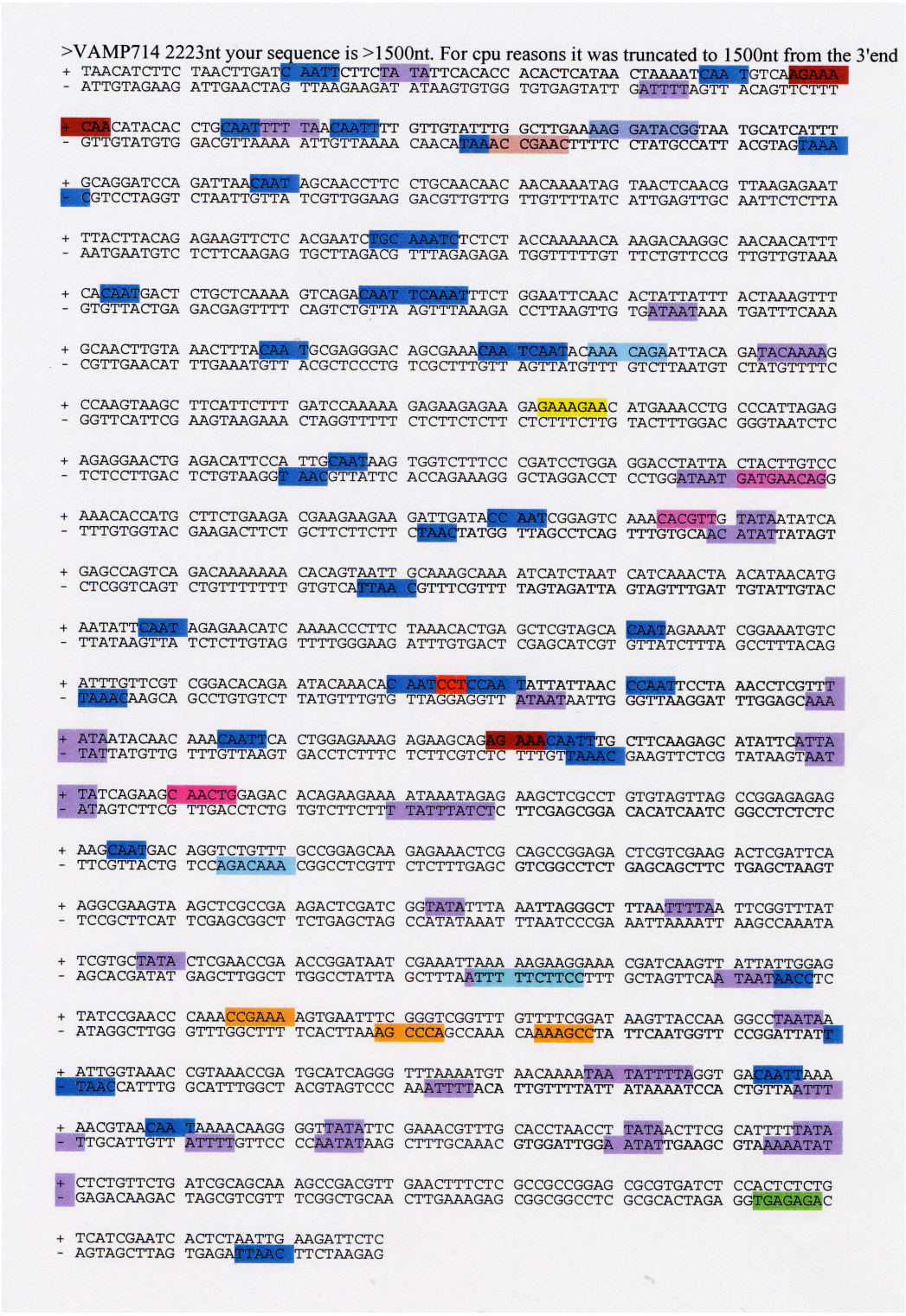

Annex 8

Table 1: Hygromycin segregation of Dominant Negative transgenics

Plant No	Hygromycin ^{R}	Hygromycin $_{S}$	Ratio
1	52	8	6:1
2	46	14	**3:1**
3	56	4	14:1
4	48	15	**3:1**
5	47	15	**3:1**
6	58	2	29:1
7	50	10	5:1
8	45	14	**3:1**
9	53	7	7:1
10	55	5	11:1